Air Force Institute of Technology
AFIT Scholar

Theses and Dissertations | Student Graduate Works

9-1-2013

Metrics for Emitter Selection for Multistatic Synthetic Aperture Radar

Sean R. Stevens

Follow this and additional works at: https://scholar.afit.edu/etd

Part of the Signal Processing Commons, and the Systems and Communications Commons

Recommended Citation

Stevens, Sean R., "Metrics for Emitter Selection for Multistatic Synthetic Aperture Radar" (2013). *Theses and Dissertations*. 906.
https://scholar.afit.edu/etd/906

This Thesis is brought to you for free and open access by the Student Graduate Works at AFIT Scholar. It has been accepted for inclusion in Theses and Dissertations by an authorized administrator of AFIT Scholar. For more information, please contact richard.mansfield@afit.edu.

METRICS FOR EMITTER SELECTION FOR MULTISTATIC SYNTHETIC APERTURE RADAR

THESIS

Sean R. Stevens, Civilian, USAF

AFIT-ENG-13-S-03

DEPARTMENT OF THE AIR FORCE
AIR UNIVERSITY

AIR FORCE INSTITUTE OF TECHNOLOGY

Wright-Patterson Air Force Base, Ohio

DISTRIBUTION STATEMENT A. APPROVED FOR PUBLIC RELEASE;
DISTRIBUTION UNLIMITED

The views expressed in this thesis are those of the author and do not reflect the official policy or position of the United States Air Force, the Department of Defense, or the United States Government.

This material is declared a work of the U.S. Government and is not subject to copyright protection in the United States

AFIT-ENG-13-S-03

METRICS FOR EMITTER SELECTION FOR MULTISTATIC SYNTHETIC APERTURE RADAR

THESIS

Presented to the Faculty

Department of Electrical and Computer Engineering

Graduate School of Engineering and Management

Air Force Insitute of Technology

Air University

Air Education and Training Command

in Partial Fulfillment of the Requirements for the

Degree of Master of Science in Electrical Engineering

Sean R. Stevens, B.S.E.E.

Civilian, USAF

September 2013

DISTRIBUTION STATEMENT A. APPROVED FOR PUBLIC RELEASE;

DISTRIBUTION UNLIMITED

AFIT-ENG-13-S-03

METRICS FOR EMITTER SELECTION FOR MULTISTATIC SYNTHETIC APERTURE RADAR

Sean R. Stevens, B.S.E.E.
Civilian, USAF

Approved:

Julie A. Jackson, PhD (Chairman) — 22 Aug 2013 — Date

Michael A. Temple, PhD (Committee Member) — 19 Aug 2013 — Date

Peter J. Collins, PhD (Committee Member) — 19 AUG 2013 — Date

Alan D. Kerrick, PhD (Committee Memeber) — 19 Aug 2013 — Date

Abstract

A bistatic synthetic aperture radar (SAR) implementation forms images of the earth's surface from an aircraft using emitters and receivers which are separated by some distance. Possible sources of illumination for such radars, when not using cooperative emitters, are ground based communications systems. The lack of radar specific waveforms in communications systems means that the radar system may have poor performance in some respects. One way to improve performance of such systems is a multistatic radar implementation, where multiple bistatic radar systems operate together. Of particular interest here is a single receiver, multiple emitter multistatic implementation. This leads to the problem of selecting from a potentially large set of emitters, a subset of which may be used in the image formation process.

A framework for selecting between sets of emitters is proposed using multiple objective optimization. This approach requires use of objective functions to score the different objectives of the selection process. Four objective functions are selected to score the sets of emitters: multistatic Signal to Noise Ratio (SNR), Integrated Sidelobes (ISL) of the multistatic ambiguity function (MAF), effective multistatic resolution area (EMRA), and contrast ratio. In this work, the high definition television (HDTV) standard, long term evolution (LTE) cellular standard, worldwide interoperability for microwave access (WiMAX) wireless internet standard, and analog frequency modulated (FM) radio standard are used as a set of representative communications standards.

Calculating objective function values through simulation can take a significant amount of time. To obtain these objective functions faster, an approximation is found for the SAR point spread function (PSF) to facilitate calculation of EMRA and contrast ratio. This approximate PSF is compared to the PSF obtained through backprojection with results showing close agreement. Following development of the fast PSF approximation, the definition of EMRA is developed. Simulation is performed for multiple emitter

configurations for bistatic and multistatic radar implementation in order to compare the results of fast approximation and backprojection based simulation. Results of this simulation show agreement between the approximation and backprojection. Contrast ratio is developed as an objective function for multistatic SAR and simulation is performed to compare with the approximation results. The results of this simulation show that approximation is useful for determining differences between sets of emitters for the purpose of selection.

A qualitative example using multiple objective optimization is presented. The previously defined objective functions are determined by approximation for a randomly selected set of emitters. The potential sets of emitters are ranked, and the resulting image from simulation based on backprojection is presented for different ranked sets to illustrate the effectiveness of the selection process. The selection approach shows the potential for significantly reducing the time required to choose a set of emitters over image simulation and comparison.

To my family

Acknowledgments

I would like to thank my advisor, Dr. Jackson, for her advice and guidance, and the Air Force Research Lab for funding my training at AFIT including this research.

Sean R. Stevens

Table of Contents

Bibliography . . . 188

List of Figures

List of Tables

List of Symbols

List of Abbreviations

Abbreviation		Page
SAR	Synthetic Aperture Radar	1
FM	Frequency Modulated Radio	2
PSF	Point Spread Function	3
EMRA	Effective Multistatic Resolution Area	3
DTCR	Distributed Target Contrast Ratio	3
PTCR	Point Target Contrast Ratio	3
MNR	Multiplicative Noise Ratio	4
ISLR	Integrated Sidelobe Ratio	4
AMBR	Ambiguity Ratio	4
SNR	Signal to Noise Ratio	4
ISL	integrated sidelobes	4
MAF	Multistatic Ambiguity Function	4
Tx	Transmitter	6
Rx	Receiever	6
RF	Radio Frequency	11
BP	Backprojection	13
CAT	Computer Aided Tomography	17
GLRT	Generalized Likelihood Ratio Test	20
CNR	Clutter to Noise Ratio	23
QNR	Quantization Noise Ratio	24
PRI	Pulse Repetition Interval	24
PRF	Pulse Repetition Frequency	24
LTE	Long Term Evolution	24
WiMAX	Worldwide Interoperability for Microwave Access	24

Metrics for Emitter Selection for Multistatic Synthetic Aperture Radar

1 Introduction

Synthetic aperture radar (SAR) is used to form images of the earth's surface from an aircraft. Traditionally this is done with a monostatic radar - an implementation in which both the transmitter and receiver are co-located and usually share one antenna [7, 20]. Another implementation of radar, the bistatic case, makes use of a transmitter and receiver which are separated by some distance. Recently, the extension of SAR to the bistatic case has received interest [14, 15, 31, 40, 43]. Passive bistatic SAR implementations use transmitters of opportunity for illumination with a non-collocated receiver. Foreknowledge of the emitter, including knowledge of the transmitted signal and emitter location, is required in order to perform image formation. These requirements encourage use of stationary ground based transmitters. Unfortunately, ground based radar systems such as air traffic control radars, tend to be focused on illumination of airborne targets. However, communications systems, such as broadcast television or cell phone towers, tend to be designed for primarily transmitting signals to receivers on the ground. The lack of radar specific waveforms means that passive radar systems may have poor performance in some respects [16, 17]. The performance may be improved by a multistatic implementation of radar, where multiple bistatic radar systems operate together [5, 9, 41, 43]. This thesis is focused on the problem of selecting between possible sets of emitters to use in the implementation of a passive multistatic SAR system.

1.1 Problem Description

The problem of waveform design for passive radar is the fundamental lack of control over nearly all parameters of the radar system. Any settings made are in response to some available waveform. Furthermore, the communications waveforms being used are not designed with consideration of radar performance. The different classes of communication system may provide poor performance by one criteria of waveform design, such as resolution, but have better performance with respect to another criteria. An interesting problem then is to clarify the selection criteria of a communication system for use as the illumination source for a SAR implementation. When a multistatic approach is used for image formation, the problem takes on the form of finding ways to use the strengths of the available communications transmissions to offset their weaknesses. A scene of interest may be illuminated by dozens of television stations, commercial frequency modulated (FM) radio stations, cell phone towers, and even wireless internet communications relays [12, 13]. However, the challenge comes from the limitations of a receiving system which can only collect a few of the available signals. The optimal subset of the available emitters to use may be a collection of the best available signals, or a combination of signals which may not be individually optimal, but which work best together. The problem this thesis seeks to answer is formulating a process to select a limited subset of the available signals which can be combined in a multistatic SAR system.

1.2 Motivation

The primary motive for this thesis is the need to determine a way to select part of a potentially large set of emitters in order to form a SAR image. Part of what makes this challenging is the limitation on how data from various emitters can be collected simultaneously. The collection platform is assumed to have limitations on how much of the spectrum can be collected from one receiver. Trying to address the variety and number

of emitters available might take the form of collecting across a broad frequency range. Doing so would require higher sampling rates to collect what may be mostly unimportant data. Alternatively, channelized systems could be used to collect all available signals. Doing so might require too much additional hardware for specific antenna beams, local oscillators, filters, and analog-to-digital converters. A better solution may be using a methodical approach to select a limited set of transmitters for use which would be best suited for the SAR application.

Currently, the planning phase of a SAR collection, especially for the purpose of exploring the implementation of passive multistatic SAR, has few tools to help make these decisions. Selection may be based on a few factors from a bistatic perspective, like individual emitter bandwidth and power. A selection process that takes the various emitters' multistatic combination into account may perform better. Furthermore, weighting these multistatic characteristics of the SAR system may provide a way to tailor the selection process for specific applications.

1.3 Contributions and Goals

There are three main contributions from this thesis to the field of passive multistatic SAR imaging:

- Development of a computationally efficient point spread function (PSF) approximation for bistatic and multistatic SAR
  - Used to estimate effective multistatic resolution area (EMRA)
  - Supports faster emitter selection
- Development of multistatic distributed target contrast ratio (DTCR) and point target contrast ratio (PTCR) by extending the monostatic definition provided in [7] involving

  - Development of bistatic multiplicative noise ratio (MNR) using the definition provided in [7]
  - Development of fast approximation of integrated sidelobe ratio (ISLR) contributing to MNR
  - Development of fast approximation of ambiguity ratio (AMBR) contributing to MNR

- Dynamic emitter selection procedure making use of multiple objective optimization
  - using multistatic signal to noise ratio (SNR), EMRA, DTCR/PTCR, and an integrated sidelobes (ISL) of the multistatic ambiguity function (MAF) based penalty
  - uses fast approximations of objective functions to speed up selection process
  - using possible limitations to rule out emitters and speed up the selection process, including minimum bistatic SNR, limited antenna beams, radar horizon, and bistatic angle

The main goal of this thesis is to describe a process for selecting a subset of potential transmitters for use in SAR image formation in a timely manner during off-line processing. Choosing a subset of emitters requires a framework for making the selection, and criteria used to judge the merit of potential selections. The framework needs to be straightforward for different SAR applications and potentially expandable to future work, which is why multiple objective optimization is selected. The criteria need to be relevant to the SAR image formation and also arguably accurate when extended to the multistatic case. The four selected for this thesis are objectives of good SNR, resolution, contrast ratio, and low ambiguity of the waveforms used. These will contribute to the selection process, but there are other practical concerns for this process.

Making sure the selection is appropriate and useful requires work on showing the criteria used in the selection process can be performed quicker than full simulation. Additionally they must be in line with the results of simulation. The desire to quickly make a selection is due to the potentially large set of combinations of transmitters. Faster selection would reduce overhead, potentially shorten the lead time to a data collection and support "real-time" selection of emitters. The goal of reconciling the quick selection to simulation verifies that the approach is at least as valid as the simulation used.

1.4 Organization

This introduction has focused on describing the problem being addressed and the goals for this research. It is followed by a chapter containing background information for the thesis. The background sets up three chapters concerning the computationally efficient PSF approximation and multistatic resolution, contrast ratio, and the dynamic emitter selection process respectively. Each of these chapters is organized as development, followed by a description of the setup used to verify the development against theory using simulation, and a presentation and discussion of the results. The final chapter is a conclusion and summary of the work done in this thesis.

2 Background

The information included in this chapter provides a foundation for the development of the selection process, the estimates for the objective functions' values and the SAR model used to check them. The first section is a brief overview of elliptic geometry to the extent it is useful in bistatic and multistatic radar. This information is included because in a two dimensional bistatic implementation of radar, the regions of constant range for these systems follow elliptical contours. The second section is a description of the signal processing needed to form images for a SAR system. Next is a short description of distributed and point target contrast ratio. Following this, a brief overview is given for each of four communications systems used for examples and in simulation. The background then focuses on the description of multiple objective waveform optimization that will serve as a framework which is generic enough to be useful to the selection process, granted the objective functions are available. Thus it is followed by description of two multistatic radar evaluation criteria developed in prior work, which are used as objective functions. Finally, background information on bistatic and multistatic resolution is given.

2.1 Elliptic Geometry

The equations for an ellipse from the perspective of the transmitter (Tx)-receiver (Rx) pair are important for bistatic radar. The distance to an object observed by the bistatic radar will be measured by the total range from the transmitter to the reflecting object, and back to the receiver. This observed total range places the object along an "isorange contour," where all points have the same total range. This isorange contour has the same definition as the ellipse, with the transmitter and receiver serving as the foci. Defining the isorange contours as ellipses has implications for the formulation for bistatic SAR and can be useful for estimating some of the SAR criteria.

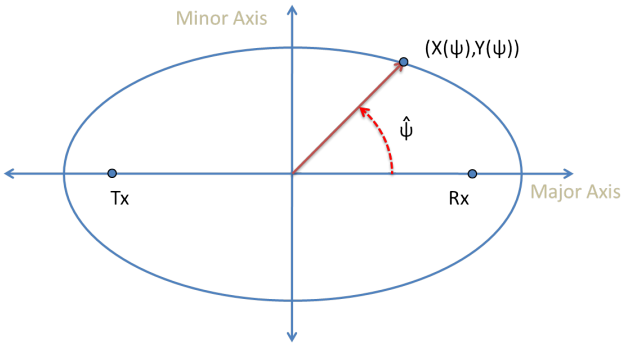

Figure 2.1: Illustration of $\hat{\psi}$

To start, the parametric equation of the ellipse can be expressed as [6, pp. 198-200]:

$$\begin{aligned} X(\psi) &= a\cos\psi \\ Y(\psi) &= b\sin\psi \end{aligned} \tag{2.1}$$

where a is the length from the center of the ellipse to the point at which the ellipse intersects the major axis (the line connecting the two foci), and b is the length from the center of the ellipse to the point where the ellipse intersects the minor axis (the line through the center of the ellipse perpendicular to the major axis), and ψ is a parametric variable ranging between 0 and 2π. In the case of a circle, where $a = b$, ψ corresponds to the angle to the point $(X(\psi), Y(\psi))$ from the major axis. However because $a \neq b$ in general for an ellipse, ψ is not always equal to the angle to the point from the major axis of the ellipse. The variable $\hat{\psi}$, the corrected angle, is the angle to the point $(X(\psi), Y(\psi))$ measured from the major axis and relative to the center of the ellipse as shown in Figure 2.1. Because this angle is generally more significant to other calculations, $\hat{\psi}$ is put in terms of the parametric ψ to a given point on the ellipse:

$$\begin{aligned} \hat{\psi} &= \arctan\left(\frac{b\sin\psi}{a\cos\psi}\right) \\ \hat{\psi} &= \arctan\left(\frac{b}{a}\tan\psi\right) \end{aligned} \tag{2.2}$$

and likewise ψ is found for the desired angle $\hat{\psi}$ as

$$\psi = \arctan\left(\frac{a}{b}\tan\hat{\psi}\right) \tag{2.3}$$

In a bistatic scenario, the foci of the ellipse are the Tx and Rx, and so the coordinate system used can be chosen such that the major axis corresponds to the x-axis, and the ellipse is centered at the origin. For a multistatic scenario, even if the coordinate system is chosen such that one pair of Tx and Rx correspond to the foci of an ellipse centered at the origin and with the major axis along the x-axis, all others will not. Thus, the center of the ellipse for other Tx-Rx pairs will be offset from the reference coordinate system's origin and are not likely to have a "baseline," the line connecting the transmitter and receiver, which is parallel with the x-axis. In order to adjust the equation of the ellipse to match the SAR scenario, the x and y coordinates of the ellipse must be rotated and translated as:

$$\begin{aligned} \begin{bmatrix} \hat{X}(\psi) \\ \hat{Y}(\psi) \end{bmatrix} &= \begin{bmatrix} X_c \\ Y_c \end{bmatrix} + \begin{bmatrix} X(\psi) \\ Y(\psi) \end{bmatrix} \begin{bmatrix} \cos\xi & \sin\xi \\ -\sin\xi & \cos\xi \end{bmatrix} \\ \hat{X}(\psi) &= X_c + a\cos\psi\cos\xi + b\sin\psi\sin\xi \\ \hat{Y}(\psi) &= Y_c - a\cos\psi\sin\xi + b\sin\psi\cos\xi \end{aligned} \tag{2.4}$$

where (X_c, Y_c) is the center of the ellipse located at the halfway point between the transmitter and receiver, and ξ is the angle between the scene's x-axis and the baseline as

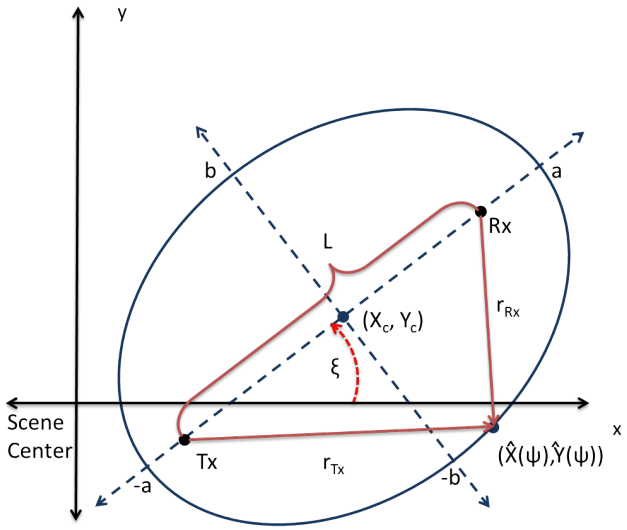

Figure 2.2: Rotated and shifted ellipse.

shown in Figure 2.2. In (2.4), a, b are

$$\begin{aligned} a &= \frac{r_{Tx} + r_{Rx}}{2} \\ b &= \sqrt{a^2\left(1 - e^2\right)} \end{aligned} \tag{2.5}$$

where b is related to the eccentricity of the ellipse,

$$e = \frac{L}{r_{Tx} + r_{Rx}} \tag{2.6}$$

by the distance, L, between the two foci, and the ranges r_{Tx} and r_{Rx} from the transmitter and receiver foci locations to the point $(\hat{X}(\psi), \hat{Y}(\psi))$ as shown in Figure 2.2.

The area of an ellipse becomes important when associating the extent of isorange contours with some width. Contour width is a consideration because a radar system has some resolution associated with it and so all measurements of total range are not infinity precise. The area of an ellipse is presented in [6] as $A = \pi ab$. The area for a segment of an

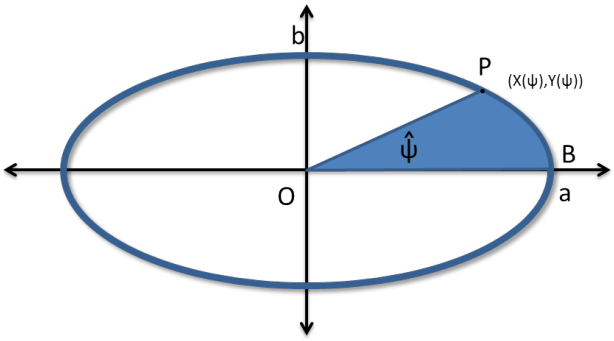

Figure 2.3: Segment of an ellipse as described in [6]

ellipse, shown as a shaded region in Figure 2.3, is presented as [6]

$$Area_{BOP} = \frac{ab}{2} \arccos\left(\frac{X(\psi)}{a}\right) \tag{2.7}$$

where $X(\psi)$ is as defined in 2.1 and so the area can be rewritten as

$$\begin{aligned} Area_{BOP} &= \frac{ab}{2} \arccos\left(\frac{a\cos\psi}{a}\right) \\ &= \frac{ab}{2} \arccos\left(\cos\psi\right) \\ &= \frac{ab}{2}\psi \\ &= \frac{ab}{2} \arctan\left(\frac{a}{b}\tan\hat{\psi}\right). \end{aligned} \tag{2.8}$$

Now the area is in terms of the angle between the major axis and the point on the ellipse, and so the area of a segment between two different angles can be found as

$$\begin{aligned} Area_{P_2OP_1} &= Area_{BOP_2} - Area_{BOP_1} \\ &= \frac{ab}{2}\left(\arctan\left(\frac{a}{b}\tan\hat{\psi}_2\right) - \arctan\left(\frac{a}{b}\tan\hat{\psi}_1\right)\right), \end{aligned} \tag{2.9}$$

assuming that $Area_{BOP_2} > Area_{BOP_1}$. The area of a segment will be used to represent regions of ambiguous returns in Chapters 4 when developing contrast ratios. Next, a brief description of synthetic aperture radar and the point spread function are given where the application of elliptical geometry should become apparent.

2.2 Synthetic Aperture Radar and the Point Spread Function

SAR is used to form images of a scene by measuring the reflection of radio frequency (RF) energy off of it. This is accomplished by carrying the SAR on an aircraft flying some distance away from the scene. By combining measurements taken from different positions the SAR can create synthetic elements of an aperture to improve its resolution. Measurements at each of these synthetic elements populate a "phase history" of the scene. This thesis focuses on the spotlight mode implementation of SAR, where the flightpath of the aircraft is along a circle centered around the scene of interest. A move-look-move model of SAR is assumed throughout, where the velocity of the receiver is assumed to be small relative to the speed of light, and thus the Doppler shift within a pulse for any given scatterer in the scene is assumed small enough to ignore.

There are many references which present the signal processing development of SAR image formation from transmission to reception, such as [20]. Others describe some of the more practical aspects of implementations, such as [7]. General digital image processing is found in [19] and in [27] a development is presented for spotlight mode SAR where the projection slice theorem is used for image formation for SAR. For the purposes of this thesis, a brief description of the basics of spotlight mode SAR based on [18–20, 27] should be sufficient to explain the approach to simulation and some of the development in the objective functions later in this chapter. Note that for the sake of generality the equations used in the following development do not assume that the transmitter is collocated with the receiver. These equations convert to the monostatic case by simply setting the positions of the Tx and Rx equal.

2.2.1 Basic Signal Processing Steps. In a broad sense of the SAR process, a signal, call it $s(t)$, is modulated from its baseband frequency to a higher frequency and transmitted. The signal then travels to, and is reflected off of a scene to be imaged, represented by reflectivity function $g(x, y, z)$. The reflected signal travels back to the receiver and is demodulated back to the baseband frequency. Thus the returned signal at the receiver is a combination of the various reflected copies of $s(t)$ with different delays and scaling due to the reflectors at different points in the scene. Assuming a small receiver velocity, relative to the speed of light, this combined return is equivalent to a convolution of $s(t)$ and $g(x, y, z)$ [20]. The delay time between transmission from point (x_{Tx}, y_{Tx}, z_{Tx}), reflection at point (x, y, z), and reception at point (x_{Rx}, y_{Rx}, z_{Rx}) is defined in terms of the spatial coordinates as [18]

$$\begin{aligned} \tau(x, y, z) &= \frac{\sqrt{(x_{Tx} - x)^2 + (y_{Tx} - y)^2 + (z_{Tx} - z)^2}}{c} + \\ &\quad \frac{\sqrt{(x_{Rx} - x)^2 + (y_{Rx} - y)^2 + (z_{Rx} - z)^2}}{c}, \end{aligned} \tag{2.10}$$

where c is the speed of light. The transmitted signal is put in terms of τ_0, the delay from the transmitter to the scene center at point $(0, 0, 0)$, as $s(t - \tau_0)$. The scene reflectivity function is put in terms of the delay as $g(t - \tau(x, y, z))$. All returns at the same range, r, will add together at the receiver, and thus the received signal at a given time t is the combination of returns from all angles ψ along an isorange contour as shown in Figure 2.4 given by

$$r(t) = \int_0^{2\pi} s(t - \tau_0) * g(t - \tau(x, y, z)) d\psi. \tag{2.11}$$

where $*$ is the convolution operator [18]. The scene reflectivity function can be recovered by deconvolution of the transmitted waveform from the received signal. The matched-filter is one method for recovering an estimate of the scene reflectivity function.

The matched-filter may be implemented via correlation of the received, demodulated return with the original signal. For some implementations of passive systems, which would not have access to the original signal, a recreation could also be used for matched-filtering. The result of matched filtering is recovery of a one dimensional Fourier transform of the scene, $P(k, \phi)$, in terms of spatial frequency, k, and the collection angle, ϕ, from the received processed signal [20]. The spatial frequency in the bistatic case with a small bistatic bisector, β, is shown in [15] (eq 4.2.6) to be

$$k = \frac{4\pi f}{c} \cos\left(\frac{\beta}{2}\right) \tag{2.12}$$

2.2.2 Backprojection. The basic premise of backprojection (BP) is that a two dimensional image of a scene or object can be formed by processing many one dimensional projections taken from different look angles. The application of this idea is formed around the Projection-Slice Theorem, which states that the Fourier transform of the projection of the scene reflectivity function at an angle ϕ is a slice of the two dimensional Fourier transform of the scene reflectivity function, $G(k_X, k_Y)$ taken at the

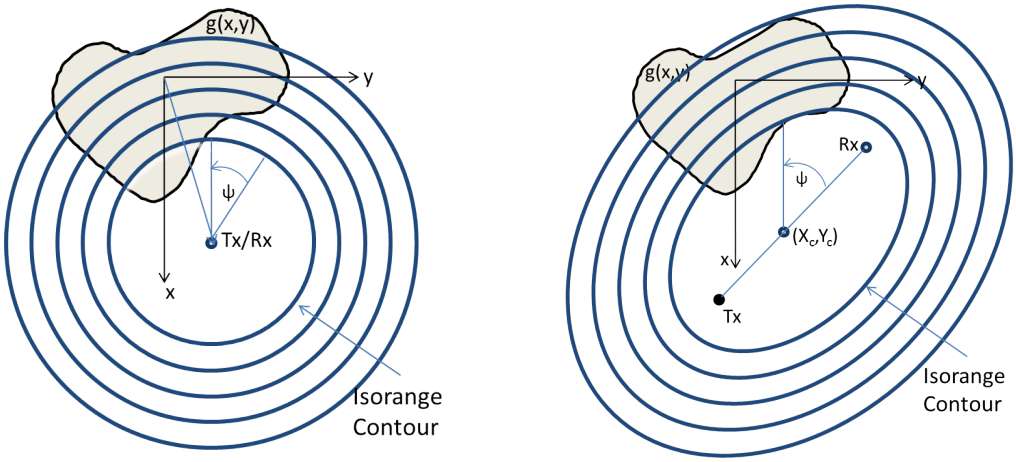

(a) Monostatic (b) Bistatic

Figure 2.4: Depiction of constant range contours [18]

angle ϕ [27]. A collected signal can thus be put in terms of spatial frequency, with spatial frequency in the x direction k_X and spatial frequency in the y direction k_Y, as shown in Figure 2.5. From this, if the one dimensional Fourier transform of the scene is put in terms of the angle along which it is collected, that is $P(k, \phi)$, it can be expressed as

$$\begin{aligned} P(k,\phi) &= G(k_X \cos\phi, k_Y \sin\phi) \\ &= \mathcal{F}\left(\int_{x=-\infty}^{x=\infty}\int_{y=-\infty}^{y=\infty} g(x,y)\delta(x(\phi)-y(\phi))dxdy\right), \end{aligned} \tag{2.13}$$

where the δ function operator (equal to one when its argument is zero, and zero when the argument is not) is used to limit the evaluation to a line. The accumulation of these measurements is known as the phase history. The formation of projections from a function by taking line integrals is called a Radon transform, $\mathcal{R}$ [19]. For SAR applications the line integral is taken over isorange contours, so the phase history may be more accurately expressed in terms of the delay to a point in the scene reflectivity function. If the scene

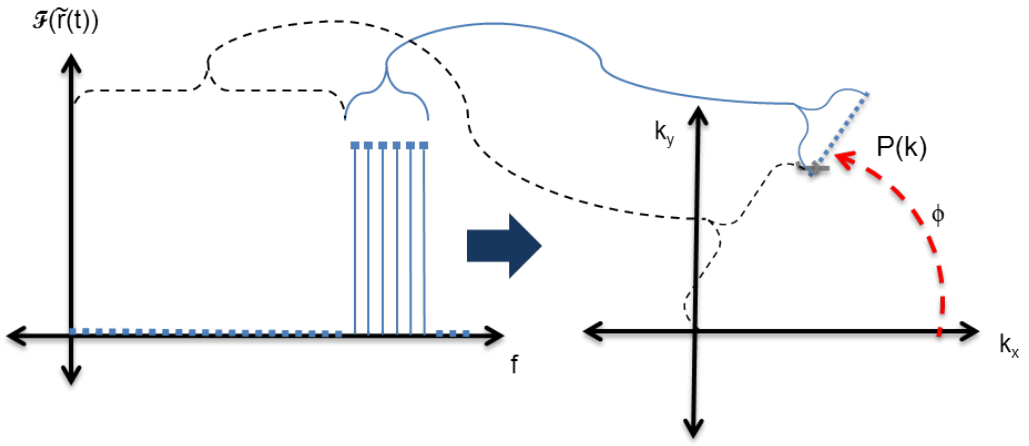

Figure 2.5: Signal frequency support effect on spatial frequency.

reflectivity function is treated as a set of isotropic point scatterers indexed by m,

$$g(x,y) = \sum_{m=0}^{\infty} A_m \delta(x - x_m)\delta(y - y_m), \tag{2.14}$$

the phase history can be expressed as an accumulation of the effect of all the points in the scene as

$$\begin{aligned} P(k,\phi) &= \mathcal{F}\left(\sum_{m=0}^{\infty} A_m \delta(t - (\tau_0 - \tau_m))\right) \\ &= \sum_{m=0}^{\infty} A_m e^{j\Delta\tau(m,\phi)2\pi f} \end{aligned} \tag{2.15}$$

where τ_m is the total delay from Tx to the mth point to Rx. Note that the shift due to the delay results in $\Delta\tau(m,\phi)$, the differential delay to point m from the receiver at collection angle ϕ. The differential delay is the difference between the round trip delay from Tx to the scene center to Rx, and the round trip delay from Tx to the point m to Rx. It is convenient at this point to express the phase history in terms of an index, n, corresponding to discrete collection points, so that the angle is given as ϕ_n. Also, phase history would be more appropriately expressed in terms of k, rather than f. So (2.12) is substituted into (2.15), and the differential delay multiplied by the speed of light is converted to a differential range,

$$\Delta R(m,\phi_n) = c\Delta\tau(m,\phi_n) \tag{2.16}$$

to give

$$P(k,\phi_n) = \sum_{m=0}^{\infty} A_m e^{\frac{j\Delta R(m,\phi_n)k}{2\cos(\beta/2)}} \tag{2.17}$$

The differential range to point m located at (x, y, z) can be found in the near field case, used when the isorange contours are expected to be less linear with respect to the scene being imaged, as

$$\Delta R(n, x, y, z) = R(n, x, y, z) - R_{SAR}(n) \tag{2.18}$$

where $R(n, x, y, z)$ is the total bistatic range to a point:

$$\begin{aligned} R(n, x, y, z) &= \sqrt{(x_{Tx}(n) - x)^2 + (y_{Tx}(n) - y)^2 + (z_{Tx}(n) - z)^2} + \\ &\quad \sqrt{(x_{Rx}(n) - x)^2 + (y_{Rx}(n) - y)^2 + (z_{Rx}(n) - z)^2}, \end{aligned} \tag{2.19}$$

and $R_{SAR}(n)$ is the total range to the scene center:

$$\begin{aligned} R_{SAR}(n) &= \sqrt{x_{Tx}(n)^2 + y_{Tx}(n)^2 + z_{Tx}(n)^2} + \\ &\quad \sqrt{x_{Rx}(n)^2 + y_{Rx}(n)^2 + z_{Rx}(n)^2}. \end{aligned} \tag{2.20}$$

In the far field case, which is valid when the isorange contour is expected to be nearly linear relative to the scene, the differential range is given as [40]

$$\begin{aligned} \Delta R(n, x, y, z) &= x(\cos(\theta_{Tx}(n))\cos(\phi_{Tx}(n)) + \cos(\theta_{Rx}(n))\cos(\phi_{Rx}(n))) + \\ &\quad y(\cos(\theta_{Tx}(n))\sin(\phi_{Tx}(n)) + \cos(\theta_{Rx}(n))\sin(\phi_{Rx}(n))) + \\ &\quad z(\sin(\theta_{Tx}(n)) + \sin(\theta_{Rx}(n))), \end{aligned} \tag{2.21}$$

where for the n^{th} collection, $\theta_{Tx}(n)$ is the elevation from the scene center to the transmitter, $\theta_{Rx}(n)$ is the elevation from the scene center to the receiver, $\phi_{Tx}(n)$ is the azimuth from the x-axis to the transmitter, and $\phi_{Rx}(n)$ is the angle from the x-axis to the receiver.

The explanation of phase history gives a convenient way to generate $P(k, \phi_n)$ during simulation, however the task of recovering an image of the scene remains. Now backprojection enters into the image recovery process. Backprojection maps a set of projections, which are generally in terms of angle and distance from the origin, into spatial coordinates as [19]

$$b(x, y) = \int_0^{\pi} \hat{g}(x\cos(\phi) + y\sin(\phi), \phi) d\phi \tag{2.22}$$

where $\hat{g}(u, \phi) = \mathcal{R}g(x, y)$. Backprojection of a pixel ideally requires projections from all directions. However, an estimate of a pixel value can be formed from limited information and in [27] it was shown that backprojection, as used in computer aided tomography (CAT) could be extended to spotlight mode SAR. Recalling from (2.15) that a collection point in phase history corresponds to the Fourier transform of such a projection, the estimate of the scene formed through backprojection would be:

$$\tilde{g} = \int_0^{2\pi} \mathcal{F}^{-1}\left(P(k, \phi)\right) d\phi \tag{2.23}$$

Due to practical implementation, a SAR image is sampled from a finite number,N_p, of discrete positions indexed by n. So the estimate of the scene is given by

$$\tilde{g} \approx \sum_{n=0}^{N_p} \mathcal{F}^{-1}\left(P(k, \phi_n)\right) \tag{2.24}$$

The phase history is filtered by multiplying by the corresponding frequency to account for the different patch sizes essentially created by sampling on a polar coordinate system, as shown in Figure 2.6. This means that (2.23) can be rewritten using the phase history as

$$\tilde{\tilde{g}} = \sum_{n}^{N_p} \mathcal{F}^{-1}\left(|f(k)|P(k, n)\right). \tag{2.25}$$

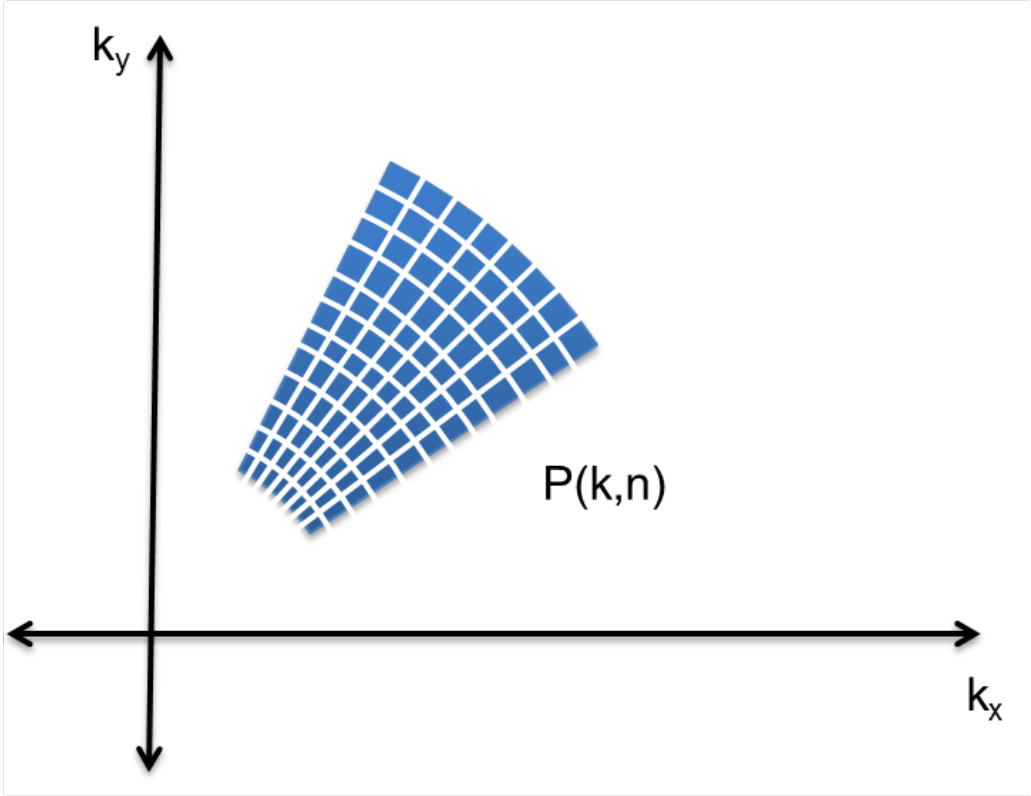

Figure 2.6: Phase history

expressing the result of the inverse Fourier transform in (2.25) as

$$\hat{p}(\Delta\tau, \phi_n) = \mathcal{F}^{-1}\left(|f(k)|P(k, \phi_n)\right), \tag{2.26}$$

then (2.25) becomes:

$$\tilde{\tilde{g}}(x, y, z) = \sum_{n}^{N_p} \hat{p}(\Delta\tau(n, x, y, z), \phi_n) \tag{2.27}$$

The development of $\tilde{\tilde{g}}(x, y, z)$ gives a convenient way to recover an estimate of the scene reflectivity function from the phase history for a bistatic or monostatic system. The estimate of $g(x, y, z)$ for the multistatic system requires some additional assumptions.

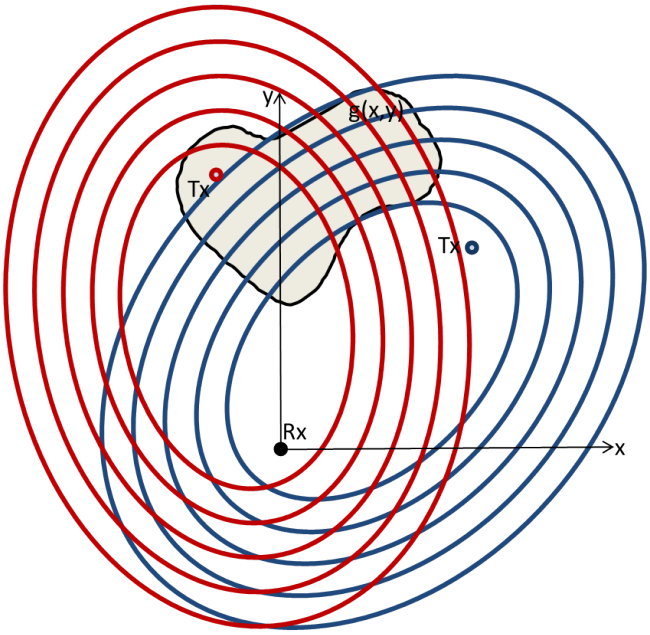

Figure 2.7: Depiction of constant range contours for Radon transform "projections" in the case of multi-static SAR with two transmitters and one receiver. Color denotes constant range contours for each bistatic pair [18].

2.2.3 Multistatic Radar. A multi-static radar scenario, as shown in Figure 2.7, will have multiple transmitter and receiver pairs. One assumption made for working with multistatic radar is that the signals used will be separable: they are assumed to be orthogonal. Starting from this assumption, the received signal is extended from (2.11) by superposition to be the sum of the individual transmitted, reflected signals:

$$r(t) = \sum_{i=0}^{N_T} \int_0^{2\pi} f(t - \tau_{i,0}) * g(t - \tau_i(x, y, z))d\psi. \tag{2.28}$$

where N_T transmitters are indexed by i. Because (2.28) is a linear operation, it can be accomplished by using the bistatic SAR development and summing the image formation results from multiple Tx-Rx pairs. For a given point (x,y), the projections corresponding to the appropriate constant range contours from the various bistatic pairs will be summed

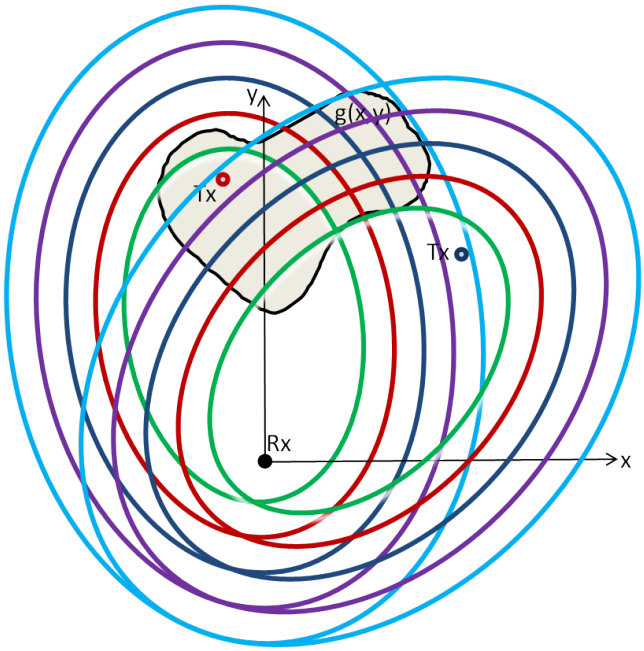

Figure 2.8: Depiction of constant range contours for Radon transform "projections" in the case of multi-static SAR with two transmitters and one receiver. Colors denote constant range. That is, all reflections from points along a single color will be collected at the same time at the receiver [18].

to give the return from that point. Thus the added projections have the form of an intersection of ellipses, as shown in Figure 2.8.

Alternatively, the combination of SAR images from different Tx-Rx pairs can be viewed as similar to the use of sub-apertures within a flight path. For monostatic radar, these sub-apertures are combined by a generalized likelihood ratio test (GLRT) [39]. The GLRT approach compares the separately formed images pixel by pixel, and the largest pixel value is taken for use in the combined image. GLRT multistatic image formation precludes the impact of phase information since the separate images are not being added, and the pixel values are the absolute value of the backprojection process output.

2.2.4 Point Spread Function. A common measure of the SAR system's quality is the point spread function. The PSF is similar to an impulse response in that it is the image

the SAR would create if a single isotropic point scatterer was located at the scene center [37]. Measuring the extent of the PSF's mainlobe, at a -3dB drop from the peak, provides one way to to determine the resolution in SAR systems. The PSF is also useful for calculating the integrated sidelobe level, which is used to calculated the MNR as shown in Section 4.1.

2.2.5 Related Research. The theoretical background for the SAR simulation was presented without going into much detail about how it would be feasibly implemented for a passive bistatic SAR. However, the approach to simulation used is partially supported by [31], where experimentation is performed with OFDM waveforms based on the WiMAX standard. The results of these experiments help validate the use of simulated phase history and the filtered backprojection approach to forming images which is similar to the approach used in this thesis. In [31], the image formation was carried out using a bistatic radar, scaled down to fit on a table top and used to collect reflected signals off of metal plates. The results of this imaging showed that images formed from the collected phase history were consistent with the simulated phase history.

Another assumption made for simulation is that there will be coherence between the transmitter and receiver. It is assumed that it is possible to use the synchronization symbols and knowledge of the transmitter and receiver locations to maintain coherence. In [14] the results of experimentation using an X-band airborne radar with a monostatic and bistatic component includes demonstrated maintenance of synchronization of a bistatic receiver located on the ground. Thus the possibility of maintaining coherence seems plausible, though not trivial.

2.3 Point and Distributed Target Contrast Ratio

A useful measure of a SAR's ability to distinguish targets is contrast ratio. Contrast ratio is important when attempting to determine the presence of some feature within an

area or background which may not have a substantially different backscatter coefficient. In [23], mention is made of using contrast ratio as a image quality metric; however, a clearer explanation is found in [7]. In [7], two types are specified, point target contrast ratio (PTCR) and distributed target contrast ratio (DTCR). PTCR is useful for determining the visibility of a point target in clutter and noise. DTCR is useful when attempting to detect a change in the local clutter from one level to another within a larger scene. In both cases the ratio is presented as the expected value of the signal return to the expected background, including clutter and noise.

For monostatic radar, PTCR is presented by [7] as

$$\text{PTCR} = \frac{\frac{\sigma_t \cos(\psi_{ac})}{\rho_a \rho_r} + \sigma_n + \text{MNR}\bar{\sigma}_0}{\sigma_0 + \sigma_n + \text{MNR}\bar{\sigma}_0} \tag{2.29}$$

where σ_t, σ_n, σ_0, $\bar{\sigma}_0$, are the backscatter coefficients of the point target, additive noise, local clutter near the point, and clutter from ambiguous regions outside the scene respectively; ρ_a and ρ_r are the crossrange and downrange resolutions; ψ_{ac} is the grazing angle and MNR is the multiplicative noise ratio. DTCR is presented as [7]

$$\text{DTCR} = \frac{\sigma_{0h} + \sigma_n + \text{MNR}\bar{\sigma}_0}{\sigma_{0l} + \sigma_n + \text{MNR}\bar{\sigma}_0} \tag{2.30}$$

where σ_{0l} is the lower level backscatter coefficient and σ_{0h} is the higher level backscatter coefficient. As an illustration of the DTCR concept, [7] gives an example of an asphalt road with σ_{0l} of -26 dB, running through a grassy area with σ_{0h} of -13 dB surrounded by an area with rough ground, farm buildings and trees with a $\bar{\sigma}_0$ of -10 dB.

2.3.1 Additive Noise Backscatter Coefficient. Additive noise in the preceding equations is actually an effective backscatter coefficient representing the additive noise

figure. This term is related to the common clutter to noise ratio (CNR) by

$$\sigma_n = \frac{\sigma_0}{CNR}. \tag{2.31}$$

The average clutter backscatter coefficient will be canceled out by the CNR which is simply recalculating the SNR, as presented in Section 2.6.1, with the radar cross section replaced by the clutter backscatter coefficient [3]. This means that the effective noise reflectivity is found from the SNR to be [41]

$$\sigma_n = \frac{(4\pi)^3 k_b T_S B_n (R_T R_R)^2_{max} L_T L_R}{P_T G_T G_R \lambda^2 F_T^2 F_R^2} \tag{2.32}$$

where R_T and R_R are the Tx to target and Rx to target ranges, P_T is the transmitter power output, G_T and G_R are the Tx and Rx antenna gain, F_T and F_R are the attenuation pattern propagation factors for Tx to target and Rx to target paths, k_b is Boltzmann's constant (not to be confused with spatial frequency), T_S is the Rx system noise temperature, B_n is the noise bandwidth of the Rx filter, sufficient to pass the spectrum of the Tx signal, and finaly L_T and L_R are the Tx and Rx system losses.

2.3.2 Multiplicative Noise Ratio. MNR is the ratio of the power within a resolution cell from the radar scatterers within that cell to power which is aliased into that cell from other external scatterers or from sources within the SAR [21]. The usage here is different from another related use of the term, such as in [10], which describes radar fading which results in speckle [21]. Though MNR is generally found through empirical analysis of a given radar system [37], an approximation for MNR is deemed to be sufficient for comparison and is found using the components listed in [7]:

$$\text{MNR} = \text{ISLR} + \text{QNR} + \text{AMBR}. \tag{2.33}$$

The integrated side lobe ratio (ISLR) is defined by [7] as the ratio of energy in the sidelobes of the system impulse response to energy in the mainlobe, where the division between these areas is considered to be the first null. In the formation of the MNR, ISLR represents the combined effect of all scatterers outside of a given pixel, excluding scatterers which fold into the pixel due to ambiguity.

The quantization noise ratio (QNR) reflects primarily analog to digital conversion quantization errors. It is modeled as white Gaussian noise and in general is assumed to be about -5dB per bit [7]. Compared to other sources of error, this error is relatively small for modern analog to digital converters which may have 8 or 12 bits. Because of this, and because the QNR value would be the same regardless of the scenario, it is not included in the determination of the MNR for this application.

The ambiguity ratio (AMBR) includes the range and azimuth ambiguities due to the pulse repetition interval (PRI)/pulse repetition frequency (PRF) and antenna sidelobes which fold into a given measurement.

2.4 Communication Standards

Four different communications standards are selected to serve as example possible transmitter types in this research. The standards are the long term evolution (LTE) cellular communications standard, the worldwide interoperability for microwave access (WiMAX) wireless internet access standard, the US high definition television (HDTV) standard, and analog frequency modulated (FM) radio. LTE and WiMAX represent two-way communication, while HDTV and FM radio represent broadcast communications. An important distinction between signal types is the way in which the message of each is modulated. LTE and WiMAX are orthogonal frequency division multiplexing (OFDM) signals, which are common for digital communication. HDTV is an eight symbol vestigial side band (8-VSB) modulated signal, which is not as common, but in some ways closer resembles a traditional radar waveform. Finally, though digital FM radio is starting to

become more popular, the version being investigated here is the classic analog signal. The transmit signal types are limited to a set of four for the sake of brevity, though this work may be extended to additional signal types. In Sections 2.4.1-2.4.4, the different communications standards are described in enough detail to understand the implementation for simulation used in the multiple objective waveform optimization section.

There has been a fair amount of research lately into the use of different communications standards for passive covert/coherent/bistatic radar. The communications standards selected for examples were based in part on similar work which had shown some experimental basis for using WiMAX, TV, and FM radio for passive radar. In [15], use of OFDM was examined for use as the waveform for SAR, with particular attention paid to WiMAX. The approach in [15] used simulation and experimental generation of a representative message with focus on using the preamble of the downlink for matched filtering. This was analyzed through the bistatic ambiguity function and also in experimental SAR image formation. In [16] non-cooperative television transmitters were used for the transmitter portion of a bistatic radar system. Airborne targets were tracked at ranges of 260 km from the receiver and 150 km from the transmitter. The processing focused on using measurements of bearing through direction of arrival (DOA) and velocity through Doppler shift. The signal used was the vision carrier of a non-digital television signal. The use of Doppler shift removes the necessity of synchronizing with the television transmitter as long as the carrier frequency is stable. In [17] experiments with non-cooperative FM transmitters were used to track airborne targets up to 150 km from the receiver. The approach performed matched filtering by correlation of a received reflection, and a direct path collection of the transmission from a dedicated reference antenna.

2.4.1 High Definition Television. HDTV provides a broadcast to an area, using a high output power and one-way communication. A good overview of US HDTV can be

found in [33], however [2] provides more current technical details of the implementation. Unlike many modern digital television standards, US HD television uses 8-VSB instead of OFDM modulation. 8-VSB is a type of amplitude modulation using 8 “symbols”, also called levels, that form the representation of the data to be transmitted. One symbol represents some digital value, and thus in this case can represent three bits of audio/video data. These symbols are allowed to take on the values -7,-5,-3,-1,1,3,5 and 7, where the corresponding amplitude of these levels is not specified, though the final transmission power is determined by the Federal Communications Commission (FCC). A pilot tone, an always present spectral component at DC, is added to the signal by increasing all of these levels by 1.25. Symbols are transmitted at a rate of 10.762 MHz [2], and an accumulation of 832 symbols is called a “segment”. Thus, the transmitted signal can be modeled as

$$s_{HDTV} = A\left(\sum_{n=0}^{832} d_n rect(t - nT) + 1.25\right) \tag{2.34}$$

where A is the amplification prior to broadcasting, d_n is symbol n’s amplitude and T is the symbol period, the reciprocal of the symbol rate. Each segment has a specific format wherein the first four symbols form the synchronization component, d_0 to d_3, follow a [5, -5, -5, 5] pattern. The rest of the frame contains the audio and video data which is randomized, encoded using Reed-Solomon coding for forward error correction, one-sixth-data-field interleaving and two-thirds-rate trellis coded modulation [2]. Because the rest of this information is not specified a-priori, and the randomization and encoding are not applied to the synchronization symbols, the synchronization symbols are assumed to be the portion of the signal which will be usable for SAR without collecting a reference signal, or decoding and reconstructing the signal. The segments, and thus the synchronization symbols, repeat at a rate of 77.3 μs.

A broadcaster is allocated a 6 MHz channel [2] and in order to make maximum use of the available bandwidth, a filter is used to remove the lower side-band of the modulated

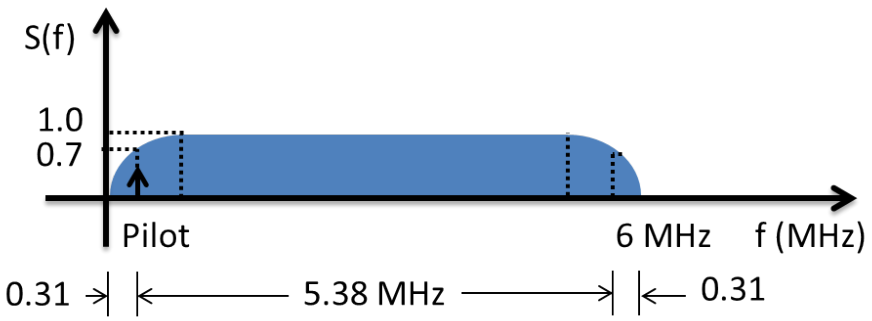

Figure 2.9: US HDTV channel occupancy described in [2]

signal. First, $s_{HDTV}(t)$ is converted to an intermediate frequency, then filtered with a specified roll off allowing some of the lower side band to remain, hence the name vestigial side band. This is accomplished by filtering the signal with a root raised cosine filter, which removes all but .31 MHz of bandwidth at IF which falls below the pilot [2] as shown in Figure 2.9. The root raised cosine filter can be defined as the square root of a raised cosine filter described in [36] as:

$$H_{RC}(\omega) = \begin{cases} T, & 0 \le |\omega| \le (1-\alpha)W \\ 0, & |\omega| > (1+\alpha)W \\ \frac{T}{2}\left\{1 - \sin\left[\frac{\pi}{2\alpha W}\left(|\omega| - W\right)\right]\right\}, & \text{else} \end{cases} \tag{2.35}$$

where W = π/T, and the roll off factor α = 0.1152 [2]. Thus, the transmitted signal spectrum is

$$\tilde{S}_{HDTV}(\omega) = \left[\frac{1}{2}S_{HDTV}(\omega - \omega_{IF}) + \frac{1}{2}S_{HDTV}(\omega + \omega_{IF})\right] H_{RRC}(\omega) \tag{2.36}$$

where $S_{HDTV}(\omega)$ is the Fourier transform of $s_{HDTV}(t)$ mixed up to an intermediate frequency, and $H_{RRC}(\omega)$ is the root raised cosine filter. The signal is then modulated up to the carrier frequency and amplified. When the transmitted signal is received, it is mixed to

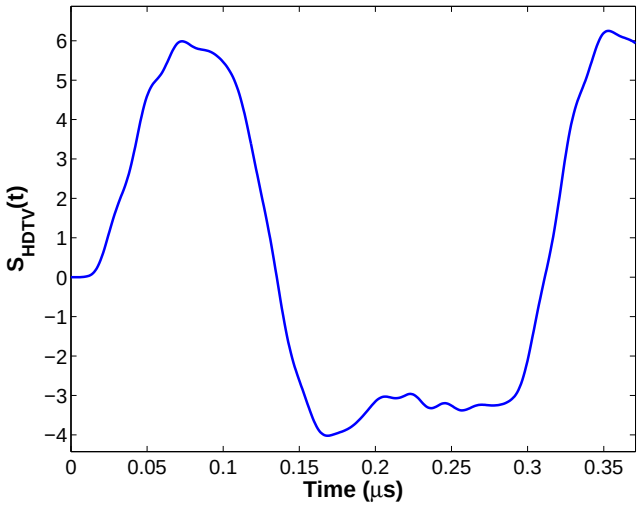

Figure 2.10: Non-zero portion of simulated HDTV sync signal in amplitude versus time

baseband such that the original signal is reproduced. The HDTV synchronization signal used was generated by creating the four synchronization symbols [5,-5,-5,5], mixing the signal to an intermediate frequency, filtering using a root raised cosine filter to reduce the bandwidth to 6 MHz. To simulate the received signal, the signal was then mixed down to baseband, and finally filtered to remove the high frequency component. The resulting signal is shown in Figure 2.10 for the synchronization portion of the signal to show the waveform at baseband.

2.4.2 Long Term Evolution (LTE). LTE is a cellular standard which allows for the transfer of large amounts of data. The term long term evolution describes the development of the Universal Terrestrial Radio Access (UTRA) standard into a new standard, known as Evolved-UTRA (E-UTRA). Since this signal will be part of a cell network, there will be downlink as well as uplink activity, distributed over several base stations in a given area. The signal makes use of OFDM to modulate symbols onto non-interfering sub-carriers spaced 15 kHz apart, with each sub-carrier modulated as either binary phase shift keying (BPSK), quadrature phase shift keying (QPSK), 16-ary quadrature amplitude modulation

(QAM), or 64-ary QAM [1]. The modulated sub-carriers are then converted into a time based signal by means of an inverse fast Fourier transform (IFFT). The set of symbols is organized into a "frame" which contains not only structure in terms of timing as was the case for the "segments" used in HDTV, but also in terms of spectral occupancy [1]. Because most aspects of the signal can be dynamically determined, the signal of interest for radar application is the primary synchronization (P-SCH) signal that is used to synchronize the mobile user equipment during downlink. There are three P-SCH signals, assigned to a given cell in order to avoid duplicating the signal of a neighboring cell [29]. The P-SCH signal is defined by the coefficients that are modulated onto 62 sub-carriers around the central or DC sub-carrier. These coefficients are a Zadoff-Chu sequence described by [29]:

$$d_u(m) = \begin{cases} \exp\left(-j\frac{\pi um(m+1)}{63}\right) & m = 0,1,...,30 \\ \exp\left(-j\frac{\pi u(m+1)(m+2)}{63}\right) & m = 31,32,...,61 \end{cases} \tag{2.37}$$

where m is mapped according to (2.37) onto sub-carriers -31 to 31, excluding the DC sub-carrier, with a guard band of five sub-carriers on either side of this sequence. Thus the modulation of the subcarriers, in terms of the subcarrier index, n, is

$$d_n = \begin{cases} 0 & n = -36,-35,..., -32 \\ d_u(n+31) & n = -31,-30,..., -1 \\ 0 & n = 0 \\ d_u(n+31) & n = 1, 2, ..., 31 \\ 0 & n = 32,33,...,36 \end{cases} \tag{2.38}$$

The variable u is either 25, 29, or 34 and defines the P-SCH signal [29]. The P-SCH symbols are transmitted twice during every 10 ms frame, with the signals placed 5 ms

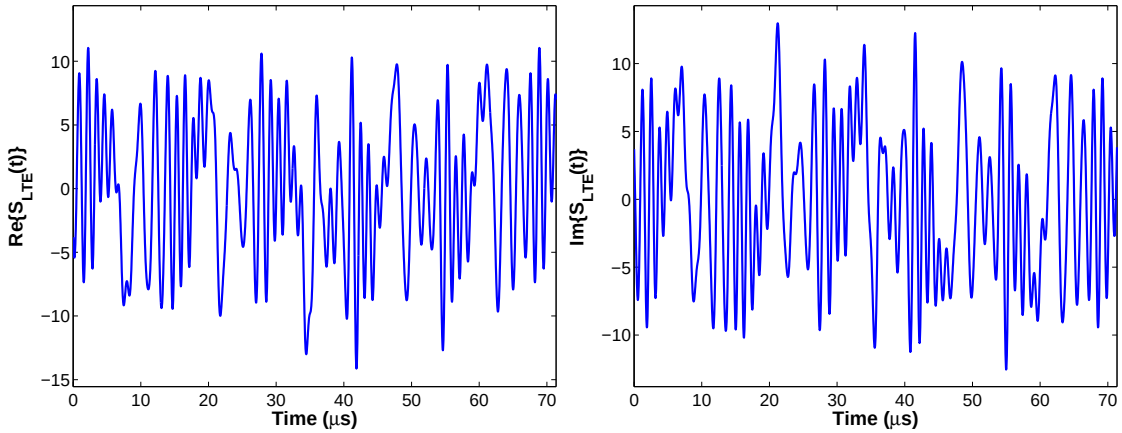

(a) Real component (b) Imaginary component

Figure 2.11: Non-zero portion of simulated LTE sync signal amplitude vs. time

apart [1]. Using the OFDM transmitted signal model:

$$s_{LTE}(t) = e^{j2\pi f_c t} \sum_{n=-N/2}^{N/2} d_n e^{jn2\pi\Delta f t} \quad 0 \leq t < T_s \tag{2.39}$$

where f_c is the carrier frequency, Δf is the subcarrier spacing, and T_s is the duration of the signal. Excluding a cyclic prefix $T_s = 1/15000$ seconds. When a cyclic prefix is used T_s becomes $(N_{CP}/N + 1)$ times longer. For a normal cyclic prefix $N = 2048$ and $N_{CP} = 144$, so $T_s = (144/2048 + 1)/15000$ seconds [1]. The signal is usually constructed at baseband, and then modulated to the carrier frequency. The LTE synchronization signal used was generated at baseband for $u = 25$, and the non-zero portion of the signal is shown in Figure 2.11.

2.4.3 Worldwide Interoperability for Microwave Access (WiMAX). The Worldwide Interoperability for Microwave Access (WiMAX) is a wireless network standard used for providing Internet access within a few miles of the base station [15]. Like LTE, this communication makes use of OFDM modulation. Three physical layer (PHY) configurations are specified in [24]: single carrier, 256-point OFDM for fixed

stations and orthogonal frequency division multiplex access (OFDMA) with up to 2048 subcarriers for mobile subscribers. WiMAX also has two different types of frame structures: frequency division duplexing (FDD), where uplink and downlink channels use different frequencies, and time division duplexing (TDD) where the uplink and downlink channels share a frequency but are separated in time so that they do not overlap [24]. In [15], WiMAX was investigated for use as a radar waveform assuming 256-point OFDM configuration with a TDD frame structure, in a 2 - 11 GHz frequency band, and so that configuration is used for this thesis.

For the purpose of SAR, the features of the waveform which are known a priori are of particular interest. A first assumption for radar application is that the downlink will be more powerful and possibly more predictable than the uplink, and so only the downlink is being investigated. The duration of the frame, including the uplink and downlink sub-frames, will be determined by the base station and should not be changed; otherwise all the subscriber stations (receivers) would have to resynchronize to the base station [24]. Therefore the frame length is assumed to determine a consistent PRI for the signal when using it for radar applications. The set of possible frame durations are: 2.5, 4, 5, 8, 10, 12.5, and 20 ms [24].

Furthermore, the frame structure has within the downlink subframe a portion called the preamble which is used for synchronization and equalization as shown in Figure 2.12. There are two different symbols used for the OFDM PHY preamble. The first uses only subcarriers which are multiples of 4, resulting in a time domain waveform which repeats every 64 samples. This symbol can be written as [24]

$$P_1 = \begin{cases} \sqrt{2}\,\sqrt{2}P^*_{ALL}(k) & k_{mod4} = 0 \\ 0 & k_{mod4} \neq 0 \end{cases} \tag{2.40}$$

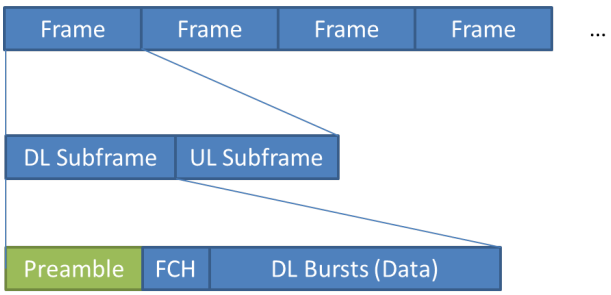

Figure 2.12: Example of TDD frame structure as described in [24]

where P^* denotes the complex conjugate of P, and the double square roots here are an explicit statement of the root mean square power associated with the data section and a 3dB boost for the preamble. P_{ALL} is a sequence provided in the standard [24] as shown in Table 2.1.

The second preamble symbol uses only even subcarriers, resulting in a time domain waveform which repeats every 128 samples and is given by [24]:

$$P_2 = \begin{cases} \sqrt{2}P_{ALL}(k) & k_{mod2} = 0 \\ 0 & k_{mod2} \neq 0 \end{cases} \tag{2.41}$$

Though there are other preamble configurations for space time encoding regions and adaptive antenna systems, they are not considered here. The two preamble symbols are run consecutively at the start of every downlink frame and each has a cyclic prefix (CP) [24] . The CP is a segment of the symbol in the time domain copied from the end of the symbol and appended to the start of that symbol as shown in Figure 2.13. The length, G, of this segment is either 1/4, 1/8, 1/16, or 1/32 of the symbol duration [24]. In [15] the CP was investigated for the effect it would have on matched filtering. If not taken into account, this could change the estimation of the range of a return; however it is assumed from now on that the CP will be known. Each symbol in the OFDM PHY has a duration determined by the desired bandwidth of the WiMAX signal. The total symbol duration is

Table 2.1: Table of P_{ALL} values as listed in [24]

P_{ALL} -100:-80	P_{ALL} -79:-59	P_{ALL} -58:-38	P_{ALL} -37:-17	P_{ALL} -16:4	P_{ALL} 5:25	P_{ALL} 26:46	P_{ALL} 47:67	P_{ALL} 68:88	P_{ALL} 89:100
1-1j	1-1j	-1-1j	-1+1j	-1-1j	-1-1j	1-1j	1-1j	-1+1j	1-1j
1-1j	-1-1j	1+1j	1+1j	-1-1j	1+1j	1-1j	1-1j	1-1j	-1+1j
-1-1j	1+1j	1-1j	1+1j	1+1j	1+1j	-1-1j	-1+1j	1+1j	1+1j
1+1j	1-1j	1-1j	-1-1j	-1-1j	1+1j	1+1j	-1-1j	1-1j	1+1j
1-1j	1-1j	-1+1j	1+1j	-1-1j	-1-1j	1-1j	-1+1j	1-1j	1+1j
1-1j	-1+1j	1-1j	1+1j	-1-1j	1+1j	-1-1j	-1+1j	-1-1j	-1-1j
-1+1j	1-1j	1-1j	1+1j	1-1j	1-1j	-1-1j	1+1j	-1+1j	-1-1j
1-1j	1-1j	1-1j	-1+1j	-1+1j	1-1j	-1-1j	1-1j	-1+1j	-1-1j
1-1j	1-1j	1+1j	1-1j	1-1j	1-1j	-1+1j	1-1j	-1+1j	-1-1j
1-1j	1+1j	-1-1j	-1+1j	1-1j	-1+1j	1+1j	1-1j	1+1j	1+1j
1+1j	-1-1j	1+1j	-1+1j	-1+1j	-1+1j	-1+1j	-1-1j	-1-1j	1-1j
-1-1j	1+1j	1+1j	1-1j	1-1j	-1+1j	-1+1j	1+1j	-1-1j	1-1j
1+1j	1+1j	-1-1j	-1+1j	-1+1j	-1+1j	-1-1j	1+1j	1-1j	
1+1j	-1-1j	1+1j	1-1j	-1+1j	1-1j	1+1j	-1+1j	-1-1j	
-1-1j	1+1j	-1-1j	1-1j	-1-1j	-1-1j	1+1j	1-1j	-1+1j	
1+1j	-1-1j	-1-1j	1+1j	1+1j	-1-1j	1+1j	-1+1j	-1-1j	
-1-1j	-1-1j	1-1j	-1-1j	0+0j	-1+1j	-1-1j	-1+1j	1-1j	
-1-1j	1-1j	-1+1j	-1-1j	-1-1j	1-1j	1-1j	-1+1j	1-1j	
1-1j	-1+1j	1+1j	-1-1j	1+1j	1+1j	1-1j	1-1j	-1+1j	
-1+1j	1-1j	1+1j	-1+1j	-1+1j	1+1j	1+1j	1+1j	-1+1j	
1-1j	1-1j	1-1j	1-1j	-1+1j	-1+1j	-1-1j	1+1j	-1+1j	

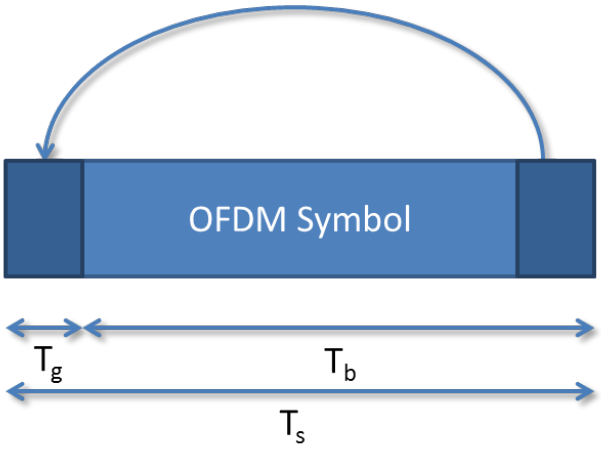

Figure 2.13: WiMAX symbol with cyclic prefix as described in [24]

the combination of the time required by the OFDM symbol, T_b, and the cyclic prefix time, T_g which are defined as

$$T_b = \frac{1}{\Delta f} \tag{2.42}$$

$$T_g = GT_b \tag{2.43}$$

where as previously mentioned G takes on one of four values, and the subcarriers are spaced Δf Hz apart, where

$$\Delta f = \frac{F_s}{N_{FFT}}. \tag{2.44}$$

Here N_{FFT} is 256, and F_s is determined as

$$f_s = 8000 \left\lfloor \frac{\eta B}{8000} \right\rfloor \tag{2.45}$$

where η is determined based on the factorization of the bandwidth in the order shown in Table 2.2 [24]. The first 28 (-128:-101), and last 27 (101:127) subcarriers are all left as

Table 2.2: Table of η values from [24]

Channel Bandwidth (B) is a multiple of	η
1.75 MHz	8/7
1.5 MHz	86/75
1.25 MHz	144/125
2.75 MHz	316/275
2.0 MHz	57/50
Other	8/7

zero in order to serve as guard bands; and the DC subcarrier is also left as zero as shown in Figure 2.14. An example preamble signal is shown in Figure 2.15.

For the simulation and estimation in this thesis, only the preamble is being considered. It is assumed that there will be limited impact from the rest of the signal on the signal recovery and matched filtering to form a SAR image. There may be some impact, but the repetitive structure of the preamble and additional amplification it receives are expected to offset this. The effect of the rest of the signal may appear as noise in the channel when a WiMAX signal is used for SAR. Additionally, the repetitive structure within the preamble may cause some ghosting. This assumption also precludes use of the rest of the signal for image formation by recovering and recreating the entire frame as suggested in [15].

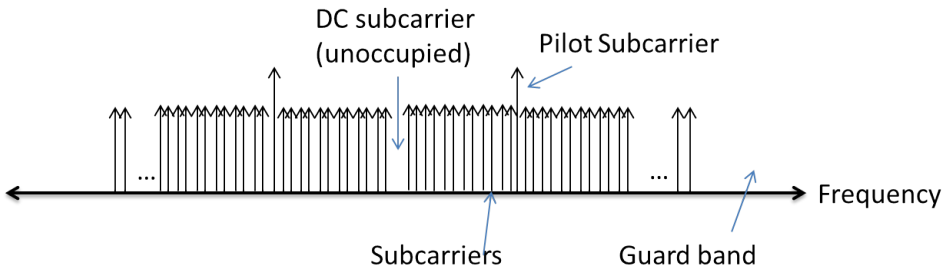

Figure 2.14: OFDM frequency domain illustration based on description in [24]

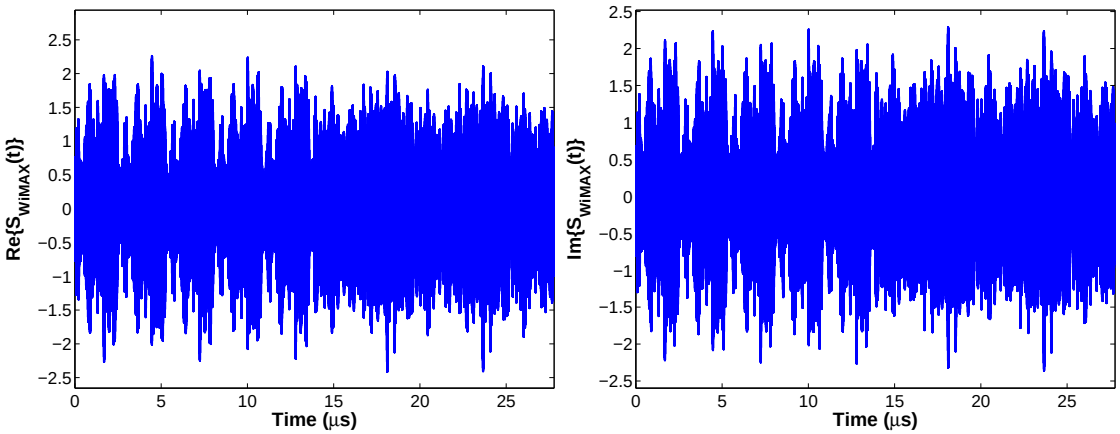

(a) Real component (b) Imaginary component

Figure 2.15: Simulated WiMAX sync signal amplitude vs. time

2.4.4 Analog FM Radio. Unlike digital communications standards, analog frequency modulated (FM) radio is generated without synchronization which could be used for matched filtering. So a direct path signal needs to be collected. A specific type of FM radio modulation called stereo FM, described in [30], is common for music broadcast. For that reason, stereo FM is used in this thesis to represent FM radio. This section provides a brief overview of the modulation procedure.

In the first step to creating a stereo FM modulated signal, two message signals are used to provide slightly different signals to different speakers. These two signals, called left, $m_l(t)$, and right, $m_r(t)$, are added and subtracted to create sum, $m_s(t)$, and difference, $m_d(t)$, signals:

$$\begin{aligned} m_s(t) &= m_l(t) + m_r(t) \\ m_d(t) &= m_l(t) - m_r(t) \end{aligned} \tag{2.46}$$

These two channels are then separately filtered using pre-emphasis filters [30]. The pre-emphasis filter is used to counteract the effect of the noise power-spectral density, shown in [30] to be parabolic after FM demodulation. After reception, the demodulated signal is run through a de-emphasis filter in order to return the message to its original power spectral density while reshaping that of the noise. The pre-emphasis filter for stereo FM radio is a first order high pass RC filter with a time constant of 75 μs:

$$H_p(f) = 1 + j\frac{f}{f_0}, \tag{2.47}$$

where for FM radio, $f_0 = (2\pi 75\mu\text{s})^{-1} = 2100$ Hz [30]. After this filtering, $m_s(t)$ occupies the frequency band between 0 and 15 KHz. To seperate it from $m_s(t)$, $m_d(t)$ is modulated by double side band suppressed carrier (DSB-SC) amplitude modulation (AM). DSB-SC is achieved by multiplying the message signal $m_d(t)$ with a carrier signal, $c(t)$, giving the

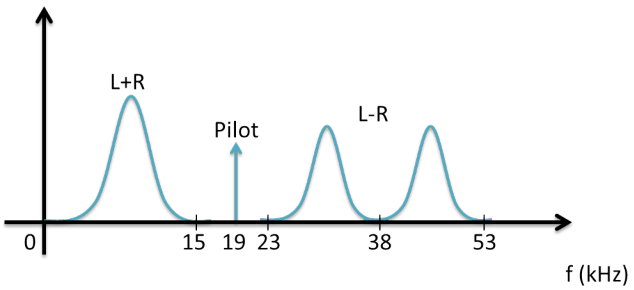

Figure 2.16: Stereo FM signal conceptual spectrum as described in [30]

modulated signal

$$\tilde{m_d}(t) = m_d(t)c(t) = m_d(t)\cos(2\pi f_i t + \phi_c) \tag{2.48}$$

where f_i is a 38 kHz intermediate carrier generated from a 19 kHz oscillator, and ϕ_c is the carrier phase (assumed to be unknown but constant). Since the message signal is a real valued function, after multiplying it by the carrier it will have both side bands centered around the carrier. As long as the message does not contain a DC component, there is no impulse at the carrier frequency, hence "suppressed carrier". Addition of a carrier to the modulated signal is useful for demodulation since the message can be recovered with a simple envelope detector, so a pilot tone, $m_p(t)$, is added at 19 kHz [30]. The spectrum of the combination of $m_s(t)$, $\tilde{m_d}(t)$, and the pilot is shown in Figure 2.16. The resulting message signal,

$$\tilde{m}(t) = m_s(t) + m_p(t) + \tilde{m_d}(t) \tag{2.49}$$

is then used to frequency modulate a carrier. FM modulation is accomplished as [30]

$$s_{FMRadio}(t) = A_c \cos[2\pi f_c t + \phi(t)] \tag{2.50}$$

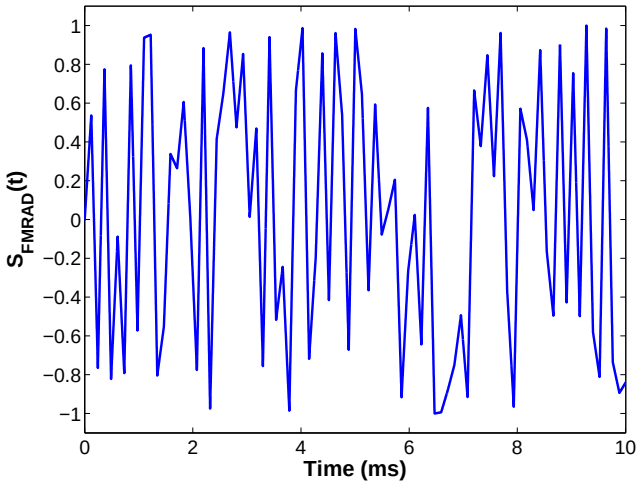

Figure 2.17: Simulated stereo FM radio signal amplitude vs. time

with

$$\phi(t) = 2\pi k_f \int_{-\infty}^{t} \tilde{m}(\tau) d\tau. \tag{2.51}$$

Here k_f is the frequency deviation constant. This term is used to convert the maximum amplitude deviation of the message signal into the desired peak frequency deviation of the modulated signal, Δf_{max}. FM radio has Δf_{max} fixed at 75 kHz with 200 kHz carrier separation [30]. Assuming that the message signal is normalized, $\Delta f_{max} = k_f$. The resulting signal might look something like Figure 2.17.

2.5 Multiple Objective Waveform Optimization

The goal of this work is to create a framework for evaluating multiple sets of possible emitters for multistatic SAR. A possible good solution for the evaluation is multiple objective optimization, where there are several different objectives being evaluated for a set of possible design criteria. The general multi-objective optimization problem is posed as

$$\arg\min_{\mathbf{x}} \mathbf{F}(\mathbf{x}) = [F_1(\mathbf{x}), F_2(\mathbf{x}), ..., F_I(\mathbf{x})]^T \tag{2.52}$$

subject to $g_j(\mathbf{x}) \leq 0, j = 1, 2, ..., J$ and $h_l(\mathbf{x}) = 0, l = 1, 2, ..., L.$. The notation indicates there are I objective functions, $F(\mathbf{x})$, J inequality constraints, $g_j(\mathbf{x})$, and L equality constraints, $h_l(\mathbf{x})$ [8, 26]. The vector of design variables, $\mathbf{x}$, is comprised of n independent variables and n is not necessarily equal to I. Note that in these equations, bold indicates that the variable is a vector. The feasible design space, $\mathbf{X}$, is a set of design vectors defined to be $\{\mathbf{X} \,|\, g_j(\mathbf{x}) \leq 0, j = 1, ...J; h_l(\mathbf{x}) = 0, l = 1, ..., L\}$. One way to solve this would be to find the Pareto optimal solution, which is defined to be the vector of design variables $\mathbf{x}^*$ such that there is no other set in $\mathbf{X}$ such that $\mathbf{F}(\mathbf{x}) \leq \mathbf{F}(\mathbf{x}^*)$ and additionally there is no case where $F_i(\mathbf{x}) < F_i(\mathbf{x}^*)$ [26]. One problem with this solution is that for the limitations for emitter selection, the Pareto optimal may not exist among the set of possible design variables. Rather than finding a Pareto optimal solution to this problem, there is the possibility of a compromise solution [26]. The compromise solution is found as the design variable vector which gives the minimum distance between the vector of objective functions $\mathbf{F}(\mathbf{x})$, and the utopia point, $\mathbf{F}^0$. The utopia point is a vector of the minimum individual functions, $F_i(\mathbf{x})$, possible for all $\mathbf{x}$ in $\mathbf{X}$. The compromise solution using the Euclidean distance between these two functions is then:

$$\arg\min_{\mathbf{x}} N(\mathbf{x}) = |\mathbf{F}(\mathbf{x}) - \mathbf{F}^0| = \left\{ \sum_{i=1}^{k} \left[F_i(\mathbf{x}) - F_i^0 \right]^2 \right\}^{1/2}. \tag{2.53}$$

However, if the functions have different units (2.53) does not hold up. The magnitude of the difference between objective functions and the utopia point may not be appropriate for comparison when using different units. As an example, resolution in meters is on a different scale than signal to noise ratio in dB. To account for different units, the functions

are normalized. One approach is to find

$$F_i^{trans}(\mathbf{x}) = \frac{F_i(x)}{|F_i^{max}|}, \tag{2.54}$$

where $|F_i^{max}|$ is the maximum value of the set of possible $F_i(\mathbf{x})$ for $\mathbf{x}$ in $\mathbf{X}$ [26]. Note that normalizing helps with different units for the objective functions, but does not account for cases where the objective function would be desirable, or undesirable, for all possible outcomes. In the event of a uniformly good or bad outcome, small changes would not be significant, despite becoming large after normalization.

In addition to the compromise solution in (2.53), the evaluation to determine which set of design variables should be selected can be based on a weighted global criterion method. This approach uses a utility function to take into account the preferences for different objective functions by weighting them [8]. A simple way to do this is using a weighted exponential sum [42],

$$U = \left\{ \sum_{i=1}^{k} w_i^p \left[F_i^{trans}(\mathbf{x}) - F_i^0 \right]^p \right\}^{1/p}, \tag{2.55}$$

which, with $p = 2$ as in the compromise solution, has the form of a weighting of the Euclidian distance between the utopia point and a given set of objective functions. The set of weights, w, is selected by a user, and there are a large number of approaches available for selecting and utilizing weighting [26]. However, two straightforward approaches are ranking (simply incrementing the weight value from least to most important) and categorization (different objectives are grouped by categories such as highly and moderately important).

Multiple objective optimization requires use of several different relevant objective functions. For the emitter selection problem of passive multistatic SAR, the selected objectives are: improving signal to noise ratio (SNR), and contrast ratio, and reducing

EMRA and ambiguities. To that end, two of these objective functions are described in the following subsections and two are developed in Chapters 3 and 4.

2.6 Objective Functions of Previously Defined Multistatic Radar Criteria

This section will give a brief description of two of the objective functions, SNR maximization and ambiguity penalty. These criteria have been well defined in the multistatic radar context in other research [5, 40, 41] . They require little, if any, adaptation to the approach of this thesis and so are presented as background. Background on bistatic resolution is also given, since it is useful to check the multistatic resolution estimate and informs some of the constraints in Section 5.1.1. Additionally some background is given on prior work on multistatic resolution.

2.6.1 Multistatic SNR maximization. One of the objective functions of interest, SNR maximization has already been formulated. In [41], the radar range equation is extended to the bistatic case for determining the maximum range product, $(R_t R_R)_{max}$ as

$$(R_T R_R)_{max} = \left[\frac{P_{av} t_0 G_T G_R \lambda^2 \sigma_B F_T^2 F_R^2}{(4\pi)^3 k_b T_S B_n (SNR)_{min} L_T L_R} \right]^{1/2} \tag{2.56}$$

where R_T and R_R are the Tx to target and Rx to target ranges, P_T is the transmitter power output, G_T and G_R are the Tx and Rx antenna gain, σ_B is the bistatic radar target cross section, F_T and F_R are the attenuation pattern propagation factors for Tx to target and Rx to target paths, k_b is Boltzmann's constant (not to be confused with spatial frequency), T_S is the Rx system noise temperature, B_n is the noise bandwidth of the Rx filter, sufficient to pass the spectrum of the Tx signal, $(SNR)_{min}$ is the minimum SNR required for detection, and finally L_T and L_R are the Tx and Rx system losses. Equation (2.56) should apply for all types of waveforms [41]. Rearranging the equation to find the SNR in terms of the

other variables yeilds

$$SNR = \frac{P_T G_T G_R \lambda^2 \sigma_B F_T^2 F_R^2}{(4\pi)^3 k_b T_S B_n (R_T R_R)^2 L_T L_R} \tag{2.57}$$

For the purpose of this application, the terms which are constant between all scenarios can be grouped together. These scenarios assume multiple transmitters and only one receiver. Additionally, the gain for the transmitters is assumed to be broad, such that the gain in any given direction will be the same. System loss for transmitters are assumed unknown, but are accounted for in the effective radiated power of the transmitter. Based on these assumptions, the bistatic SNR equation can be grouped as

$$SNR = \left(\frac{P_T \lambda^2 \sigma_B}{B_n (R_T R_R)^2}\right)\left(\frac{G_T G_R F_T^2 F_R^2}{(4\pi)^3 k_b T_S L_T L_R}\right), \tag{2.58}$$

where the first set of terms represent those which change between scenarios and are separated out to be calculated for each Tx-Rx pair; the second set represent those which are essentially constant based on the previously stated assumptions. Note that full consideration of the aspect dependence of the bistatic radar target cross section is beyond the scope of this thesis; however, there may be frequency dependence which could help differentiate the SNR for different transmitters. To that end, σ_B is treated as a backscatter coefficient which depends on the frequency, and the type of clutter/scenery being represented in a scenario. For multistatic radar, [41] gives the equation for system signal to noise ratio for n_r receivers and n_t transmitters operating coherently as

$$SNR = \frac{\sigma_B \Sigma_T^2 \Sigma_R^2}{(4\pi)^2 k_b} \tag{2.59}$$

where the two Σ terms are the sum of the transmitter and receiver components. Specifically they are presented as

$$\Sigma_T = \sum_{i=1}^{N_T} \left(\frac{P_{Ti} G_{T_i} F_{Ti}^2}{R_{Ti}^2 L_{Ti}} \right)^{1/2}, \tag{2.60}$$

and

$$\Sigma_R = \frac{\sum_{j=1}^{N_R} \left(\frac{A_{R_j} F_{Rj}^2}{R_{Rj}^2 L_{Rj}} \right)^{1/2}}{\sum_{j=1}^{N_R} T_{sj} B_{nj}}, \tag{2.61}$$

where the variables are as described in the previous section, with indices corresponding to the transmitter or receiver they are derived from. The receiving aperture, A_{Rj} is related to the antenna gain as

$$A_{Rj} = \frac{G_{Rj} \lambda_j^2}{4\pi}. \tag{2.62}$$

Putting (2.62) into (2.61) and then into (2.59) along with (2.60) to get a more familiar SNR function gives

$$SNR = \frac{\sigma_B \left[\sum_{i=1}^{N_T} \left(\frac{P_{Ti} G_{T_i} F_{Ti}^2}{R_{Ti}^2 L_{Ti}} \right)^{1/2} \right]^2 \left[\sum_{j=1}^{N_R} \left(\frac{G_{R_j} \lambda_j^2 F_{Rj}^2}{R_{Rj}^2 L_{Rj}} \right)^{1/2} \right]^2}{(4\pi)^3 k_b \left(\sum_{j=1}^{N_R} T_{sj} B_{nj} \right)} \tag{2.63}$$

Note that the wavelength, λ, is associated with the receiver's aperture gain term, and has now been given an index corresponding to the receiver, though the receive frequency is determined by the transmitter frequency.

The preceding formulation relies on the assumption that coherence can be maintained between the transmitter and the receiver. Coherence may be difficult to implement, though

possible if knowledge of the original signal's transmission time is available. Accurate estimation of the timing of the original signal would rely on synchronization and knowledge of the distance of the transmitter from the receiver. Digital communications signals are designed so that a receiver separate from the transmitter may be synchronized in order to demodulate and decode the original message. Based on this synchronization, coherence for digital communications signals are assumed to be possible. Synchronization in this manner is not possible for analog signals, which lack the synchronization structure. To obtain coherence for analog signals, the system is assumed to make use of a separate antenna to collect a reference signal that will be coherent with the reflected signal. Thus, the assumption of coherence used in this thesis is reasonable, if it is accompanied by the assumption that the position of the transmitter and receiver are known. Since the same assumption is required for the formation of images using backprojection as previously described, it is maintained.

2.6.2 Waveform Ambiguity Penalty/Integrated Side Lobe. Ambiguities due to the waveform being transmitted can be used as another objective function. The geometry of a scenario and waveforms being used by the transmitters have been shown to contribute to resolution based on the bandwidth and frequency of the signal being used. Beyond the main lobe resolution, there may be ambiguities which add uncertainty as to whether a return is from one or several reflectors. Ambiguities in the waveforms are due to parts of the signal which resemble other parts, such that during matched filtering they produce peaks at places other than the main lobe. This is separate from ambiguous returns from reflections at ranges ambiguous due to the signals PRI. Note that this is also being treated separately from the question of resolution. ISL is focused on relative ambiguities with a main lobe. To account for this in an objective function, the ratio of the integrated side lobe level to main lobe of the waveform's ambiguity function (MAF) is found. ISL is defined as the ratio of the integral of all points in the MAF above the -3dB cutoff to the integral of

those points below:

$$ISL = \frac{\iint_{\{x,y:10\log_{10}(\Psi(x,y))>-3dB\}} \Psi(x,y)dxdy}{\iint_{\{x,y:10\log_{10}(\Psi(x,y))\leq-3dB\}} \Psi(x,y)dxdy} \tag{2.64}$$

To find the ISL value, it is first necessary to define how the MAF, $\Psi(x, y)$ will be calculated. Next, differences between how the ambiguity function is calculated for digital and analog signals need to be determined. Note that though ISL has a similar name to ISLR developed in Section 2.3.2, ISLR is the integrated side lobes of a PSF, whereas ISL is the integration of the sidelobes of the ambiguity function. Due to the assumption of an isotropic point scatterer used in the development of the multistatic SAR simulation, the phase history is treated as if the signal could be perfectly de-convolved; however, a more realistic scene would involve more interference.

2.6.2.1 Multistatic Ambiguity Function. A traditional, monostatic ambiguity function compares a signal to a copy of itself which has been delayed and offset in frequency. In [38], the ambiguity function was extended to the bistatic case, and put in terms of the bistatic delay and Doppler of a target at a given angle. However for the purpose of a MAF, the geometry assumptions in [38] are hard to maintain. Thus, going to a more general statement, the ambiguity function represents the comparison of a signal reflected off of a target to the signal for a false hypotheses of the state of that target. These false hypotheses evaluate targets at different ranges and Doppler shifts [25, 32]. The ambiguity function gives information about how much the false hypotheses resemble the true, and also for SAR applications how reflectors outside of the point being evaluated may contribute to the measured return for that point. To calculate the MAF, it is necessary to look at the function in terms of a sum of signals, put in a slightly altered version of the

traditional form [5]

$$\Psi(\tau_a, \tau_H, \omega_a, \omega_H) = \left| \int_{-\infty}^{\infty} s(t-\tau_a) s^*(t-\tau_H) e^{j(\omega_{DH}-\omega_{Da})t} dt \right|^2, \tag{2.65}$$

where $s(t)$ is the combination waveform being evaluated, τ_a and ω_{Da} are the actual delay and Doppler shift, and τ_H and ω_{DH} are the hypothesized delay and Doppler shift. Note that, due to the different ranges from the transmitter to a point target, to a receiver due to a given scenario's geometry, the delays will not be consistent, meaning that the combination waveform is of the form

$$s(t-\tau) = \sum_{i=1}^{N_T} s_i(t-\tau_i). \tag{2.66}$$

Now N_T transmitter signals are added together, each delayed by its own τ_i depending on the range. In [5], the solution to this disconnect between the various delays is to set up the ambiguity function in terms of a position in space, giving the appropriate relative delays. The Doppler shift could be put in terms of hypothesized velocity of the point target. Changing to notation of the ambiguity function, as suggested in [5], based on a position and velocity based approach would lead to a restatement of (2.65) as:

$$\Psi(x_a, y_a, vx_a, vy_a, x_h, y_h, vx_h, vy_h) = \left| \int_{-\infty}^{\infty} s(t, x_a, y_a, vx_a, vy_a) s^*(t, x_h, y_h, vx_h, vy_h) dt \right|^2, \tag{2.67}$$

where x_a, y_a, vx_a, and vy_a are the actual x and y coordinates and x and y velocity components, and x_h, y_h, vx_h, and vy_h are the hypothesized x and y coordinates and x and y velocity components. Bistatic Doppler shift calculations which could be used for the individual signals contributing to the ambiguity function are provided in [38]. However, for the purpose of SAR image formation, the ambiguities due to velocities are assumed to

be small for the move-look-move model of receiver collection which should be appropriate when the scene is in the far field. The signal is then a function of the sum of the various delays due to location as

$$s(t,x,y) \quad = \quad \sum_{i=1}^{N_T} A_i s_i(t-\tau_i(x,y)) \tag{2.68}$$

where the delay of signal i to point (x,y) is given by

$$\tau_i(x,y) = \frac{\sqrt{(X_{Txi}-x)^2+(Y_{Txi}-y)^2}}{c} - \frac{\sqrt{(X_{Rxi}-x)^2+(Y_{Rxi}-y)^2}}{c}. \tag{2.69}$$

The signal has to take into account attenuation due to path loss, given by the coefficient A_i, as well as transmitter and receiver location relative to the point target location. Substituting (2.68) into (2.67), and setting actual and hypothesized velocities equal, yields

$$|\Psi(x_a,y_a,x_h,y_h)| = \left| \int_{-\infty}^{\infty} \left(\sum_{i=1}^{N_T} A_i s_i\left(t-\tau_i(x_a,y_a)\right) \right) \left(\sum_{m=1}^{N_T} A_m s_m\left(t-\tau_m(x_h,y_h)\right) \right)^* dt \right|^2 . \tag{2.70}$$

Presumably the individual communication signals in an area will be designed to not interfere with each other. The cross terms in (2.70) are thus assumed to be uncorrelated and can be removed to give

$$|\Psi(x_a,y_a,x_h,y_h)| = \left| \int_{-\infty}^{\infty} \sum_{i=1}^{N_T} A_i^2 s_i\left(t-\tau_i(x_a,y_a)\right) s_i^*\left(t-\tau_i(x_h,y_h)\right) dt \right|^2 . \tag{2.71}$$

Rearranging the sum and integral operations, this becomes

$$|\Psi(x_a,y_a,x_h,y_h)| = \left| \sum_{i=1}^{N_T} A_i^2 \left(\int_{-\infty}^{\infty} s_i\left(t-\tau_i(x_a,y_a)\right) s_i^*\left(t-\tau_i(x_h,y_h)\right) dt \right) \right|^2 . \tag{2.72}$$

Now the MAF can be seen as a weighted sum of the individual bistatic pair ambiguity functions. The sum of these ambiguity functions is normalized, so that the maximum value will be 1, and the resulting ambiguity function, for a set area is evaluated to determine the integrated sidelobe level. Examples of the individual bistatic ambiguity functions for the four transmitter types, and their combined ambiguity function are shown in Figures 2.18 and 2.19. The combination of transmitters all at the same azimuth does not give a good indication of the way the MAF will behave in general, and so the azimuth values of the transmitters are changed and the ambiguity functions are reformed in Figure 2.20. The MAF in Figure 2.21 shows the addition of bistatic pairs with down ranges in the different direction.

The ambiguity penalty objective function is then simply the value of the ISL found by using the ambiguity function based on the approach described in [5]. In the development in [5] the geometry and waveforms were more traditional with transmitters and receiver assumed to be on separate aircraft, and P3, P4, and Frank polyphase coded waveforms used to generate the ambiguity function. In [4] experimentation carried out in a lab environment was performed to confirm that the approach to the ambiguity function worked as expected.

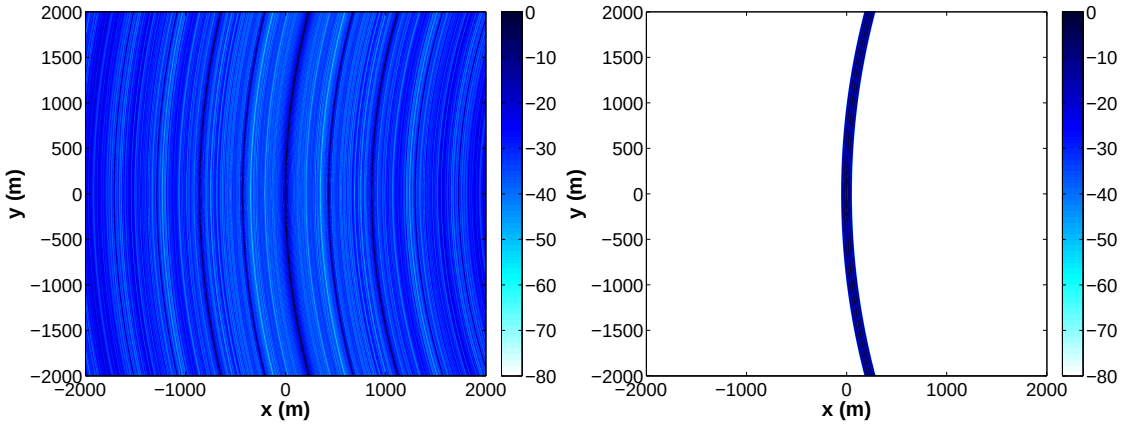

(a) WiMAX with F_c = 2GHz, B = 20MHz, and $\phi_{Tx} = 0°$

(b) HDTV with F_c = 470MHz, B = 6MHz, and $\phi_{Tx} = 0°$

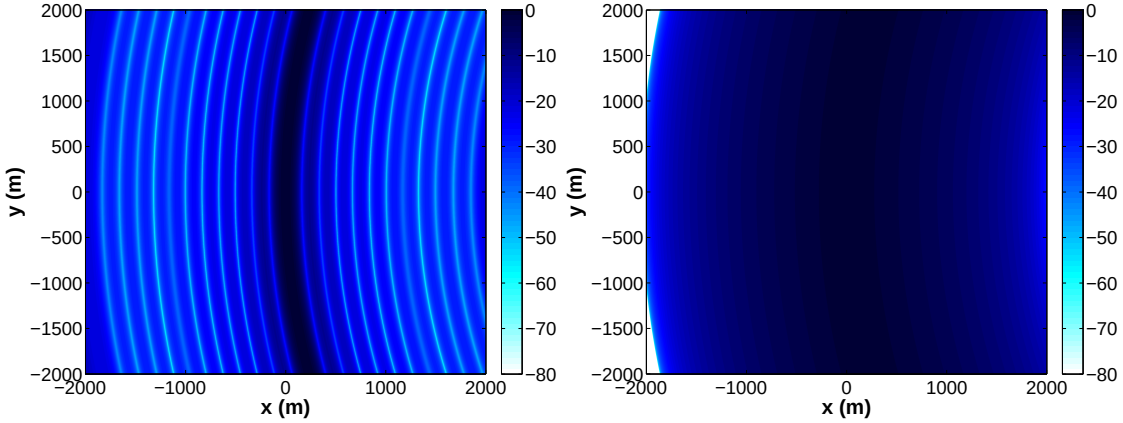

(c) LTE with F_c = 1.85GHz, B = 945kHz, and $\phi_{Tx} = 0°$

(d) FM Radio with F_c = 88MHz, B = 75kHz, and $\phi_{Tx} = 0°$

Figure 2.18: Bistatic ambiguity function in dB for example transmitters and a receiver at zero azimuth

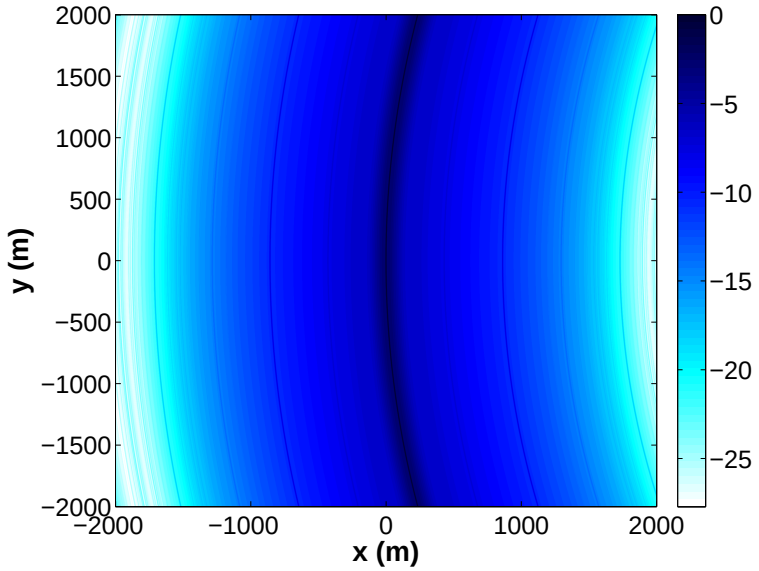

Figure 2.19: Ambiguity function in dB for combination of example transmitters in Figure 2.18 using (2.72)

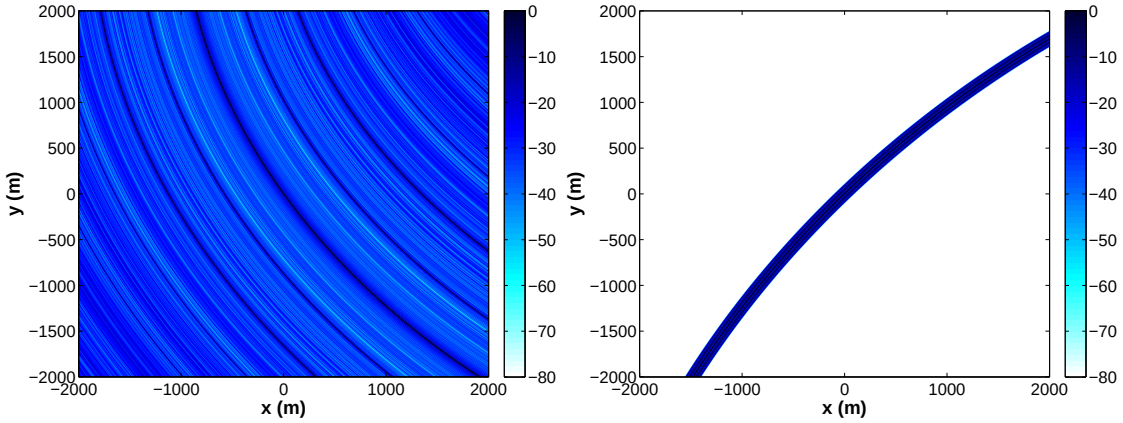

(a) WiMAX with $F_c = 2$GHz, $B = 20$MHz, and $\phi_{Tx} = 63°$

(b) HDTV with $F_c = 470$MHz, $B = 6$MHz, and $\phi_{Tx} = -83°$

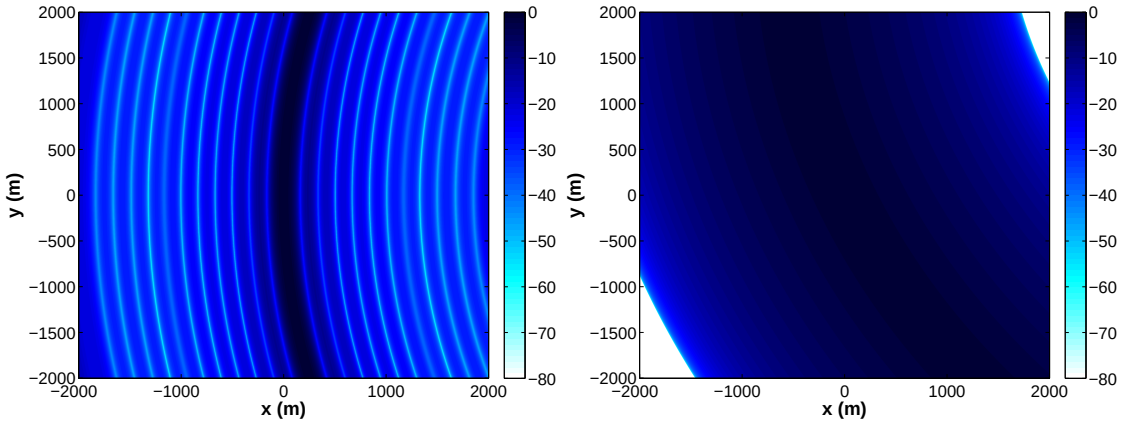

(c) LTE with $F_c = 1.85$GHz, $B = 945$kHz, and $\phi_{Tx} = 0°$

(d) FM Radio with $F_c = 88$MHz, $B = 75$kHz, and $\phi_{Tx} = 45°$

Figure 2.20: Bistatic ambiguity function in dB for example transmitters at various azimuths and a receiver at zero azimuth

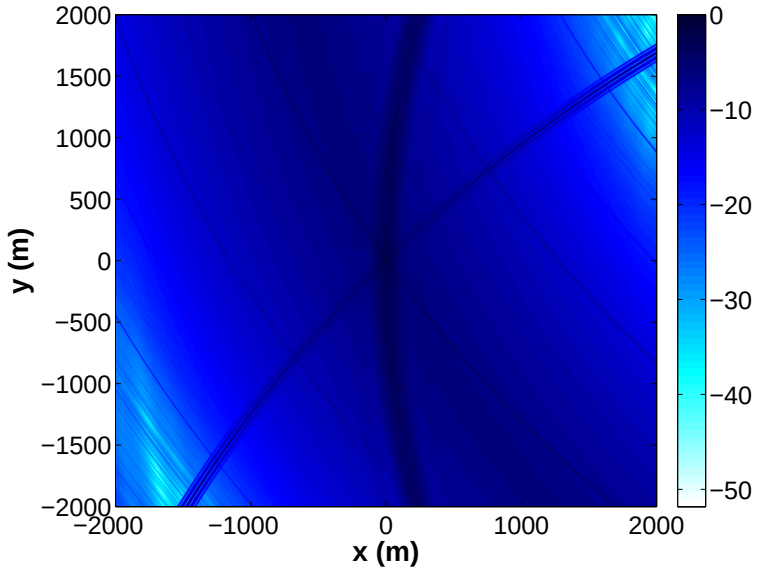

Figure 2.21: Ambiguity function in dB for combination of example transmitters in Figure 2.20 using (2.72) with the WiMAX Tx at 63°, the HDTV Tx at -83°, the LTE Tx at 0°, and the FM radio Tx at 45°

2.6.3 Bistatic SAR Resolution. Though not an objective function itself, bistatic SAR resolution is used to check the resolution estimate from the PSF approximation in Chapter 3. In [40] formulas for down and cross range bistatic resolution are developed based on far field approximations. The cross range resolution is determined to be [40]

$$\delta_{cr} = \frac{c}{4f_c \sin\left(\frac{\Delta\phi}{2}\right)\cos\bar{\theta}_b \cos(\beta/2)} \tag{2.73}$$

where f_c is the carrier frequency, $\Delta\phi$ is the angular extent of the phase history relative to the scene center, $\bar{\theta}_b$ is the elevation look angle of the SAR image as shown in Figure 2.22, and β is the bistatic angle between the transmitter and receiver. The angular extent of the phase history is expressed as [40]

$$\Delta\phi = \max\left(\tan^{-1}\left(\frac{f_y(f,\tau)}{f_x(f,\tau)}\right)\right) - \min\left(\tan^{-1}\left(\frac{f_y(f,\tau)}{f_x(f,\tau)}\right)\right) \tag{2.74}$$

where

$$f_x(f,\tau) = \frac{f}{2}\left[\cos\phi_t(\tau)\cos\theta_t(\tau) + \cos\phi_r(\tau)\cos\theta_r(\tau)\right] \tag{2.75}$$

$$f_y(f,\tau) = \frac{f}{2}\left[\sin\phi_t(\tau)\cos\theta_t(\tau) + \sin\phi_r(\tau)\cos\theta_r(\tau)\right] \tag{2.76}$$

$$f_z(f,\tau) = \frac{f}{2}\left[\sin\theta_t(\tau) + \sin\theta_r(\tau)\right], \tag{2.77}$$

τ is the slow time of the collection (similar to the previously defined ϕ_n, except time of collection instead of angle), ϕ_t and ϕ_r are the azimuth angles to the transmitter and receiver from the scene center, and likewise θ_t and θ_r are the elevation angles. The bistatic elevation look angle is defined by [40] as

$$\bar{\theta}_b = \tan^{-1}\left(\frac{f_z(f,0)}{\sqrt{f_x(f,0)^2 + f_y(f,0)^2}}\right) \tag{2.78}$$

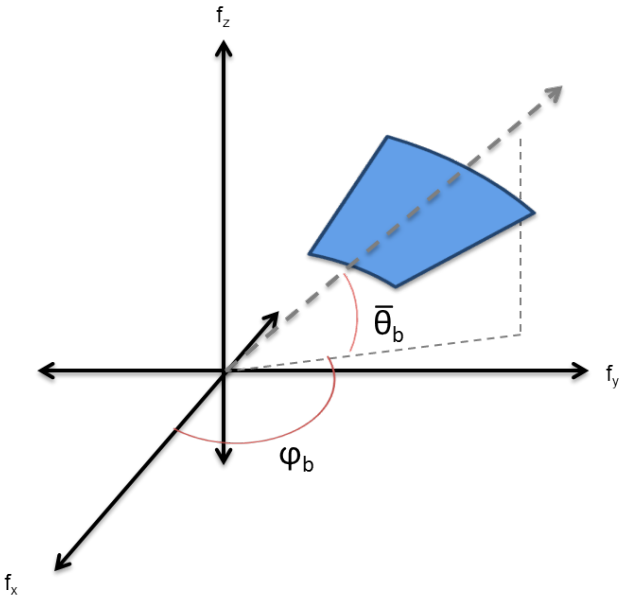

Figure 2.22: Phase history in three dimensions as described in [40]

The down range resolution is found in [40] to be

$$\delta_r = \frac{c}{2B\cos(\beta/2)} \tag{2.79}$$

where B is the bandwidth of the waveform being used. Projecting to the ground plane, the equation for down range resolution becomes [40]:

$$\delta_{r_B} = \frac{c}{2B\cos(\beta/2)\cos\bar{\theta}_b}, \tag{2.80}$$

while the cross range resolution is already in the ground plane.

2.6.4 Prior Research on Multistatic Resolution. Though the EMRA objective function used in this thesis follows a different approach, it has some inspiration from previous work on bistatic resolution and multistatic resolution in the non-coherent addition case. In [43], the generalized ambiguity function (GAF) is determined for bistatic

radar pairs with respect to spatial coordinates instead of delay and Doppler, similar to [5]. The GAF is shown to be the product of the power spectrum of the transmitted waveform and the inverse Fourier transform of the power ratio of the received and transmitted signals. This is used to show the effect of the collection manifold as an antenna pattern and the waveform spectrum on the resulting resolution, allowing for an expression for resolution in any direction. In [9] the idea of the GAF is again pursued and resolution is defined as a set of vectors and a resolution ellipse. The GAF is extended to multistatic systems in [9] using a non-coherent summation of ambiguity functions and the resulting resolution was shown to be the intersection of the individual bistatic radar resolution ellipses. The results of this theoretical development are checked in [9] against a scenario using three GPS satellites as non-cooperative transmitters. These approaches, however, do not explore coherent or GLRT combination of bistatic pairs. They do however give some insight into ways in which the resolution of a combination of bistatic pairs can be formed. This informs the developments in Section 3.2.

2.7 Summary of Background Material

This chapter has given the necessary background on elliptical geometry, bistatic and multistatic SAR, contrast ratio, communications standards, multiple objective optimization, as well as previous work on multistatic SAR parameters. This provides a foundation from which to develop the framework for dynamic emitter selection. In Chapter 3, the background on SAR in Section 2.2 is used as the starting point for the development of a computationally efficient point spread function. This is followed by a development of the EMRA objective function based on the background in Sections 2.6.3 and 2.6.4. Chapter 4 uses the background on elliptical geometry in Section 2.1, SAR in Section 2.2, and contrast ratio in Section 2.3 to develop an approximation of the multistatic contrast ratio. Chapter 5 uses the multiple objective optimization approach described in Section 2.5, using SNR from Section 2.6.1, ISL from Section 2.6.2, EMRA

from Chapter 3, and contrast ratio from Chapter 4 as objective functions. The development in each chapter is checked against simulation based on Section 2.2 using transmitter parameters from the communications standards in Section 2.4.

3 Computationally Efficient Point Spread Function Approximation

This chapter contains the derivation of a computationally efficient approximation of the point spread function for a bistatic radar. The PSF approximation serves to reduce the number of calculations required in order to find an approximation of the effective multistatic resolution area (EMRA). The PSF approximation is compared to backprojection for a number of scenarios to show agreement. The approach to finding the EMRA is described next. Following the development, test scenarios are described to show how bistatic resolution observed in the PSF approximation compares to that formed through backprojection and theory. Next, scenarios for forming effective resolution from the two PSFs under different carrier frequencies, bandwidths and bistatic angles are presented. The EMRA is compared between the fast approximation and backprojection for these scenarios to show the utility of the fast approximation.

3.1 Deriviation of PSF Approximation

The process of forming a phase history and performing backprojection in a simulation can take a significant amount of time, especially for a scene with a large number of pixels and many samples along the flightpath. However, it is possible to make a much faster rough approximation of the point spread function if a few key conditions are satisfied. This section develops the approximation and shows the resulting PSF for a simple example of the point spread function using WiMAX transmitter bandwidth and frequency characteristics (20MHz and 2GHz) located at an azimuth of 45 degrees above the scene's x axis and a receiver moving from -0.5 degrees to 0.5 degrees azimuth, and a constant 20 degrees elevation. The PSF generated for this scenario through simulated backprojection as described in Section 2.2 is shown in Figure 3.1.

The PSF approximation development starts by re-writing the image formation process described in (2.25), and including the form of phase history from (2.15) using

frequency notation. For an arbitrary set of point reflectors, the image is

$$\begin{aligned} IM(x,y,z) &= \sum_{n=1}^{N_p} \mathcal{F}_f^{-1}\left\{\sum_{m=1}^{M} A_m f e^{j2\pi f \Delta R_{nm}(x,y,z)/c}\right\}(\Delta\tau(n,x,y,z)) \\ &= \sum_{n=1}^{N_p}\sum_{m=1}^{M} A_m \mathcal{F}_f^{-1}\left\{f e^{j2\pi f \Delta\tau_m(n,x,y,z)}\right\}(\Delta\tau(n,x,y,z)). \end{aligned} \tag{3.1}$$

The notation $\mathcal{F}_f^{-1}\{X(f)\}(t)$ indicates the inverse Fourier transform of X expresed in terms of frequency f, evaluated at t. The differential delay, $\Delta\tau$, is put in terms of the PSF's evaluation point, (x, y, z), as well as the receiver collection point index n. Note that for the point spread function, the only point used is located at the scene center. Thus $m = 1$ and the differential range of the point is $\Delta R_{nm}(0,0,0) = \Delta\tau_m(0,0,0) = 0$, and the exponential term containing this will be equal to one. The point's amplitude for the PSF is presumably only dependent on propagation loss and the reflectivity coefficient of the point, and is left

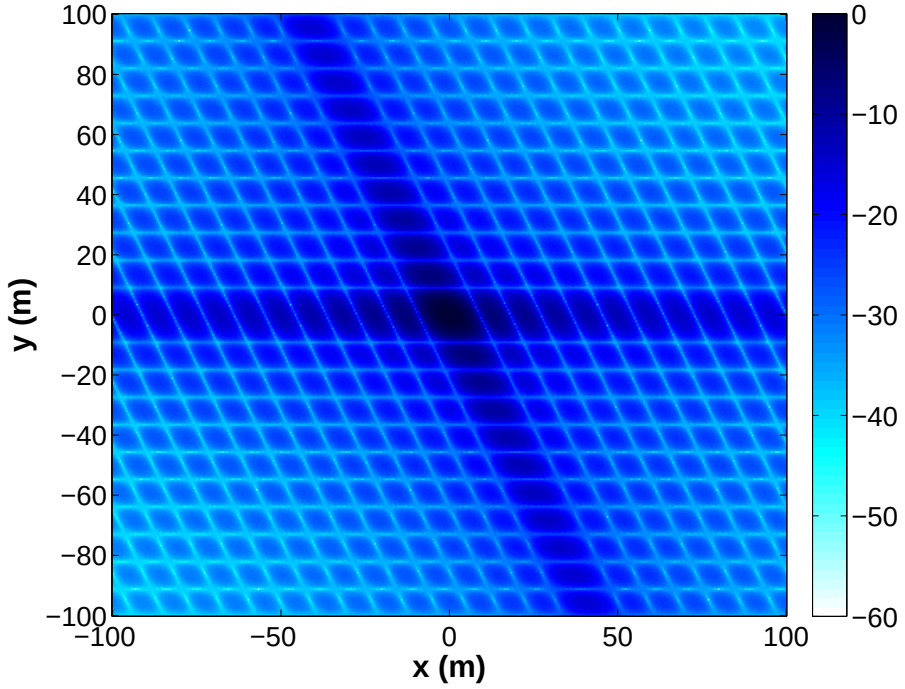

Figure 3.1: $|PSF(x,y,z)|$ for example transmitter, in dB

as a constant A. Additionally, taking into account that the phase history is bounded in frequency by half the bandwidth on the upper and lower ends, it is useful to explicitly write this restriction using the rectangular function so that the PSF becomes

$$PSF(x,y,z) = A\sum_{n=1}^{N_p}\mathcal{F}_f^{-1}\left\{f\Pi\left(\frac{f-F_c}{B}\right)\right\}(\Delta\tau(n,x,y,z)). \tag{3.2}$$

where

$$\Pi(x) = \begin{cases} 1 & |x| \leq 1/2 \\ 0 & \text{otherwise} \end{cases}. \tag{3.3}$$

The result of taking the inverse Fourier transform is found as follows

$$\begin{aligned}
\mathcal{F}_f^{-1}\left\{f\Pi\left(\frac{f-F_c}{B}\right)\right\}(\Delta\tau) &= \int_{-\infty}^{\infty} f\Pi\left(\frac{f-F_c}{B}\right)e^{j2\pi f\Delta\tau}df \\
&= \int_{F_c-B/2}^{F_c+B/2} fe^{j2\pi f\Delta\tau}df \\
&= \frac{e^{j2\pi f\Delta\tau}(1-j2\pi f\Delta\tau)}{4\pi^2\Delta\tau^2}\Bigg|_{F_c-B/2}^{F_c+B/2} \\
&= \frac{e^{j2\pi(F_c+B/2)\Delta\tau}(1-j2\pi(F_c+B/2)\Delta\tau)}{4\pi^2\Delta\tau^2} - \\
&\quad \frac{e^{j2\pi(F_c-B/2)\Delta\tau}(1-j2\pi(F_c-B/2)\Delta\tau)}{4\pi^2\Delta\tau^2} \\
&= \frac{e^{j2\pi F_c\Delta\tau}}{4\pi^2\Delta\tau^2}\Big(e^{j\pi B\Delta\tau} - j2\pi(F_c+B/2)\Delta\tau e^{j\pi B\Delta\tau} \\
&\quad -e^{-j\pi B\Delta\tau} + j2\pi(Fc-B/2)\Delta\tau e^{-j\pi B\Delta\tau}\Big) \\
&= \frac{e^{j2\pi F_c\Delta\tau}}{4\pi^2\Delta\tau^2}\Big(e^{j\pi B\Delta\tau} - j2\pi F_c\Delta\tau e^{j\pi B\Delta\tau} - \\
&\quad j\pi B\Delta\tau e^{j\pi B\Delta\tau} - e^{-j\pi B\Delta\tau} + \\
&\quad j2\pi F_c\Delta\tau e^{-j\pi B\Delta\tau} - j\pi B\Delta\tau e^{-j\pi B\Delta\tau}\Big)
\end{aligned} \tag{3.4}$$

where Euler's formula allows further simplification to

$$\begin{aligned}
\mathcal{F}_f^{-1}\left\{f\Pi\left(\frac{f-F_c}{B}\right)\right\}(\Delta\tau) &= \frac{e^{j2\pi F_c\Delta\tau}}{4\pi^2\Delta\tau^2}\Big(j2\sin(\pi B\Delta\tau) - j^2 2^2\pi F_c\Delta\tau\sin(\pi B\Delta\tau) - \\
&\quad j2\pi B\Delta\tau\cos(\pi B\Delta\tau)\Big) \\
&= \frac{je^{j2\pi F_c\Delta\tau}}{2\pi^2\Delta\tau^2}\Big(\sin(\pi B\Delta\tau) - j2\pi F_c\Delta\tau\sin(\pi B\Delta\tau) - \\
&\quad \pi B\Delta\tau\cos(\pi B\Delta\tau)\Big) \\
&= \frac{jBe^{j2\pi F_c\Delta\tau}}{2B\pi^2\Delta\tau^2}\Big((1 - j2\pi F_c\Delta\tau)\sin(\pi B\Delta\tau) - \\
&\quad \pi B\Delta\tau\cos(\pi B\Delta\tau)\Big) \\
&= \frac{jBe^{j2\pi F_c\Delta\tau}}{2\pi\Delta\tau}\Big((1 - j2\pi F_c\Delta\tau)\mathrm{sinc}(\pi B\Delta\tau) - \\
&\quad \cos(\pi B\Delta\tau)\Big) \qquad (3.5)
\end{aligned}$$

which would make the PSF

$$\begin{aligned}
&PSF(x,y,z) = \\
&\frac{jAB}{2\pi}\sum_{n=1}^{N_p}\frac{e^{j2\pi F_c\Delta\tau(n,x,y,z)}}{\Delta\tau(n,x,y,z)}\Big((1 - j2\pi F_c\Delta\tau(n,x,y,z))\,\mathrm{sinc}(\pi B\Delta\tau(n,x,y,z)) - \\
&\qquad \cos(\pi B\Delta\tau(n,x,y,z))\Big). \qquad (3.6)
\end{aligned}$$

An example of the image for the previously described scenario for the analytically arrived at PSF in (3.6) is shown in Figure 3.2.

Using (3.6), it may be possible to approximate the PSF with fewer operations. First, a few constraints on the scenario allow the differential delay to be simplified. The constraints are that the flightpath be centered around zero and maintain a constant elevation, that $\phi_R(n)$ be small for all n, and that the transmitter be stationary. The condition that $\phi_r(n)$ be small leads to $\cos\phi_r(n) \approx 1$ and $\sin\phi_r(n) \approx \phi_r$ for all n. Thus the differential delay can be separated out into constant and varying terms as

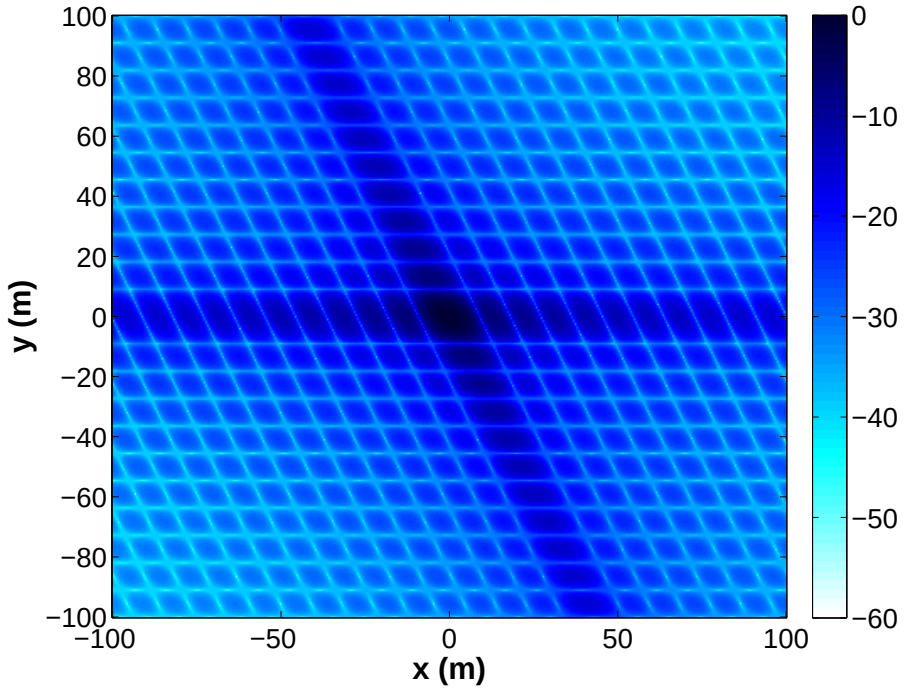

Figure 3.2: $|PSF(x, y, z)|$ for example transmitter in dB after evaluating Fourier transform

$$\begin{aligned}
\Delta\tau(n, x, y, z) &= \frac{1}{c}(-x(\cos(\phi_T(n))\cos(\theta_T(n)) + \cos(\phi_R(n))\cos(\theta_R(n))) \\
&\quad -y(\sin(\phi_T(n))\cos(\theta_T(n)) + \sin(\phi_R(n))\cos(\theta_R(n))) \\
&\quad -z(\sin(\theta_T(n)) + \sin(\theta_R(n)))) \\
&\approx \frac{1}{c}(-x(\cos(\phi_T(n))\cos(\theta_T(n)) + \cos(\theta_R(n))) \\
&\quad -y(\sin(\phi_T(n))\cos(\theta_T(n)) + \phi_R(n)\cos(\theta_R(n))) \\
&\quad -z(\sin(\theta_T(n)) + \sin(\theta_R(n)))) \qquad (3.7)
\end{aligned}$$

Gathering all constant terms and dropping their dependence on n

$$\begin{aligned}\Delta\tau(n,x,y,z) &\approx \frac{1}{c}(-x(\cos\phi_T\cos\theta_T+\cos\theta_R)\\ &\quad -y(\sin\phi_T\cos\theta_T)-z(\sin\theta_T+\sin\theta_R)\\ &\quad -y\phi_R(n)\cos(\theta_R(n)))\\ &\approx \overline{\Delta\tau}(x,y,z)-\frac{y\phi_R(n)\cos\theta_R}{c}\end{aligned} \tag{3.8}$$

where

$$\overline{\Delta\tau}(x,y,z)=\frac{-x(\cos\phi_T\cos\theta_T+\cos\theta_R)-y(\sin\phi_T\cos\theta_T)-z(\sin\theta_T+\sin\theta_R)}{c} \tag{3.9}$$

not only represents all of the terms which are constant for all collection points, but is also the differential delay found from the midpoint of the flightpath, where $\phi_R(m_p)=0$.

The foregoing changes to the differential delay lead to another modification to the PSF approximation to decrease the number of calculations required. Note that because the summation of the exponential in (3.6) is for a finite number of pulses, it resembles a DFT multiplied by a scale factor. If the remaining term in the summation,

$$\begin{aligned}\text{Term}_1 &= \frac{\Big((1-j2\pi F_c\Delta\tau(n,x,y,z))\,\text{sinc}(\pi B\Delta\tau(n,x,y,z))-\cos(\pi B\Delta\tau(n,x,y,z))\Big)}{\Delta\tau(n,x,y,z)}\\ &= \frac{\text{sinc}(\pi B\Delta\tau(n,x,y,z))-\cos(\pi B\Delta\tau(n,x,y,z))}{\Delta\tau(n,x,y,z)}-\\ &\quad j2\pi F_c\text{sinc}(\pi B\Delta\tau(n,x,y,z))\end{aligned} \tag{3.10}$$

can be shown to be nearly constant, it could be moved outside. If this could be shown to be the case, the DFT could be solved and calculating the PSF would require many fewer operations. The first step to determine that Term_1 is nearly constant is to show that for a given point, the difference in the differential delays for the middle collection point, $n=m_p$

and another collection point is minimal relative to the midpoint's differential delay:

$$\begin{aligned} \left|\frac{\Delta\tau(m_p) - \Delta\tau(n)}{\Delta\tau(m_p)}\right| &\ll 1 \\ \left|1 - \frac{\overline{\Delta\tau}(x,y,z) - \frac{y\phi_R(n)\cos\theta_R}{c}}{\overline{\Delta\tau}(x,y,z) - \frac{y\phi_R(m_p)\cos\theta_R}{c}}\right| &\ll 1 \end{aligned} \tag{3.11}$$

Since $\phi_R(n)$ is zero for the midpoint of the flightpath by definition, this changes to

$$\begin{aligned} \left|1 - \frac{\overline{\Delta\tau}(x,y,z) - \frac{y\phi_R(n)\cos\theta_R}{c}}{\overline{\Delta\tau}(x,y,z)}\right| &\ll 1 \\ \left|1 - 1 + \frac{\frac{y\phi_R(n)\cos\theta_R}{c}}{\overline{\Delta\tau}(x,y,z)}\right| &\ll 1 \\ \left|\frac{y\phi_R(n)\cos\theta_R}{c\overline{\Delta\tau}(x,y,z)}\right| &\ll 1 \\ |\phi_R(n)| &\ll \left|\frac{c\overline{\Delta\tau}(x,y,z)}{y\cos\theta_R}\right|. \end{aligned} \tag{3.12}$$

Inserting (3.9) into (3.12)

$$\begin{aligned} |\phi_R(n)| &\ll \left|\frac{-x(\cos\phi_T\cos\theta_T + \cos\theta_R) - y(\sin\phi_T\cos\theta_T) - z(\sin\theta_T + \sin\theta_R)}{y\cos\theta_R}\right| \\ |\phi_R(n)| &\ll \left|\frac{-x(\cos\phi_T\cos\theta_T + \cos\theta_R)}{y\cos\theta_R} - \frac{(\sin\phi_T\cos\theta_T)}{\cos\theta_R} - \frac{z(\sin\theta_T + \sin\theta_R)}{y\cos\theta_R}\right|. \end{aligned} \tag{3.13}$$

Thus, as $y\cos\theta_R/c$ goes to zero the right side becomes infinity large and the condition is easily met. A plot of $y\cos\theta_R/c$ in Figure 3.3 shows that for the ranges of y and θ_R expected for this application, the term does not become excessively large and the division of $\overline{\Delta\tau}(x,y,z)$ by this term does not become small relative to the flightpath. Thus, the remaining consideration is the case where $\overline{\Delta\tau}(x,y,z)$ becomes small. Account for this case requires placing a second condition on Term_1 being treated as a constant: that when the first condition is not met due to a small $\overline{\Delta\tau}(x,y,z)$, then the difference between Term_1

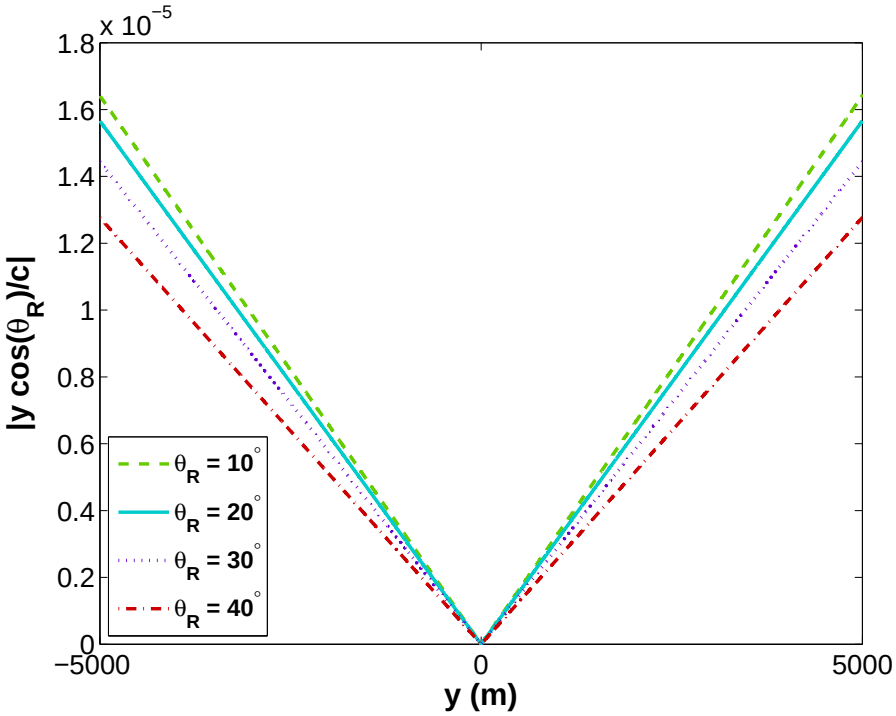

Figure 3.3: $|y\cos\theta_R/c|$ versus y for given receiver elevations θ_R

evaluated at the midpoint and some other point is small relative to Term_1 evaluated at the midpoint:

$$\frac{\text{Term}_1(m_p) - \text{Term}_1(n)}{\text{Term}_1(m_p)} << 1 \tag{3.14}$$

However, when $\overline{\Delta\tau}(x, y, z)$ goes to zero, the differential delay from (3.8) depends only on the term $y\phi_R(n)\cos\theta_R/c$. Thus the difference term in (3.14) can be evaluated by replacing

$\Delta\tau(n, x, y, z)$ with $y\phi_R(n)\cos\theta_R/c$

$$\begin{aligned}
&\text{Term}_1(m_p) - \text{Term}_1(n) = \Delta\text{Term}_1 = \\
&\frac{\text{sinc}(\pi B\frac{y\phi_R(m_p)\cos\theta_R}{c}) - \cos(\pi B\frac{y\phi_R(m_p)\cos\theta_R}{c})}{\frac{y\phi_R(m_p)\cos\theta_R}{c}} - j2\pi F_c\text{sinc}(\pi B\frac{y\phi_R(m_p)\cos\theta_R}{c}) - \\
&\frac{\text{sinc}\left(\pi B\frac{y\phi_R(n)\cos\theta_R}{c}\right) - \cos\left(\pi B\frac{y\phi_R(n)\cos\theta_R}{c}\right)}{2\pi\frac{y\phi_R(n)\cos\theta_R}{c}} + j2\pi F_c\text{sinc}(\pi B\frac{y\phi_R(n)\cos\theta_R}{c}) \\
&= \frac{c}{y\cos\theta_R}\Big(\frac{\text{sinc}(\pi B\frac{y\phi_R(m_p)\cos\theta_R}{c}) - \cos(\pi B\frac{y\phi_R(m_p)\cos\theta_R}{c})}{\phi_R(m_p)} - \\
&\qquad \frac{\text{sinc}(\pi B\frac{y\phi_R(n)\cos\theta_R}{c}) - \cos(\pi B\frac{y\phi_R(n)\cos\theta_R}{c})}{\phi_R(n)}\Big) - \\
&\qquad j2\pi F_c\left(1 - \text{sinc}\left(\pi B\frac{y\phi_R(n)\cos\theta_R}{c}\right)\right)
\end{aligned} \tag{3.15}$$

accounting for division by $\phi_R(m_p)$ requires using L'Hopital's rule. Noting that in general:

$$\begin{aligned}
\lim_{x\to 0}\frac{(\text{sinc}(ax) - \cos(ax))}{x} &= \lim_{x\to 0}\frac{\frac{\partial}{\partial x}(\text{sinc}(ax) - \cos(ax))}{\frac{\partial}{\partial x}x} \\
&= \lim_{x\to 0}\frac{\frac{ax\cos(ax)-\sin(ax)}{ax^2} + a\sin(ax)}{1}
\end{aligned} \tag{3.16}$$

and since

$$\begin{aligned}
\lim_{x\to 0}\frac{ax\cos(ax) - \sin(ax)}{ax^2} &= \lim_{x\to 0}\frac{\frac{\partial}{\partial x}(ax\cos(ax) - \sin(ax))}{\frac{\partial}{\partial x}(ax^2)} \\
&= \lim_{x\to 0}\frac{a\cos(ax) - a^2x\sin(ax) - a\cos(ax)}{2ax} \\
&= \lim_{x\to 0}\frac{-a\sin(ax)}{2} \\
&= 0
\end{aligned} \tag{3.17}$$

then

$$\lim_{x\to 0}\frac{(\text{sinc}(ax) - cos(ax))}{x} = 0 \tag{3.18}$$

Thus, the value from (3.15) simplifies to

$$\Delta\text{Term}_1 = \frac{-c}{y\phi_R(n)\cos\theta_R}\left(\text{sinc}\left(\pi B\frac{y\phi_R(n)\cos\theta_R}{c}\right) - \cos\left(\pi B\frac{y\phi_R(n)\cos\theta_R}{c}\right)\right) - j2\pi F_c\left(1 - \text{sinc}\left(\pi B\frac{y\phi_R(n)\cos\theta_R}{c}\right)\right) \tag{3.19}$$

From the previous use of L'Hopital's rule, it is evident that (3.19) also goes to zero as the product $y\phi_R(n)$ does, but further from $y\phi_R(n) = 0$, it can take on larger values quickly. However when compared to the term from the center of the flightpath, shown from the previous calculations to be equal to $-j2\pi F_c$, the change is not so large:

$$\begin{aligned}\frac{\Delta\text{Term}_1}{\text{Term}_1(m_p)} &= \frac{-jc}{2\pi F_c y\phi_R(n)\cos\theta_R}\left(\text{sinc}\left(\pi B\frac{y\phi_R(n)\cos\theta_R}{c}\right) - \cos\left(\pi B\frac{y\phi_R(n)\cos\theta_R}{c}\right)\right) + \\ &\quad \left(1 - \text{sinc}\left(\pi B\frac{y\phi_R(n)\cos\theta_R}{c}\right)\right)\end{aligned} \tag{3.20}$$

Evaluating (3.20) with several possible values of $\phi_R(n)$, and allowing y to vary, results in the plots shown in Figure 3.4. Note that the range of y values is selected to extend to the expected resolution from (2.73) for the given parameters. This should indicate that the approximation will be accurate up to at least the first null. Based on the conditions of the approximation, it could become less accurate further along the y axis and near points with small differential delay. However, the mainlobe of the PSF is the region of primary concern for resolution, and so the condition is deemed sufficient. The error that is being accepted with these approximations is explored through comparison with PSF's generated through backprojection in Section 3.1.2.

The result of this formulation is that the relative difference is small for values of y near the expected resolutions, and thus the term in (3.10) is effectively constant. Thus

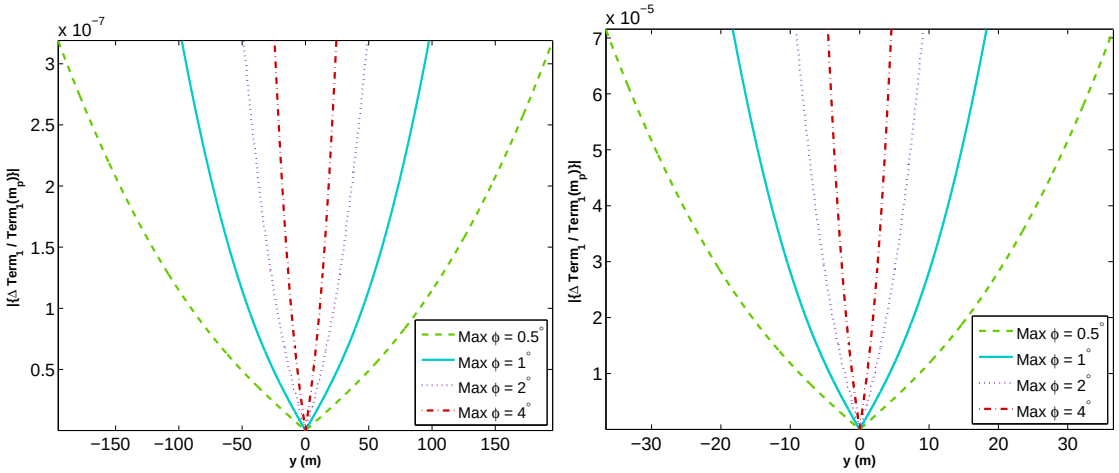

(a) FM radio (88MHz with 75kHz BW) (b) HDTV (470MHz with 6MHz BW)

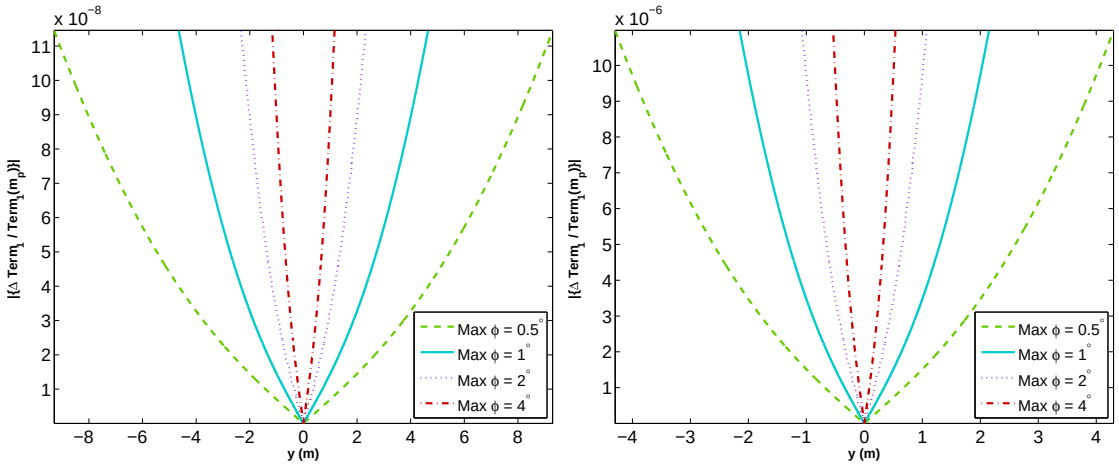

(c) LTE (1.85 GHz with 945kHz BW) (d) WiMAX (4 GHz with 20MHz BW)

Figure 3.4: Plot of (3.20) vs. y for various transmitter types. Note that plots (a)-(d) are on different scales to show the value of (3.20) is small near the expected resolution of the given communication type

(3.10) can be pulled outside the summation using the differential delay from the center of the flight path, $\overline{\Delta\tau}(x,y,z)$. The PSF can now be approximated as

$$\widetilde{PSF}(x,y,z) = \frac{jBA}{4\pi F_c \overline{\Delta\tau}(x,y,z)}\Big(\Big(1 + j2\pi F_c \overline{\Delta\tau}(x,y,z)\Big)\,\mathrm{sinc}\Big(\pi B\overline{\Delta\tau}(x,y,z)\Big) - \cos\Big(\pi B\overline{\Delta\tau}(x,y,z)\Big)\Big)\sum_{n=1}^{N_p} e^{j2\pi F_c \Delta\tau(n,x,y,z)}, \tag{3.21}$$

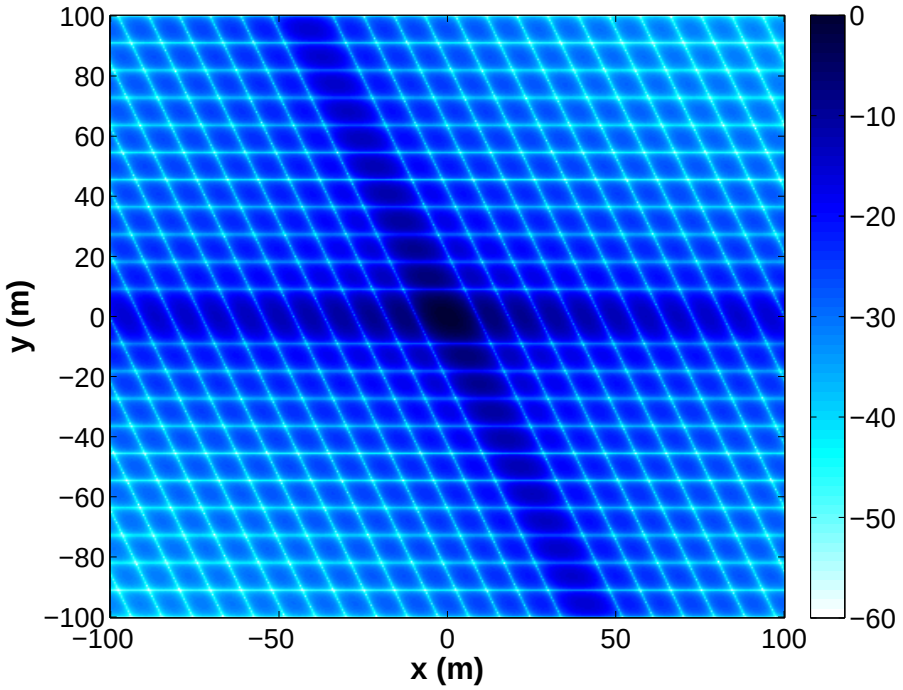

Figure 3.5: $|\widetilde{PSF}(x, y, z)|$ for Example Transmitter

which results in a PSF approximation for the previously described scenario as shown in Figure 3.5. The second term in this approximation can be rewritten as

$$\begin{aligned}
\sum_{n=1}^{N_p} e^{j2\pi F_c \Delta\tau(n,x,y,z)} &= \sum_{n=1}^{N_p} e^{j2\pi F_c \overline{\Delta\tau}(x,y,z)} e^{-j2\pi F_c \frac{y\phi_R(n)\cos\theta_R}{c}} \\
&= e^{j2\pi F_c \overline{\Delta\tau}(x,y,z)} \sum_{n=1}^{N_p} e^{-j2\pi F_c \frac{y\phi_R(n)\cos\theta_R}{c}} \\
&= e^{j2\pi F_c \overline{\Delta\tau}(x,y,z)} \sum_{n=-\infty}^{\infty} \Pi\left(\frac{\phi_R(n)}{\Delta\phi_R}\right) e^{-j2\pi F_c \frac{y\phi_R(n)\cos\theta_R}{c}}
\end{aligned} \tag{3.22}$$

where now the portion outside the summation is a constant phase term, and the summation resembles an inverse DFT of a rectangular function with width $\Delta\phi_R$ with a scaled frequency variable $F_c \cos(\theta_R)/c$. Evaluating (3.22) would result in a Dirichlet sinc (periodic sinc due to digital sampling) [28], however this is approximated by a standard sinc due to the sampling assumptions. Substituting the sinc function for (3.22) and

rearranging terms, the approximation of the PSF is

$$\begin{aligned}\widetilde{\widetilde{PSF}}(x,y,z) &= \frac{jBAN_p}{4\pi F_c\overline{\Delta\tau}(x,y,z)}e^{j2\pi F_c\overline{\Delta\tau}(x,y,z)}\text{sinc}\left(\frac{\pi F_c\cos\theta_R\Delta\phi_R y}{c}\right)\\ &\quad\left(\left(1+j2\pi F_c\overline{\Delta\tau}(x,y,z)\right)\text{sinc}\left(\pi B\overline{\Delta\tau}(x,y,z)\right)-\right.\\ &\quad\left.\cos\left(\pi B\overline{\Delta\tau}(x,y,z)\right)\right).\end{aligned} \tag{3.23}$$

Clearly each time an assumption is required, the PSF approximation becomes more limited in how it can be applied and how accurate the result is; however, the computation becomes faster. Backprojection, an $O(N^3)$ operation [40], is replaced by an approximation which is $O(N^2)$, where N is the number of pixels in the PSF. The assumptions used are not unreasonable, and comparing Figures 3.2 and 3.6, the difference in the shape of the approximation near the center appears to be small. In Section 3.1.1 scenarios will be set up to test these differences more rigorously with the results of these comparisons presented in Section 3.1.2.

3.1.1 Analysis of Fast PSF Approximation. To analyze the fast PSF approximation, a set of arbitrary transmitter characteristics were selected to be representative of bandwidths and carrier frequencies that would be found in some of the communication modulation types being considered. Furthermore, a range of possible transmitter azimuths was used to check for angle dependence. These possible values are shown in Table 3.1. All transmitters are 50 m above the ground and 7 km away from the scene center. The receiver is located 10 km away from the scene center at an elevation of 20°. The receiver follows a flightpath of −0.5° to 0.5° in 0.001° steps. All possible combinations of the given values are evaluated, varying bandwidth first, then carrier frequency, then transmitter azimuth.

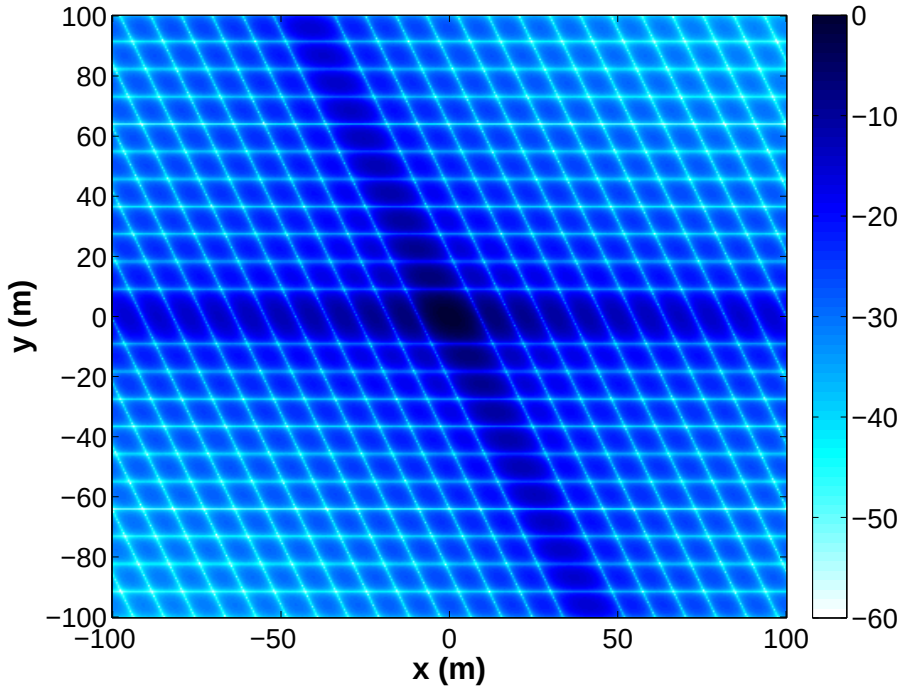

Figure 3.6: $|\widetilde{\widetilde{PSF}}(x, y, z)|$ for example transmitter

Table 3.1: Table of Transmitter Characteristics for Bistatic Resolution

Bandwidth (MHz)	Carrier Frequency (GHz)	Azimuth (degrees)
4.0	0.47	-50.4
5.5	0.8525	-44.8
7.0	1.235	-28.0
8.5	1.6175	0
10.	2.0	39.2
		89.6

PSF images are formed through backprojection and the fast approximation method for all configurations for a scene ranging from -150 m to 150m in 0.25m steps along both the x and y axis. The difference between the absolute value of all corresponding pixels

and their ratios are examined, as well as the absolute value of the difference between corresponding pixels. Additionally the phase of the difference, and the difference of the phases of corresponding pixels are examined. The results are presented as a histogram of results from all configurations, a plot of difference by configuration, as well as PSF difference images for a small number of example configurations.

3.1.2 Fast PSF Approximation Results. The PSFs for a given Tx-Rx configuration, generated both through backprojection and the fast approximation are compared pixel by pixel. A pixel from the PSF formed through the fast approximation is subtracted from the corresponding pixel from the PSF formed through backprojection. The resulting magnitude of the difference is accumulated for all pixels in all PSFs. For the set of all pixels in all PSFs for all configurations, the resulting set of differences is shown as a histogram in Figure 3.7 for the magnitude of the difference between pixels. The mean for the magnitude of the difference between all pixels is 6.45e-4, and the standard deviation is 7.99e-4. These results show good agreement in the magnitude and phase of the PSF, so that the coherent combinations of PSFs formed through the fast approximation should closely resemble the PSFs formed through backprojection.

To help illustrate the differences in the magnitude, configuration 150, with a transmitter using a bandwidth of 10MHz, a carrier frequency of 2GHz, and an azimuth of 89.6° is used as an example. The configuration number is from the progression of values in Table 3.1 according to the order described in Section 3.1.1. The PSFs for this configuration formed through backprojection and fast approximation are shown in Figure 3.8 for configuration 150. Figure 3.9(a) presents an image of the magnitude of the difference between all pixels for the PSFs formed through backprojection and fast approximation on a dB scale, $||\text{PSF}_{BP}| - |\text{PSF}_{Approx}||$. Figure 3.9(b) presents an image of the absolute value of the difference of the magnitude of all pixels for the PSFs formed through backprojection and fast approximation on a dB scale, $|\text{PSF}_{BP} - \text{PSF}_{Approx}|$.

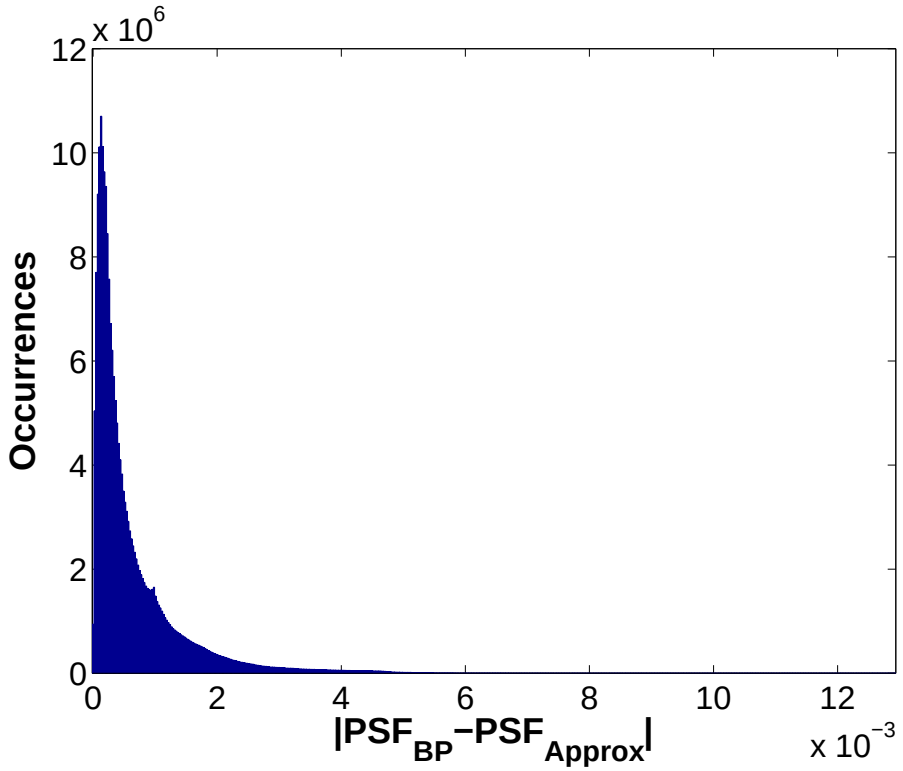

Figure 3.7: Histogram of differences between corresponding pixel intensities

Again, configuration 150 is used as an example to examine the effect of these trends on the phase of the PSFs for an individual bistatic pair. In Figure 3.10(a) the phase of the difference between all pixels is shown, and as expected the phases appear uniformly random. In Figure 3.10(b) the difference between the phases of all pixels is shown. The phases in Figure 3.10(a) tends to be close to 0° near the peaks of the main and sidelobes, and approaches $\pm\pi$ closer to the nulls. In general though, measuring the effective resolution, which will be discussed in Section 3.2, will rely more on those pixels closer to the center of the main and sidelobes.

The statistics of the accumulated difference between pixels illustrates that in general, the approximated PSF matches well with the backprojection PSF. Looking at the statistics for all pixels within a given configuration provides some additional information. The mean of the magnitude of pixel differences is plotted in Figure 3.11 by configuration with

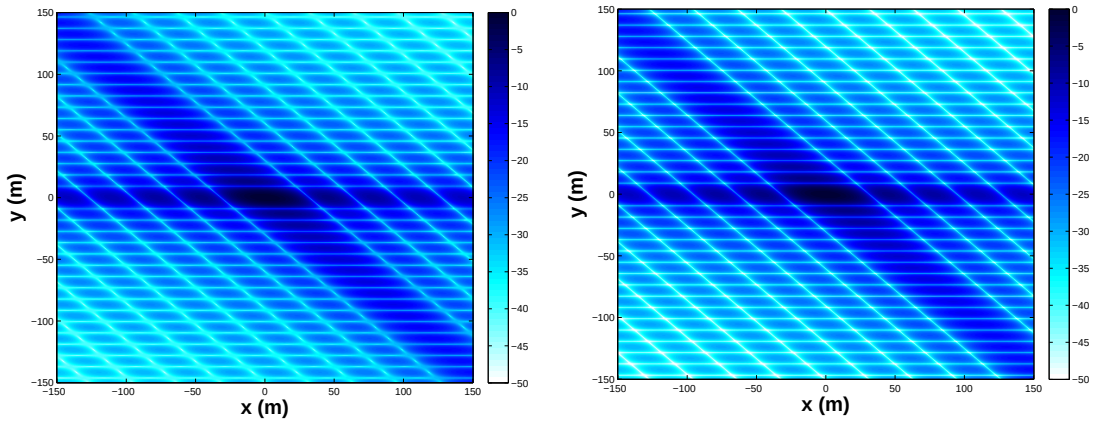

(a) $|\mathrm{PSF}_{BP}|$ (b) $|\mathrm{PSF}_{Approx}|$

Figure 3.8: PSF images for configuration 150 formed through (a) backprojection and (b) fast approximation

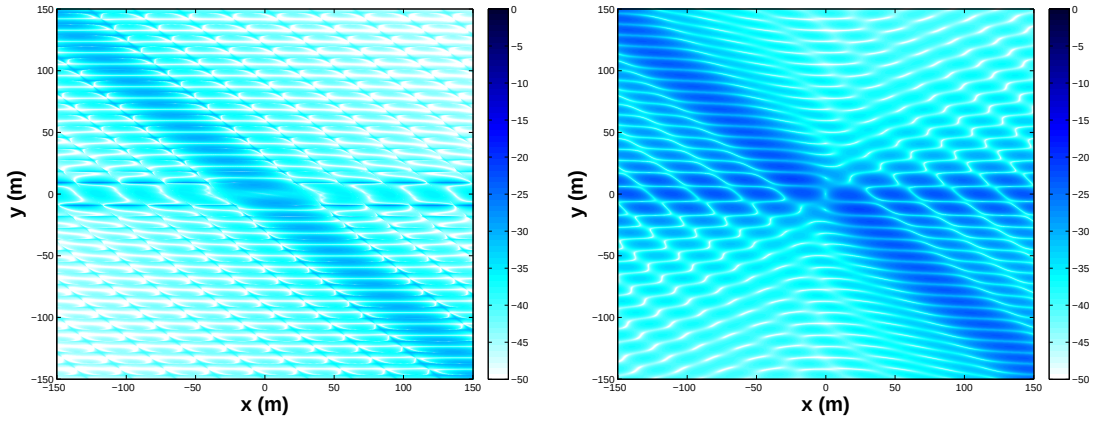

(a) $||\mathrm{PSF}_{BP}| - |\mathrm{PSF}_{Approx}||$ (b) $|\mathrm{PSF}_{BP} - \mathrm{PSF}_{Approx}|$

Figure 3.9: Images of the differences between PSFs for configuration 150 in dB scale

the standard deviation of the pixel difference shown as an error bar. These results show that there is variation in the agreement between pixel values from one configuration to another. In particular increasing bandwidth tends to decrease variability, increasing frequency tends to increase the variability, and increasing the absolute value of the bistatic

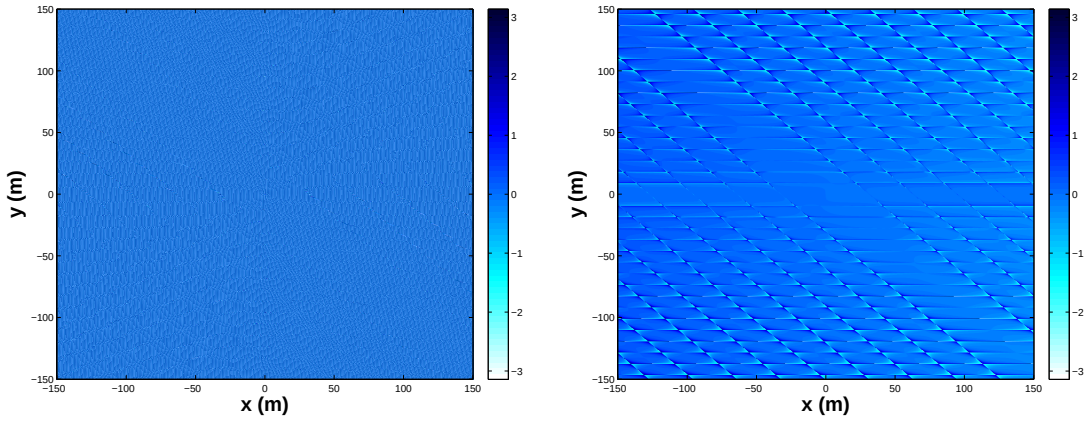

(a) phase($\mathrm{PSF}_{BP} - \mathrm{PSF}_{Approx}$) (b) phase($\mathrm{PSF}_{BP}$) − phase($\mathrm{PSF}_{Approx}$)

Figure 3.10: Images of the differences between PSFs phase for configuration 150 in radians

angle tends to increase variability. Again note the parameters of the configuration follow the progression of values in Table 3.1 according to the order described in Section 3.1.1, denoted by hash marks for the first progression through a given parameter in Figure 3.11.

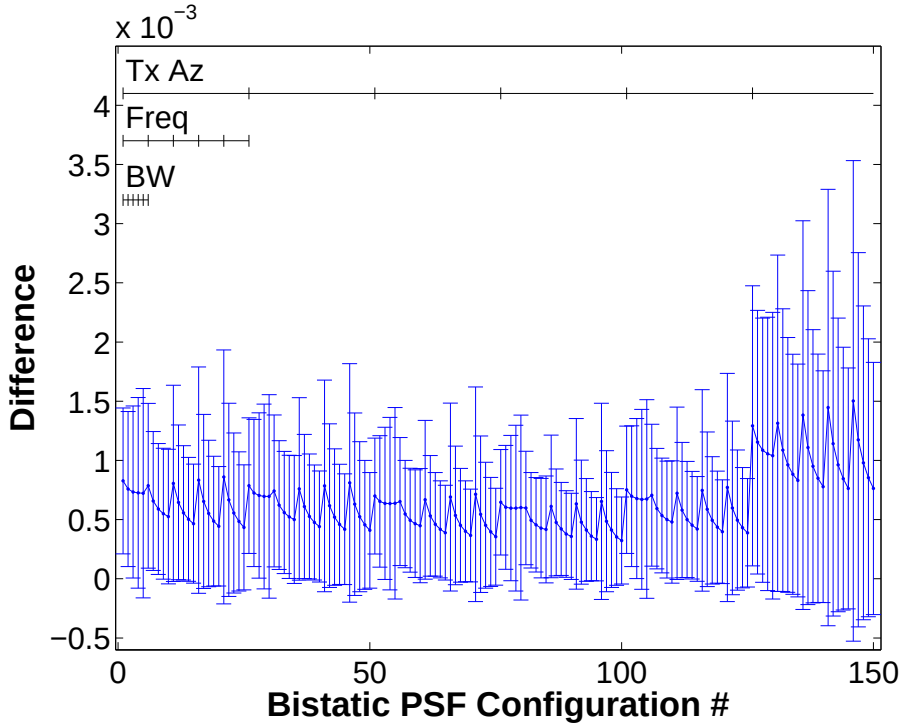

Figure 3.11: Statistics for the magnitude of pixel differences by configuration

3.2 Development of Effective Multistatic Resolution Area

3.2.1 Analysis of Bistatic Resolution Estimation. Though bistatic resolution has been previously described, comparison of the approximation and backprojection to theoretical values are made. Checking the results of bistatic resolution against the theoretical values provides a first step in using the PSF approximation for multistatic resolution. To analyze the bistatic resolution estimation, the same parameters listed for the fast PSF approximation analysis are used, as listed in Table 3.1. All possible combinations of the given values are evaluated, varying bandwidth first, then carrier frequency, then transmitter azimuth.

Measuring the cross range resolution is accomplished by evaluating PSF(x, y) for

$$\begin{aligned} x &= r\cos\left(\frac{\beta}{2}+\frac{\pi}{2}\right) \\ y &= r\sin\left(\frac{\beta}{2}+\frac{\pi}{2}\right) \end{aligned} \tag{3.24}$$

where $\beta/2$ is the bistatic bisector, and the range from the scene center, r, was a set of values between zero and 100 m in 0.05m increments. Since the PSF generated both through backprojection and through the approximation method previously developed using these parametrically defined x and y coordinates is along a line extending from the center and perpendicular to the bistatic bisector, the first null is taken to be the cross range resolution. Measuring the down range resolution requires a slightly different approach than simply using

$$\begin{aligned} x &= r\cos\left(\frac{\beta}{2}\right) \\ y &= r\sin\left(\frac{\beta}{2}\right), \end{aligned} \tag{3.25}$$

because backprojection and approximation can result in point spread functions such as the PSF approximation shown in Figure 3.12, where the first null the radial line will intersect is due to the cross range limitation, rather than the down range extent δr. To avoid selecting the wrong range, the first null along the x axis is found resulting in δx. The first x axis null is used to find the true down range resolution as

$$\delta r = \delta x\cos\left(\frac{\beta}{2}\right) \tag{3.26}$$

Measuring the first null is straightforward: find the first inverse peak. Thus the first step in the analysis of the bistatic resolution approximation is comparing the down and cross range to the theoretical down and cross range values for the backprojection PSF and

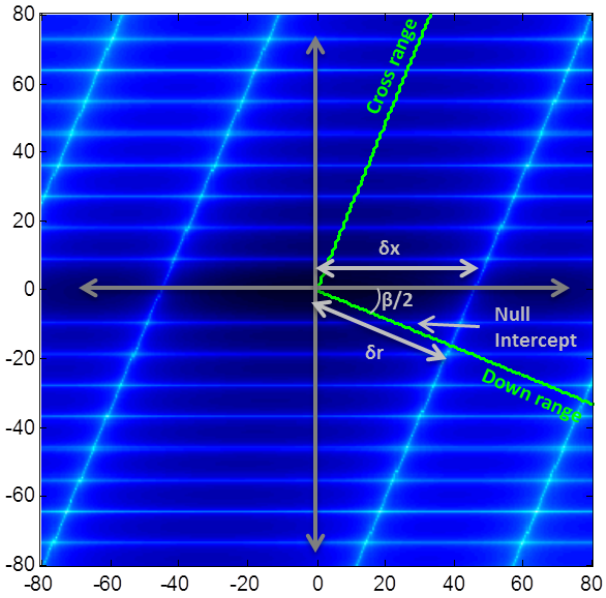

Figure 3.12: Point spread function approximation with overlain down and cross range markers in green

PSF approximation. Following this, the resolution measurements using a -3dB threshold are evaluated. Comparison for a -3dB threshold is done because this threshold is used for evaluating the multistatic resolution due to the presence of grating lobes. Only the backprojection PSF and PSF approximation are compared, since the theoretical values are for a resolution measured to the first null.

3.2.2 Bistatic Resolution Approximation Results. The results of comparing down and cross range for the bistatic scenario is largely in agreement between the fast approximation and backprojection. In Figure 3.13, the null-to-null resolution for the PSF formed through backprojection (BP) are shown as blue dots, the null-to-null resolution of the PSF approximation are shown as red x's, and the theoretical down and cross range are shown as black plus signs. Both measurements of down and cross range follow the theoretical values well. As expected, down range resolution responds more to changes in bandwidth than carrier frequency, and cross range resolution responds more to changes in

frequency. Also as expected, both have finer resolutions for transmitters at zero azimuth, as seen in configurations 76 through 100. Note that the configuration numbering comes from the progression through the values in Table 3.1 as described in Section 3.2.

Comparing the ratio of the measurements with the theoretical values found using (2.73) and (2.80) and each other, shown in Figure 3.14, provides additional information. The ratio of the measurements of the PSF formed through backprojection to the estimate, using asterisk markers in the plot, show good agreement. The ratio of the BP measurements to theoretical values, shown as blue dots, as well as the ratio of the estimate to the theoretical values, shown as red x's, show that these are close to the theoretical values. However, both backprojection and approximation tend to be larger for the down range resolution, and become worse as the transmitter azimuth, and consequently the

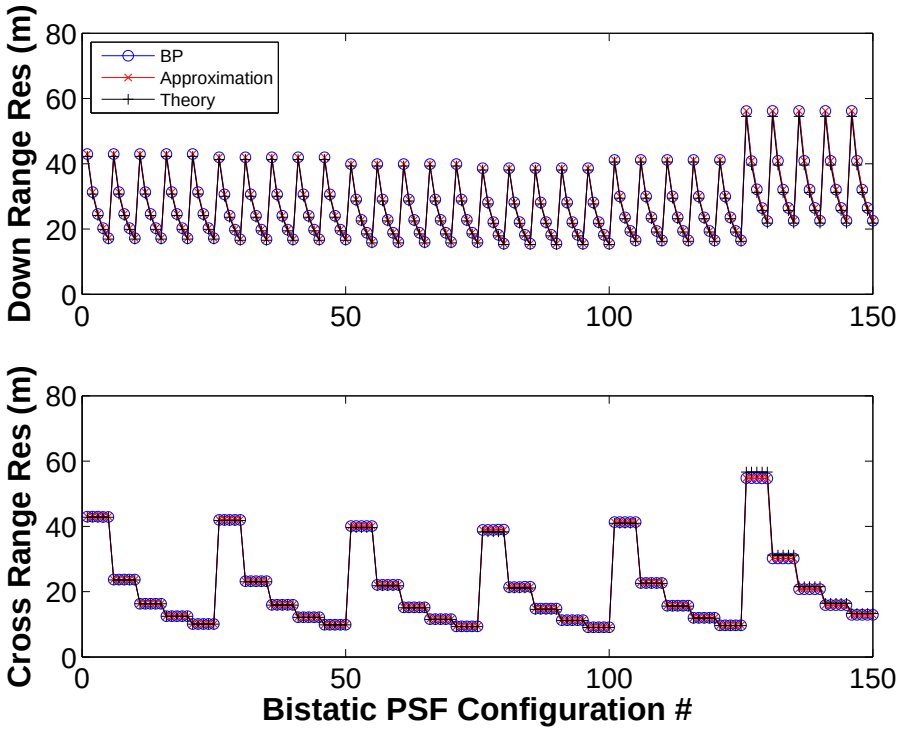

Figure 3.13: Results of null-to-null down and cross range resolution for bistatic system, where configuration varies first by bandwidth, then by carrier frequency, then by transmitter angle using values from Table 3.1

bistatic angle, becomes larger as shown in configurations 126 through 150 where the Tx azimuth is 89 degrees. This is not entirely surprising due to the assumption in Section 2.2 that the bistatic angle would be small. Again in Figure 3.15 showing the -3dB threshold resolution, the BP -3dB resolution and the PSF approximation -3dB resolution are in agreement and follow the same pattern. However looking at the ratio of BP -3dB resolution to approximation -3dB resolution shown in Figure 3.16 there is a consistent tendency for the PSF approximation's resolution to be slightly larger than the resolution measured from the PSF formed through backprojection.

One potential problem when comparing the two, which was discovered and corrected to produce the results in this section, comes from the interpolation of the zero padded phase history in backprojection. Increasing the zero padding of the IFFT from a total of 2^{13} points to 2^{17} smoothed out the PSF and improved the agreement between BP and approximation -3dB resolution. In Figure 3.17 an example of the difference in zero padding is provided by showing the down and cross range radial slices of the PSF for backprojection (blue) and approximation (red dashed) together with a line at the -3dB threshold (green) for both the 2^{13} and 2^{17} point FFT cases.

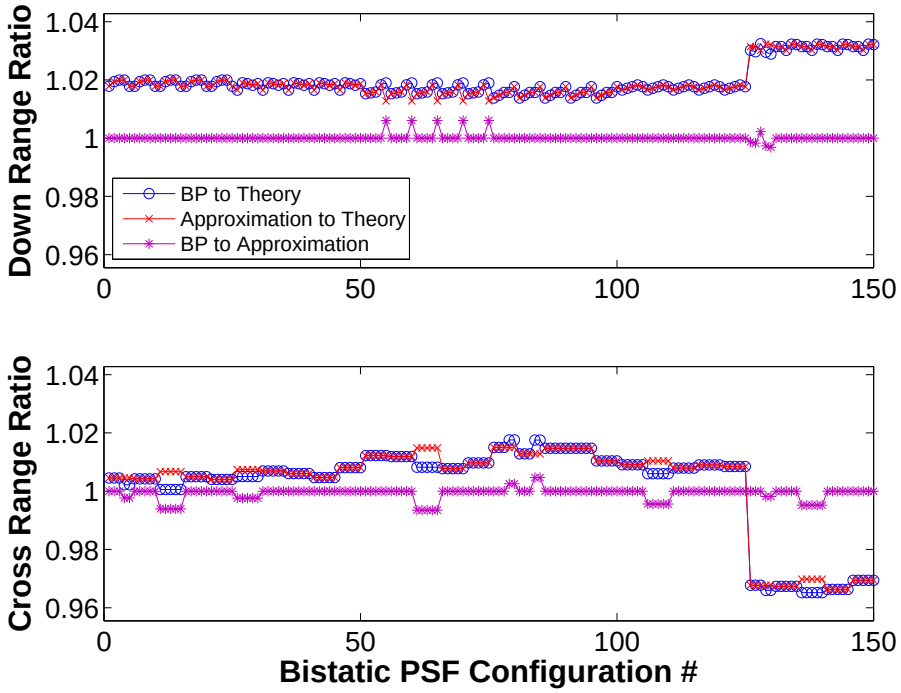

Figure 3.14: Ratios of null-to-null down and cross range resolution for bistatic system

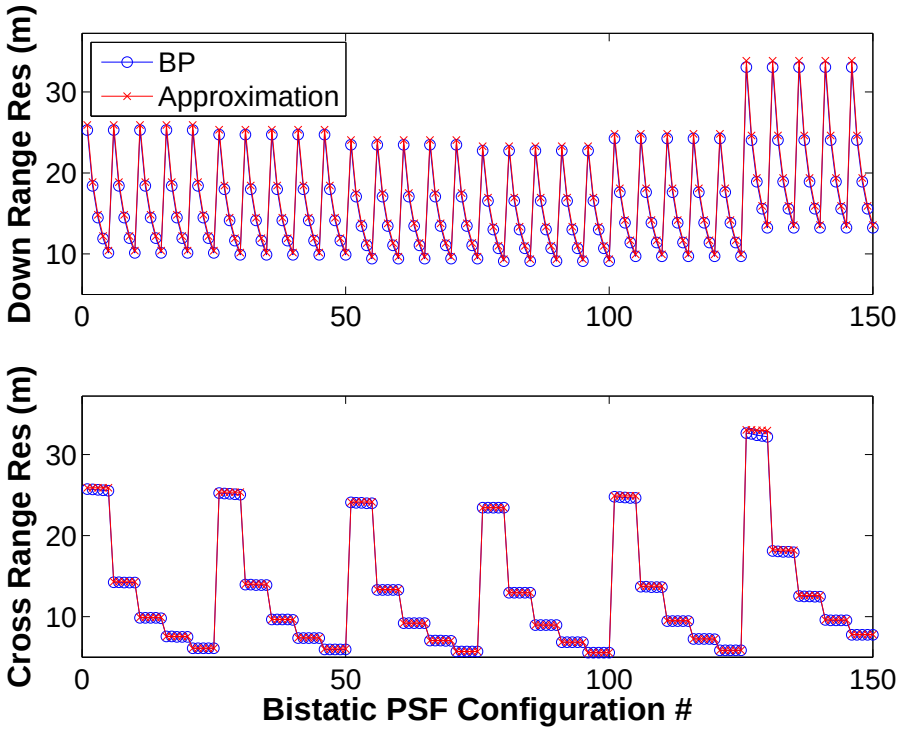

Figure 3.15: Results of down and cross range resolution using a -3dB threshold for bistatic systems varying configuration first by bandwidth, then by carrier frequency, then by Tx angle using values from Table 3.1

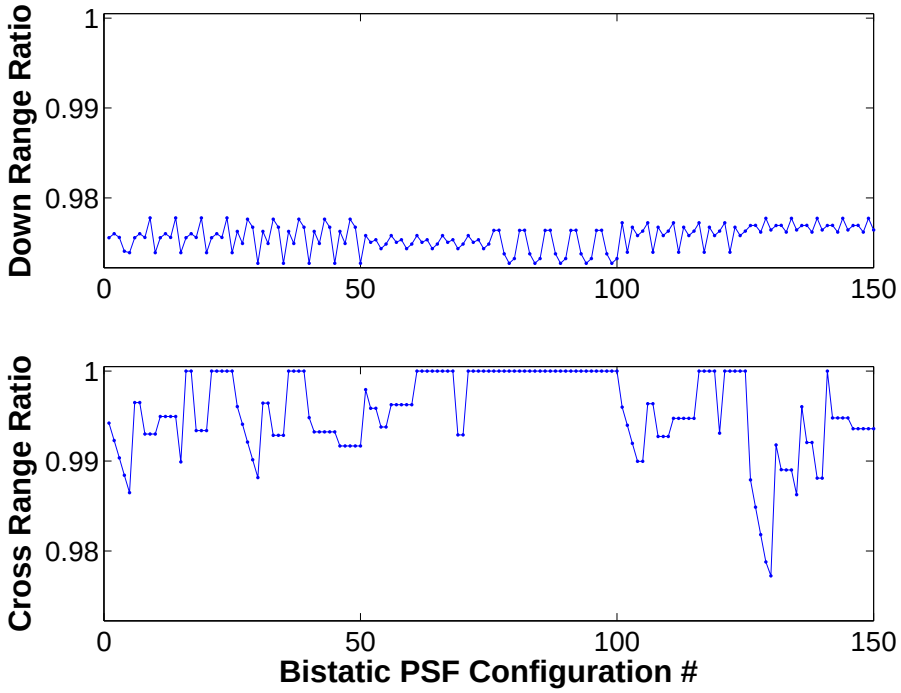

Figure 3.16: Ratio of BP down range resolution to approximation down range resolution (top) and ratio of BP cross range resolution to approximation cross range resolution (bottom) using a -3dB threshold for bistatic systems varying configuration first by bandwidth, then by carrier frequency, then by Tx angle using values from Table 3.1

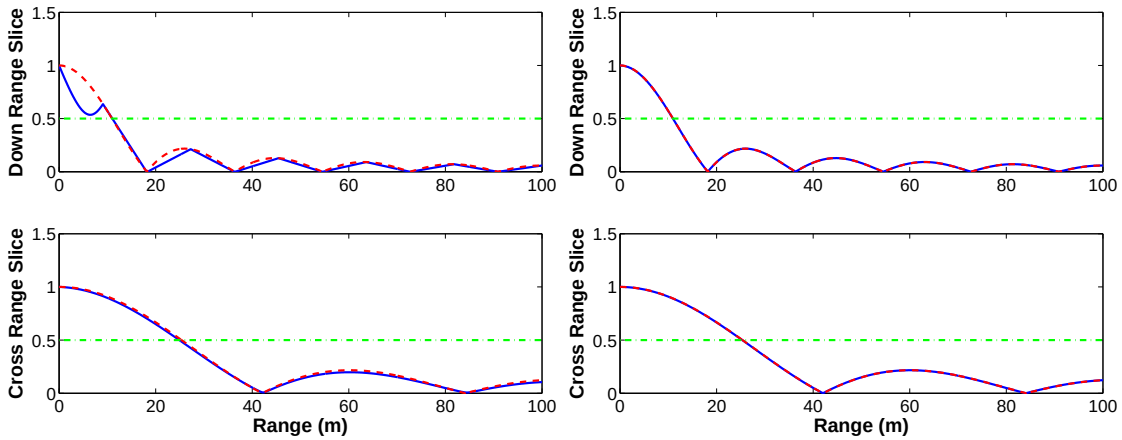

(a) Slices using a 2^{13} point FFT

(b) Slices using a 2^{17} point FFT

Figure 3.17: Example radial slice of PSF approximation (red dash) and BP PSF (blue) with -3dB point marked in green for configuration 30, with 10MHz bandwidth, 470MHz carrier frequency, and -44.8° Tx azimuth

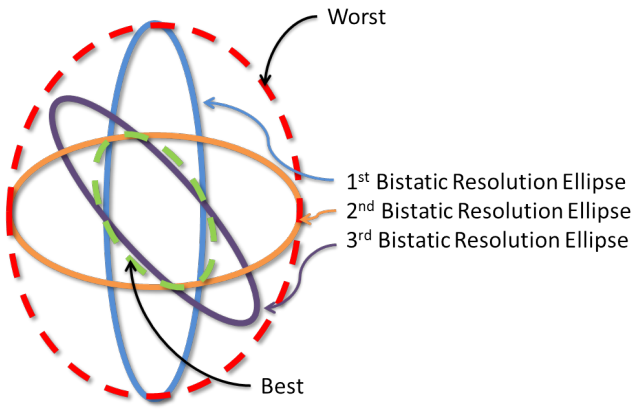

Figure 3.18: Conceptual best and worst case combined resolution

3.2.3 Multistatic SAR Resolution. Multistatic SAR resolution is not extensively documented, and so this section will attempt to explain the methods used to arrive at an evaluation of the EMRA of a multistatic SAR. The effect on the resolution of combining data from multiple bistatic pairs will clearly depend on the way their individual images are combined into a multistatic image. If the images are coherently added, the resolution will be different than if a GLRT approach is used to combine the images. In previous work on multistatic resolution, such as in [9], resolution from individual bistatic pairs is treated as an ellipse. Non-coherent addition and GLRT combination of images will result in multistatic resolution which is at best the intersection of the individual resolutions, and at worst bounding their union, as shown in Figure 3.18.

Use of ellipses to describe multistatic resolution is appropriate, because the overlap and combination of resolutions does not follow the definition of down and cross range in a traditional sense. To measure the resolution ellipse, the point spread function is weighted by the effective radiated power and propagation loss, and combined for the various bistatic pairs forming the multistatic system. Because the phase history placement for the various Tx-Rx pairs are irregularly spaced, the coherent combination of the images formed from them contain grating lobes. Grating lobes can be hard to predict and are expected to

effectively increase the area of minimum separability of targets. An example of this is presented in Figure 3.20 where the three bistatic PSF's shown in Figure 3.19 are coherently combined into a multistatic PSF. In that image, the portion of the normalized multistatic PSF above the -3dB threshold is shown along with the bistatic resolution ellipses. Figure 3.20 highlights a case where grating lobes appear outside the intersection of the individual bistatic resolution ellipses but within their union. Because of this, we define the outer boundary of where the combination of N_T different PSFs cross a -3dB threshold, shown as a magenta ellipse in Figure 3.20, as the EMRA used for comparison of different possible sets of transmitters. EMRA is treated as the area of an ellipse which bounds all points above -3dB from the peak of the PSF.

To calculate the combined resolution ellipse, it is first necessary to determine the individual point spread functions and scale them by the propagation loss to the point. The multistatic PSF is then formed using either the GLRT or coherent combination approach. For estimating the GLRT approach, the maximum value for a given (x, y) coordinate from all the bistatic PSFs is found and used as the combined PSF. For coherent addition, the complex value of the pixels at (x, y) from all PSF are added. To improve the speed of estimating the resolution, a faster method of approximating the PSF was developed in Section 3.1.

To find the resolution ellipse, a set of points is generated by finding all parts of the combined PSF above the threshold:

$$(\mathbf{X}, \mathbf{Y}) \quad = \quad \{(x, y) | 10 \log_{10}(\text{PSF}(x, y)) \geq -3\} . \tag{3.27}$$

The parameters of the ellipse are then found in a straightforward manner by using singular value decomposition (SVD), which factors a matrix into three new matrices in the form of $\mathbf{A} = \mathbf{U}\mathbf{\Sigma}\mathbf{V}^T$ [35]. This factoring is of particular interest since the matrices can be used to find the a, b and ξ parameters of the ellipse. The length of the major axis of the ellipse, a,

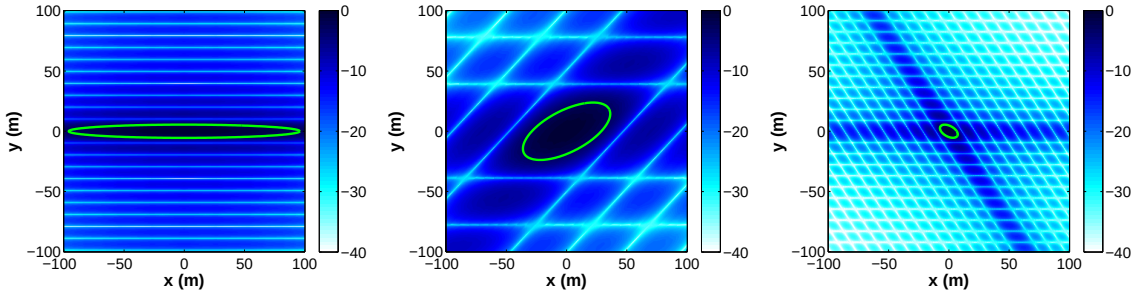

Figure 3.19: PSF for three bistatic pairs used in generating multistatic PSF (Tx1: LTE, az = 0°, range = 7km, F_c = 1850MHz, BW = 945kHz, u=25, Tx2: HDTV, az = −83° , range = 8062km, F_c = 470MHz, BW = 6 MHz, TX3: WiMAX, az = 63°, range=4472km, F_c=2GHz, BW=20MHz, Rx: az = −0.5° to 0.5° in 5e − 4° steps, el = 20°, range = 10km

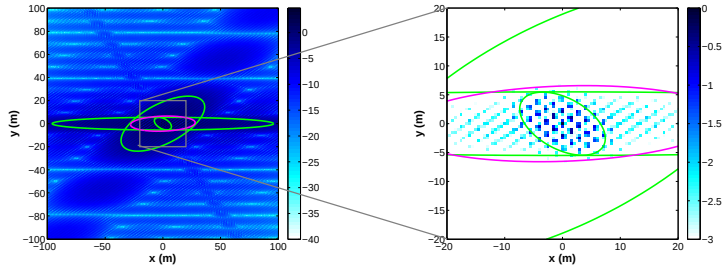

Figure 3.20: Combination of three bistatic PSFs into multistatic PSF with grating lobes outside of resolution ellipse intersection

can be found by multiplying the first element of the matrix $\mathbf{\Sigma}$, the first singular value, by the largest element in the first column of $\mathbf{U}$. Likewise the distance of the minor axis of the ellipse, b, is found by multiplying the second element of the matrix $\mathbf{\Sigma}$, the second singular value, by the largest element in the second column of $\mathbf{U}$. The orientation of the major axis, ξ, is found from $\mathbf{V}$, as it is a matrix with columns representing the orthonormal bases of the row space of the original matrix [35]. The association of the first singular value to the first column of $\mathbf{U}$ is based on the assumption that it is a rotated and scaled set of coordinates corresponding to ($\mathbf{X}$, $\mathbf{Y}$), only along the axis provided by $\mathbf{V}$. This assumed orientation is shown in Figure 3.21. Since it is assumed that the first axis of $\mathbf{V}$ is parallel with the major axis of the ellipse, the largest element of the first column of $\mathbf{U}$ is the

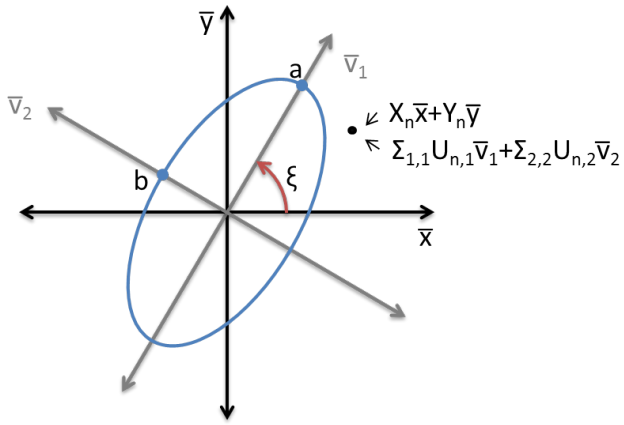

Figure 3.21: Assumed orientation of **V** with respect to resolution ellipse

furthest point along that axis. Likewise the association of the second singular value to the second column of **U** is based on a presumed association with the minor axis. Thus

$$a = \Sigma_{1,1} \max(U_{:,1}) \tag{3.28}$$

$$b = \Sigma_{2,2} \max(U_{:,2}) \tag{3.29}$$

$$\xi = \operatorname{atan}\left(\frac{V_{2,1}}{V_{1,1}}\right) \tag{3.30}$$

3.2.4 Analysis of EMRA Approximation. To analyze the EMRA approximation, combinations of different transmitters at different locations are desirable. In order to set up a large number of unique combinations with limited simulation overhead, a small set of permissible locations for the transmitters is used, along with a set of representative modulation configurations . For determining the accuracy of the EMRA predictions, the set of potential positions puts transmitters at the locations in Table 3.2. Height is treated as a constant 50 meters for all transmitter positions.

The six different potential positions are shown in Figure 3.22. A representative configuration for each modulation is used in each position, with the exception of FM radio

Table 3.2: Table of Potential Positions for EMRA

Azimuth (degrees)	Range (m)
-55	4000
-30	9000
0	4000
15	9000
40	4000
65	9000

which was excluded due to a large expected resolution. For HDTV, the configuration uses a carrier frequency of 470 MHz, near the bottom of the band, with a transmission power of 91 kW, based on the mean power of the reported stations in [13]. The WiMAX configuration uses a frequency of 4 GHz, near the middle of the band, with a bandwidth of 20 MHz, a frame duration of 2.5 milliseconds, a quarter length cyclic prefix, and a 85 dBm power level, or about 316 kW, the same as was assumed in [15]. Finally, for LTE the configuration uses a carrier frequency of 1.85 GHz, near the bottom of the usable band, a Zadoff-Chu sequence based on $u = 25$, and a transmission power of 85 dBm. To avoid interfering frequencies, which would occur when the same communication standard is used at different positions, the frequency is offset based on the position it occupies. The carrier frequency of each signal type is offset by adding a multiple of the index of the position being occupied, based on what modulation was being used. For HDTV the multiples are 6 MHz, for WiMAX the offset is 20 MHz, and for LTE the offset is 5 MHz. This offset allows different images to be added together without consideration of possible interference due to frequency reuse. In addition, a blank modulation corresponding to no transmitter present is also included to account for cases where there are fewer than six transmitters being used for image formation. To facilitate computation time, PSF

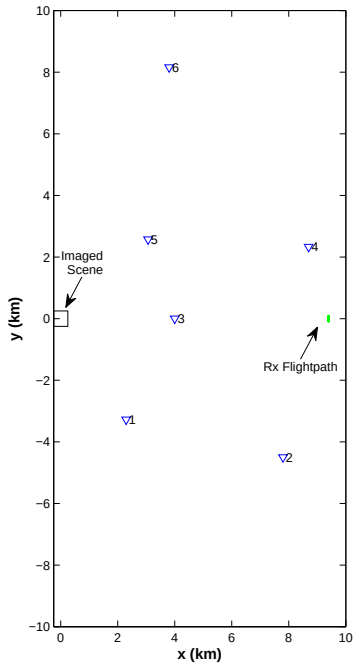

Figure 3.22: Transmitter positions used for multistatic resolution analysis

formation from a given transmitter at a given position is performed before combination and saved for later use, so that backprojection is performed to form the PSF only twenty four times for the EMRA measurements. In summary, for EMRA measurements there will be a combination of four modulation schemes with six possible Tx positions, a total set of $(4^6 - 1) = 4095$ possible combinations excluding the no transmitter case.

In order to compare the theoretical EMRA, a point spread function is used in image formation for each bistatic pair and then combined to form the multistatic image. The image is formed for a square grid of pixels around the center point, representing -150m to 150m in .25m steps in both dimensions. This .25m step resolution is smaller than the smallest expected bistatic resolution (7m). To evaluate the worst case resolution, the multistatic image is formed from a GLRT combination of the separate bistatic images. This means that the image is formed by taking the pixel by pixel maximum absolute value

of the bistatic pair PSFs. For the best case resolution, the point spread functions are added coherently. Because each image is formed from phase history which occupies different frequencies and azimuth angles in phase history space, the irregular sampling leads to the creation of grating lobes as shown in Figure 3.23(b). Rather than ignore this effect, the effective resolution is measured, the EMRA, defined to be the area of an ellipse enclosing the set of points above a threshold of -3dB below the maximum point as described in Section 3.2.

In both cases, the parameters of the resolution ellipse are determined by examining the set of points above the cutoff:

$$(\mathbf{X}, \mathbf{Y}) \quad = \quad \{(x, y) | 10 \log_{10}(\text{PSF}(x, y)) \geq -3\} \tag{3.31}$$

SVD is used to find the parameters of the error ellipse fit to the points as described in (3.28) - (3.30) .

To compare the backprojection simulation result to the fast approximation, the two EMRAs are computed as described in Section 3.2.3, and then plotted together to compare results. The results for all combinations are examined using plots, including plots of the ratio between the approximated and simulated areas and histograms of the difference between the EMRAs.

3.2.5 Multistatic Resolution Results. Comparison of EMRA between the approximated PSF and the PSF formed through backprojection showed more variability for coherent combination of transmitters than GLRT combination. In Figure 3.24(a) the EMRAs are shown for all transmitter configurations for both the combination of PSFs generated through BP and approximation where coherent combination was used. Figure 3.24(b) shows the same results, but for GLRT combination. This plot shows some difference between the two; however, other comparisons provide more insight into the

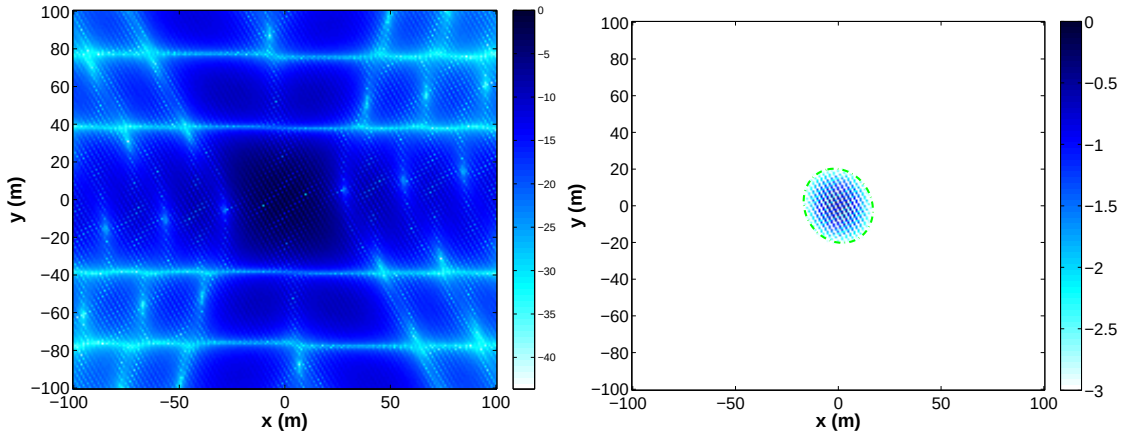

(a) Coherent combination of PSFs

(b) Coherent combination above -3dB

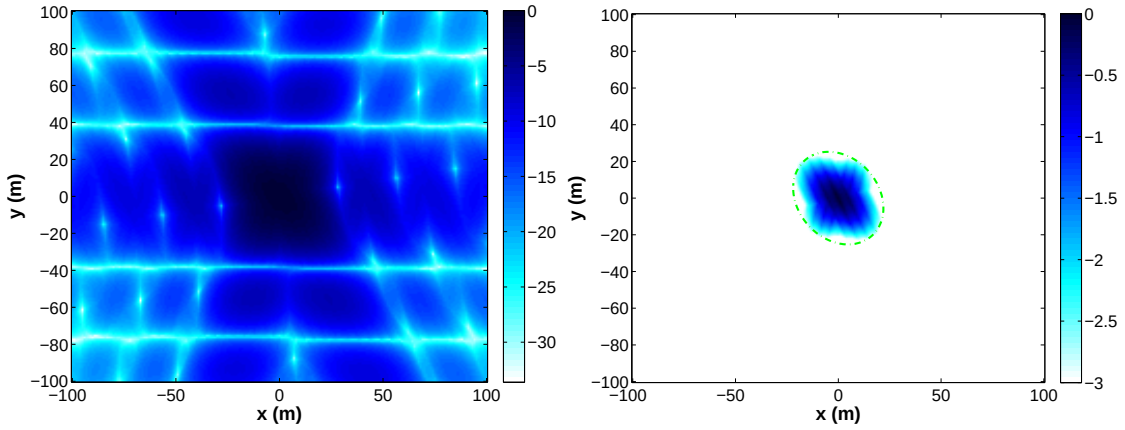

(c) GLRT combination of PSFs

(d) Portion of GLRT combination above -3dB

Figure 3.23: Example of coherent and GLRT combination of two PSFs and resulting portions above -3dB cutoff (Tx1: az=45°, range = 5km, F_c=470MHz, BW=6Mhz, Tx2: az = −25°, range = 5km, F_c=482Mhz, BW = 6MHz, Rx: az = −0.5° to 0.5° in $5e-3$° steps, el = 20°, range = 10km

performance. Examining a histogram of the error between the two EMRA values for each configuration, determined as the difference between the measurement of the resolution for the combination of PSFs generated through backprojection and that of the combination of PSF approximations, shows a tendency toward small error in Figure 3.25.

By itself, measurement of error fails to take into account the difference between cases where error is large but EMRA is also large, such that the error is minor relative to the

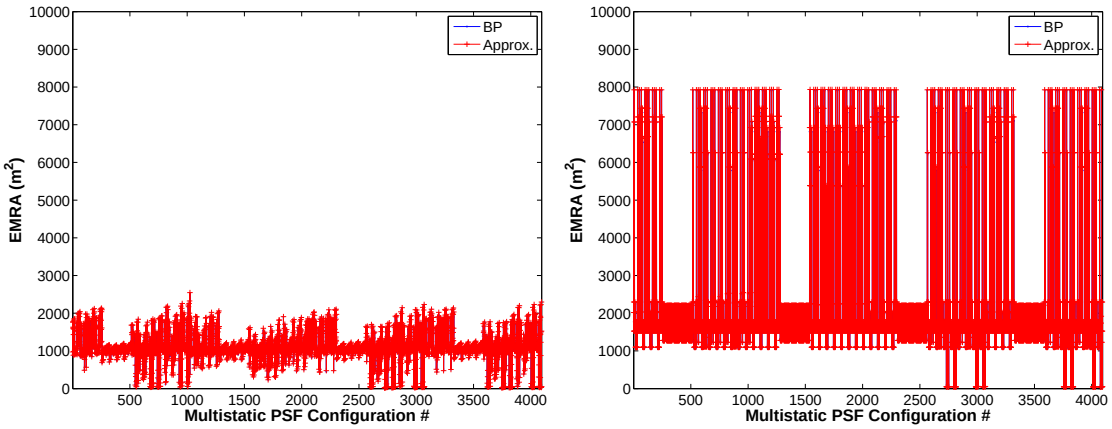

(a) Coherent combination (b) GLRT combination

Figure 3.24: EMRA area for BP PSF and PSF approximation

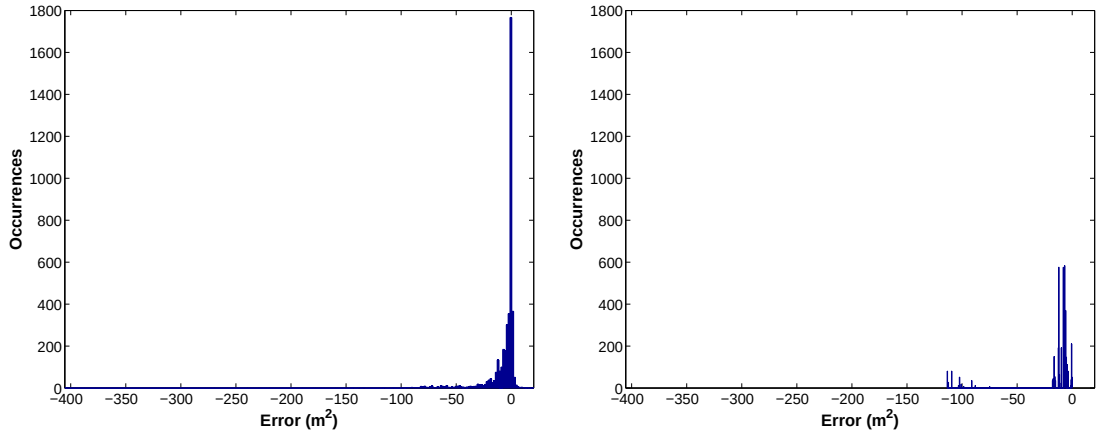

(a) Coherent combination (b) GLRT combination

Figure 3.25: Histogram of error between EMRA from BP PSF to resolution area from PSF approximation

EMRA; and cases where the relative error is large compared to the EMRA, but both are small on an absolute scale. However, examining the results of the ratio of the EMRAs helps mitigate this problem and show results which are generally close. Comparing the ratio between the simulation and the estimate, as seen in Figure 3.26(a) shows that though

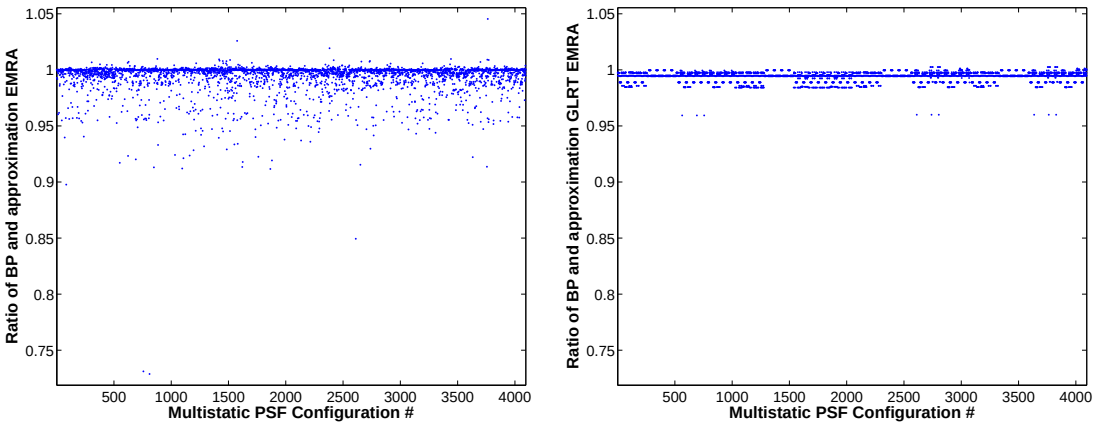

(a) Coherent combination (b) GLRT combination

Figure 3.26: Ratio of EMRA for BP PSF to EMRA for PSF approximation. Coherent combination has a mean ratio of 0.994 and standard deviation of 0.01341. GLRT combination has a mean ratio of 0.994 and standard deviation of 0.00433

there are many cases where the two EMRAs are nearly the same, the mean of the set of ratios being 0.994 with a standard deviation of 0.0134. There are some cases where either the EMRA from the simulation or the estimate is up to 1.37 times the other EMRA.

In contrast to the coherent combination results, the EMRA of the GLRT combination approach seem to be dominated by a few or even one main transmitter. This results in EMRA which are repetitive as shown in Figure 3.24(b). A histogram of the difference between the two GLRT EMRAs is shown in Figure 3.25(b) which highlights the fact that the EMRA from the PSF approximation tends to be larger than the EMRA formed through back projection. In the histogram there are a few values which show up repeatedly, creating a sparse histogram. The ratios are similarly repetitive as shown in Figure 3.26(b). Here the results of simulation and estimation tend to be closer, having a mean ratio of 0.994 and a standard deviation of 0.00433, and range between extremes of 0.959 and 1.003.These differences in the results between coherent addition and GLRT prompted a closer look at some of the more extreme errors.

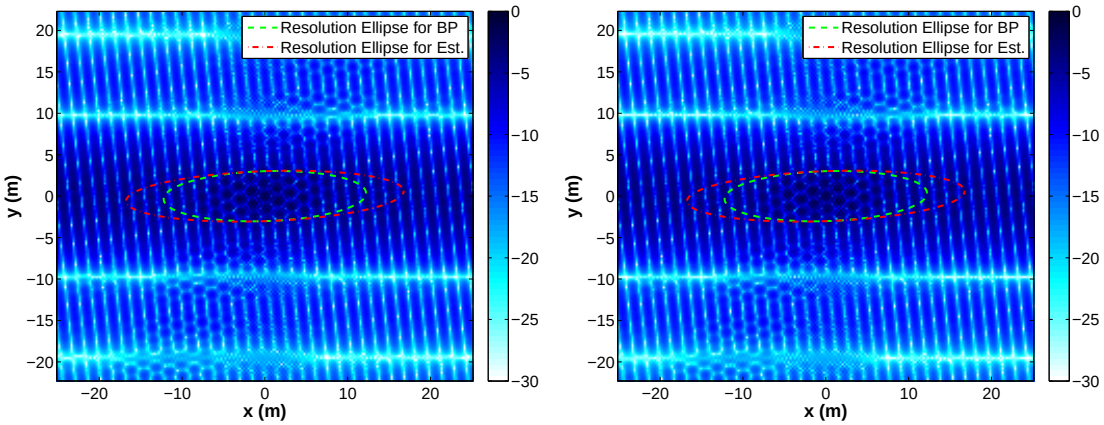

(a) Backprojection (b) Fast Approximation

Figure 3.27: Multistatic PSF for run 811 formed through coherent combination of (a) BP bistatic PSFs and (b) fast approximation bistatic PSFs, with resolution ellipses

The run with the lowest ratio of EMRA from backprojection to EMRA from fast approximation is run 811, with a ratio of 0.729. This run consists of five transmitters, two LTE transmitters at 15°, and 65°, and three WiMAX transmitters at -55°, -30°, and 0°. This corresponds to carrier frequencies at 1.87 GHz, 1.88 GHz, 4.02 GHz, 4.04 GHz, and 4.06 GHz respectively. The multistatic PSFs for run 811 are shown in Figure 3.27. Reducing the extent of the approximate PSF to show only the portion above -3dB in Figure 3.28 shows where the difference comes from. The approximate PSF, as shown in 3.28 (b) has pixels located at (-16.75,-0.5) and (16.75,0.5) which are -2.998 dB down from the maximum value. This may indicate that setting the threshold of the EMRA at -3dB in accordance with convention will not alway results in the best agreement between the approximation and backprojection.

The run with the highest ratio of EMRA from backprojection to EMRA from fast approximation is run 3763, with a ratio of 1.05. This run consists of four transmitters, one LTE Tx at -30°, and three WiMAX transmitters at −55°, 15°, and 40°. This corresponds to carrier frequencies at 1.86GHz, 4.02GHz, 4.08 GHz, and 4.1 GHz respectively. The

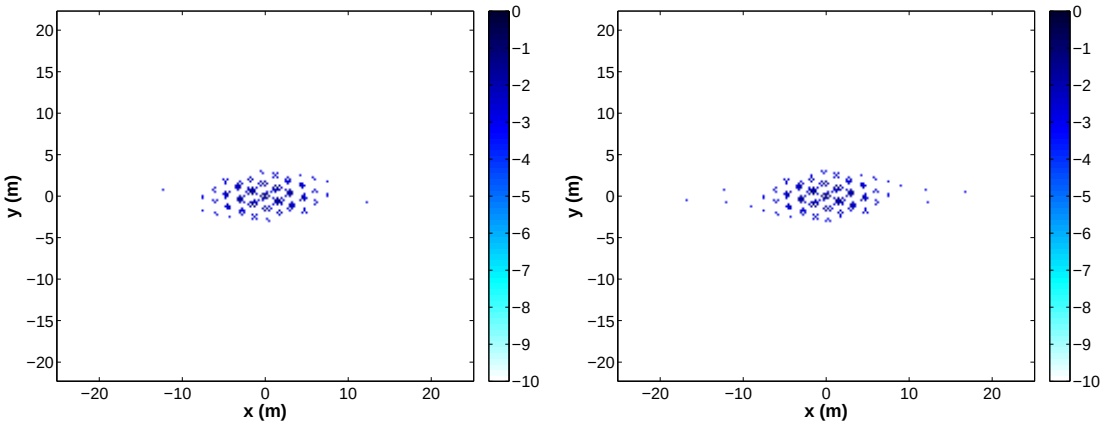

(a) Backprojection PSF above -3 dB (b) Approximated PSF above -3 dB

Figure 3.28: Approximate and backprojeciton multistatic PSF for run 811 above -3 dB threshold formed through coherent combination

multistatic PSFs for run 3763 are shown in Figure 3.29. The same approach as was used to display the difference the threshold made for run 811 is applied to 3763. Reducing the extent of the approximate PSF to show only the portion above -3dB in Figure 3.30 shows the differences between the approximation and backprojection PSF. This time, pixels in the approximation PSF located at (-5.5,1.25) and (5.5,-1.25) having normalized values of -2.998 have changed the resolution ellipse enough that the area is slightly larger than the backprojection PSF.

In the case of GLRT combination, runs 564, 692, and 756 all have a ratio of BP to approximation EMRA of 0.959 and similar PSFs to each other. Runs 2731, 2735, 2747, 2751, 2795, 2799, 2811, 2815, 3755, 3759, 3771, 3775, 3819, 3823, 3835, and 3839 all have a ratio of BP to approximation EMRAs of 1.003 and similar PSFs to each other. Run 564 is examined as an example of one of the worst ratios of EMRA for the GLRT combination. Run 564 consists of four transmitters, three LTE Tx at $-30°$, $15°$, and $65°$, and one WiMAX transmitter at $40°$. This corresponds to carrier frequencies at 1.86GHz, 1.87GHz, 1.88 GHz, and 4.1 GHz respectively. The multistatic PSFs for run 564 are

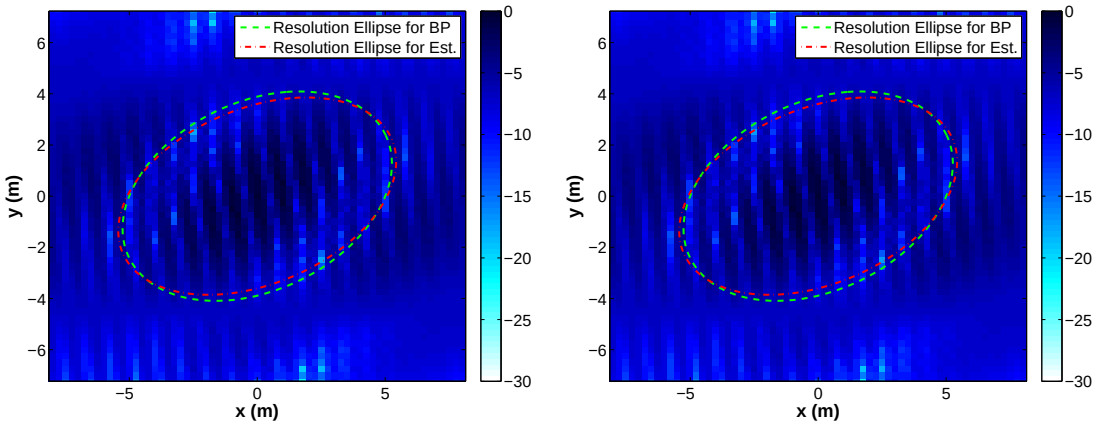

(a) Backprojection (b) Fast Approximation

Figure 3.29: Multistatic PSF for run 3763 formed through coherent combination of (a) BP bistatic PSFs and (b) fast approximation bistatic PSFs, with resolution ellipses

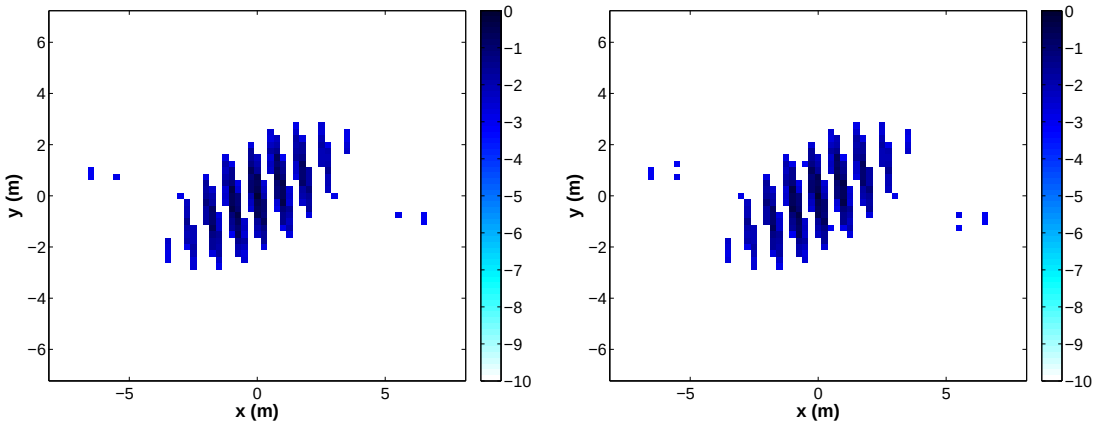

(a) Backprojection PSF above -3 dB (b) Approximated PSF above -3 dB

Figure 3.30: Approximate and backprojeciton multistatic PSF for run 3763 above -3 dB threshold formed through coherent combination

shown in Figure 3.31. The two PSFs appear similar and have very little difference, except that the approximation PSF contains multiple pixels further along the cross range above the threshold.

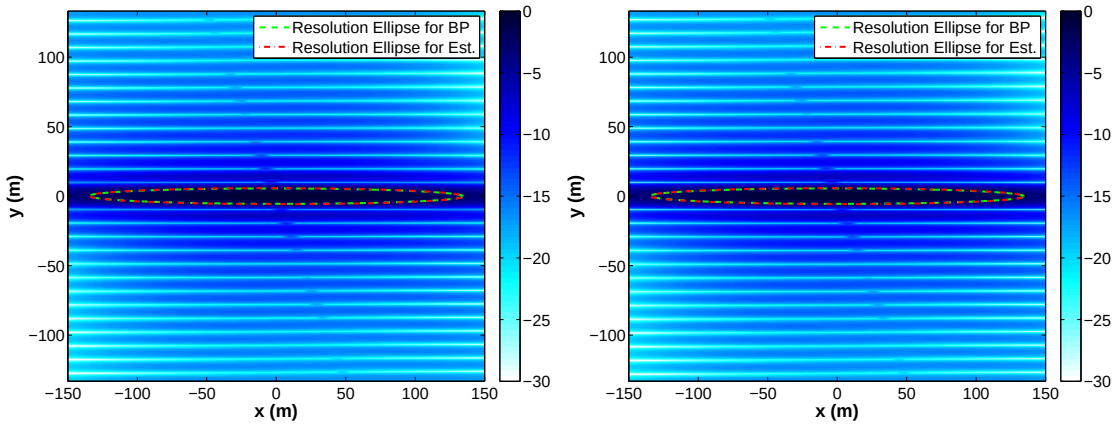

(a) Backprojection (b) Fast Approximation

Figure 3.31: Multistatic PSF for run 564 formed through GLRT combination of (a) BP bistatic PSFs and (b) fast approximation bistatic PSFs, with resolution ellipses

Differences in the way the PSF images formed through backprojection and through the PSF approximation add constructively and destructively are assumed to be the main cause of variation between the EMRAs for a given transmitter configuration. The threshold of the EMRA was originally set at -3dB, however it would change the agreement between EMRA for backprojection and approximation if the threshold is changed slightly. For example, if the threshold is changed to -2.5 dB, the set of ratios would then have a mean of 0.994 and standard deviation of 0.0154 with a maximum ratio of 1.157 and a minimum of 0.626. Likewise if the threshold is changed to -3.5 dB, the set of ratios would then have a mean of 0.995 and standard deviation of 0.0177 with a maximum ratio of 1.82 and a minimum of 0.815. The -3dB threshold is maintained as a conventional cutoff, however the potential effect a single pixel difference due to the threshold on the EMRA should be understood.

Another factor influencing the EMRA results is the PSF's pixel size. Previously, 0.25 m square pixels were used. To check the dependence on pixel size, the test is run with 0.15 m square pixels and a -3dB threshold. The histogram of the difference between the

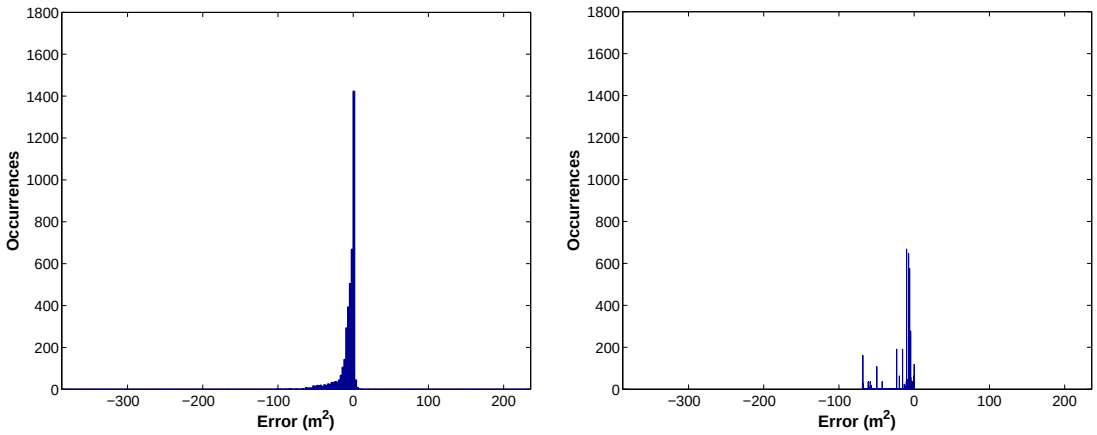

(a) Coherent combination (b) GLRT combination

Figure 3.32: Histogram of error between EMRA from BP PSF to EMRA from PSF approximation when using 0.15 m by 0.15 m pixels to determine EMRA

area from backprojection and the area from approximation shown in Figure 3.32. Ratios of the area for backprojection to the area from approximation are shown in Figure 3.33. For the ratios of the coherently combined PSFs, the mean is 0.994, the standard deviation is 0.0136, the maximum ratio is 1.36 for configuration 1096, and the minimum ratio is 0.627 for configuration 1187. For the ratios of the PSFs combined through GLRT, the mean is 0.994, the standard deviation is 0.00461, the maximum ratio is 1 for 108 different configurations; and the minimum ratio is 0.944 for configurations 2988, 2992, 3052, 3056, 4012, 4016, 4076, and 4080.

The variability in the EMRA results between fast approximation and backprojection are much smaller when using the smaller pixels. This would be expected as small differences in the grating lobes is captured by finer calculation of the PSF. As a check on the effect, Figure 3.34 shows the results for run 811 using the smaller pixels. In this case, more pixels above the threshold are captured.

Though in general, the agreement between backprojection and the fast approximation is improved by using smaller pixels to calculate the EMRA, there are two notable outliers,

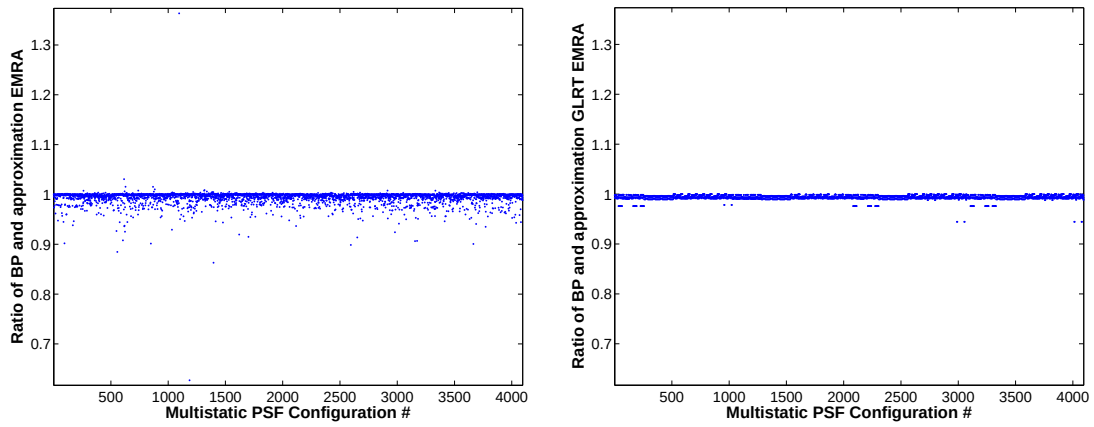

(a) Coherent combination (b) GLRT combination

Figure 3.33: Ratio of EMRA for BP PSF to EMRA for PSF approximationusing 0.15 m by 0.15 m pixels to determine EMRA, coherent combination has a mean ratio of 0.994 and standard deviation of 0.0136, GLRT combination has a mean ratio of 0.994 and standard deviation of 0.00461

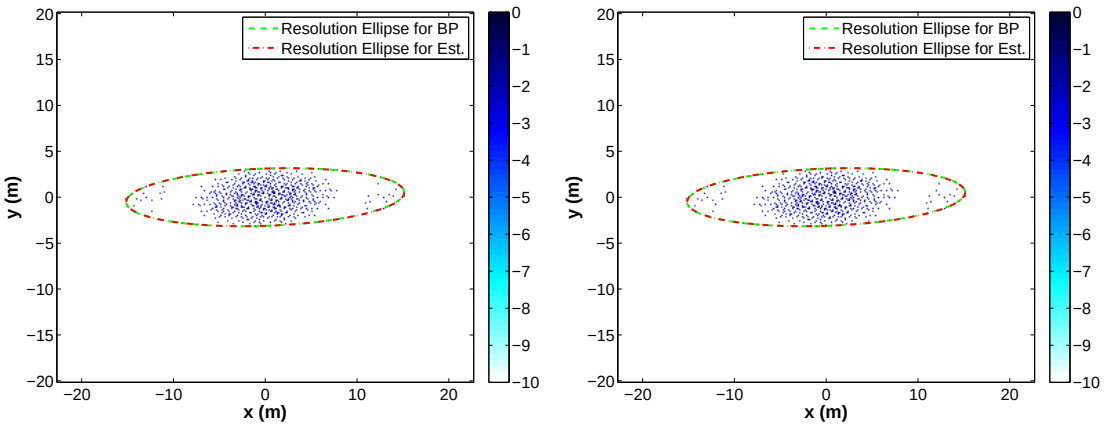

(a) Backprojection (b) Fast approximation

Figure 3.34: Approximate multistatic PSF for run 811 formed through coherent combination for 0.15 m square pixels by (a) backprojection and (b) fast approximation, with resolution ellipses

configurations 1096 and1187. As in runs 811 and 3763 for the 0.25 m by 0.25 m pixel case, the large difference between the backprojection and fast approximation EMRA can be attributed to a few pixels with values close to the threshold for both configurations. Run 1096 has pixels at (-2.4,11.85) and (2.4,-11.85) with a normalized value of -2.998 dB in the backprojection PSF which is below the threshold in the fast approximation. Run 1187 has pixels at (-52.2,0.15) and (52.2,-0.15) with a normalized value of -3dB in the fast approximation which is below the threshold in the backprojection PSF.

Based on the results of comparison between the EMRA generated through fast approximation and backprojection, the fast approximation is determined to be appropriate for the purpose of comparing different sets of emitters. The fast approximation will tend to be pessimistic and on average produce slightly larger EMRA values. When calculating the EMRA, the effect of the PSF's pixel size should be considered, since smaller pixels will produce more consistent results but require more time to compute.

4 Multistatic Contrast Ratio

This chapter develops the multistatic DTCR and PTCR. To facilitate this, fast approximations of the ISLR and AMBR are developed to allow speedy calculation. Once these are developed, test scenarios are presented for comparison of the fast approximations against simulation using backprojection. The results of the comparison are presented following the scenario to demonstrate the appropriateness of the approximation. After development and simulation of both the ISLR and AMBR approximations, multistatic DTCR and PTCR are developed. Scenarios to compare the approximation to a simulation of DTCR are presented. PTCR is assumed to have the same dependence on an accurate calculation of MNR, but because DTCR allow for a simulation that includes the average effect in a region, only DTCR is examined. The chapter is concluded by the result of the comparisons between approximation and simulated DTCR.

4.1 ISLR Approximation

Rather than simulate a large number of scatterers, then measure their effect on a given pixel, it is simpler to measure the ratio of energy in the pixels outside a single scatterer to the pixel containing it. This assumes that when forming an image, scatterers exist at all points around a measured pixel, such that through superposition the effect is that of the sums of all points outside of the center. Thus, in the evaluation of ISLR for this application, the ratio is determined by examining the point spread function (PSF) for the various bistatic configurations within the scenario. The ISLR estimate is determined based on descriptions in [7] and [37] as

$$\text{ISLR} = \frac{\sum_{\{x,y:\text{PSF}(x,y)<-3dB\}} |\text{PSF}(x,y)|}{\sum_{\{x,y:\text{PSF}(x,y)\geq-3dB\}} |\text{PSF}(x,y)|}. \tag{4.1}$$

Assuming that the PSF has been normalized, such the maximum value in the mainlobe is 0 dB. A faster approximation of this value may be obtained using the PSF approximation, thus

$$\widetilde{\text{ISLR}} = \frac{\sum_{\left\{x,y:\widetilde{\widetilde{\text{PSF}}}(x,y)<-3dB\right\}} \left|\widetilde{\widetilde{\text{PSF}}}(x,y)\right|}{\sum_{\left\{x,y:\widetilde{\widetilde{\text{PSF}}}(x,y)\geq-3dB\right\}} \left|\widetilde{\widetilde{\text{PSF}}}(x,y)\right|}. \tag{4.2}$$

4.1.1 Analysis of Integrated Sidelobe Ratio. ISLR is present in all simulation involving multiple reflectors, since the addition of side lobes from a different reflector into a pixel can change the measurement of a given reflector. This section looks at two aspects of simulating the ISLR, the effect of pixel size on the results, and the possibility of using the fast approximation to arrive at a similar value to that produced by backprojection, but faster. The PSF of bistatic pairs are generated through backprojection and fast approximation for a range of possible values of transmitter locations, bandwidths, and frequencies based on the communications standards discussed in Section 2.4. The selected values for this simulations used throughout this chapter are shown in Table 4.1. The PRI will not impact the way ISLR is calculated, and so this is not used as a variabile during simulation, however it is presented here as part of the set of variables used for simulation in AMBR and DTCR. Transmitters are given a height of 25 m, which is not expected to impact the ISLR calculations significantly, but does reduces some of the required calculations for the AMBR and DTCR tests, by decreasing the radar horizon.

The simulation uses a receiver flying at an elevation of 20° and azimuth between −0.5° and 0.5° in 1/1500° steps at a range of 7 km. The transmitters are simulated having the values in Table 4.1 progressing through carrier frequency first, then bandwidth, then finally transmitter azimuth values. Thus, the first transmitter would have an azimuth of −50°, a 470 MHz carrier, and a 4 MHz bandwidth, followed by a transmitter with a 1235 MHz carrier frequency, but otherwise the same values. Likewise the fourth transmitter

Table 4.1: Table of Potential Tx Parameters for DTCR Simulations

Carrier (MHz)	Bandwidth (MHz)	PRI (μs)	Azimuth (deg)	Range (m)	Height (m)
470	4.0	60	-50	5000	25
1235	5.875	105	-28		
2000	7.75	150	-0		
			-89		

simulated would have the same values as the first except the bandwidth would change to 5.875 MHz. This progression continues until the final transmitter having an azimuth of 89°, a 2000 MHz carrier, and a 7.75 MHz bandwidth.

The extent of the PSF formed by backprojection and the fast approximation has to be fixed at some value for calculation. The limit used in this simulation is found based on the theoretical cross range resolution, as presented in (2.73), multiplied by the number of samples along the flight path. Cross range resolution is used because it is expected to be smaller than down range, and thus be more limiting. This is similar to limitation on the size of a scene to be imaged discussed in [20]. The resulting PSF is separated out into points above the -3dB threshold below the maximum value and those points below it in order to be added together according to (4.1) for the simulation and (4.2) for the approximation. The resulting ISLR is compared for different square pixel sizes based on oversampling the cross range resolution of the bistatic pair. The oversampling values used are 0.5 (representing a coarser resolution than the pair provides), 1 (representing the expected resolution), 2, and 4. The ISLR based on oversampling factors of 8 and 16 are calculated using only the fast approximation method to check that the results settle into similar values as the oversampling factor increases. The results are plotted together for comparison.

4.1.2 ISLR Approximation Results. The result of various oversampling factors comparing backprojection and fast approximation ISLR is shown in Figure 4.1. In each of the four oversampling factor values used, the pattern of the change from one configuration to another is similar between ISLR determined using backprojection and ISLR determined using the fast approximation. However the values of ISLR for the approximation tend to be smaller than the ISLR from backprojection. Unfortunately, for those configurations with a transmitter azimuth of 89° (runs 28-36), the patterns of the change due to changes in frequency and bandwidth of the two ISLR values appear to diverge more than for other azimuth values. Furthermore, the ISLR arrived at through both methods depends on the oversampling. By increasing the oversampling, the ISLR for a given configuration first becomes large, as the number of pixels outside the mainlobe increases. The increase due to finer sampling can be seen in the difference between Figures 4.1(a) and (b). The ISLR then starts to decrease with increased oversampling as more pixels within the mainlobe of the PSF begin to be incorporated in the numerical integration. The decrease due to finer sampling can be seen in the difference between Figures 4.1(c) and (d).

As would be expected with numerical integration, the trend of the ISLR value should be to settle into one value for larger and larger oversampling factors. To check the trend, the ISLR from more oversampling factors than were previously used are calculated. In this case, only the fast approximation is used, though the previous results indicate that backprojection would have similar dependence on the configuration, though a larger ISLR. The set of ISLR values are shown in Figure 4.2, and this indicates that as the oversampling increases, the ISLR settles into a fixed value for a given configuration. For ease of comparison, an expanded view of 4,8 and 16 times oversampling is shown in Figure 4.3. These results would seem to indicate that an oversampling factor of at least four would be preferable when finding the ISLR. However, in Section 4.3.2, results of simulation of DTCR indicate better agreement for simulation purposes may be achieved

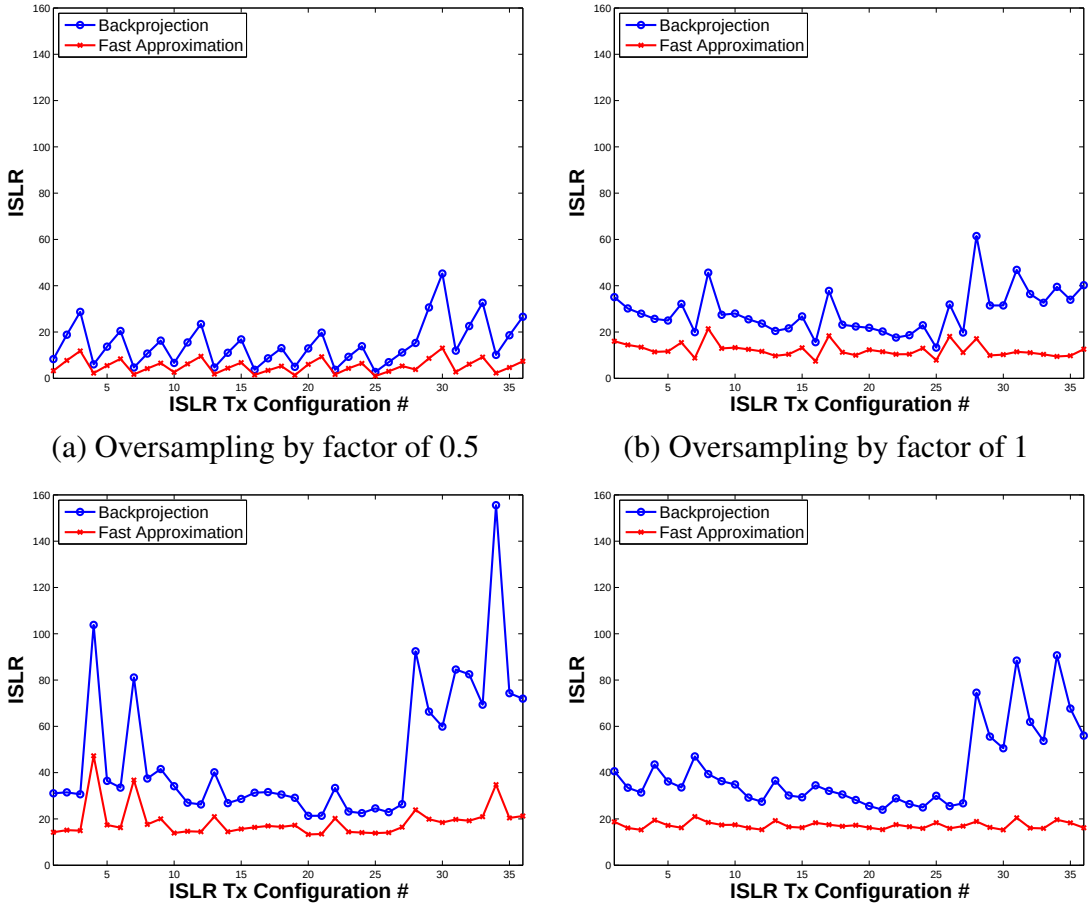

(a) Oversampling by factor of 0.5

(b) Oversampling by factor of 1

(c) Oversampling by factor of 2

(d) Oversampling by factor of 4

Figure 4.1: Plot of ISLR results from backprojection and fast PSF approximation using different oversampling factors for the pixel resolution

by matching the resolution of the ISLR evaluation with the point scatterer spacing used to generate the phase history.

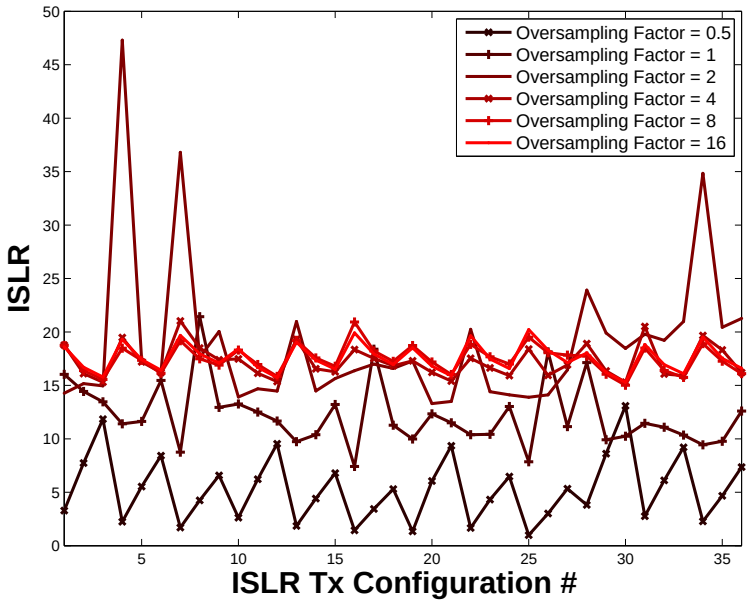

Figure 4.2: ISLR from multiple oversampling values generated using the fast approximation method

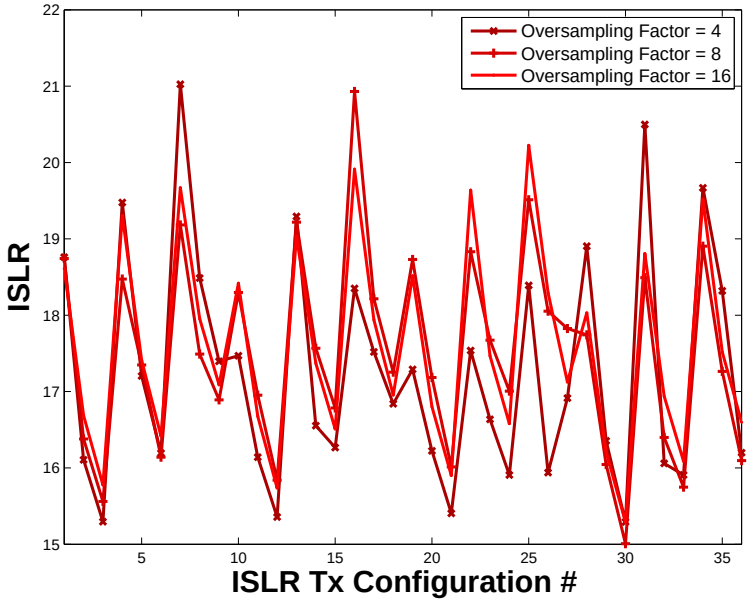

Figure 4.3: Expanded view of ISLR from 4, 8, and 16 times oversampling values generated using the fast approximation method

4.2 AMBR Approximation

Based on the approach for image formation being used, the ambiguities due to Doppler shifts surpassing half the PRF are assumed to be filtered out prior to image formation, leaving PRI as the primary source of ambiguities. For a given scenario, the ambiguities are assumed to be coming from the expected clutter returns from isorange contours of the bistatic radar at multiples of the PRI as shown in Figure 4.4. Thus, a fast approximation of the AMBR is developed as the numerical integral of all portions of all ambiguous isorange ellipses which fold into the scene.

The first step to approximating the AMBR is to limit the number of calculations to only the necessary isorange ellipses. The number and extent of the isorange contours folding into the scene center are limited by the radar horizon of the bistatic radar. The radar horizon is assumed to be primarily limited by the transmitter, which will be near the ground and thus have a much more limited horizon than the aircraft. Thus, the radar horizon varies between bistatic pairs. The radar horizon range, R_h is given in [3] as

$$R_h = \sqrt{h_a^2 + 2h_a a_e} \tag{4.3}$$

Where h_a is the height above the earth and a_e is the effective radius of the earth, modeled as $\frac{4r_e}{3}$. The radius of the earth is approximated as 6371 km [3]. The FCC website gives information about the height of TV and FM transmitters height relative to the average terrain. For TV, tower height ranges between -1156 and 2530.3 meters, with an average of 132.9 meters [13]. For FM, tower height ranges between -827 and 1531 meters, with an average of 87.4 meters [12]. LTE and WiMAX are assumed to be between 50 and 200 meters above the ground [11]. Clearly there is no single height estimate which will be representative, but rather height will depend on the scenario.

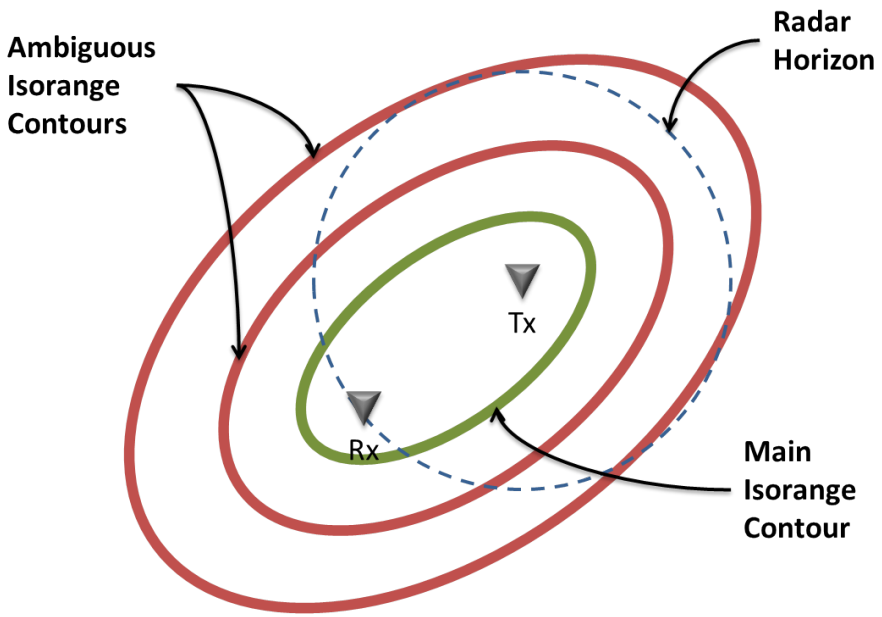

Figure 4.4: Ambiguous isorange contours and radar horizon

The number of ambiguous isorange contours to be included, N_a, can be found by using (2.5), given a total range to the last ambiguity, N_a, of

$$R_{tot} = R_{Tx} + R_{Rx} = c(T_c + N_a\text{PRI}), \tag{4.4}$$

where T_c is the delay to the scene center, which is assumed to be closer than any ambiguities, but in the general case could be the result of taking the modulus of the delay with respect to the PRI. Note that R_{Rx} is assumed to be constant for all pulses for spotlight mode SAR. To determine N_a, the distance from the transmitter to the nearest point on the isorange contour for the N_a^{th} ambiguity must be less than the radar horizon. Since the major axis parameter a will always be the range from the center of the Tx-Rx pair to the

point on the isorange contour closest to the Tx:

$$\begin{aligned} a - \frac{L}{2} &\leq R_h \\ \frac{R_{Tx} + R_{Rx}}{2} - \frac{L}{2} &\leq R_h \\ \frac{c(T_c + N_a(PRI))}{2} - \frac{L}{2} &\leq R_h \\ T_c + N_a(\text{PRI}) &\leq \frac{2R_h + L}{c} \\ N_a &\leq \frac{1}{\text{PRI}}\left(\frac{2R_h + L}{c} - T_c\right) \end{aligned} \tag{4.5}$$

where L is the baseline length, the distance between the transmitter and receiver. So, to find the number of ambiguities for the approximation, pick

$$N_a = \left\lfloor \frac{1}{\text{PRI}}\left(\frac{2R_h - L}{c} - T_c\right)\right\rfloor \tag{4.6}$$

Now, the AMBR can be expressed as the sum of the reflected signal from the various ambiguous isorange contours which fold into the scene, with the average clutter backscatter coefficient divided out:

$$\widetilde{\text{AMBR}} = \frac{1}{\sigma_0}\sum_{n=1}^{N_a}\int_{\psi:R_{Txn}(\psi)\leq R_h} S_n(\psi)d\psi \tag{4.7}$$

where ψ is the angle to the point on the ellipse. The reflected signal power, $S_n(\psi)$, can be found similar to the previously described SNR in (2.58), for the range ambiguities as

$$S_n = \left(\frac{P_T\lambda^2 A_n\sigma_0}{(R_{Txn}(\psi)R_{Rxn}(\psi))^2}\right)\left(\frac{G_T G_R F_T^2 F_R^2}{(4\pi)^3 L_T L_R}\right), \tag{4.8}$$

Note that the reflectivity is expressed as the product of a clutter reflectivity factor, σ_0, and the area of clutter illuminated, A_n [34]. The average clutter reflectivity factor is multiplied by the MNR in the DTCR/PTCR equations, and so this term is removed while calculating

the AMBR. The inclusion of the area implies that the isorange contours are treated as having some width. This width is determined by the radar's resolution, δ_r. Also note that now the ranges from the transmitter and receiver to a point on the n^{th} ambiguous isorange ellipse, R_{Txn} and R_{Rxn} are put in terms of the angle ψ. ψ is the angle to a point on the ellipse defined by (2.4) from the center of the bistatic pair. So now rewriting (4.7) gives

$$\widetilde{\text{AMBR}} = \left(\frac{P_T \lambda^2 G_T G_R F_T^2 F_R^2}{(4\pi)^3 L_T L_R}\right) \sum_{n=1}^{N_a} \int_{\psi: R_{Txn}(\psi) \leq R_h} \left(\frac{A_n}{(R_{Txn}(\psi) R_{Rxn}(\psi))^2}\right) d\psi \tag{4.9}$$

The ranges from the transmitter to a point on the n^{th} ambiguous contour at $(\hat{X}_n(\psi), \hat{Y}_n(\psi), \hat{Z}_n(\psi))$ are, for the sake of clarity, explicitly:

$$\begin{aligned} R_{Txn}(\psi) &= \sqrt{\left(X_{Tx} - \hat{X}_n(\psi)\right)^2 + \left(Y_{Tx} - \hat{Y}_n(\psi)\right)^2 + \left(Z_{Tx} - \hat{Z}_n(\psi)\right)^2} \\ R_{Rxn}(\psi) &= \sqrt{\left(X_{Rx} - \hat{X}_n(\psi)\right)^2 + \left(Y_{Rx} - \hat{Y}_n(\psi)\right)^2 + \left(Z_{Rx} - \hat{Z}_n(\psi)\right)^2}. \end{aligned} \tag{4.10}$$

To simplify the calculation, the integration indicated in (4.9) is performed numerically by splitting the N isorange contours into M discrete segments. The center of each isorange contour segment is found using (2.4). Though this provides a point, and thus the ranges required, the area of the isorange contour segment A_n is still needed to calculate (4.9). Thus each isorange contour segment is assumed to have an angular extent to the bisector between itself and its neighboring points, and a width dependent on the radar's resolution, δ_r. In (2.9), the area of a segment of an ellipse was provided, so the area of an isorange contour segment could be found from the difference betweenA_{+nm} which is a an ellipse segment with total range increased by half δ_r, and A_{-nm}, an ellipse segment decreased by half δ_r, as shown in Figure 4.5. Thus the area of the n^{th} isorange contour's m^{th} segment is then given by

$$A_{nm} = A_{+nm} - A_{-nm}, \tag{4.11}$$

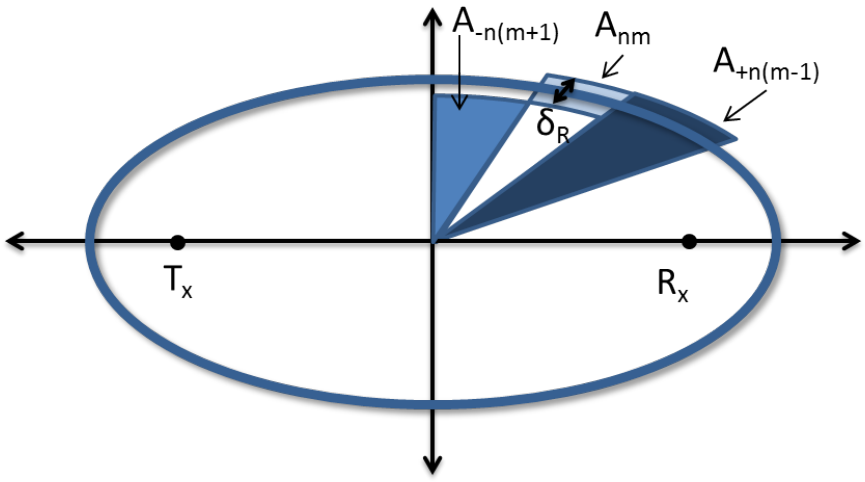

Figure 4.5: Wedges of ellipse used to find area of a segment

However increasing the extent of the ellipse wedge by $\delta_r/2$ requires evaluating (2.9) with different values of a and b. The n^{th} ellipses a and b parameters are found for upper and lower bounds of the segment using (4.4) and (2.5) to produce:

$$\begin{aligned} a_{+n} &= \frac{c(T_c + n(PRI)) + \delta r}{2} \\ b_{+n} &= \sqrt{a_{+n}^2\left(1 - \left(\frac{L}{c(T_c + n(PRI)) + \delta r}\right)^2\right)} \\ a_{-n} &= \frac{c(T_c + n(PRI)) - \delta r}{2} \\ b_{-n} &= \sqrt{a_{-n}^2\left(1 - \left(\frac{L}{c(T_c + n(PRI)) - \delta r}\right)^2\right)} \end{aligned} \tag{4.12}$$

So now, using (2.9), the area of the larger ellipse segment is:

$$\begin{aligned} A_{+nm} = \frac{a_{+n}b_{+n}}{2}\Bigg(&\arctan\left(\frac{a_{+n}}{b_{+n}}\tan\left(\hat{\psi}_m + \frac{\pi}{M}\right)\right) - \\ &\arctan\left(\frac{a_{+n}}{b_{+n}}\tan\left(\hat{\psi}_m - \frac{\pi}{M}\right)\right)\Bigg), \end{aligned} \tag{4.13}$$

and the smaller ellipse segment is

$$A_{-nm} = \frac{a_{-n}b_{-n}}{2}\Bigg(\arctan\left(\frac{a_{-n}}{b_{-n}}\tan\left(\hat{\psi}_m + \frac{\pi}{M}\right)\right) - \arctan\left(\frac{a_{-n}}{b_{-n}}\tan\left(\hat{\psi}_m - \frac{\pi}{M}\right)\right)\Bigg). \tag{4.14}$$

Now, (4.9) is implemented as a summation, with the limits of integration replaced by the unit step function,

$$u(x) = \begin{cases} 0 & x < 0 \\ 1 & x \geq 0 \end{cases}, \tag{4.15}$$

to become:

$$\widetilde{\text{AMBR}} = \left(\frac{P_T\lambda^2 G_T G_R F_T^2 F_R^2}{(4\pi)^3 L_T L_R}\right)\sum_{n=1}^{N_a}\sum_{m=1}^{M}\frac{u(R_h - R_{Txn}(\hat{\psi}_m))A_{nm}}{(R_{Txn}(\hat{\psi}_m)R_{Rxn}(\hat{\psi}_m))^2} \tag{4.16}$$

4.2.1 Analysis of Ambiguity Ratio. Analysis of AMBR uses the same scenarios as in Section 4.1.1 but now must include the effect of PRI in Tabel 4.1. In order to simulate the effects of the AMBR, the area outside of the scene is simulated. A set of points centered around the transmitter, ambiguous with the scene being imaged, and within the radar horizon, is added to the phase history at 71.4 m steps in the x and y axis, to create a 2000m x 2000m scene with 29x29 pixels. The clutter backscatter coefficient is $\bar{\sigma_0} = -10$dB as in [7]. An example of the resulting scene is shown for the first configuration in Figure 4.6 where both full and partial ambiguous isorange contours are visible. The phase history generation and backprojection were performed using the near field equations so that differential ranges resulting in delays greater than the PRI for a given transmitter could be adjusted to create ambiguities. Inclusion of ambiguities into phase history was accomplished by taking the modulus of the range to the scene center, as

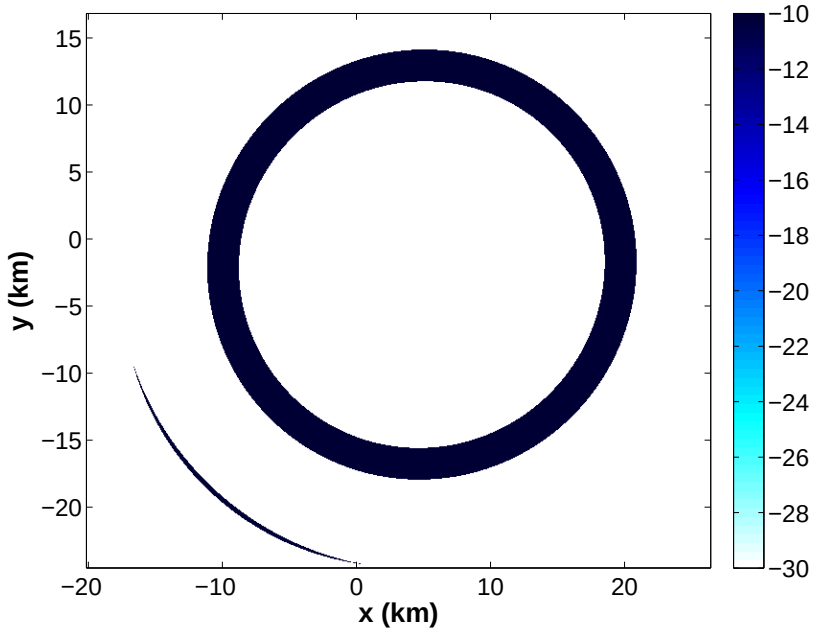

Figure 4.6: Example scene used for simulating AMBR via phase history generation and image formation through backprojection, for configuration 1 with Tx. azimuth -50°, carrier frequency 470 MHz, PRI 60 μs, and bandwidth 4 MHz

well as the modulus of the range to all points within the scene, with respect to the PRI and then finding the difference between the two.

$$R_c = \sqrt{X_{Tx}^2 + Y_{Tx}^2 + Z_{Tx}^2} + \sqrt{X_{Rx}^2 + Y_{Rx}^2 + Z_{Rx}^2} \tag{4.17}$$

is the range to the scene center, and

$$\begin{aligned} R_s \quad = \quad & \sqrt{(X_{Tx} - X_S)^2 + (Y_{Tx} - Y_S)^2 + (X_{Tx} - Z_S)^2} + \\ & \sqrt{(X_{Rx} - X_S)^2 + (Y_{Rx} - Y_S)^2 + (X_{Rx} - Z_S)^2} \end{aligned} \tag{4.18}$$

is the range to a given point 'S'. The modulus is taken so that the new values are

$$\begin{aligned} \hat{R}_c &= c\,\mathrm{PRI}\left(\frac{R_c}{c\,\mathrm{PRI}} - \left\lfloor \frac{R_c}{c\,\mathrm{PRI}} \right\rfloor\right) \\ \hat{R}_s &= c\,\mathrm{PRI}\left(\frac{R_s}{c\,\mathrm{PRI}} - \left\lfloor \frac{R_s}{c\,\mathrm{PRI}} \right\rfloor\right) \end{aligned} \tag{4.19}$$

so that now the differential range used in image formation, modified to allow for ambiguities is

$$\Delta R = \hat{R}_c - \hat{R}_s \tag{4.20}$$

The resulting AMBR is found by creating an image through backprojection for a scene of 29x29 pixels corresponding to a 2000m x 2000m region centered on the scene center. This spacing provides a scene which is within the expected resolution of any of the transmitter configurations used. The number of pixels used effectively creates a number of sample points (841 in this case) where the ambiguous backscatter fold in is measured. Thus, the mean backscatter in the recovered image is divided by the scene's average backscatter coefficient $\bar{\sigma_0}$ to obtain the simulated AMBR. The results of the fast approximation of the AMBR and the simulated AMBR are compared by plotting results by configuration on linear and log scales.

4.2.2 AMBR Approximation Results. The AMBR measurement resulting from simulation are shown in Figure 4.7. The fast approximation seems to be a pessimistic estimate of the AMBR, since the AMBR values arrived at through the backprojection based simulation are much smaller. On average the fast approximation AMBR is 263.49 times larger than the backprojection based simulations AMBR values, for those points where both values are not zero. However, the trends seem to follow the same pattern of decreasing AMBR as the frequency and bandwidth of the emitter is increased. For both

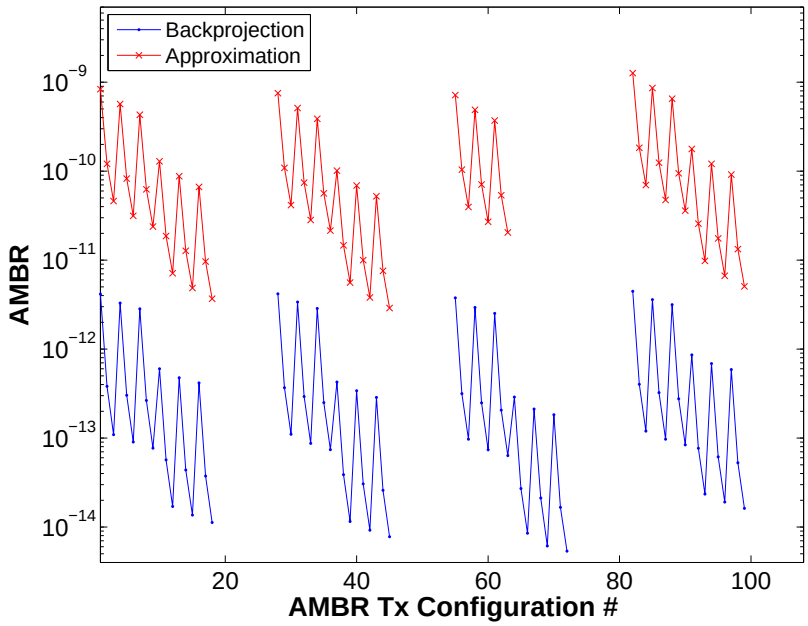

Figure 4.7: AMBR values generated through simulation of phase history generation and BP of a scene and the fast approximation method plotted together with a log scale y axis

methods, the AMBR decreases with the increase in PRI, as would be expected since more points on ambiguous isorange contours are excluded as it moves further away from the transmitter. The approximation also seems to follow the trend of the simulation with respect to the angle of the emitter, that is increasing with larger bistatic angles. The large difference between the approximation and simulation may be due to the assumption that all ambiguous regions will add constructively in the scene of interest. In the simulation, there may have been some destructive interference from different ambiguous scatterers which reduced the resulting AMBR.

For some of the configurations, 64 through 72, the fast approximation method determines no ambiguous points will fold in to the scene center, yet the backprojection based simulation has non zero values for AMBR. In these cases, the radar horizon is close enough to an ambiguous isorange contour that the backprojection based simulation,

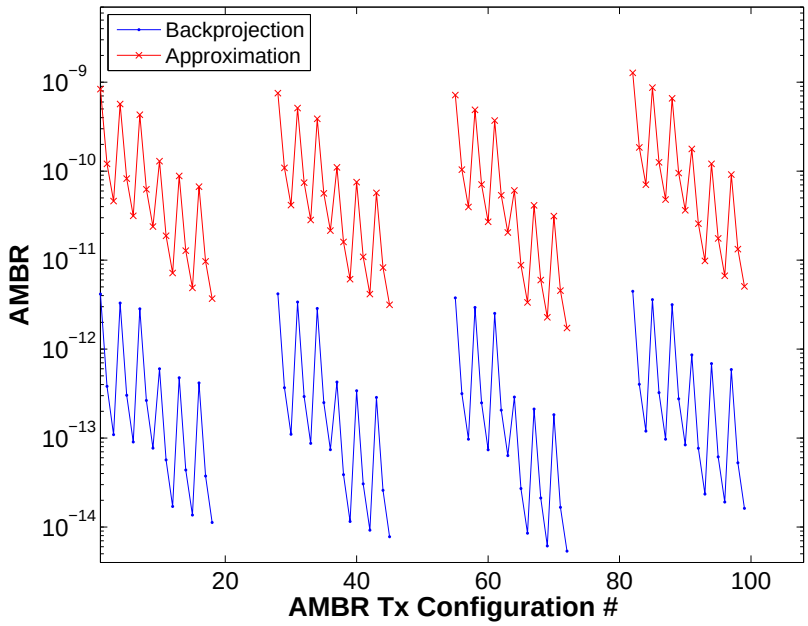

Figure 4.8: AMBR values generated through simulation of phase history generation and BP of a scene and the fast approximation method plotted together with a log scale y axis, with point cutoff based on simulation scene extent instead of bistatic radar resolution

consisting of all points which are ambiguous with the scene, calculates AMBR for points within a much thicker isorange contour which fall within the radar horizon as shown in Figure 4.6. The fast approximation on the other hand is based on the resolution of the bistatic radar for a isorange contour passing through the scene center only. If the limits of this calculation are changed to match the backprojection based simulation, by making contour segment exclusion based on the scene extent instead of the resolution, the results do include AMBR for these points. A plot of these results is shown in Figure 4.8. Including the scenes limits allows the AMBR approximation to better account for an entire scene.

To check that the impact of the AMBR does not increase dramatically with the height of the transmitter, and thus the radar horizon and number of ambiguous isorange contours, a quick check is performed using the fast approximation. The AMBR is recalculated for

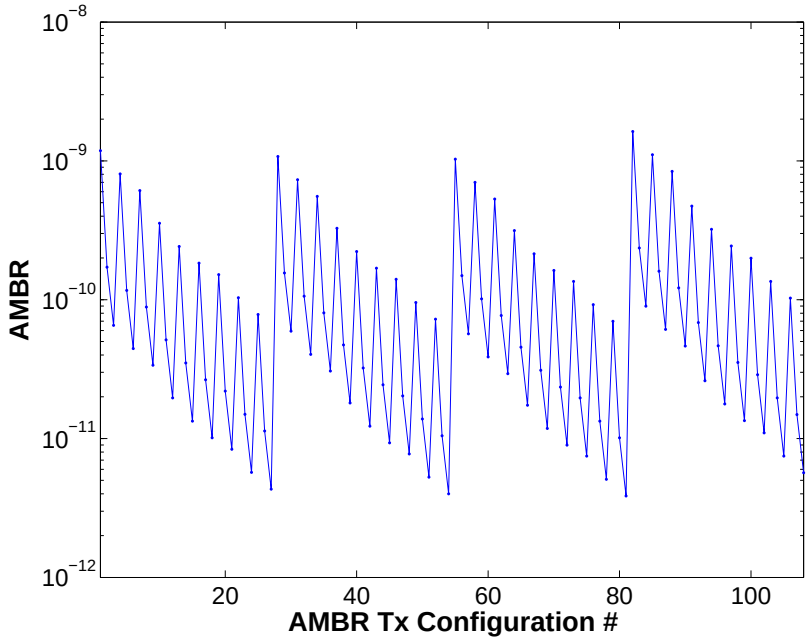

Figure 4.9: AMBR values generated through the fast approximation method, reseting the transmitter height to 2.394 km to match the receiver

all of the previous configurations; however, the transmitter height is set to match the receiver. The receiver height is 2.394 km based on the scenario configuration of a 20° elevation from the scene center and 7 km range. Figure 4.9 shows the results of re-running the AMBR calculations with the new transmitter heights. As expected, the AMBR increases for the higher emitters. Additionally, more ambiguities fold into the scene center, thus no AMBR values calculated with the parameters presented in Table 4.1 are zero.

Because the relative changes in the simulated AMBR tend to correspond to the fast approximation, the approximation is deemed to be acceptable for the purpose of comparing emitters in the multiple objective optimization. Note that in general the AMBR is several orders of magnitude smaller than the ISLR for the same configuration (see Section 4.1.2) thus it will have considerably less impact on the MNR. However the AMBR, and thus the MNR, will be slightly more pessimistic when using the

approximation. Even when the transmitter is given more height and hence more possible ambiguities, it appears that AMBR is still a less significant contributing factor (see Section 4.3.2). Despite this, the fast approximation requires little calculation time, and so is left in the MNR calculations used in Chapter 5.

4.3 Multistatic DTCR

Since both the PTCR and DTCR are a ratio of the expected received signal for the areas of high and low backscatter coefficient, it may be extended to the multistatic case by making the assumption, as was previously done while presenting the background on multistatic SAR, that the signals are non-interfering and separable. Thus, they combine using the principle of superposition for the coherent addition approach. This means that the PTCR and DTCR for a multistatic image generated by the coherent addition of bistatic images are expected to become

$$\mathrm{PTCR}_c = \frac{\sum_{i=1}^{N}[\frac{\sigma_{ti}\cos(\psi_{aci})}{\rho_{ai}\rho_{ri}} + \sigma_{ni} + \mathrm{MNR}_i\bar{\sigma}_{0i}]}{\sum_{i=1}^{N}[\sigma_{0i} + \sigma_{ni} + \mathrm{MNR}_i\bar{\sigma}_{0i}]} \tag{4.21}$$

$$\mathrm{DTCR}_c = \frac{\sum_{i=1}^{N}[\sigma_{0hi} + \sigma_{ni} + \mathrm{MNR}_i\bar{\sigma}_{0i}]}{\sum_{i=1}^{N}[\sigma_{0li} + \sigma_{ni} + \mathrm{MNR}_i\bar{\sigma}_{0i}]} \tag{4.22}$$

When using a GLTR approach to combining bistatic images into a multistatic image, the form of the PTCR and DTCR would be

$$\mathrm{PTCR}_g = \frac{\max_i[\frac{\sigma_{ti}\cos(\psi_{aci})}{\rho_{ai}\rho_{ri}} + \sigma_{ni} + \mathrm{MNR}_i\bar{\sigma}_{0i}]}{\max_i[\sigma_{0i} + \sigma_{ni} + \mathrm{MNR}_i\bar{\sigma}_{0i}]} \tag{4.23}$$

$$\mathrm{DTCR}_g = \frac{\max_i[\sigma_{0hi} + \sigma_{ni} + \mathrm{MNR}_i\bar{\sigma}_{0i}]}{\max_i[\sigma_{0li} + \sigma_{ni} + \mathrm{MNR}_i\bar{\sigma}_{0i}]} \tag{4.24}$$

Note that the various backscatter coefficients for the different bistatic pairs may have different values depending on the frequencies used and aspect dependency, the development of which is beyond the scope of this thesis. However, the manner in which

the multiplicative noise ratios differ from one bistatic pair to another is assumed to be sufficiently useful as a comparative measurement.

4.3.1 Analysis of Distributed Contrast Ratio. The set of possible scenarios as presented in Section 4.1.1 is reused. Because the AMBR is expected to have minimal impact, the PRI is held constant at 60μs. However, to check the impact of AMBR, a second set of simulations is run holding the azimuth constant at -50° while varying first carrier frequency, then bandwidth, then PRI according to Table 4.1. For a distributed target, the ratio is between the average value of two regions. The numerator is the expected value of an image formed in an area with a higher backscatter coefficient in the presence of noise and clutter. The denominator is the expected value of the image formed in an area with a lower backscatter coefficient in the presence of noise and clutter. The scene being used has a general background clutter scattering coefficient, $\bar{\sigma}_0$ equal to -10 dB, with a small area with a lower backscatter coefficient σ_{0l} equal to -26 dB, containing another area with a higher backscatter coefficient σ_{0h} equal to -13 dB as in [7]. This scenario is illustrated in Figure 4.10(a). To simulate the DTCR in a similar manner as the AMBR, a set of points was simulated within the scene at 71.4 m steps along the x and y axis. An inner rectangle of 15x29 points was given the lower backscatter coefficient, and two 7x29 rectangles on either side were given the higher backscatter coefficient. Note that there are 406 pixels of higher backscatter and 435 pixels of lower backscatter, so that the image contains nearly the same number of pixels for both coefficients. Outside of this scene are a number of scatterers within the radar horizon as shown in Figure 4.10(b) representing the clutter. Thousands of reflectors have to be added to the phase history, causing each scenario to take a great deal of time to simulate.

Normally in simulating the image formation, the thermal noise, clutter, and two area backscatter coefficients would all be random values. However this analysis is focused on the accuracy of the combined expected effect. To this end, using non-random realizations

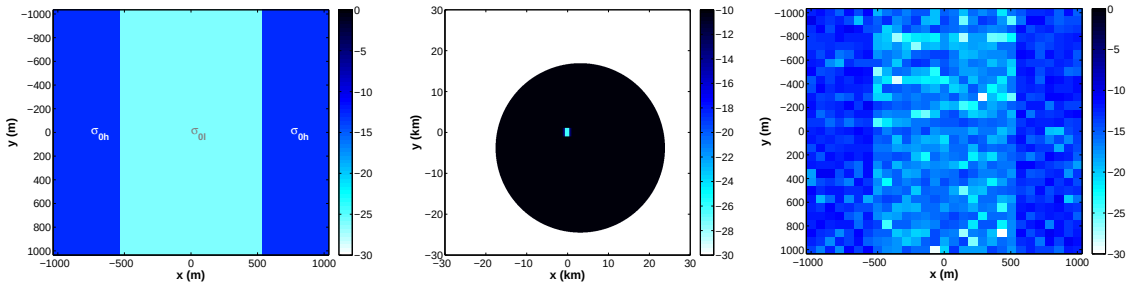

(a) Scene used (b) Broader view (c) Example resulting image

Figure 4.10: Scene used in DTCR simulation, scene within simulated clutter, and example image formed by BP for Scene plus clutter, both shown with backscatter coefficients in dB

of these values is assumed to be sufficient. Additionally thermal noise is left out of the simulation and fast approximation of DTCR. Despite this, the exact effect of adding complex valued side lobes and ambiguities from individual point scatterers are hard to predict, leading to images such as that shown in Figure 4.10(c). Thus, for measuring DTCR the mean value of the regions was used to find the ratio between the high backscatter (σ_{0h}) and low backscatter (σ_{0l}) region. Plots of the simulated DTCR and DTCR formed from the fast approximation of the ISLR and AMBR are presented.

4.3.2 DTCR Approximation Results. The first observation about the simulations used to find the DTCR was a large variations in the measurements for the configurations with transmitters at zero degrees azimuth. Looking into this, it appears that the images for these runs all have a region of higher returns close to zero on the y axis, as shown in Figure 4.11(a). This is different from a run with a larger DTCR, as shown in Figure 4.11(b). At first this was thought to be caused by points along the baseline between the transmitter and receiver only, however it appears that the transmitter angle also contributes to this. As an example, a point is simulated midway between a transmitter at a range of 5km and receiver at 7 km with azimuth ranging between $-0.5°$ and $0.5°$, and as shown in Figure 4.12 (a), the point can contribute strongly to a scene centered at the origin.

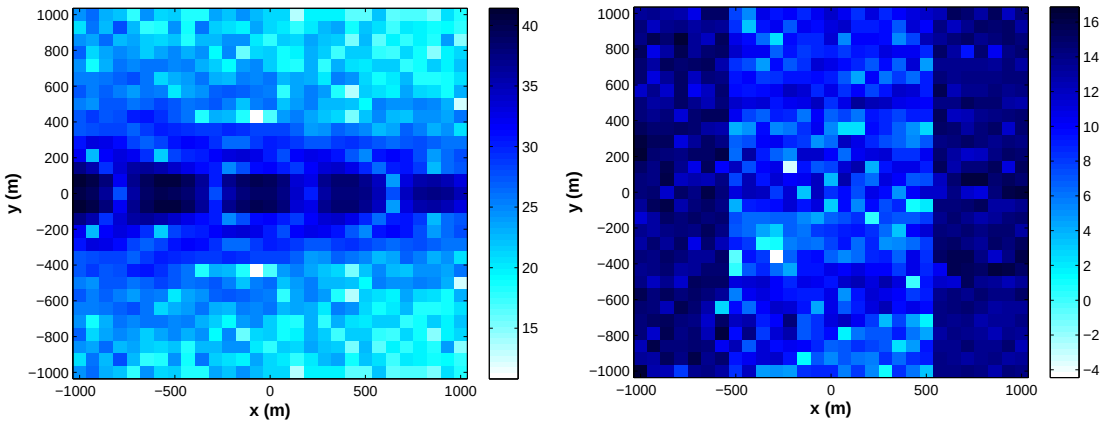

(a) Small DTCR (b) Large DTCR

Figure 4.11: Image for configurations with different DTCR values

However, a point midway between the receiver and a transmitter at an azimuth other than zero tends to have less influence on a scene located at the origin, as shown in Figure 4.12(b). When simulating a scene, the large SNR of points close to the transmitter can have a disruptive impact on the image formed. For this reason, the simulation is re-run with an assumption that the transmitter antennas have a non-isotropic antenna pattern that exclude points within 1km of the transmitter. This is unlikely to be the case for a real communication system, but it is assumed that a realistic receiver would attempt to avoid the direct signal from the emitter unless it was collecting a reference signal.

With that anomaly resolved, the simulated DTCR is plotted by configuration in Figure 4.13. The DTCR for ISLR calculations based on a eight times oversampling factor is shown in Figure 4.14. Though the approximated value is smaller, it is expected to have changes in the DTCR between configurations behave in a consistent manner (i.e. both increase from one to another and decrease from that configuration to the next, etc...). This does not appear to be the case. The DTCR from the simulated scene increases with bandwidth and frequency and decreasing azimuth. The approximated DTCR decreases with frequency and azimuth angle. However when the ISLR is calculated with the fast

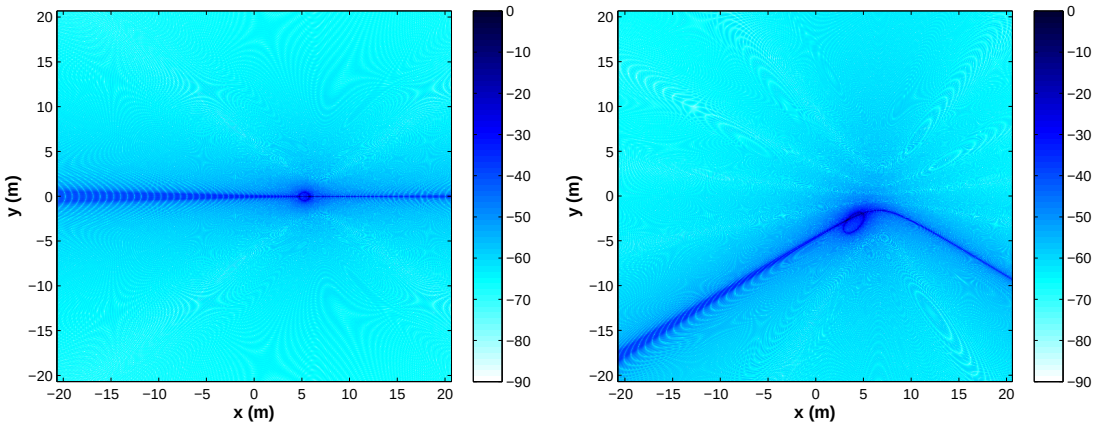

(a) Point at (5789m,0m), Tx at 0° Az (b) Point at (4896m,-1915m), Tx at −50° Az

Figure 4.12: Image for points along Tx-Rx pair baseline

approximation using the same pixel size used to create the results in Figure 4.13, the results have a very similar relative dependence on the configuration as shown in Figure 4.15. When using the 71.4 m square pixel size, both the DTCR from the simulated scene using backprojection and the fast approximation of the DTCR tend to decrease as the bistatic angle increases, increase as the frequency increases, and increase as the bandwidth changes. This behavior could be due to the decreasing mainlobe extent used to calculate the ISLR expected to result from these changes, since the mainlobe of the PSF will be smaller for a constant scatterer spacing. As shown in Section 4.1.2, the results from fast approximation and backprojection ISLR will be similar for a given pixel size, so the fast approximation is not the source of the differences. The source of this behavior is the spacing of the points added to phase history in the simulation. Since ISLR is the influence of all scatterers outside of a given pixel, then the addition of scatterers at a set interval can best be found by evaluating the PSF at the same step size, to simulate superposition of all scatterers outside a given pixel. Thus, when simulating phase history the best approach to find ISLR will be to use the spacing at which scatterers are added. Conversely, when planning for an actual collection, ISLR calculated with higher oversampling is expected to

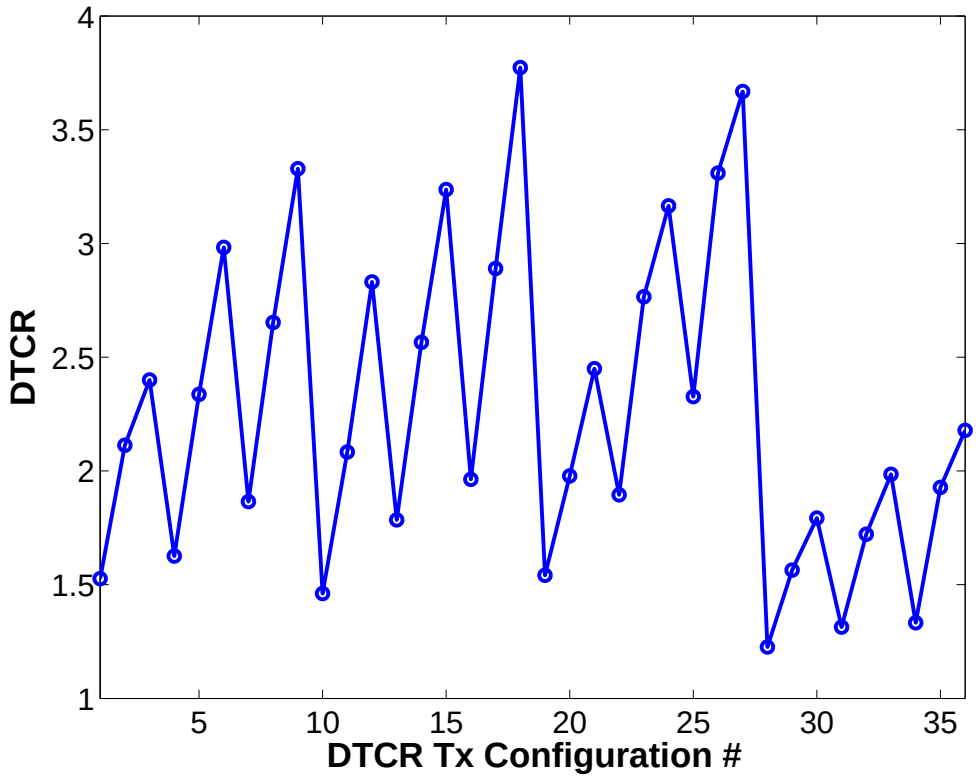

Figure 4.13: Plot of DTCR from backprojection

be a better predictor of performance. Thus the calculation of DTCR in Chapter 5 will use the spacing of the scatterers added to phase history to approximate ISLR.

Examining the set of runs where azimuth is held constant and PRI is allowed to vary shows that though AMBR is expected to be small, there are some minor changes in the DTCR. In Figure 4.16 small increases to the DTCR are observable as the PRI increases, corresponding to fewer ambiguous reflectors folding into the scene. Changes to the DTCR due to PRI still represents a marginal change compared to the differences caused by changing the carrier frequency or bandwidth, as indicated on the plot.

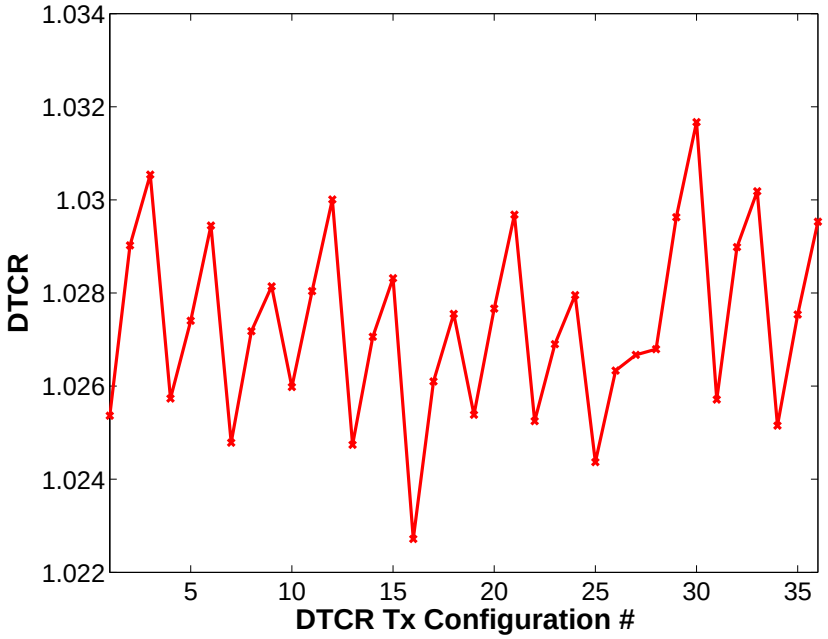

Figure 4.14: Plot of DTCR from ISLR using fast approximation and eight times oversampling

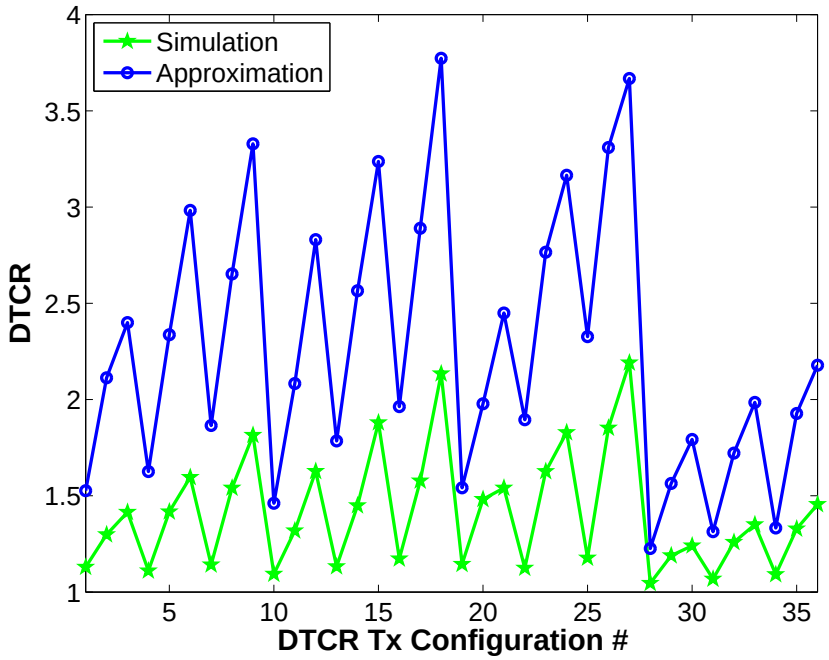

Figure 4.15: Plot of simulated DTCR and approximated DTCR from ISLR using fast approximation and pixel size based on backprojection simulation resolution

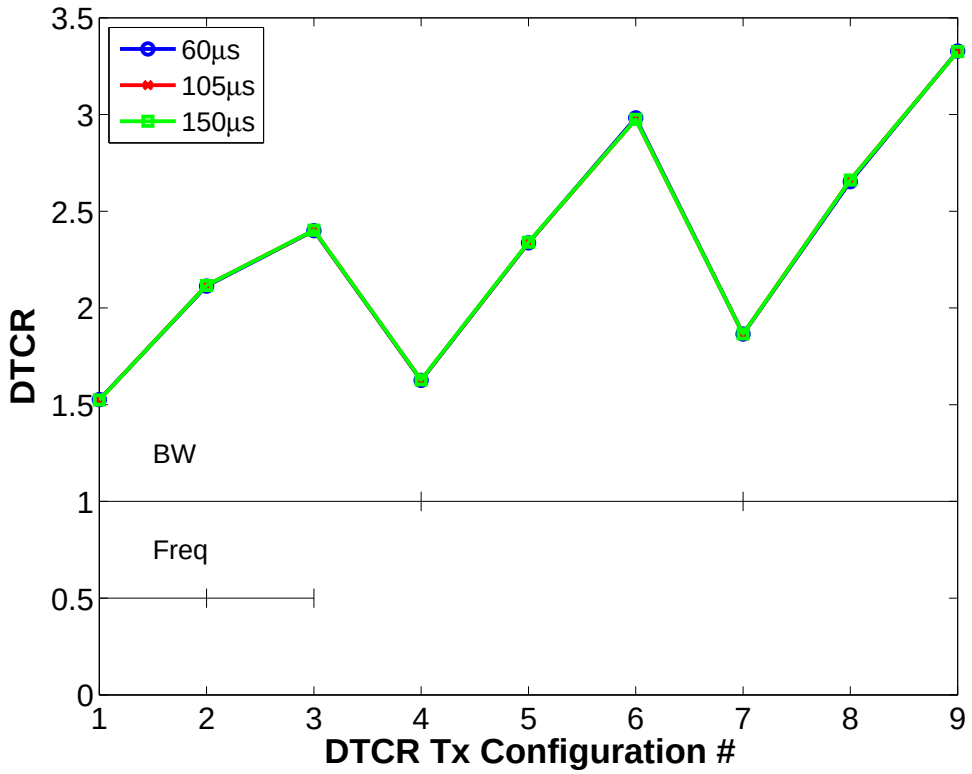

Figure 4.16: Plot of DTCR for scenarios holding azimuth constant and varying PRI

5 Dynamic Emitter Selection

This chapter presents a qualitative example of the dynamic emitter selection process. It starts with a description of the implementation of the multiple objective optimization process. It then describes the constraints used to limit the design space. Next, details of the implementation of objective functions are described. This is followed by the setup of a scenario to perform the selection process on, and a scene to use in simulating image formation. Finally results are presented for the evaluation of the different emitter sets under different weightings, along with some representative multistatic images generated using a Matlab simulation.

5.1 Multiple Objective Optimization Function Implementation

The scoring of all possible transmitter combinations takes the form of the multiple objective optimization as described in Section 2.5. The values of the objective functions are found for the combination, where

$$\begin{aligned} F_1 &= \frac{1}{SNR(\mathbf{T_x}, R_x)} \\ F_2 &= EMRA_C(\mathbf{T_x}, R_x) \\ F_3 &= EMRA_G(\mathbf{T_x}, R_x) \\ F_4 &= \frac{1}{DTCR_C(\mathbf{T_x}, R_x)} \\ F_5 &= \frac{1}{DTCR_G(\mathbf{T_x}, R_x)} \\ F_6 &= \frac{1}{PTCR_C(\mathbf{T_x}, R_x)} \\ F_7 &= \frac{1}{PTCR_G(\mathbf{T_x}, R_x)} \\ F_8 &= ISL(\mathbf{T_x}, R_x). \end{aligned} \tag{5.1}$$

Where $\mathbf{T_x}$ represents the set of transmitters, and likewise R_x is the receiver. $EMRA_C$ and $EMRA_G$ are the effective multistatic resolutions areas (EMRA) respectively found by coherent and generalized likelihood ratio test (GLRT) combination. Likewise, coherent or GLRT distributed target contrast ratio (DTCR) and point target contrast ratio (PTCR) are denoted by the C and G subscript respectively. The values of the signal to noise ratio (SNR), DTCR, and PTCR objective functions are inverted, such that minimizing the resulting objective produces a desirable outcome. The objective functions are evaluated for all permissible combinations of transmitters in the scenario. The largest result for a given objective function for all permitted configurations is then used to normalize all the results for that objective function. The utopia point is likewise found as the set of minimum values of each of the objective functions. To facilitate the selection process, the first step is to use the constraints to rule out transmitters. The minimum bistatic SNR, radar horizon, and bistatic angle constraints are used to remove individual transmitters from consideration. In a practical implementation, bistatic multiplicative noise ratio (MNR) for use in objective function evaluation is calculated first, then re-used to speed up objective function calculation. This saves repeated calculations for different combinations of transmitters. All combinations of between one and four transmitters, not ruled out by the constraints, are evaluated. The consideration of a given combination is however constrained by the maximum allowable number of antenna beams prior to evaluation.

5.1.1 Multiple Objective Optimization Function Constraints. A major part of limiting the calculations required to find the optimal combination of transmitters lies in limiting the search space. To this end, a set of constraints of the form $g_j(\mathbf{x}) \leq 0$ for $j = 1, 2, ..., J$ and $h_l(\mathbf{x}) = 0$ for $l = 1, 2, ...L$, are used to limit the set of possible solutions, $\mathbf{x}$. The constraints being considered are a minimum bistatic signal to noise ratio at the scene center, a limit on the number of antenna beams to allow, a requirement that the transmitters radar horizon includes the scene center, and a limit on the maximum bistatic

angle. Primarily, these represent precluding a transmitter/receiver pair based on some characteristic of the pair on its own, and not considered in relation to any other possible selections. The exception is the antenna beam constraint.

5.1.1.1 Bistatic SNR Constraint. Constraining bistatic SNR is meant to rule out signals which are simply too weak to be of much use when obscured by system noise. The limit on SNR for a bistatic pair illuminating the scene center is set to SNR_{min} and the constraint can be expressed as $SNR > SNR_{min}$. The SNR is calculated using (2.58) and assuming unity for the gain, system losses, propagation factors, and radar cross section.The variable SNR_{min} has for this implementation been set to a low threshold of -30dB. This is to accommodate signals which may potentially have other desirable features when combined with additional signals.

5.1.1.2 Antenna Beam Constraint. The antenna beam constraint refers to the selection of how many transmitters to use. The constraint is that the number of available receive antenna beams be less than or equal to the number of antenna beams required by that transmitter. The receiver is assumed to have a maximum of N_B possible beams which can be used concurrently. The type of transmitter determines how many antennas are required to use it. Analog signals are assumed to require two beams due to the necessity of collecting a reference signal, as described in Chapter 2.6.1. For digital signals, only one antenna is assumed to be necessary, since they presumably have a repetitive segment known a priori. Letting $N_B = 4$, the possible combinations are limited to no more than four transmitters.

5.1.1.3 Radar Horizon Constraint. In order for a transmitter to be capable of illuminating a scene of interest, it should have a line of sight to the scene center. For this reason all transmitters being considered must be closer to the scene center than their radar

horizon, as described in Section 4.2. Though some transmitters may be capable of propagating beyond the line of sight, this possibility is not considered here.

5.1.1.4 Bistatic Angle Constraint. The angle between the transmitter and receiver with respect to the scene center, known as the bistatic angle, will be limited to be no greater than 90 degrees. In cases where the bistatic angle exceeds 90 degrees, the resolution suffers, as described in (2.80). Additionally, issues of aspect dependence are not well explored, especially for the forward scattering case and are beyond the scope of this thesis.

5.1.2 PTCR Implementation. The multistatic PTCR is calculated using (4.21) and (4.23). The bistatic grazing angle for this calculation uses the bistatic grating angle definition found in [40], and is written for this application as

$$\psi_{aci} = \frac{\psi_{Txi} + \psi_{Rx}}{2} \tag{5.2}$$

where ψ_{aci} is the equivalent bistatic grazing angle of the i^{th} bistatic pair and ψ_{Txi} and ψ_{Rx} are the transmitter and receiver grazing angles, equal to their elevation angle (for flat terrain). The resolution term, $\rho_{ai}\rho_{ri}$, in (4.21) and (4.23) is replaced by the bistatic resolution area found as in Chapter 3.2. The point's backscatter coefficient, σ_{ti}, is -13 dB, the same as σ_{0h} in the DTCR calculations. The local clutter backscatter coefficient σ_{0i} is -10 dB, the same as the average backscatter coefficient, $\bar{\sigma}_{0i}$.

5.1.3 Ambiguity Penalty Implementation. In order to implement the ambiguity penalty, there are different approaches for digital and analog signals. The difference in the implementation for this thesis are explained here. Details of the signal used to modulate the FM Radio are also provided.

Though the exact contents of a communication signal may not be known in advance, most digital communications signals contain a predetermined portion which may periodically repeat. In the case of WiMAX,the preamble is used, and in the case of HDTV and LTE a set of synchronization symbols is used. Having these symbols, as described in Section 2.4, allows matched filtering against a portion of the communication symbol which is known a-priori. The synchronization also provides a PRI and pulsewidth defined as they would be in traditional radar waveforms. Additionally, the extent of the multistatic ambiguity could be set based on the maximum expected pulsewidth, or minimum expected PRI. Of the digital communications standards selected, the maximum possible pulsewidth belongs to the WiMAX, with a preamble consisting of two symbols with cyclic prefix attached. The case where the bandwidth is minimum (1.25 MHz) and an FFT size is 2048 leads to a maximum pulse width of 3.5 ms. The minimum PRI of the signal set is, 77.3 μs, belongs to the HDTV signal. Based on these parameters, the extent of the scene being imaged should not be larger than 23 km.

Unlike digital signals, there may be no repeating section of an analog communication signal. However, it may be possible to match the received signal against a reference. So, for analog signals, two signals must be collected, the reflection of the signal off of the target area, and the direct path signal from the transmitter. Since there is no real pulsewidth or PRI, it is necessary to determine how long to sample a signal, and how often. For the purpose of determining ambiguity, the PRI is effectively infinite, and the pulsewidth is arbitrary, but has been selected to be the inverse of the bandwidth, 1/(75kHz)=13.33 μs, such that the time bandwidth product will be one. More advanced approaches may use a larger time bandwidth product to improve resolution; however, such an approach is not considered in this thesis.

In order to simulate the FM radio signal for ambiguity determination, a wave file containing an 8 second segment of classical music is loaded, then split into left and right

components, with the right signal arbitrarily delayed by about 9 ms to simulate the equivalent of a three meter difference in separation from the source of sound between microphones. These signals are FM modulated to an IF frequency of 10.7 MHz [30] and then a section of the signal, corresponding to the pulsewidth, is selected to serve as the signal to autocorrelate, and use in forming the ambiguity function. The section used is a randomly selected segment of the recording.

5.1.4 Noise Implementation. A useful characteristic of the backprojection image formation process is that it is a linear operation. Because of linearity, the Gaussian thermal noise component of SNR can be treated as a separate image formation process. Two useful properties of Gaussian random variables are then used to simplify noise generation. First, linear transformations like the inverse Fourier transform of a set of Gaussian random numbers is expected to result in another set of Gaussian random numbers [22]. Second, summation of several Gaussian random numbers, as would then be done in the backprojection process, is expected to result in another Gaussian random variable [22]. Thus, noise can be added to either the phase history or the final image of the scene. To generate the images in Section 5.3, the noise is added to the phase history. To generate the noise, the peak power is found, then using the SNR as defined in Section 2.6.1 to scale the variance, a single realization of noise is found for each point in phase history or each pixel as:

$$N_{tot} = \mathcal{N}\left(0, \frac{|P_{peak}|}{2\text{SNR}}\right) + j\mathcal{N}\left(0, \frac{|P_{peak|}}{2\text{SNR}}\right) \tag{5.3}$$

5.2 Test Scenarios

The goal of this demonstration is to evaluate the optimization approach and show whether it produces quantitative ranking which are in line with qualitative image results. A simulated scene is used in the examples shown. Different weighting criteria are

presented to attempt to highlight the impact of different objective functions scores. In order to highlight all the effects being investigated, it is necessary to use a scene that includes components which can be used to qualitatively observe some of the different effects. With the scene determined, a set of possible transmitters is selected and positioned randomly, and then the objective function is used to determine which subset should produce the best results. The results of the combinations for optimal and suboptimal are displayed to highlight the strengths of the approach.

5.2.1 Weighting of Criteria. The weighted distance from the utopia point is found using two sets of weights:

$$\begin{aligned} \mathbf{w_C} &= [1,1,0,1,0,1,0,1] \\ \mathbf{w_G} &= [1,0,1,0,1,0,1,1] \end{aligned} \tag{5.4}$$

where the weights correspond to the objective functions in the order shown in (5.1). These weights indicate that optimization is performed under separate assumptions of how the bistatic images are combined into a multistatic image: coherent combination for $\mathbf{w_C}$ and GLRT combination for $\mathbf{w_G}$. Also, all weights are set equal to zero or one so that all objectives that are used are given equal priority. The score for a given combination is then found using (2.55) for these functions and weightings. After all combinations are scored and ranked, some of the images formed for the top ranking combinations are presented, along with some of the poorer ranking combinations to provide a qualitative indication of the emitter selection's performance. The process is repeated with a new set of weights to show the effect of a more targeted selection:

$$\begin{aligned} \mathbf{w_C} &= [1,1,0,1,0,.5,0,.1] \\ \mathbf{w_G} &= [1,0,1,0,1,0,.5,.1] \end{aligned} \tag{5.5}$$

In (5.5), the SNR, EMRA, and DTCR receive equal weighting of 1, however PTCR, with a weighting of 0.5, is smaller because the targets in the image are distributed. ISL receives an even lower weight (0.1) because it is not taken into account in the simulation the same way as the other values, but could be informative.

5.2.2 Scene Characteristics. The scene used for qualitative analysis contains some features which allow observation of the effect of the different objective functions. The scene takes the form of a group of letters in a 7500m x 7500m grid with 50m x 50m pixels. To demonstrate the effect of SNR, the scene is large enough that some parts are better illuminated than others. In order to test the resolution, the scene is set up to contain different sized letters. To demonstrate the DTCR the scene includes regions of different backscatter coefficients, outlining of the letters, and points outside of the scene representing background clutter. The scene is simulated as a set of non-interacting (i.e. non-shadowing) point targets forming both clutter as well as the letters, with backscatter intensity and location shown as an image in dB in Figure 5.1.

5.2.3 Scenarios. The set of transmitters used is generated randomly within some constraints. The positions of the individual transmitters is random within an area ranging between 0 and 10km on the x axis and -10km and 10 km on the y axis, but outside the scene. There are equal numbers of each transmitter type, however the parameters of the individual transmitters are randomly selected from a set of allowable values. The set of transmitters thus created are shown in Table 5.1 in terms of their azimuth (Az) in degrees, height (H) in meters, range from scene center in meters, waveform (WF) type , carrier frequency (F_c) in MHz, bandwidth (BW) in MHz, pulse repetition interval (PRI) in μs, pulse width (PW) in μs, effective radiated power (P_t) in kW, and the u parameter of the Zadoff-Chu sequence if the waveform is LTE. The Tx positions are shown on an x-y axis along with the receiver flight path in Figure 5.2. The receiver parameters are the same as

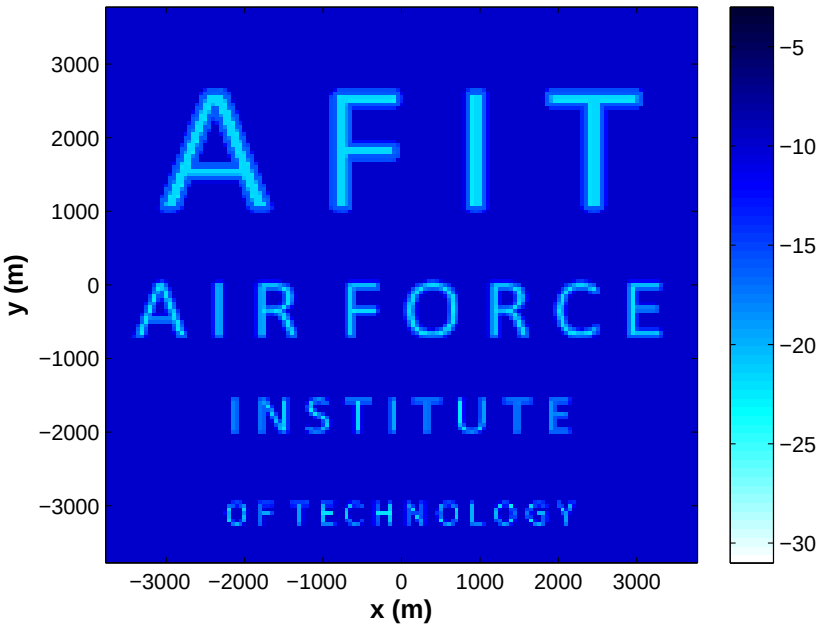

Figure 5.1: Scene used in qualitative evaluation of emitter sets

for the simulation of DTCR in Section 4.3. Additionally, clutter is added within the radar horizon and outside of the scene, except for a 1km radius around the emitter and further along the x axis than the receiver, implementing a simplistic antenna pattern.

Table 5.1: Table of Tx Parameters for Multiple Objective Optimization Qualitative Analysis

Tx	Az	H	Range	WF	F_c	BW	PRI	PW	P_t	u
1	55.5	35.6	11798	FM	92.6	0.075	∞	13.3	14.0	
2	-41.3	35.1	8486	FM	88.2	0.075	∞	13.3	14.0	
3	-8.9	35.0	8101	FM	90.4	0.075	∞	13.3	14.0	
4	-20.8	36.0	9458	FM	100.4	0.075	∞	13.3	14.0	
5	15.2	38.7	8273	FM	97.0	0.075	∞	13.3	14.0	
6	-20.0	32.5	7351	FM	90.2	0.075	∞	13.3	14.0	
7	-57.3	30.3	8459	HDTV	500	6.0	77.3	0.37	91.0	
8	-30.8	33.4	11041	HDTV	596	6.0	77.3	0.37	91.0	
9	-66.9	30.6	6284	HDTV	656	6.0	77.3	0.37	91.0	
10	-53.8	38.6	8946	HDTV	518	6.0	77.3	0.37	91.0	
11	10.2	30.6	4088	HDTV	698	6.0	77.3	0.37	91.0	
12	-76.3	35.5	6896	HDTV	470	6.0	77.3	0.37	91.0	
13	-73.2	38.3	6087	LTE	1880	0.945	5000	66.7	316.2	34
14	74.3	34.9	7668	LTE	1895	0.945	5000	66.7	316.2	25
15	0.9	33.3	8569	LTE	1925	0.945	5000	66.7	316.2	29
16	40.9	34.2	10752	LTE	1950	0.945	5000	66.7	316.2	34
17	71.6	39.8	6905	LTE	1965	0.945	5000	66.7	316.2	34
18	48.1	32.9	9394	LTE	1945	0.945	5000	66.7	316.2	34
19	41.9	37.3	10379	WiMAX	9300	3.5	2500	136	316.2	
20	52.5	37.7	6529	WiMAX	9720	5.25	10000	106.7	316.2	
21	50.3	37.9	10918	WiMAX	7620	15.25	8000	31.2	316.2	
22	-58.7	37.4	11651	WiMAX	3460	3.25	12500	155.2	316.2	
23	43.7	36.0	9570	WiMAX	9240	16.75	8000	33.5	316.2	
24	39.8	33.2	11103	WiMAX	7080	12.5	12500	37.8	316.2	

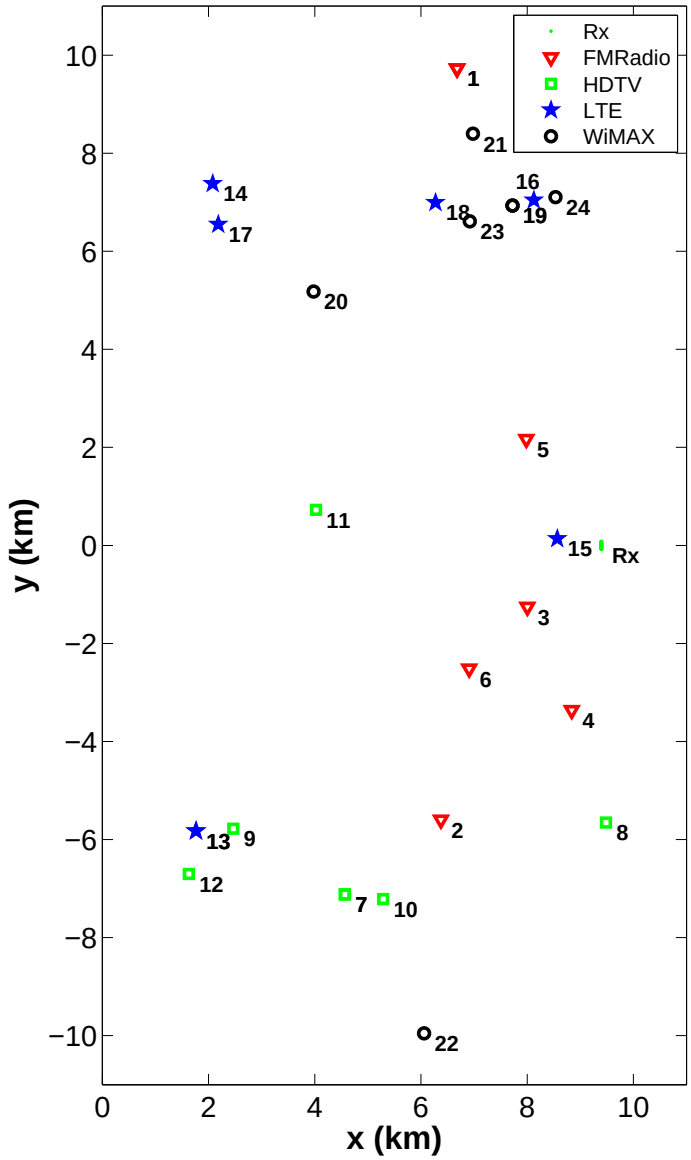

Figure 5.2: Tx positions for dynamic emitter selection qualitative analysis

5.3 Results

The Multiple Objective Optimization was carried out as described for the set of emitters presented. The constraints ruled out emitters 21,23 and 24 due to small bistatic

SNR. That brought the total number of available emitters to 21. Out of these available emitters, there were a total of 2680 different combinations that were not ruled out by the required number of antenna beams. Use of the constraints described in Section 5.1.1 has resulted is a 84.7 percent reduction from all 17550 different combinations of one to four emitters out of a set of 24.

The top ten combinations for the coherent combination cases are shown in Table 5.2 along with their objective function scoring. In addition, ten sets of emitters with higher scores are listed. The higher ranked sets are selected because they occur at a point where the scores change more drastically from the top ten. The combined image formed coherently from the first and second ranked set of emitters is shown in Figure 5.3 (a) and (b) respectively. To highlight performance of higher scored sets, the coherent multistatic image for the 1551st and 1552nd ranked sets of emitters is shown in Figures 5.3 (c) and (d). As indicated, the top ranked sets have similar scores, with different objective functions scores supporting the rank. For example, the first image has better SNR, so that letters stand out better, however the second has better DTCR, such that borders around the 'T' in "AFIT" are visible. Additionally, the last few letters in "Force" and "Institute" are more visible with the better EMRA and DTCR in Figure 5.3 (b). For the emitter set ranked 1551, the EMRA and SNR are better than the first ranked set, however the poor DTCR and ambiguous clutter contribute to the poorer visibility of letters further away from the receiver. Finally, the image for the set ranked 1552 shows much poorer performance. Beside ISL, DTCR is the only objective function worse than the top ranked set and may be the cause of the distortion. Note that the ranking of the equally weighted sets is strongly affected by ISL, which is not captured by the simulation method, so that the result is close to the top ranked sets in some respects, despite nearly doubling the score.

The image in Figure 5.3 (c) points to potential shortfall of the exclusion criteria. In Figure 5.3 (c) a large return is shown in the upper left corner of the scene. The large return

corresponds to the point where clutter close to a distant emitter with a short PRI, number7, is ambiguous with the scene. Some points close to the emitter are excluded to emulate an antenna pattern, visible as a ring around the eleventh emitter in the right side of the images in Figures 5.3 (b) and (c). When ambiguous with the scene, these points create the ring on the left half of the scene in Figure 5.3 (c). The ambiguous clutter also causes low local DTCR, with smaller SNR to counteract it. Thus, letters on the left half of the scene with poor DTCR and SNR are more distorted. Letters on the right half may have similar local DTCR, but much higher SNR. One approach to account for this effect would be to add another exclusion criteria, that unambiguous range be greater than the scene. Such a constraint may have ruled out the first scene, where the upper left corner is lighter because ambiguous clutter is outside the scene. Another approach would be to adjust AMBR calculations to account for antenna patterns and the possibility that the scene is not entirely in the unambiguous range.

In a similar way to the coherent case, Table 5.3 shows the ranks of the first ten highest, and ten lower ranked emitter sets. The image of the scene for the first, second, 1271st and 1280th transmitter sets from the GLRT ranking are shown in Figure 5.4. Comparing the first two images shows that the results are similar, except 5.4(b) contains more of the last word. The SNR may have been a more significant factor than DTCR or PTCR when both are relatively high. The set ranked 1271 has slightly poorer DTCR, but otherwise comparable SNR, EMRA and PTCR to the first two. However, in the resulting image in Figure 5.4(c) points further from the receiver are distorted by ambiguous clutter. The set ranked 1280 has poorer DTCR than the top ranked sets, visible in the bottom of the scene, and poorer EMRA, causing smearing of the letters, as shown in Figure 5.4(d).

Table 5.2: Table of top 10 ranked emitter combinations and selected emitter combinations for coherent combination (only coherent values reported)

Rank	Tx set	Score	SNR (dB)	EMRA (m^2)	DTCR	PTCR	ISL
1	12, 13	0.039689	3.60	1524	1.0090	0.982	0.595
2	11, 13	0.039784	2.71	669	1.0110	0.977	1.031
3	12, 14, 17	0.039824	7.84	1461	1.0081	0.983	1.117
4	11, 14, 17	0.039828	6.91	665	1.0092	0.981	1.869
5	13, 15	0.039845	2.49	2382	1.0086	0.982	0.781
6	14, 17	0.039853	2.19	2651	1.0090	0.982	0.533
7	12, 13, 15	0.039866	8.02	1444	1.0079	0.984	1.204
8	11, 13, 18	0.039876	6.84	671	1.0082	0.983	1.726
9	9, 11, 13	0.039901	7.19	846	1.0076	0.984	1.308
10	12, 17	0.039905	2.80	1629	1.0080	0.983	1.330
1550	9, 15, 18, 20	0.083411	6.45	922	1.0003	0.999	25.537
1551	7, 11, 16, 18	0.083427	9.32	806	1.0053	0.989	26.326
1552	9, 15, 18, 19	0.083469	5.94	924	1.0002	1.000	25.536
1553	9, 11, 16, 18	0.083632	8.81	744	1.0054	0.989	26.419
1554	11, 12, 15, 22	0.084024	8.85	983	1.0012	0.997	25.973
1555	11, 12, 15, 20	0.084407	9.28	1026	1.0003	0.999	25.954
1556	11, 12, 15, 19	0.084465	8.63	1005	1.0002	1.000	25.953
1557	7, 11, 15, 18	0.085213	9.84	830	1.0060	0.988	27.108
1558	9, 14, 15, 16	0.085388	8.74	829	1.0055	0.988	27.140
1559	8, 9, 15, 18	0.086118	8.01	898	1.0038	0.992	27.246
1560	12, 13, 14, 17	0.087829	12.01	1439	1.0090	0.982	28.280

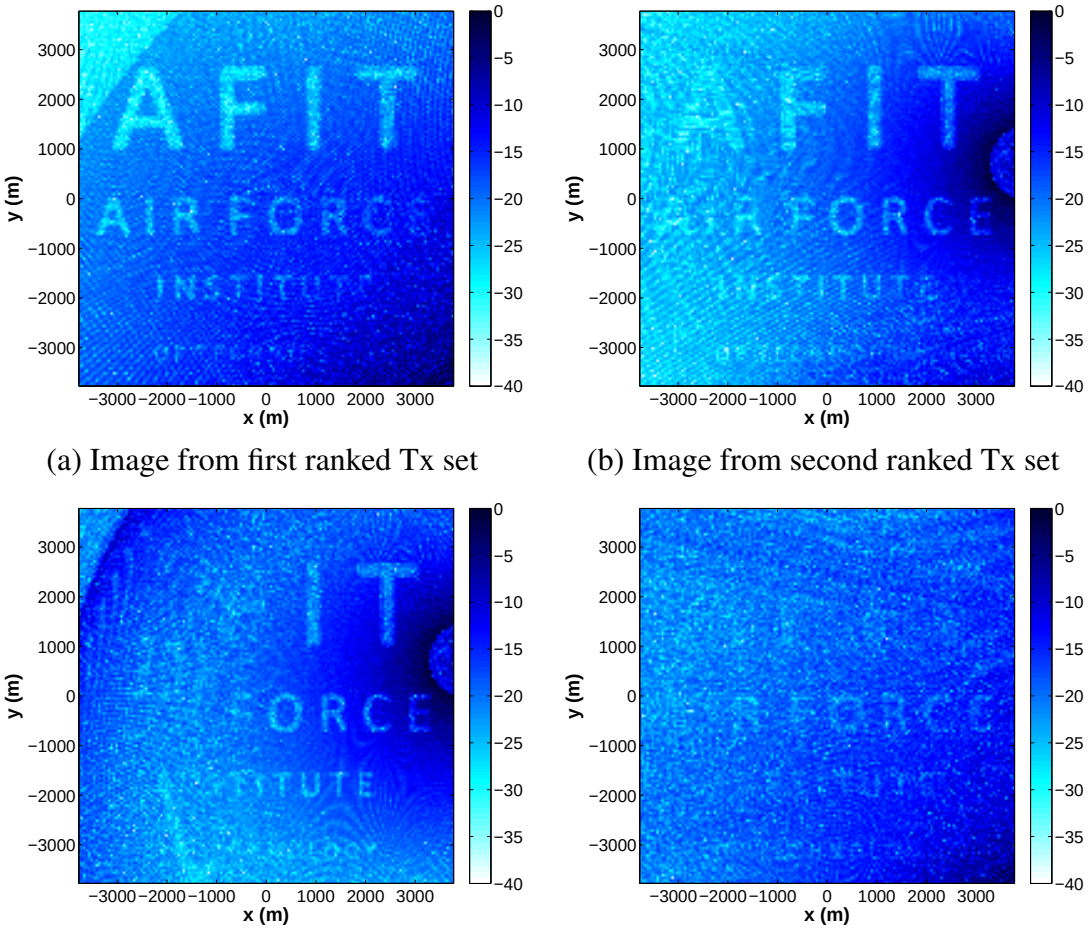

(a) Image from first ranked Tx set

(b) Image from second ranked Tx set

(c) Image from 1551st ranked Tx set

(d) Image from 1552nd ranked Tx set

Figure 5.3: Images formed coherently for different highly ranked sets of emitters

Table 5.3: Table of top 10 ranked emitter combinations and selected emitter combinations for GLRT combination (only GLRT values reported)

Rank	Tx set	Score	SNR (dB)	EMRA (m^2)	DTCR	PTCR	ISL
1	11, 13	0.039653	2.71	822	1.0096	0.980	1.031
2	11, 14, 17	0.039898	6.91	822	1.0084	0.983	1.869
3	14, 17	0.039901	2.19	2636	1.0084	0.983	0.533
4	13, 14	0.040027	2.97	2852	1.0084	0.983	1.334
5	13, 17	0.040061	3.23	2852	1.0096	0.980	1.774
6	11	0.040070	-6.45	822	1.0096	0.980	1.499
7	12, 13	0.040140	3.60	1993	1.0069	0.986	0.595
8	17	0.040180	-6.56	2636	1.0096	0.980	0.380
9	12, 14, 17	0.040186	7.84	1993	1.0069	0.986	1.117
10	12, 17	0.040225	2.80	1993	1.0069	0.986	1.330
1270	9, 10, 19, 22	0.046647	5.13	1266	1.0001	1.000	5.213
1271	10, 11, 16	0.046689	5.56	822	1.0038	0.992	7.994
1272	9, 16, 18, 20	0.046781	5.97	1270	1.0001	1.000	5.409
1273	9, 16, 18, 19	0.046810	5.40	1270	1.0001	1.000	5.409
1274	13, 14, 17, 22	0.046867	7.79	2852	1.0003	0.999	5.570
1275	7, 8, 10, 12	0.046875	7.76	1993	1.0020	0.996	7.063
1276	11, 12, 22	0.046904	5.11	1580	1.0003	0.999	5.795
1277	7, 8, 10	0.046906	2.98	1481	1.0020	0.996	7.132
1278	13, 14, 17, 20	0.047108	6.69	2852	1.0001	1.000	5.570
1279	11, 12, 20	0.047128	5.93	1580	1.0001	1.000	5.776
1280	13, 14, 17, 19	0.047137	6.90	2852	1.0001	1.000	5.570

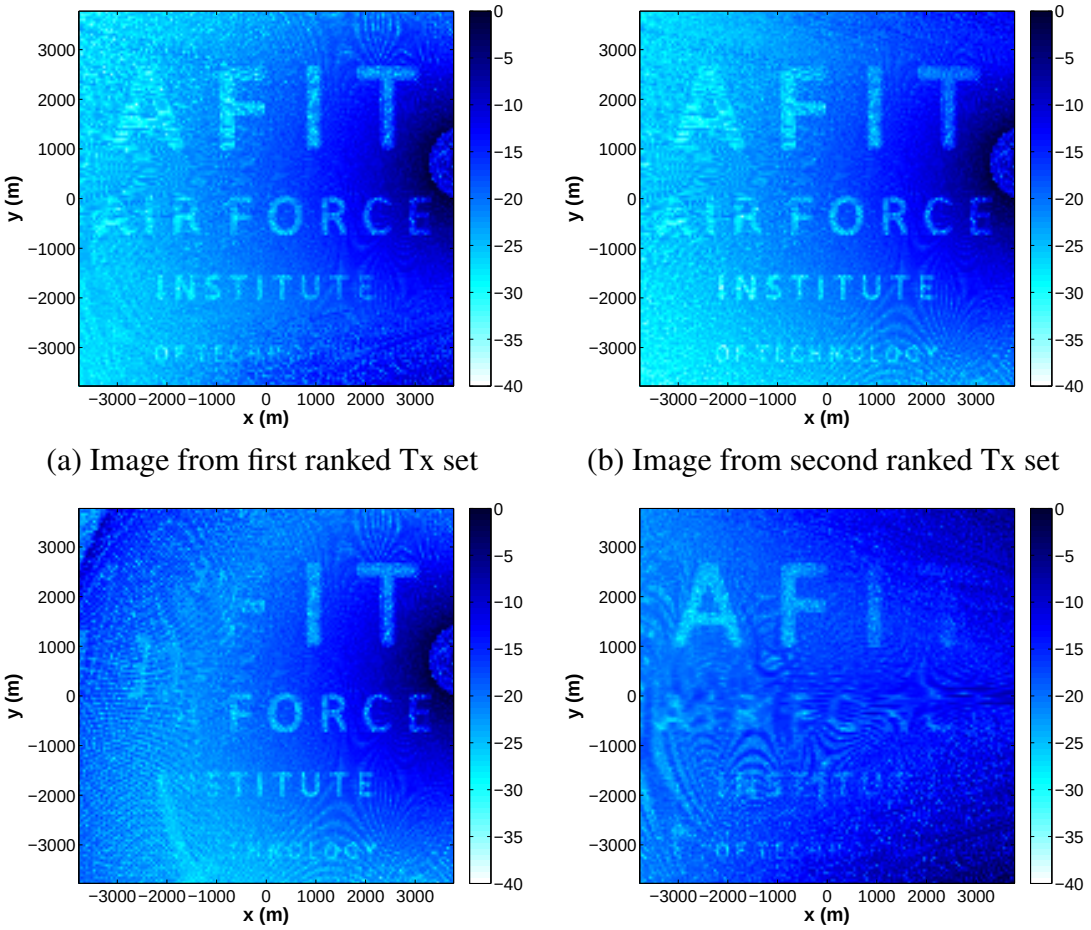

(a) Image from first ranked Tx set

(b) Image from second ranked Tx set

(c) Image from 1271st ranked Tx set

(d) Image from 1280th ranked Tx set

Figure 5.4: Images formed through GLRT for different highly ranked sets of emitters

The process is repeated for the weighting in (5.5) with the resulting top ten ranking shown in Table 5.4 for the coherent case. Again, ten sets of emitters with higher scores are also listed.The image formed by the first set, a single transmitter, is shown in Figure 5.5(a), and the image formed by the second set, which is predicted to have better SNR, EMRA, and PTCR, but poorer DTCR is shown in Figure 5.5(b). Despite the higher score, the first image is less legible than the second. The poorer EMRA appears to lead to smearing of letters in the middle of the scene. Despite the predicted good DTCR, poor SNR may be counteracting it towards the bottom of the scene. The image for the set ranked 1920 is shown in Figure 5.5(c). Here, the poor EMRA and contrast seem to work together to cause much of the scene to be unrecognizable, with ambiguous clutter further distorting the image. The set ranked 1923, shown in Figure 5.5(d), has better SNR, EMRA, and PTCR than the first ranked set, and may have been clearer, as seen in the right half. However ambiguous clutter has again distorted much of the left half of the image.

Using the weighting in (5.5), the top ten ranking sets are shown in Table 5.5 for the GLRT case, along with ten sets of emitters with higher scores than the top ten. The image formed by the first set, the same single transmitter as for the coherent case is shown in Figure 5.6(a). The image formed by the second set, which is predicted to have better SNR, EMRA, and PTCR, but poorer DTCR is shown in Figure 5.6(b). Again, despite a higher score, the first image is less recognizable than the second. The image for the set ranked 1937 is shown in Figure 5.6(c), and is expected to have better SNR, EMRA, and PTCR than the first, but worse DTCR. In the resulting image, the DTCR is made worse by ambiguous clutter. The image for the set ranked 1940 is shown in Figure 5.6(d). The set ranked 1940 is expected to have much better SNR and good DTCR and PTCR, but terrible ERMA, due to the inclusion of an FM radio, and this is apparent in the resulting image.

In all of these cases, the weighting appears to result in ranks which make sense in general. Images with low ranks seem better than those with higher ranks. However

between two low ranked sets, it would not automatically select the same set a user might want based on the images. For example, the image in Figure 5.6(b) appears to be more legible than Figure 5.6(a), however it was ranked second. Thus, a better method of selecting the weighting may help improve the outcome of the selection process. Experimentation with different weighting schemes is an area where additional research could improve the outcome. This would depend on the ability to recognize a given image for a given scenario. To make the results of such a test less subjective, different quantitative approaches, such as simply correlating the recovered image against the original, calculating a root mean squared error of the ranked images versus the true scene, or using the same automatic target recognition algorithm, could provide a measure of the weighting's success.

Table 5.4: Table of top 10 ranked emitter combinations and selected emitter combinations for coherent combination using targeted weighting (only coherent values reported)

Rank	Tx set	Score	SNR (dB)	EMRA (m^2)	DTCR	PTCR	ISL
1	13	0.034677	-5.08	2852	1.0130	0.973	0.389
2	11, 13	0.035347	2.71	669	1.0110	0.977	1.031
3	13, 17	0.035604	3.23	2628	1.0110	0.977	1.774
4	1, 11, 12	0.035636	15.28	2923	1.0110	0.977	0.517
5	11, 13, 14	0.036058	7.39	726	1.0100	0.979	5.024
6	13, 14	0.036156	2.97	2749	1.0102	0.979	1.334
7	13, 14, 17	0.036300	8.09	2582	1.0100	0.979	5.570
8	11, 14, 17	0.036627	6.91	665	1.0092	0.981	1.869
9	11, 12, 13	0.036638	8.41	945	1.0092	0.981	2.072
10	12, 13, 17	0.036678	8.64	1321	1.0092	0.981	2.950
1920	10, 12, 14, 19	0.070516	8.35	1454	1.0002	1.000	195.200
1921	7, 10, 12, 15	0.070946	9.48	1401	1.0051	0.989	209.142
1922	7, 8, 9, 16	0.071005	7.47	1170	1.0034	0.993	205.701
1923	7, 9, 16	0.072450	4.51	1219	1.0045	0.991	214.347
1924	8, 9, 12, 15	0.073966	8.74	1451	1.0039	0.992	219.656
1925	8, 9, 10, 16	0.074204	7.26	1123	1.0033	0.993	219.339
1926	7, 9, 16, 22	0.074249	6.78	1219	1.0011	0.998	214.432
1927	7, 8, 12, 15	0.074521	8.82	1545	1.0039	0.992	221.899
1928	7, 9, 16, 20	0.074691	7.52	1219	1.0003	0.999	214.353
1929	7, 12, 15	0.074753	6.30	1551	1.0057	0.988	226.556
1930	7, 9, 16, 19	0.074757	6.62	1219	1.0002	1.000	214.353

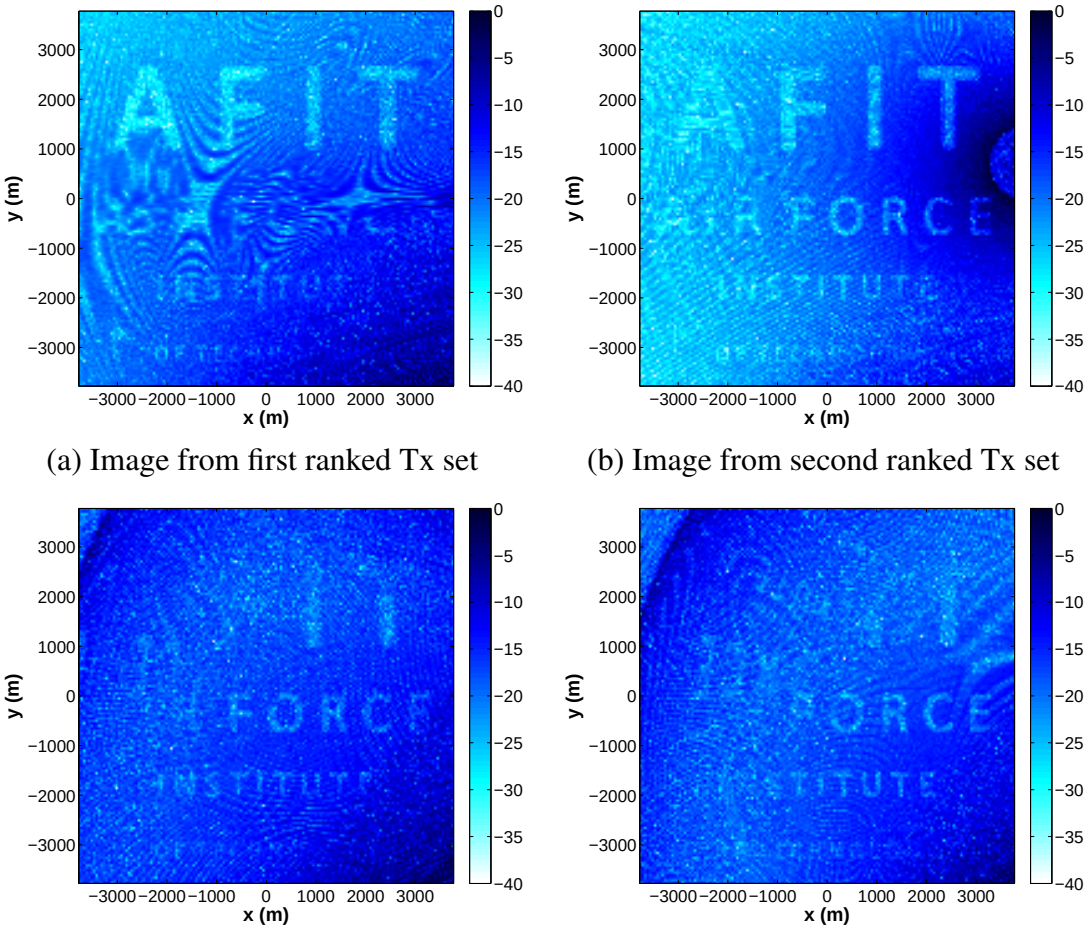

(a) Image from first ranked Tx set

(b) Image from second ranked Tx set

(c) Image from 1920th ranked Tx set

(d) Image from 1923th ranked Tx set

Figure 5.5: Images formed coherently for different highly ranked sets of emitters using targeted weighting

Table 5.5: Table of top 10 ranked emitter combinations and selected emitter combinations for GLRT combination using targeted weighting (only GLRT values reported)

Rank	Tx set	Score	SNR (dB)	EMRA (m^2)	DTCR	PTCR	ISL
1	13	0.034677	-5.08	2852	1.0130	0.973	0.389
2	11, 13	0.036331	2.71	822	1.0096	0.980	1.031
3	13, 17	0.036624	3.23	2852	1.0096	0.980	1.774
4	11	0.036697	-6.45	822	1.0096	0.980	1.499
5	17	0.036960	-6.56	2636	1.0096	0.980	0.380
6	11, 14, 17	0.037180	6.91	822	1.0084	0.983	1.869
7	11, 13, 14	0.037200	7.39	822	1.0084	0.983	5.024
8	14, 17	0.037412	2.19	2636	1.0084	0.983	0.533
9	13, 14	0.037454	2.97	2852	1.0084	0.983	1.334
10	13, 14, 17	0.037478	8.09	2852	1.0084	0.983	5.570
1935	7, 8, 10, 18	0.096873	7.70	1481	1.0020	0.996	309.841
1936	19, 20	0.107078	-19.17	48	1.0001	1.000	4.765
1937	7, 9, 12, 14	0.107810	9.94	1993	1.0045	0.991	356.051
1938	20	0.649880	-27.41	48	1.0001	1.000	1.899
1939	4, 13	0.740730	21.59	442406	1.0130	0.973	0.552
1940	4, 11, 13	0.740833	18.95	442406	1.0096	0.980	0.552
1941	4, 11	0.740833	12.86	442406	1.0096	0.980	0.552
1942	4, 13, 17	0.740833	24.15	442406	1.0096	0.980	0.552
1943	4, 17	0.740833	20.62	442406	1.0096	0.980	0.554
1944	4, 11, 17	0.740833	18.39	442406	1.0096	0.980	0.552
1945	4, 13, 14	0.740875	23.78	442406	1.0084	0.983	0.552

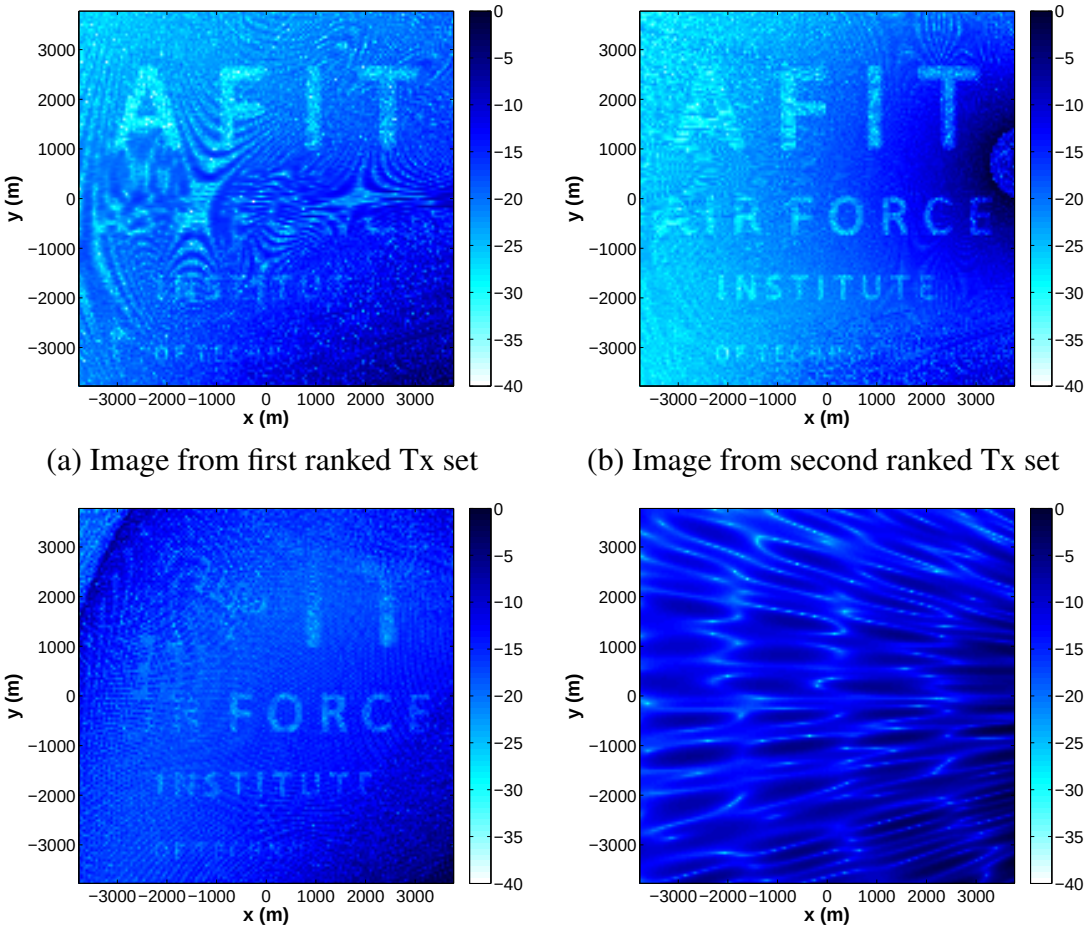

(a) Image from first ranked Tx set

(b) Image from second ranked Tx set

(c) Image from 1937th ranked Tx set

(d) Image from 1940th ranked Tx set

Figure 5.6: Images formed through GLRT combination for different highly ranked sets of emitters using targeted weighting

6 Conclusion

6.1 Summary

This thesis developed a process for selecting a subset of emitters out of a larger set to use in forming passive multistatic SAR images. As part of this development, background was given on SAR, with a focus on bistatic/multistatic SAR. Additionally, multiple objective optimization was described. The multiple objective optimization approach was used as the framework for the selection process with four different SAR criteria serving as the objective functions. Two of the objective functions, the multistatic signal to noise ratio (SNR) and integrated sidelobes (ISL) of the multistatic ambiguity function (MAF) had sufficient previous work to require little adaptation for this application. Two other criteria, effective multistatic resolution area (EMRA) and contrast ratio, required more development before they could be approximated in the selection process. To decrease the number of calculations required to form the estimates of EMRA and ISLR, an approximation for the point spread function (PSF) was developed. A fast approximation of the ambiguity ratio (AMBR) contributing to the multiplicative noise ratio (MNR) was also developed. Simulation was performed to check that the fast approximations corresponded to the values obtained when simulating with backprojection. In addition to the EMRA and MNR development, a set of criteria was presented for ruling out emitters separate from their combined effect. A qualitative example of the use of the multiple objective optimization was presented with the resulting scores of a limited number of the possible emitter combinations. A demonstration of multistatic SAR images resulting from some of these emitter sets was performed using simulation of a scene designed to highlight the effect of SNR, EMRA, and contrast ratio.

6.2 Research Contributions

The contributions from this thesis to the area of emitter selection for passive multistatic SAR are:

- Development of PSF Approximation for bistatic and multistatic SAR, reducing from an $O(n^3)$ operation [40] to an $O(n^2)$ approximation
- Formulation of effective multistatic resolution area as a criteria for judging waveforms
  - Accounts for grating lobes due to coherent combination of bistatic images into a multistatic image.
  - Use of PSF approximation to find EMRA checked against use of backprojection, showing the fast approximation is useful for estimating the EMRA
- Development of bistatic MNR using the definition provided in [7]
  - Use of PSF approximation to find approximation of ISLR contributing to MNR. The approximation was shown to follow same trends for changes in bandwidth, frequency, and bistatic angle of the system, except for bistatic angles close to 90°.
  - Development of approximation of AMBR contributing to MNR. The approximation was shown to be pessimistic, but still follow the same trends for a example set of changes in bandwidth, frequency, and bistatic angle of the system.
- Bistatic MNR used to formulate bistatic distributed target contrast ratio (DTCR) and point target contrast ratio (PTCR) using the definition provided in [7]

- Extension from bistatic to multistatic MNR, DTCR, and PTCR
- Emitter selection procedure making use of multiple objective optimization using multistatic SNR, EMRA, DTCR/PTCR, and ISL of the MAF
  - Showed multiple objective optimization could quantitatively rank sets of emitters and have images in general be qualitatively better or worse
  - Discovered that weighting is not a simple problem of trying to maximize a few desired criteria

6.3 Future Research

Though several advances are made in this work, there is much that could be done to improve selection process effectiveness. Possible topics of future work are:

- Inclusion of more transmitter types
- Inclusion of the effect of more realistic signal processing of the received signals
  - Correlation of the FM radio signal to improve resolution. Using more of the signal would allow for some pulse compression such that the bandwidth of the signal might no longer cause FM radio to have substantially worse down range resolution from the other communications standards.
  - Reconstruction of digital signals as suggested in [15] so that more of the signal than just the synchronization symbol or preamble could be used for for image reconstruction. This could stand to improve various aspects of SAR image formation, including all the criteria used for the selection process in this thesis.
- Inclusion of backscatter frequency and aspect dependence for contrast ratio estimates

- Investigation of the weighting used in the utility function to rank the emitter combinations.
- Investigation the use of genetic algorithms or other search approaches to speed up the selection process over the exhaustive search used in Chapter 5.
- Investigation of effect of antenna patterns and ambiguous clutter on the DTCR approximation and simulation
- Experimentation to validate the results of simulation in a more realistic and complex signal environment.

Appendix A: Results of Emitter Set Ranking Used in Qualitative Demonstration

This appendix contains the results of the quantitative analysis of the emitter set used in the qualitative demonstration in Chapter 5. Plots of the utility function score versus rank are shown for the four weight sets in Figures A.1 and A.2. These weight sets are the uniform coherent, $\mathbf{w_{C1}}$, uniform GLRT $\mathbf{w_{G1}}$, non-uniform coherent $\mathbf{w_{C2}}$, and non-uniform GLRT $\mathbf{w_{G2}}$ weights from Section 5.2.1. The plots of score versus rank are split into two parts due to the large difference in the first and second half of the ranked sets' scores. The signal to noise ratio (SNR) versus rank is shown in Figures A.3 - A.6 for the different weight sets used in the multi-objective optimization for emitter group selection. Figures A.7 - A.10 show the effective multistatic resolution in meters squared versus rank. Note that in these plots, the resolution is found for a coherent or GLRT combination based on whether a coherent or GLRT weighting is used. Additionally, these plots use a log scale for the y axis due to the large difference in resolution area between transmitter sets. Figures A.11-A.14 show the multistatic distributed target contrast ratio (DTCR) versus rank. Again, the DTCR is calculated for a coherent or GLRT combination based on whether a coherent or GLRT weighting is used. Figures A.15-A.18 show the multistatic point target contrast ratio (PTCR) versus rank. PTCR is calculated for a coherent or GLRT combination based on whether a coherent or GLRT weighting is used. Finally, Figures A.19 - A.22 show the integrated sidelobes (ISL) of the ambiguity function versus rank. Note that these plots use a log scale for the y axis due to the large difference between ISL values for different ranks. The different transmitter sets are shown with their rank for all weightings in Table A.1.

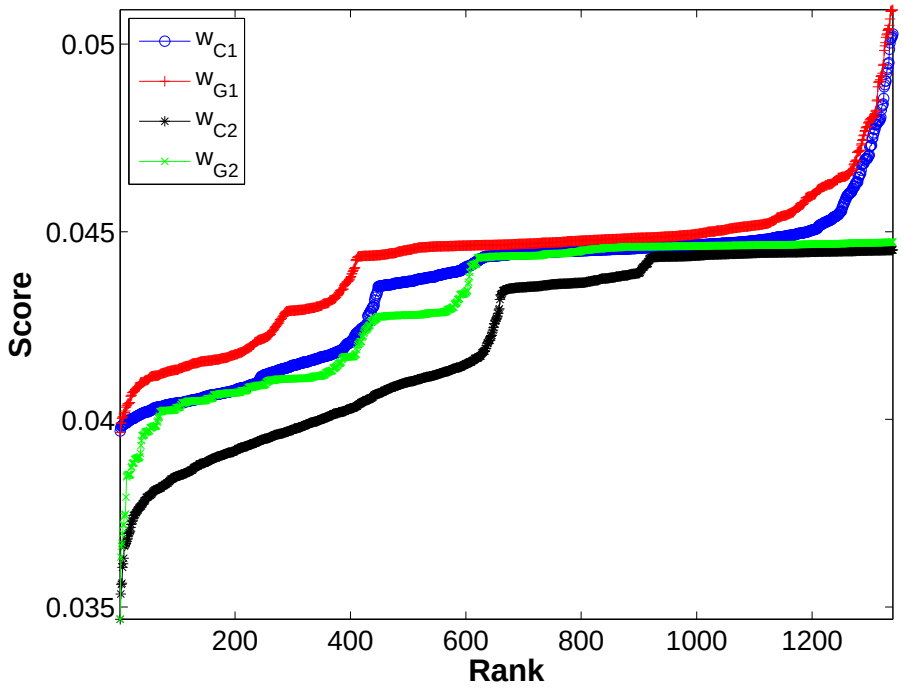

Figure A.1: Emitter set score vs. rank for different weightings, first 1340 ranked

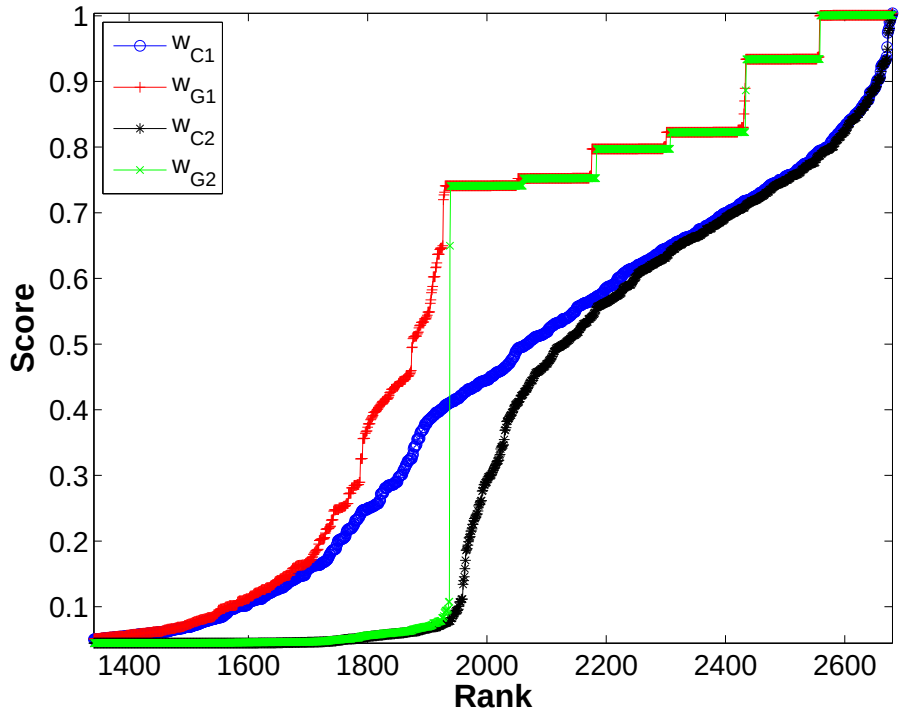

Figure A.2: Emitter set score vs. rank for different weightings, last 1340 ranked

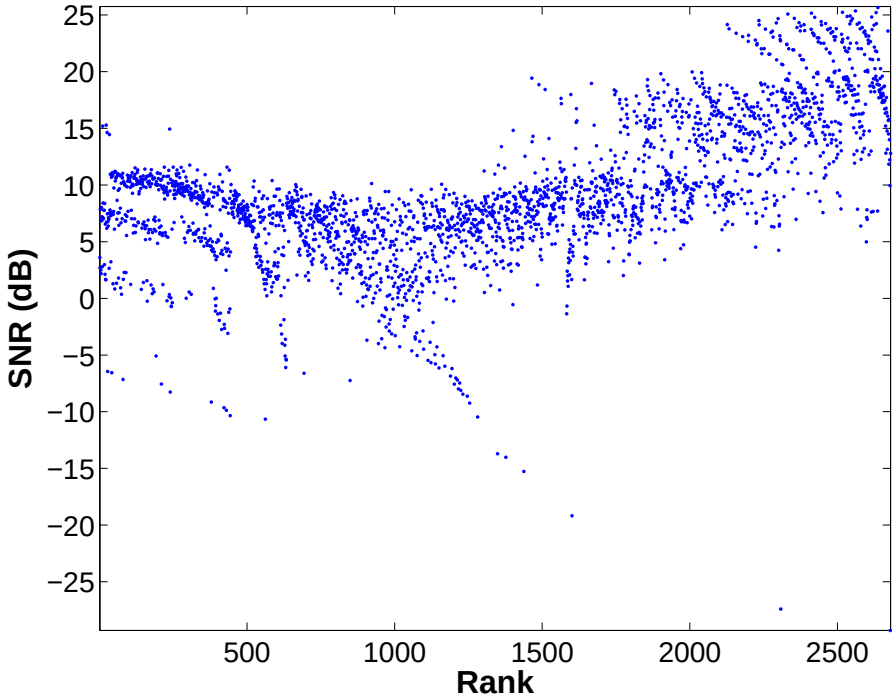

Figure A.3: Emitter set SNR in dB vs. rank for uniform coherent weighting, corresponding to Table 5.2 and Figure 5.3

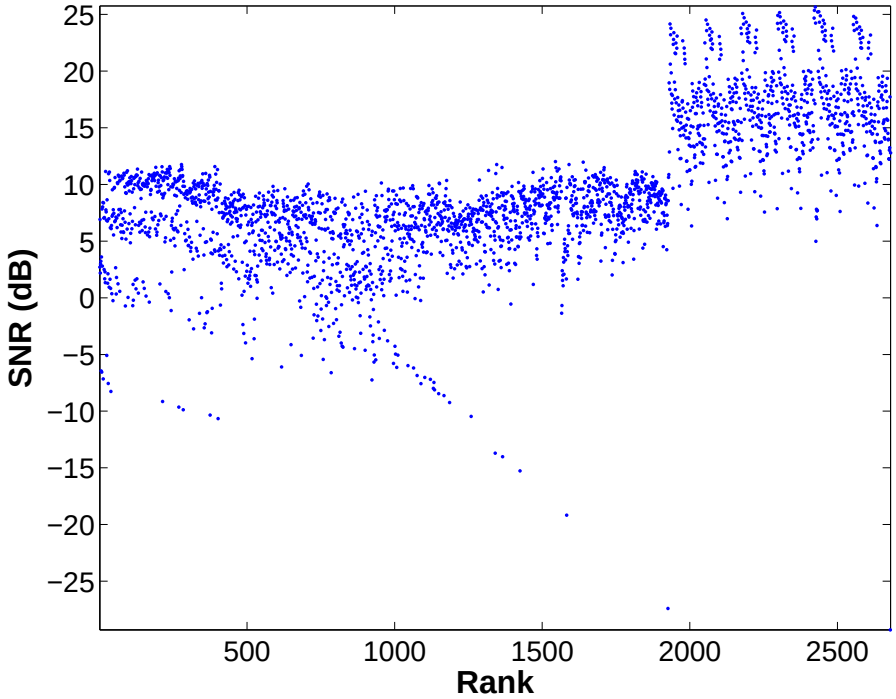

Figure A.4: Emitter set SNR in dB vs. rank for uniform GLRT weighting, corresponding to Table 5.3 and Figure 5.4

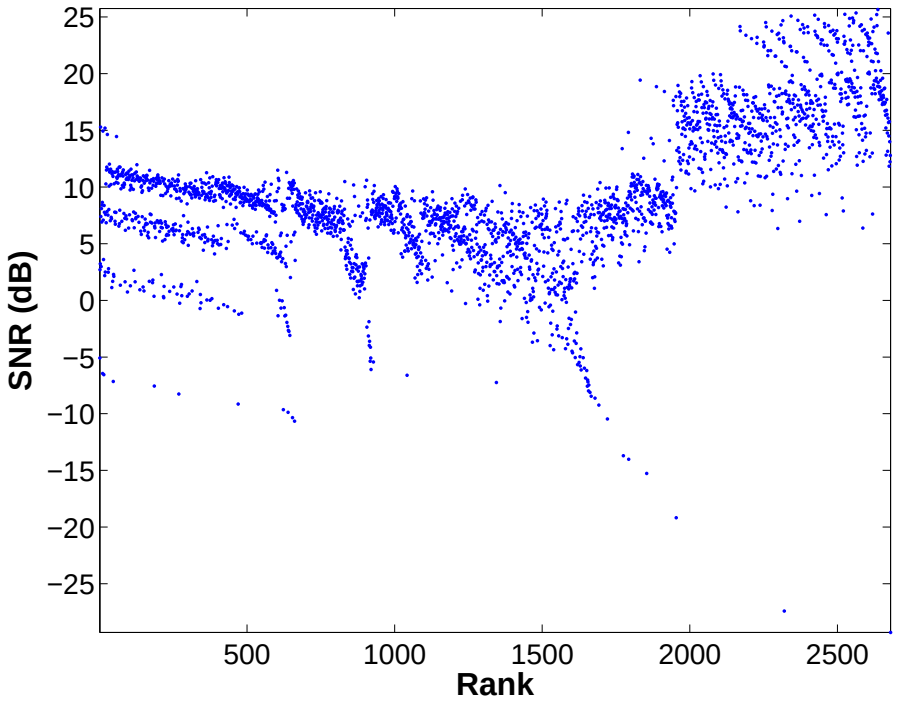

Figure A.5: Emitter set SNR in dB vs. rank for non-uniform coherent weighting, corresponding to Table 5.4 and Figure 5.5

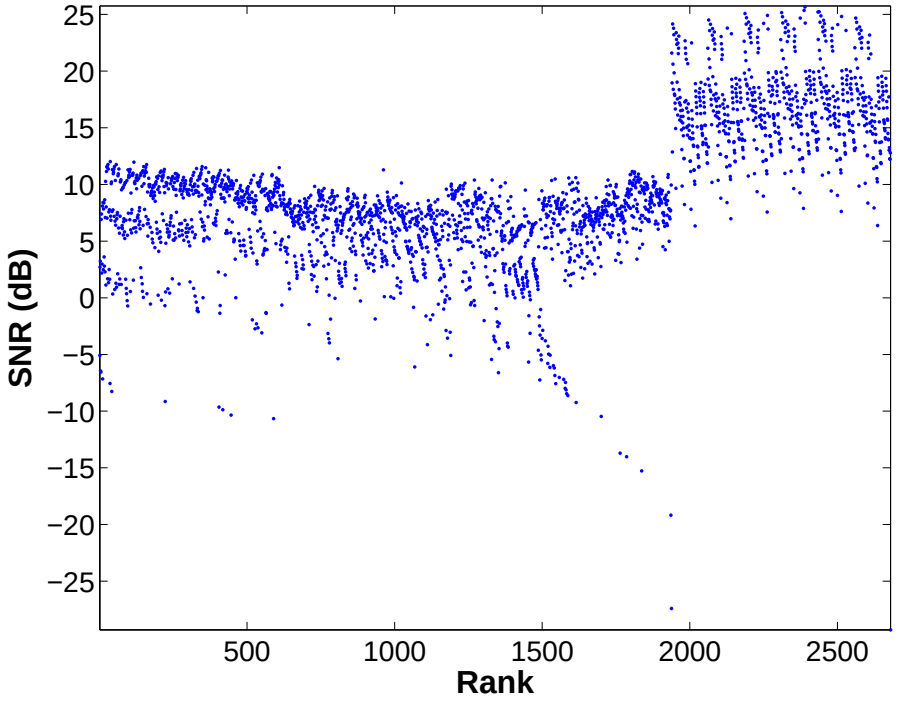

Figure A.6: Emitter set SNR in dB vs. rank for non-uniform GLRT weighting, corresponding to Table 5.5 and Figure 5.6

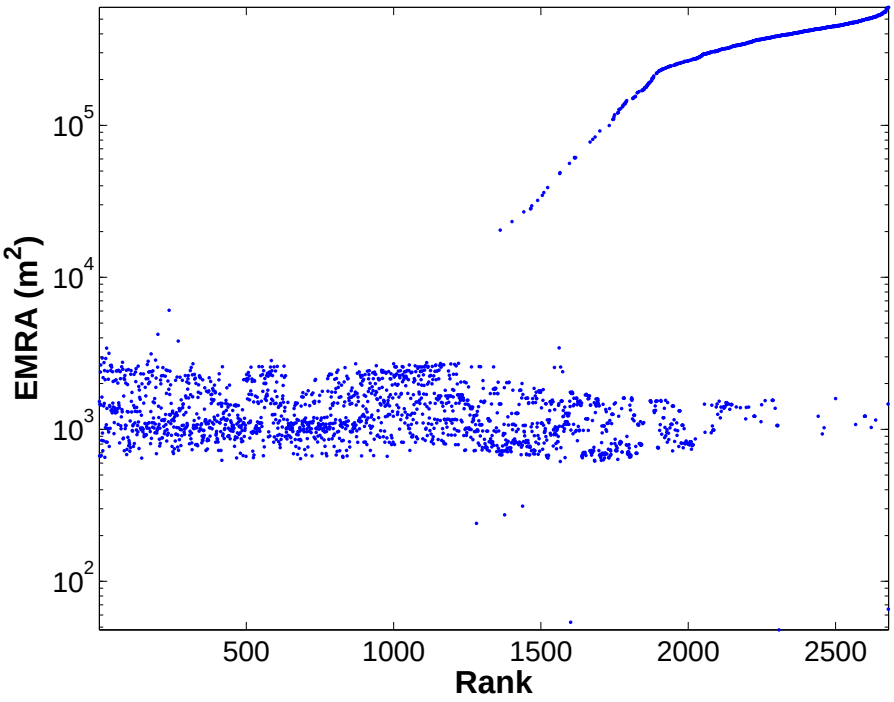

Figure A.7: Emitter set effective multistatic resolution vs. rank for uniform coherent weighting, corresponding to Table 5.2 and Figure 5.3

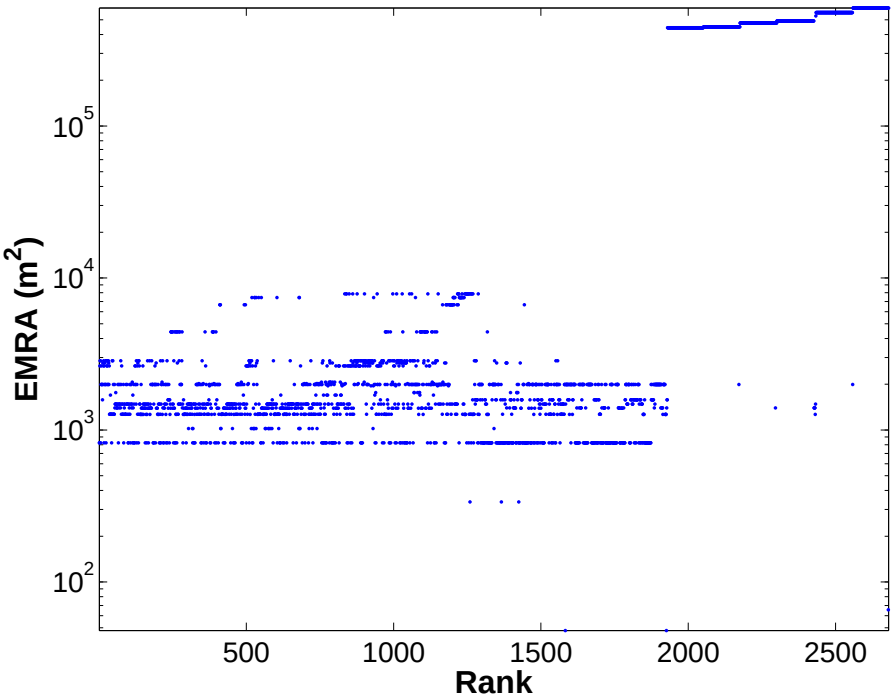

Figure A.8: Emitter set effective multistatic resolution vs. rank for uniform GLRT weighting, corresponding to Table 5.3 and Figure 5.4

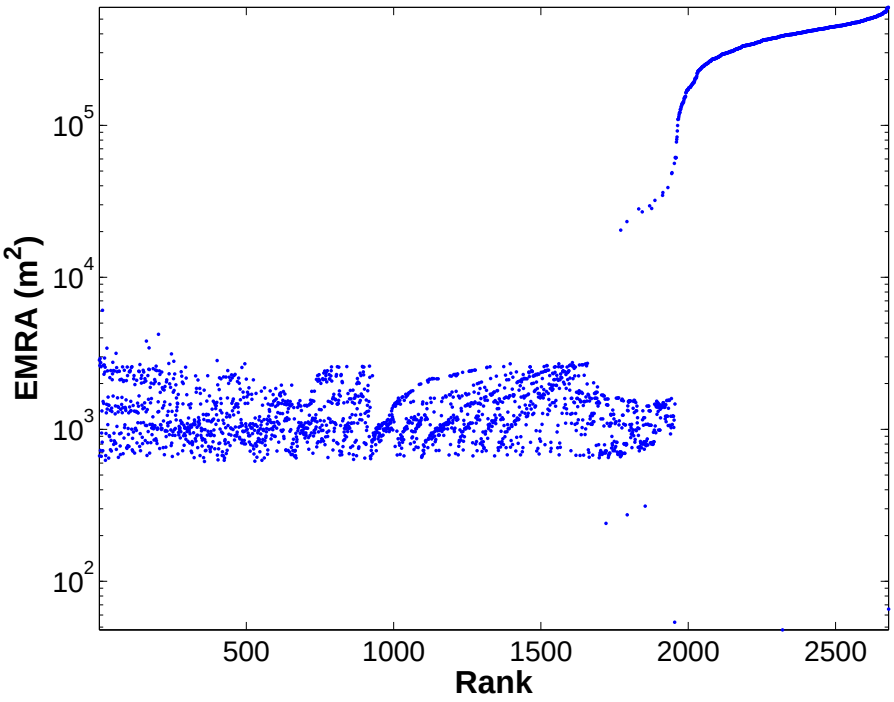

Figure A.9: Emitter set effective multistatic resolution vs. rank for non-uniform coherent weighting, corresponding to Table 5.4 and Figure 5.5

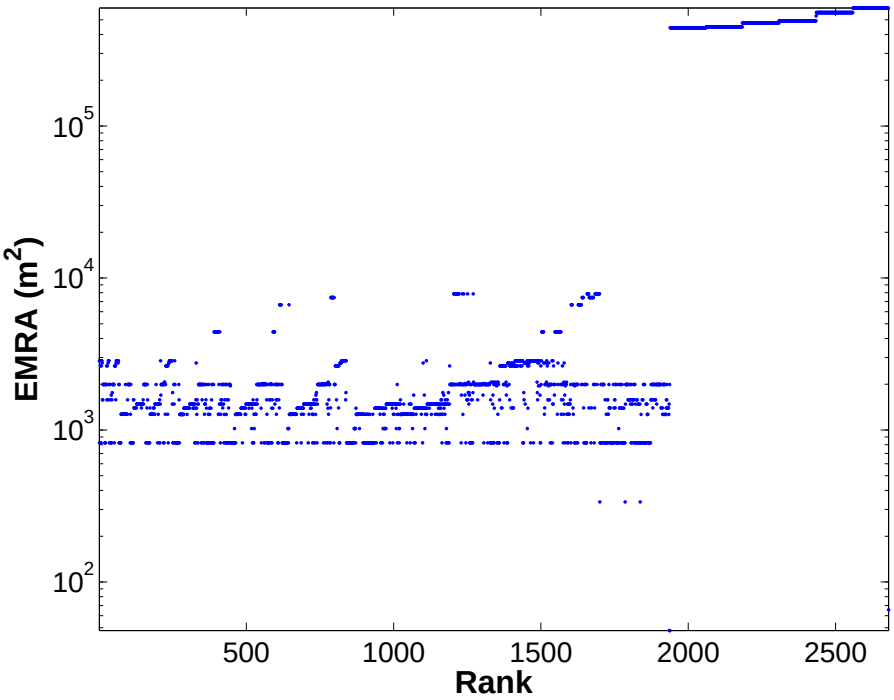

Figure A.10: Emitter set effective multistatic resolution vs. rank for non-uniform GLRT weighting, corresponding to Table 5.5 and Figure 5.6

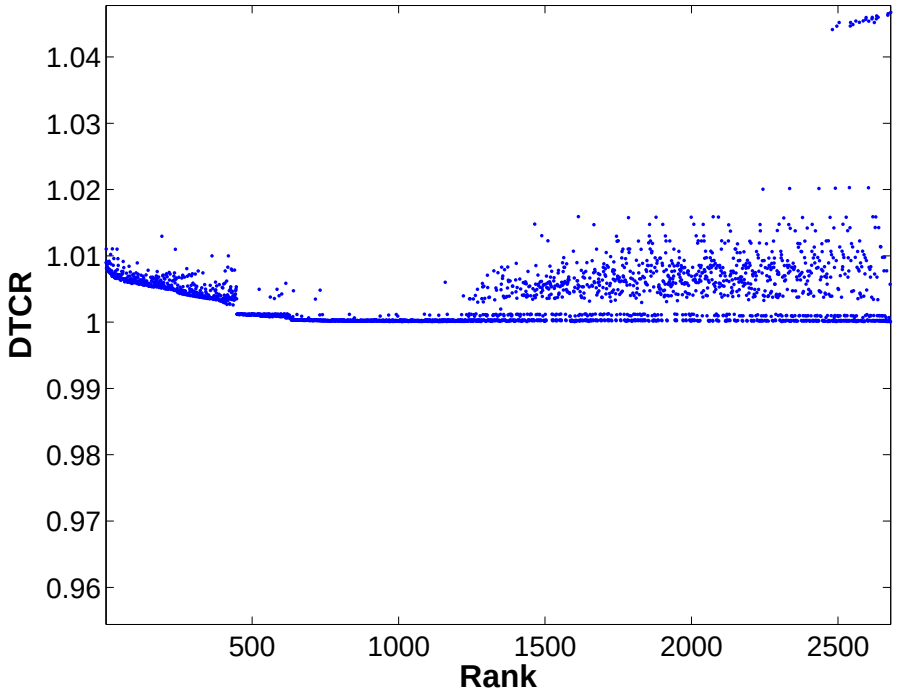

Figure A.11: Emitter set DTCR vs. rank for uniform coherent weighting, corresponding to Table 5.2 and Figure 5.3

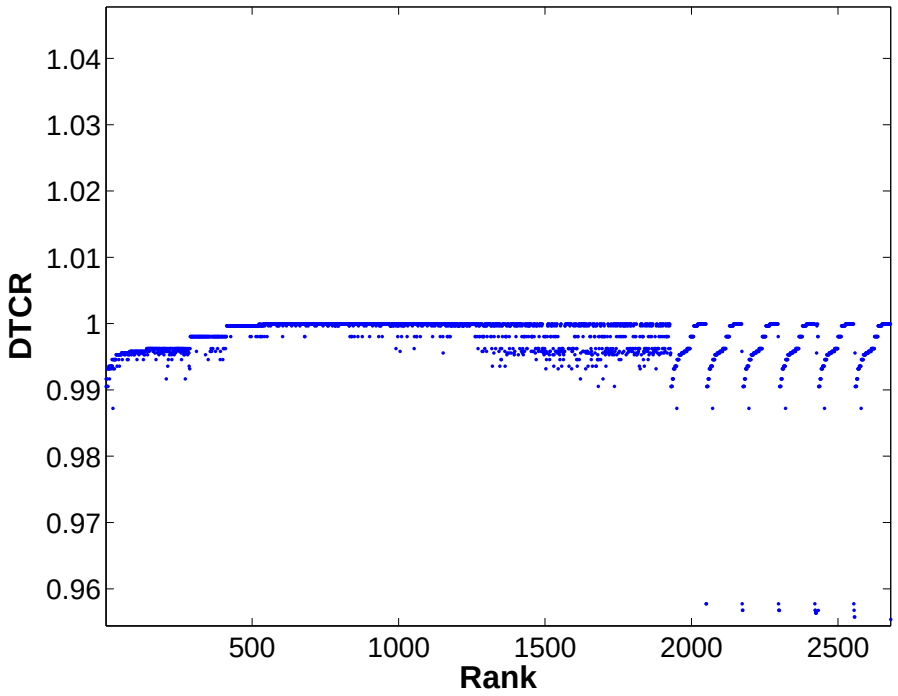

Figure A.12: Emitter set DTCR vs. rank for uniform GLRT weighting, corresponding to Table 5.3 and Figure 5.4

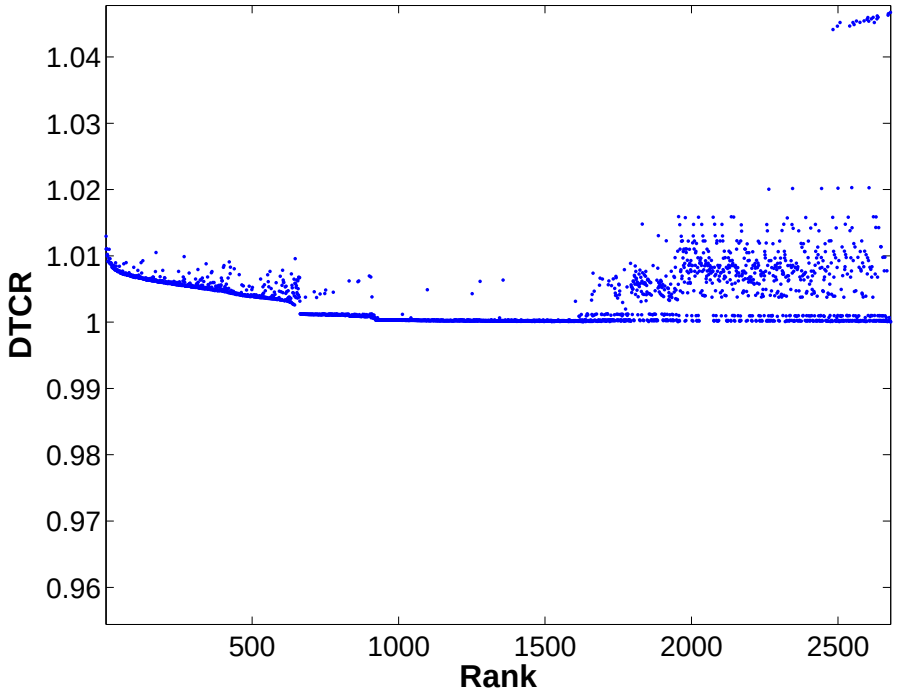

Figure A.13: Emitter set DTCR vs. rank for non-uniform coherent weighting, corresponding to Table 5.4 and Figure 5.5

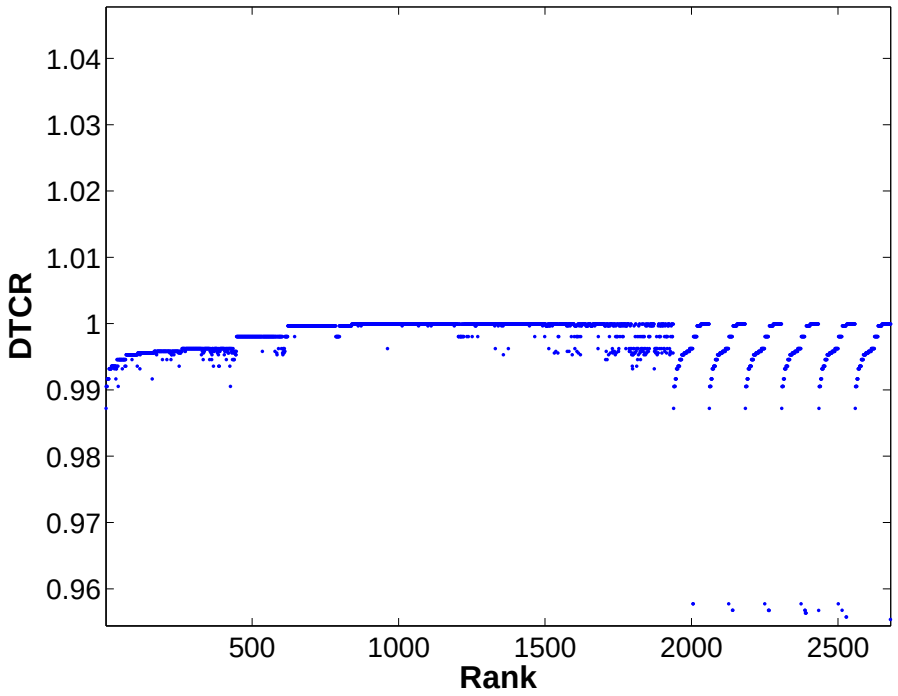

Figure A.14: Emitter set DTCR vs. rank for non-uniform GLRT weighting, corresponding to Table 5.5 and Figure 5.6

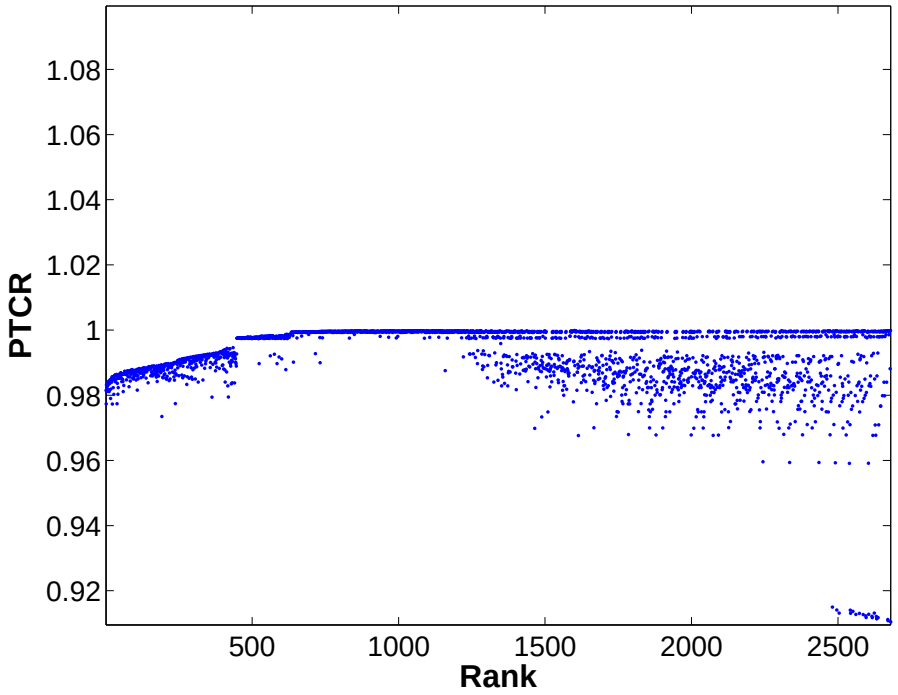

Figure A.15: Emitter set PTCR vs. rank for uniform coherent weighting, corresponding to Table 5.2 and Figure 5.3

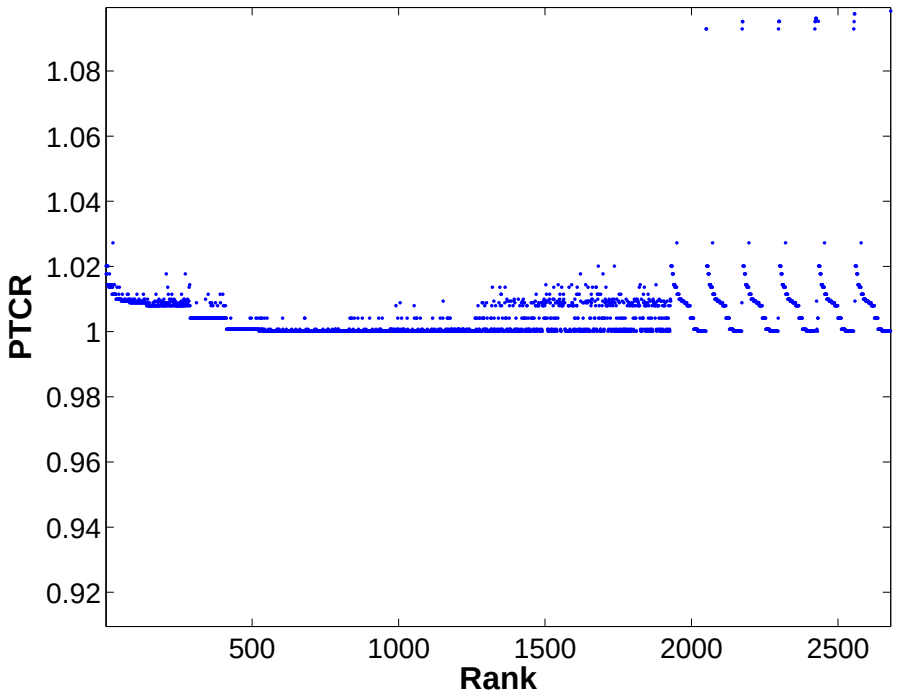

Figure A.16: Emitter set PTCR vs. rank for uniform GLRT weighting, corresponding to Table 5.3 and Figure 5.4

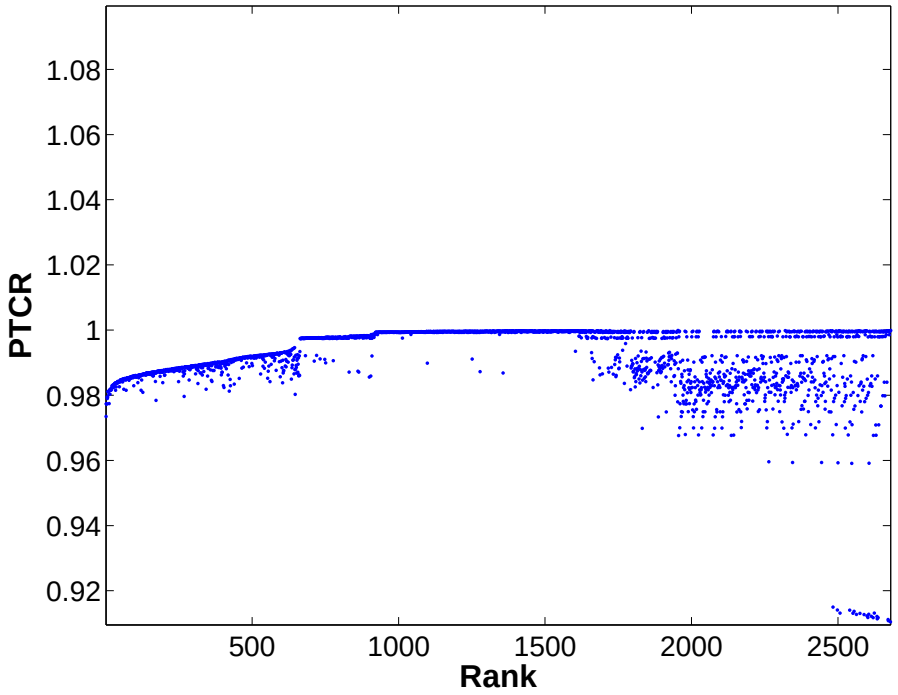

Figure A.17: Emitter set PTCR vs. rank for non-uniform coherent weighting, corresponding to Table 5.4 and Figure 5.5

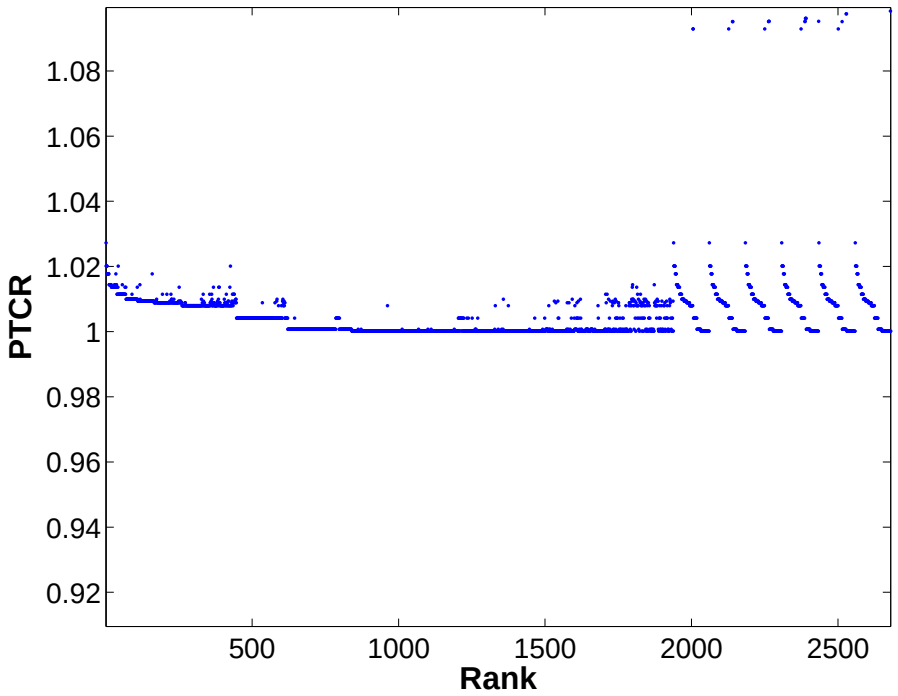

Figure A.18: Emitter set DTCR vs. rank for non-uniform GLRT weighting, corresponding to Table 5.5 and Figure 5.6

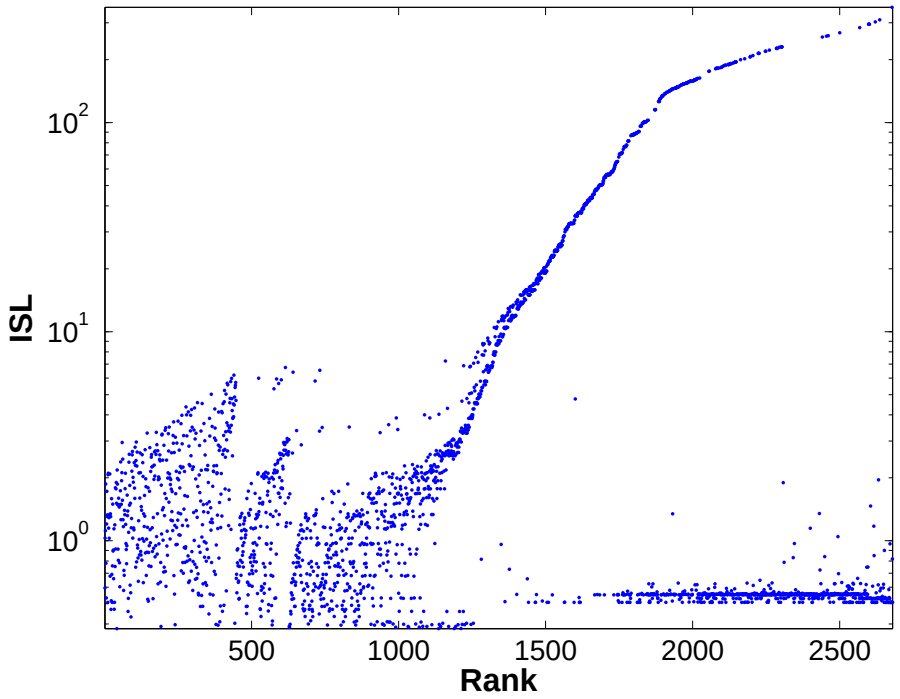

Figure A.19: Emitter set ISL vs. rank for uniform coherent weighting, corresponding to Table 5.2 and Figure 5.3

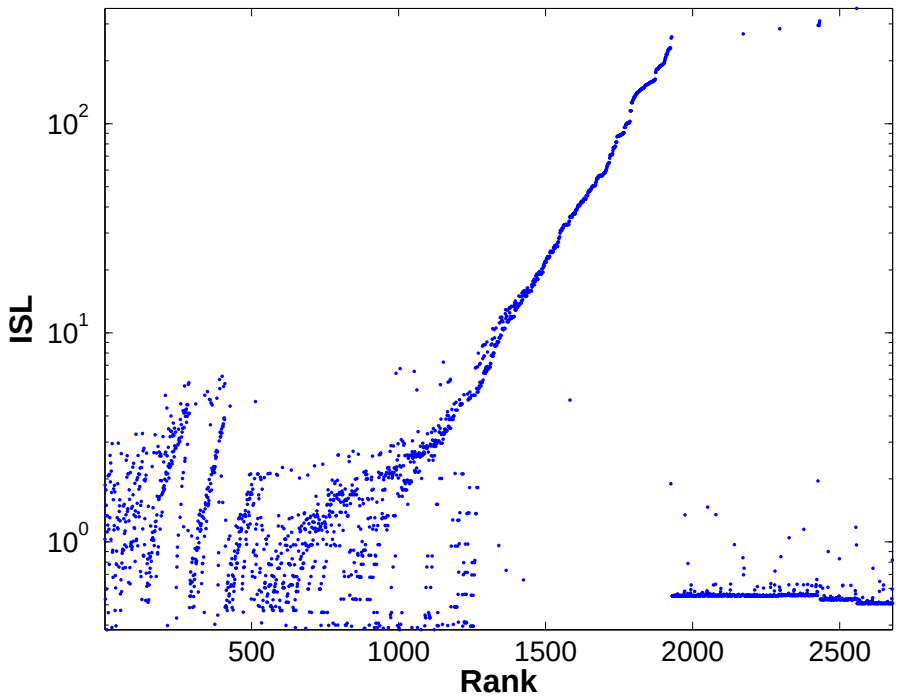

Figure A.20: Emitter set ISL vs. rank for uniform GLRT weighting, corresponding to Table 5.3 and Figure 5.4

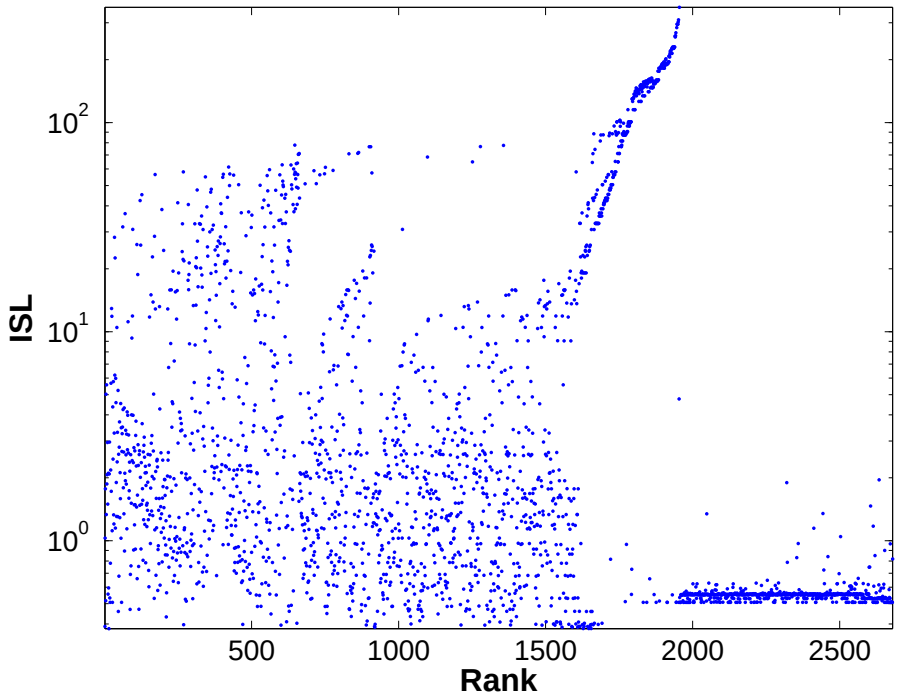

Figure A.21: Emitter set ISL vs. rank fornon-uniform coherent weighting, corresponding to Table 5.4 and Figure 5.5

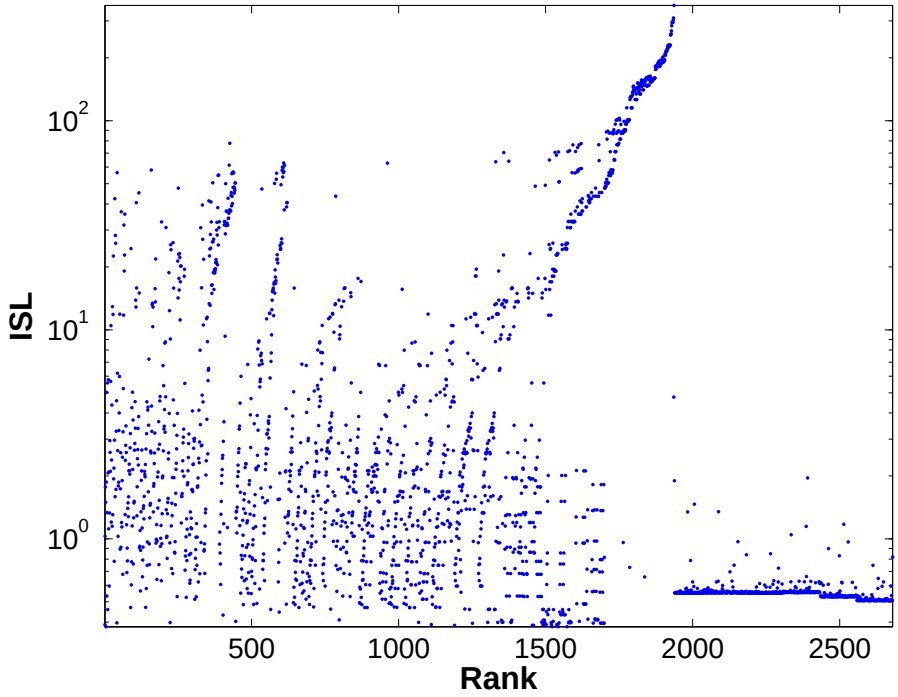

Figure A.22: Emitter set ISL vs. rank for non-uniform GLRT weighting, corresponding to Table 5.5 and Figure 5.6

Table A.1: Table of emitter combinations by rank and weighting, where $\mathbf{w_{C1}}$ is the uniform coherent weighting, $\mathbf{w_{G1}}$ is the uniform GLRT weighting, $\mathbf{w_{C2}}$ is the non-uniform coherent weighting, and $\mathbf{w_{G1}}$ is the non-uniform GLRT weighting

Rank	$\mathbf{w_{C1}}$ Tx's	$\mathbf{w_{G1}}$ Tx's	$\mathbf{w_{C2}}$ Tx's	$\mathbf{w_{G2}}$ Tx's	Rank	$\mathbf{w_{C1}}$ Tx's	$\mathbf{w_{G1}}$ Tx's	$\mathbf{w_{C2}}$ Tx's	$\mathbf{w_{G2}}$ Tx's
1	12,13	11,13	13	13	58	14,15	7,17	1,10,11	14,18
2	11,13	11,14,17	11,13	11,13	59	9,13,17	7,13,18	7,11,14,17	13,15,18
3	12,14,17	14,17	13,17	13,17	60	12,13,17	7,9,17	13,14,15,18	13,14,18
4	11,14,17	13,14	1,11,12	11	61	12,13,15,16	7,9,14,17	7,11,12,13	13,17,18
5	13,15	13,17	11,13,14	17	62	13,17,18	7,9,13,18	13,14,15,17	13,18
6	14,17	11	13,14	11,14,17	63	7,12,13,18	7,14	9,13,15,17	13,14,15,18
7	12,13,15	12,13	13,14,17	11,13,14	64	9,14,17,18	9,12,13,15	12,14,17,18	13,15,17,18
8	11,13,18	17	11,14,17	14,17	65	7,17	7,13,15	9,12,13,14	14,15,18
9	9,11,13	12,14,17	11,12,13	13,14	66	14,16,17	7,11,13	11,13,16	13,14,15,17
10	12,17	12,17	12,13,17	13,14,17	67	10,12,13	9,12,14,17	7,12,13,17	12,18
11	1,9,11	12,13,15	11	14	68	9,13,15,18	7,9,13,15	14,17,18	11,15,18
12	11,12,13	11,12,13	4,11,12	11,12,13	69	10,12,14,17	7,15	7,13,17	12,15
13	11,13,15	14	11,13,15	11,12	70	7,9,11,13	7,14,17,18	11,12,13,14	9,11,13
14	14,15,17	12,13,14	12,13	12,14,17	71	7,13,17	7,12,13	14,15	9,11,13,18
15	7,11,13	14,15,17	17	12,13,14	72	14,18	7,17,18	7,11,13,15	9,11,14,17
16	12,13,18	13,15	12,13,14	12,13	73	13,15,16	7,9,14	11,14,16,17	9,11,13,15
17	13,14	11,13,15	13,15,17	12,17	74	7,9,14,17	13,17,18	12,13,15,18	9,11
18	12,13,14	15,17	14,17	12,13,17	75	9,14	7,9,12,13	11,12,13,16	9,14,17,18
19	13,18	12,14	1,9,11	12,14	76	7,9,12,13	9,14,18	13,15,18	9,14,17
20	11,13,16	14,15	13,15	11,13,15	77	13,14,16	15,17,18	7,13,15,17	9,13,15
21	15,17	12,14,15,17	13,14,15	11,14,15,17	78	12,13,16,18	7,13,15,18	9,13,14,15	9,13,18
22	9,13	12,13,18	11,14,15,17	11,15	79	10,12,13,15	7,14,15,17	12,13,16,17	9,13,15,18
23	1,11,12	13,14,15	11,13,18	12,13,15	80	14	9,13,17	13,14,16,17	9,14,15,17
24	9,13,14	11,13,18	11,12,13,15	12,14,15,17	81	13,16	9,15,17	7,12,13,14	9,17,18
25	9,14,17	13	12,13,15,17	12,13,14,15	82	7,9,13,15	9,13,16	11,13,15,16	9,13,14
26	1,7,11	12,13,17	12,14,17	14,15,17	83	9,11,13,18	7,12,13,18	7,13,14	9,13,17
27	9,12,13	14,17,18	1,7,11	11,12,13,15	84	12,14	7,9,11,13	14,15,17,18	9,13,14,18
28	11	17,18	12,13,14,15	15,17	85	14,15,16,17	7,13,14	9,11,13,18	9,15,17
29	14,17,18	13,18	13,17,18	12,13,15,17	86	9,11,13,16	7,9,13,16	13,16,17	9,14,18
30	9,13,15	12	11,12	11,12,14,17	87	10,14,17	7,13,16	9,13	9,13,14,15
31	7,14,17	12,14,17,18	12,17	14,15	88	10,13,14	9,18	9,14,17	9,13,17,18
32	13,15,18	13,15,18	12,13,15	13,14,15	89	7,9,13	9,14,16,17	12,13,14,16	9,13
33	7,13	14,18	11,14,17,18	13,15	90	10,13	9,16,17	9,12,13	12,14,18
34	1,10,11	12,13,15,18	12,13,14,17	13,15,17	91	14,16,17,18	9,13,16,18	9,12,14,17	9,17
35	10,11,13	14,15,17,18	11,12,13,18	11,14	92	9,17,18	7,12,14,17	12,17,18	9,14
36	7,12,13	9,13	11,12,14,17	12	93	13,16,17	7,14,16,17	10,13,14,17	9,13,15,17
37	12,14,17,18	9,14,17	14,15,17	12,13,14,17	94	11,14,16,17	7,16,17	7,11,13,18	9,15
38	7,13,15	9,17	12,13,17,18	11,12,15	95	7,11,14,17	7,12,13,15	11,18	9,14,15
39	13,17	15	11,13,15,18	11,13,18	96	9,12,13,16	9,13,14,18	13,14,17,18	9,18
40	13,14,18	9,13,18	13,14,18	11,14,17,18	97	10,13,17	7,18	13,15,16,17	9,11,12,13
41	9,12,14,17	9,13,15	9,11,13	11,13,15,18	98	7,9,13,14	7,13,16,18	10,11,14,17	9,12,13
42	17	9,14	11,15	15	99	10,12,13,18	9,11,13,18	9,13,15	9,12,13,18
43	13,14,15	9,11,13	12,14,15,17	11,13,17	100	7,14,17,18	11,13,16	10,11,12,13	9,12,13,15
44	12,13,15,18	9,14,17,18	12,13,14,18	11,12,13,18	101	10,11,14,17	9,13,15,16	9,12,13,15	9,12,14,17
45	9,12,13,15	13,14,18	15,17	15,18	102	7,11,13,16	7,13,15,16	10,11,13	9,12,13,14
46	17,18	9,15	13,15,17,18	12,13,18	103	9,10,11,13	7,9,13,14	7,13,14,15	9,12,17
47	12,13,16	13,15,17	14	12,14,17,18	104	9,11,14,17	12,13,16	9,14,15,17	9,12,13,17
48	7,13,14	9,17,18	12,14	12,13,15,18	105	11,13,16,18	9,14,16	17,18	9,12
49	9,14,15,17	9,12,13	13,18	12,13,14,18	106	7,14	7,14,16	9,13,17,18	9,11,15
50	7,12,14,17	9,13,15,18	9,11,14,17	12,17,18	107	7,11,13,18	11,14,17,18	10,12,13,17	9,15,17,18
51	9,13,18	9,14,15,17	9,11,12,13	12,13,17,18	108	13,15,17	7,12,13,16	9,13,14,18	12,15,17
52	9,17	9,13,14	7,11,13	11,18	109	7,13,18	9,12,13,16	7,12,14,17	9,11,18
53	7,12,13,15	9,12,13,18	9,13,17	14,17,18	110	9,13,14,18	7,14,18	9,13,14,17	7,11,13
54	14,15,17,18	7,9,13	9,13,14	14,15,17,18	111	9,12,13,14	7,9,16,17	7,14,17	7,9,11,13
55	12,14,15,17	7,13	9,12,13,17	15,17,18	112	9,14,16,17	7,15,17	13,14,16	7,11,13,18
56	9,12,13,18	7,14,17	12,13,18	17,18	113	7,9,13,18	16,18	10,11,13,14	7,11,14,17
57	12,14,16,17	15,18	9,11,13,15	11,12,13,14	114	9,10,14,17	9,11	10,11,13,15	7,11,13,15

Continued on next page

Table A.1 – continued from previous page

Rank	$\mathbf{w_{C1}}$ Tx's	$\mathbf{w_{G1}}$ Tx's	$\mathbf{w_{C2}}$ Tx's	$\mathbf{w_{G2}}$ Tx's	Rank	$\mathbf{w_{C1}}$ Tx's	$\mathbf{w_{G1}}$ Tx's	$\mathbf{w_{C2}}$ Tx's	$\mathbf{w_{G2}}$ Tx's
115	9,13,16	15,16	11,13,16,18	7,11	177	10,14,17,18	7,9,13,17	14,16,17,18	9,13,15,16
116	7,17,18	7,9,17,18	7,12,13	7,9,11	178	10,11,13,15	10,14,15,17	12,16,17	9,13,16
117	10,11,13,18	7,11,13,16	7,13	11,12,13,17	179	14,16	13,14,16	9,10,13,17	9,16,17
118	7,12,13,16	12,13,16,18	15,17,18	9,11,12	180	7,9,14	7,10,12,13	7,11	9,13,14,16
119	10,13,15	7,13,17	13,14,15,16	7,9,14,17	181	13,14,15,16	9,10,12,13	7,17	9,14,16
120	7,10,11,13	9,11,13,16	7,12,13,15	7,9,13,18	182	10,14	9,12,17	7,9,14,17	9,16,17,18
121	7,12,13,14	7,11	11,14	7,9,13,15	183	7,13,14,16	10,12,13,16	7,9,12,13	9,13,16,17
122	9,15,17	14,16,17	10,13,17	7,9,13	184	10,12,17	9,10,11,13	7,13,15,18	9,15,16,17
123	9,10,12,13	12,14,16,17	11,12,15	7,9,17	185	7,15	7,10,11,13	9,14	7,9,13,16
124	13,16,18	16,17	7,13,15	7,9,14	186	7,14,18	7,13,14,15	12	7,9,16,17
125	13,15,16,18	12,13,15,16	10,12,13,14	7,9,13,14	187	9,10,13,17	10,11,13,16	7,11,15	7,9,14,16
126	7,13,15,18	7,13,14,18	12,14,16,17	7,9,17,18	188	7,12,17	7,12,17	7,14,15	9,15,16
127	7,10,14,17	13,16	11,12,13,17	7,9,13,17	189	12,16,17	10,12,13,18	10,14,17	9,14,16,18
128	12,13,14,16	7,11,13,18	10,13,15,17	7,14,17,18	190	7,9,10,13	15,16,17	9,17,18	7,14,16,17
129	9,10,13,15	12,13,14,18	7,9,11,13	7,14,17	191	9,10,17	7,12,13,14	13,15,16,18	7,13,16,18
130	10,12,13,14	14,16,17,18	12,13,15,16	7,13,18	192	13	11,14,16,17	7,13,16,17	7,13,15,16
131	7,15,17	9,13,14,15	12,13,16	7,13,15	193	10,13,14,16	10,12,14,17	7,9,13,15	7,13,16
132	7,13,16	14,16	7,9,13,17	7,13,15,18	194	10,13,15,16	14,16,18	10,14,15,17	12,15,17,18
133	10,14,15,17	13,16,18	9,12,13,18	7,14,15,17	195	11,13,15,16	10,14,18	9,11,13,14	7,16,17
134	9,13,16,18	9,11,14,17	9,12,17	7,17,18	196	11,12,13,16	10,12,13,15	7,13,18	7,14,16
135	9,13,15,16	9,13,14,16	13,16,17,18	7,13,14	197	9,14,16	10,16,17,18	7,10,11,13	7,13,14,16
136	10,11,13,16	13,15,16	10,13,14,15	7,13,17	198	7,10,13,17	10,15,17	7,10,13,17	7,16,17,18
137	10,13,15,18	16,17,18	14,18	7,15,17	199	7,13,16,18	9,13,17,18	9,10,13,14	11,16
138	9,13,14,15	7,13,14,16	10,11,13,18	7,14,18	200	7,14,15,17	9,10,13,14	10,12,13,18	7,13,16,17
139	7,10,12,13	7,16,17,18	7,13,14,18	7,13,14,18	201	9,10,13,16	12,16,17	12,14,18	9,16,18
140	9,13,14,16	9,10,13	9,13,18	7,13	202	9,12,17	7,10,17,18	7,14,15,17	7,15,16,17
141	9,10,13,14	9,16,17,18	9,11,13,16	7,13,14,15	203	7,10,17	9,10,17,18	9,12,13,16	7,15,16
142	16,17	9,10,13,16	9,15,17	7,17	204	7,14,16	7,10,13,14	15,16,17	7,14,16,18
143	7,10,13,15	9,12,13,14	14,15,16,17	7,13,17,18	205	10,14,18	10,11	7,13,14,16	7,11,16
144	7,9,17	10,14,17	9,14,17,18	7,9,15,17	206	7,11,13,15	7,13,16,17	10,11,13,16	11,12,13,16
145	11,14,17,18	9,10,17	10,13,14	7,14	207	7,10,13,16	11,13,14	10,13,15	9,11,16
146	7,13,15,16	7,9,10,13	9,13,15,18	7,15	208	9,11,13,15	9,13,16,17	9,14,16,17	7,16,18
147	9,10,13	9,10,14,17	7,9,13,14	7,13,15,17	209	10,13,16	13,16,17	7,17,18	13,14,17,18
148	7,10,13,14	10,17	9,11	7,14,15	210	12	10,11,13,18	10,13	15,16
149	10,17	14,15,16,17	7,12,13,18	7,18	211	10,13,16,17	7,10,14,16	7,9,13	7,12,13,16
150	9,10,13,18	7,10,13	14,16,17	7,11,12,13	212	10,13,16,18	12,13,14,15	7,10,13,14	9,12,13,16
151	10,13,18	9,10,13,18	9,17	7,15,17,18	213	9,10,14	12,13,14,16	13,16,18	12,13,16
152	10,12,13,16	10,14	13,14,16,18	7,9,12,13	214	10,16,17	18	9,14,18	12,13,16,18
153	10,15,17	7,10,13,16	14,15,18	7,12,13	215	10,11	9,10,14,16	9,15,17,18	12,14,16,17
154	10,11,12,13	10,14,16,17	10,12,14,17	7,12,13,18	216	7,9,17,18	13,14,16,18	10,13,16,17	12,13,15,16
155	10,17,18	7,10,17	7,12,17	7,12,14,17	217	13,14,15,18	7,9,14,16	15,18	12,16,17
156	9,16,17	10,16,17	13,15,16	7,12,13,15	218	9,13,16,17	9,11,13,15	11,16	12,13,14,16
157	10,13,14,18	10,11,13	7,11,13,16	7,12,13,14	219	7,9,16,17	10,12,17	7,14	7,9,11,15
158	7,9,13,16	10,15	9,11,12	7,12,17	220	7,11,12,13	10,11,14,17	7,12,13,16	12,13,16,17
159	10,13,14,15	7,10,14,17	10,13,17,18	11,13,14,17	221	9,16,17,18	7,9,10,14	10,13,15,18	7,9,11,16
160	15,17,18	9,10,13,15	10,12,13,15	7,12,13,17	222	7,16,17,18	10,15,16	11,15,16	16,18
161	7,11	7,10,13,18	7,13,17,18	7,12	223	7,10,14	7,13,17,18	10,12,17	18
162	9,15	11,13,16,18	7,15,17	7,11,15	224	9,10,17,18	7,10,15	9,13,15,16	12,16
163	7,10,13,18	9,10,14	11,15,18	7,9,14,18	225	14,16,18	9,12	10,11,12	9,15,18
164	7,13,14,18	10,14,17,18	12,13,16,18	7,9,12	226	7,9,10,17	12,17,18	7,9,13,18	9,12,17,18
165	7,10,13	13,15,16,18	9,11,15	7,11,12	227	7,10,17,18	9,10,13,17	9,11,18	14,16,17,18
166	16,17,18	7,10,13,15	9,13,16,17	11,13,16	228	7,13,16,17	7,11,13,15	10,15,17	14,16,17
167	7,14,16,17	7,10,14	9,14,15	7,11,13,16	229	15,16	7,10,13,17	14,15,16	14,15,16,17
168	15,16,17	7,11,14,17	9,13,14,16	9,11,13,16	230	10,16,17,18	10,12,13,14	15,16,17,18	16,17,18
169	13,14,16,18	10,18	13,16	11,13,16,18	231	9,10,16,17	13,14,15,16	9,10,14,17	15,16,17
170	7,9,13,17	10,14,16	7,13,14,17	11,14,16,17	232	10,14,16	11,13,15,16	7,9,15,17	16,17
171	9,14,18	10,17,18	7,14,17,18	11,13,15,16	233	9,13,17,18	7,12	11,12,16	9,13,14,17
172	10,14,16,17	13,14,15,18	11,13,17	7,11,18	234	10,13,17,18	9,11,12,13	9,13,16	15,16,17,18
173	7,13,14,15	9,10,16,17	7,11,12	7,9	235	9,11,12,13	10,15,16,17	9,10,12,13	11,15,16
174	7,16,17	7,10,16,17	10,13,14,18	9,14,15,18	236	10,15	11,12,13,16	7,14,18	14,16,18
175	9,11	7,9,10,17	10,12,13	9,14,16,17	237	15,18	10,12	7,15,17,18	14,15,16
176	12,13,14,18	10,12,13	9,10,11,13	9,13,16,18	238	4,11,12	7,11,12,13	16,17	14,16

Continued on next page

Table A.1 – continued from previous page

Rank	$\mathbf{w}_{C1}$ Tx's	$\mathbf{w}_{G1}$ Tx's	$\mathbf{w}_{C2}$ Tx's	$\mathbf{w}_{G2}$ Tx's	Rank	$\mathbf{w}_{C1}$ Tx's	$\mathbf{w}_{G1}$ Tx's	$\mathbf{w}_{C2}$ Tx's	$\mathbf{w}_{G2}$ Tx's
239	7,10,16,17	10,11,13,15	9,10,13,15	13,16,18	301	8,13,15	8,9,14	9,14,16	7,9,10,14
240	15	10,11,12,13	7,13,15,16	13,15,16	302	8,13,14,15	8,10,14	10,11,18	10,15,16
241	13,16,17,18	9,10,15	12,16,17,18	13,15,16,18	303	8,13,14	7,8,10,13	10,15,16,17	10,15,16,17
242	7,18	7,15,16,17	9,13,16,18	13,14,16	304	9,12	8,18	7,15	10,14,16,18
243	16,18	10,16	10,13,14,16	13,16,17	305	8,13,15,16	7,8,17	10,12,16,17	10,14,15
244	9,18	10,13,16	7,10,14,17	13,14,16,18	306	7,12,13,17	7,8,13,16	9,10,17,18	10,16,18
245	8,12,14,17	10,13	10,11,15	13,14,15,16	307	8,10,13,18	7,8,14,17	9,11,12,15	10,17
246	10,14,15	10,13,18	10,14,17,18	13,16,17,18	308	7,10,11	8,9,13,15	7,11,16	7,10,13,16
247	10,18	10,13,15	7,11,18	13,16	309	8,9,13,16	8,10,15	7,14,16,18	7,10,14,17
248	8,11,14,17	10,13,16,18	7,10,12,13	13,15,16,17	310	8,13,14,18	9,15,16	10,12,17,18	7,10,13,18
249	8,12,13,15	7,10,15,17	11,17,18	7,14,15,18	311	7,12	7,8,10,17	7,9,14,18	7,10,13,15
250	10,12,13,17	10,14,15	10,14,15	15,16,18	312	8,9,17,18	7,8,14	12,14,16,18	7,10,13
251	8,9,11,13	10,13,15,16	7,13,16	11,14,15	313	8,14,16,17	7,8,13,18	9,11,15,16	7,10,16,17
252	7,10,14,16	7,15,16	12,18	7,9,11,18	314	7,8,13,16	8,10,16,17	10,14	7,10,17
253	8,11,13	7,10,11	16,17,18	11,16,18	315	7,8,17,18	7,8,9,17	11,14,15	7,10,14
254	10,15,16,17	13,16,17,18	7,14,16,17	12,16,17,18	316	11,13,15,18	8,9,16,17	7,11,15,18	7,10,17,18
255	9,10,14,16	10,14,16,18	10,15,17,18	7,15,18	317	8,13,17	8,16,18	9,10,11	7,10,13,14
256	8,11,13,18	10,16,18	7,10,13,15	7,12,17,18	318	8,13,18	8,10,11,13	9,10,11,15	7,10,14,16
257	8,12,13,18	10,13,15,18	10,13,18	13,14,16,17	319	8,14,17	8,16	7,14,16	10,14
258	7,9,10,14	7,9,11	7,9,11	9,12,16	320	8,9,10,13	7,8,13,15	9,10,17	7,10,13,17
259	7,8,11,13	11,13,15,18	7,15,16,17	7,11,15,16	321	7,8,9,17	7,8,16,17	7,9,10,13	10,15,17,18
260	10,13,15,17	10,13,14	7,9,17	9,11,15,16	322	8,10,13,17	7,8,11,13	7,10,17,18	7,10,15
261	8,9,14,17	9,15,16,17	9,15,16,17	10,11,13	323	9,10,15	8,9,11,13	11,16,17,18	7,10,15,17
262	8,11,12,13	9,10,15,17	7,9,17,18	7,10,11,13	324	8,13,14,16	8,9,10,14	7,9,16,17	10,15
263	12,13,16,17	10,13,14,16	9,12	9,10,11,13	325	8,13,16,18	7,8,10,14	9,10,14,18	10,11,16
264	7,10,15,17	9,10,11	9,12,17,18	10,11,13,16	326	8,9,13	8,11,13,16	7,11,12,15	7,10,14,18
265	8,14,15,17	10,13,17	12,15,17,18	10,11,13,18	327	8,10,13,14	8,10,17,18	7,11,15,16	9,11,15,18
266	8,9,12,13	14,15,16	10,12,13,16	10,11,14,17	328	9,10,11	7,8,15	10,13,16,18	10,18
267	8,11,13,15	9,13,15,17	7,12,17,18	10,11,13,15	329	7,8,13,17	8,10,14,16	10,16,17,18	10,11,12,13
268	7,8,14,17	10,13,14,18	11,13,14,17	7,10,11	330	7,8,10,13	8,12,13	12,15	14,15,16,18
269	7,13,17,18	9	15	9,10,11	331	8,9,16,17	8,9,15	10,14,15,18	10,16
270	8,11,13,16	7,13,15,17	9,14,15,18	10,11	332	9,12,13,17	8,10,12,13	7,10,11,15	9,10
271	8,9,13,15	7,10,14,18	10,17,18	7,12,16	333	8,10,17,18	8,9,12,13	9,10,13,16	11,12,15,18
272	8,12,13,14	13,14,17	9,15	11,12,16	334	7,8,13	7,8,12,13	7,10,11	7,11,15,18
273	8,9,13,14	10,13,16,17	9,10,13,18	7,9,10,11	335	8,10,13,16	8,10,18	9,11,15,18	7,10
274	7,8,12,13	10,13,14,15	9,10,15,17	9,10,13,16	336	8,12,17	8,9,17,18	10,13,16	7,10,11,16
275	8,14,17,18	12,13,16,17	9,10,13	9,10,14,17	337	8,15,17	8,12,13,16	7,10,14,18	7,15,16,18
276	7,8,13,15	7,14,15	10,11	9,10,13,18	338	9,15,16,17	7,8,17,18	7,10,17	7,10,12,13
277	12,13,14,15	7,14,16,18	9,16,17,18	9,10,13,15	339	7,8,16,17	8,15	7,9,14,16	9,10,12,13
278	8,10,11,13	7,12,13,17	10,17	9,10,13	340	8,9,10,17	8,12,13,18	9,10,14	10,12,13,16
279	12,17,18	10,12,13,17	14,16	9,10,16,17	341	10,14,16,18	9,14,15	9,18	10,12,13
280	9,10,15,17	9,12,13,17	9,16,17	9,10,17	342	8,13,17,18	7,8,14,16	12,16	10,12,13,18
281	8,9,13,18	13,15,16,17	14,16,18	9,10,14	343	8,9,17	8,9,14,16	11,13,14,15	10,12,14,17
282	7,8,13,14	10,13,17,18	7,9,14	9,10,13,14	344	8,13,16,17	7,8,9,14	15,16	10,12,13,15
283	8,13,15,18	7,9,15,17	10,14,16,17	9,10,17,18	345	8,17,18	8,12,14,17	7,9,12	10,12,17
284	8,12,13,16	7	11,16,18	9,10,14,16	346	7,8,10,17	8,11	7,9,11,16	10,12,13,14
285	7,13,15,17	11,14,15,17	12,15,17	9,10,13,17	347	7,8,17	8,12,13,15	7,10,13,16	9,10,11,16
286	8,12,13	9,10,14,18	14,15,16,18	9,10,15	348	7,8,9,14	8,9,13,14	11,12,15,18	10,12,13,17
287	7,9,14,16	11,12	7,9,11,15	9,10,15,17	349	8,10,16,17	8,11,13,18	10,16,17	10,11,15
288	7,10,15	10,15,17,18	7,14,15,18	10,14,16,17	350	7,8,15,17	13,15,17,18	10,11,15,18	10,11,12
289	8,10,14,17	8,9,13	9,11,16	10,14,17,18	351	8,9,15,17	7,8,13,14	7,9,11,18	10,12
290	7,8,13,18	8,9,10,13	7,16,17,18	10,14,17	352	8,16,17,18	8,12,17	9,15,16	10,12,16,17
291	10,15,16	8,9,13,16	7,10,13,18	7,9,10,13	353	8,10,15,17	8,10,14,18	7,9,10,11	7,10,12
292	7,15,16,17	8,9,17	7,10,15,17	10,14,15,17	354	8,9,14	8,15,16	7,9,10,17	9,10,12
293	13,15,16,17	8,9,14,17	7,9,13,16	10,16,17	355	8,10,13	7,8	8,11,13,14	11,17,18
294	10,12	8,10,17	7,13,16,18	10,17,18	356	8,9,14,16	8,11,14,17	7,10,14	10,11,18
295	8,10,12,13	7,8,9,13	10,14,18	7,9,10,17	357	7,9,11	9,14,16,18	15,16,18	12,14,16,18
296	9,13,15,17	8,11,13	10,13,15,16	10,14,16	358	8,12,13,17	8,9	11,15,16,18	9,15,16,18
297	8,10,13,15	8,9,13,18	9,14,16,18	10,16,17,18	359	8,13,16	7,16,18	10,11,16	7,10,16,18
298	14,15,16	8,10,14,17	7,12	10,15,17	360	8,9,10,14	10,13,15,17	9,10,16,17	7,13,14,17
299	8,9,13,17	8,9,10,17	7,16,17	9,10,14,18	361	7,8,14,16	8,10,15,17	11,13,14,16	7,14,15,16
300	7,8,9,13	7,8,13	7,10,13	10,14,18	362	7,8,10,14	15,16,17,18	10,11,15,16	12,14,15,18

Continued on next page

Table A.1 – continued from previous page

Rank	$\mathbf{w}_{C1}$ Tx's	$\mathbf{w}_{G1}$ Tx's	$\mathbf{w}_{C2}$ Tx's	$\mathbf{w}_{G2}$ Tx's	Rank	$\mathbf{w}_{C1}$ Tx's	$\mathbf{w}_{G1}$ Tx's	$\mathbf{w}_{C2}$ Tx's	$\mathbf{w}_{G2}$ Tx's
363	11,13,14	8,10,11	7,11,13,14	9,11,12,15	425	8,9,10,11	10,17,22	11,15,17,18	9,10,15,16
364	7,8,14	8,12	7,18	7,10,11,15	426	9,15,16	8,11,13,22	11,13,14,18	11,17
365	8,14,18	8,11,13,15	7,9,10,14	10,15,18	427	9,14,16,18	7,8,9,11	7,8,11,13	7,10,11,12
366	7,10,14,18	7,10	12,14,16	9,10,11,15	428	7,8,10,15	9,10,17,22	8,9,13,14	10,12,18
367	8,10,14,16	8,9,13,17	7,15,16	7,11,16,18	429	11,12	10,14,17,22	10,15,16,18	10,12,14,18
368	8,10,14,18	7,8,14,18	10,14,16	12,14,15	430	7	9,13,18,22	10,16,18	11,15,16,17
369	8,10,17	7,8,13,17	10,14,16,18	9,11,16,18	431	7,8,12	10,14,22	8,14,15,17	7,12,18
370	8,15,16,17	7,8,15,17	10,11,12,15	10,11,13,14	432	12,13,17,18	9,14,22	8,11,13	9,10,14,15
371	7,8,14,18	8,9,14,18	7,10,16,17	9,14,15,16	433	7,16,18	8,9,14,22	8,12,13,18	11,14,15,18
372	8,9,14,18	8,9,15,17	8,11,14,17	10,12,16	434	8,14,15,16	7,8,13,22	7,9	12,16,18
373	8,16,17	8,11,12,13	9,10,14,16	10,11,15,16	435	8,10	8,10,14,22	8,11,13,16	10,11,12,16
374	8,13,15,17	8,12,13,14	8,11,12,13	7,10,11,18	436	8,9,12	7,10,13,22	10,12,16	11,13,17,18
375	7,14,15	16	10,12	10,14,15,18	437	8,10,16,18	7,13,22	8,13,14,18	7,11,13,14
376	7,15,16	8,10,12,17	7,14,15,16	9,10,16,18	438	7,10	10,15,22	7,8,13,14	11,13,14,18
377	8,10,14	7,8,11	9,10,11,18	10,15,16,18	439	8,9,18	7,8,17,22	9,11,13,17	11,12,18
378	10,16,18	7,8,18	9,10,11,16	9,10,11,18	440	11,12,13,18	7,17,22	7,8,13,17	7,9,15,18
379	18	8,9,11	7,10,11,18	10,11,16,18	441	7,8,9,11	7,13,16,22	8,9,14,17	12,15,16,18
380	8,14,16	8,10	10,15,18	10,14,15,16	442	9,10	9,13,15,22	8,14,17,18	7,12,14,18
381	8,10,12,17	8,10,15,16	10,15	11,15,16,18	443	16	7,14,17,22	8,9,12,13	11,13,14,16
382	8,14,16,18	9,10	8,11,13,15	7,11,12,15	444	9,16,18	8,10,15,22	7,10,16,18	9,12,14,18
383	8,14,15	8,10,12	9,15,18	7,12,16,17	445	7,9,10,11	10,16,17,22	8,10,11,13	9,12,18
384	8,9,15	8,12,16,17	8,12,13,17	10,12,17,18	446	10,12,16,17	7,10,17,22	8,13,15,18	16
385	7,8,15	8,10,13	9,10,15	9,11,13,14	447	8,9,10,15	10,11,13,22	8,9,13,15	8,10,11,13
386	8,13	8,10,13,16	7,15,18	11,15,17	448	7,14,17,22	7,14,22	7,8,14,17	7,8,11,13
387	8,15,17,18	8,10,13,18	9,14,15,16	10,11,15,18	449	9,14,17,22	9,16,17,22	8,10,13,17	8,9,11,13
388	10,15,17,18	8,10,13,15	9,10,12	11,13,14,15	450	7,9,13,22	7,8,14,22	8,13,17	8,11,13
389	8,10,15	8,10,13,14	7,10,14,16	12,14,16	451	9,13,15,22	7,13,18,22	8,12,17,18	8,11,13,16
390	8,12,16,17	8,15,18	9,16,18	11,16,17,18	452	9,13,18,22	7,9,17,22	8,13,16,17	8,11,13,18
391	8,15,16	12,13,17,18	7,10,11,16	10,13,16,18	453	7,13,15,22	8,16,18,22	7,8,12,13	8,11,14,17
392	8,17	9,16,18	9,12,16	10,13,15,16	454	9,12,13,22	7,13,15,22	8,15,17,18	8,11,13,15
393	10,16	7,8,10,11	9,11,16,18	10,13,15	455	7,13,16,22	10,18,22	7,8,13,15	8,10,11
394	8,14	8,12,13,17	7,12,16,17	10,13,18	456	9,13,16,22	7,11,13,22	12,14,15	7,8,11
395	8,16,18	7,8,12,17	12,14,15,18	10,13,16	457	9,10,13,22	7,16,17,22	9,10	8,9,11
396	8,11	7,8,10,15	8,12,13,14	10,13,15,18	458	7,10,13,22	9,10,14,22	8,13,14	7,8,10,11
397	8,10,11	8,10,13,17	11,12,15,16	10,13,14	459	7,12,13,22	9,11,13,22	8,12,13,16	8,9,10,11
398	7,14,16,18	8,9,10,11	12,15,16,17	10,13,14,16	460	10,11,13,22	7,15,22	8,9,15,17	8,16,18
399	8,10,18	8,12,14	7,10,15	10,13,17	461	7,11,13,22	7,10,14,22	8,9,13,18	7,8,9,11
400	9,10,14,18	11,12,13,18	7,10,12	10,13,14,18	462	12,13,16,22	11,13,16,22	8,13,14,16	8,11
401	8,15	8,10,14,15	8,13,14,17	10,13,16,17	463	9,11,13,22	10,14,16,22	9,10,16,18	8,9,10,13
402	7,8,11	10	11,15,17	10,13,14,15	464	10,12,13,22	9,15,22	8,9,12,17	8,11,13,14
403	7,9,15,17	7,8,12	16,18	10,13	465	12,13,18,22	10,17,18,22	10,12,14,18	8,9,10,17
404	8,9,11	8,9,12,17	11,13,17,18	10,13,17,18	466	12,14,17,22	7,8,15,22	8,12,13	8,9,14,17
405	7,8,12,17	7,9,10,11	7,16,18	9	467	11,13,16,22	9,17,18,22	7,8,15,17	8,9,13,16
406	8,18	8,10,16,18	8,11,13,18	10,13,15,17	468	9,10,17,22	12,13,22	7,8,13,18	8,9,13,18
407	15,16,17,18	8,9,18	7,11,16,18	9,12,16,17	469	10,16,17,22	8,12,13,22	8,10,14,17	8,9,13,15
408	13,15,17,18	8,9,12	10,14,15,16	9,16	470	7,16,17,22	10,12,13,22	18	8,9,10,14
409	8,10,15,16	10,12,16,17	8,13,15,17	7,16	471	7,9,17,22	8,9,15,22	7,8,12,17	8,9,16,17
410	8,12	8,14	10,11,16,18	10,13,14,17	472	7,10,17,22	8,15,22	7,10	8,9,13
411	7,8,18	8,14,16	10,15,16	7,10,15,18	473	12,13,15,22	7,12,13,22	8,10,12,13	8,9,17,18
412	8,12,14	8,14,18	9,12,16,17	11,15,17,18	474	9,16,17,22	7,17,18,22	8,10,13,14	8,9,14,16
413	9,14,15	8,18,22	7,12,16	9,10,15,18	475	10,17,18,22	9,12,13,22	8,10,13,15	8,9,17
414	8,16	8,16,22	8,13,14,15	11,12,15,16	476	7,17,18,22	12,13,16,22	8,13,15,16	8,9,13,14
415	8,15,18	8,9,13,22	8,12,14,17	7,10,15,16	477	9,17,18,22	8,10,18,22	8,9,14,15	8,9,14
416	8,9,12,17	9,10,13,22	7,15,16,18	12,15,16,17	478	7,10,14,22	7,9,14,22	8,9,17,18	8,9,13,17
417	11,14,15,17	9,13,22	8,12,13,15	10,11,12,15	479	10,14,16,22	9,14,16,22	8,13,15	8,9,15
418	8,10,12	8,9,17,22	11,15,16,17	7	480	8,11,13,22	7,14,16,22	8,12,16,17	8,9,15,17
419	13,14,17	9,13,16,22	8,9,11,13	7,9,10,12	481	9,10,14,22	12,13,18,22	7,10,15,18	8,9,14,18
420	8,10,14,15	9,17,22	9,15,16,18	7,9,14,15	482	8,9,13,22	12,14,17,22	10,16	8,10,14,17
421	7,8,10,11	9,14,17,22	10,18	9,10,12,16	483	8,10,13,22	16,18,22	7,8,14,15	8,10,16,17
422	9	11,13,22	11,13,15,17	7,10,12,16	484	9,13,14,22	8,11,22	7,8,17,18	8,10,17,18
423	8,9	8,10,17,22	8,13,17,18	7,10,14,15	485	7,8,13,22	9,13,14,22	8,14,16,17	7,8,9,13
424	7,8	7,9,13,22	8,9,13,17	11,13,15,17	486	8,9,17,22	11,22	8,9,14,18	8,10,14,16

Continued on next page

Table A.1 – continued from previous page

Rank	w_{C1} Tx's	w_{G1} Tx's	w_{C2} Tx's	w_{G2} Tx's	Rank	w_{C1} Tx's	w_{G1} Tx's	w_{C2} Tx's	w_{G2} Tx's
487	8,12,13,22	12,13,15,22	7,8,9,13	8,11,16	549	8,13,14,22	11,13,20,22	7,8,10,11	8,12,16,17
488	8,10,17,22	11,13,18,22	8,11,12	7,8,9,17	550	7,15,22	11,13,20	7,8,10,17	8,10
489	11,13,18,22	7,22	8,15,16,17	8,10,17	551	10,12,17,22	8,17,18	8,14,18	8,11,15
490	7,9,14,22	15,16,22	7,10,11,12	8,10,14	552	10,18,22	10,17,20,22	8,9,10,14	8,12,13,17
491	10,14,17,22	7,13,14,22	8,12,17	7,8,9,14	553	9,15,22	8,10,17,20	11,14,15,18	7,8,12,17
492	7,14,16,22	12,17,22	8,10,13,18	8,10,14,18	554	13,14,16,22	10,17,20	8,10,16,17	8,15,16
493	8,10,14,22	8,14,16,18	8,10,15,17	8,10,15,17	555	10,15,17,22	7,9,13,20	12,14,15,16	8,10,12
494	7,8,17,22	7,8,22	8,9,13,16	8,10,15	556	7,13,17,22	9,13,17,22	7,8,11	8,12,14
495	8,9,14,22	9,22	8,14,17	8,10,18	557	8,15,22	8,11,13,20	10,11,12,16	8,9,12,17
496	9,14,16,22	10,14,18,22	8,10,12,17	8,9,18	558	8,18,22	9,10,17,20	7,8,17	7,8,12
497	7,8,14,22	8,14,15	8,9,11,15	8,10,15,16	559	13,14,18,22	10,14,17,20	8,9,14	8,15,18
498	14,15,17,22	10,15,17,22	7,8,14,18	8,9,10,15	560	15,16,17,22	9,13,18,20	7,8,10,14	8,9,12
499	11,14,17,22	14,17,22	9,10,15,18	7,8,10,13	561	8,16,22	9,14,20,22	11,13,16,17	8,10,11,15
500	10,13,15,22	11,14,17,22	8,13,16,18	7,8,14,17	562	10	10,14,20,22	8,13,16	8,11,18
501	14,16,17,22	7,18,22	7,10,14,15	7,8,13,16	563	13,15,22	9,15,17,22	8,10,14,16	8,12,17,18
502	10,13,16,22	14,16,17,22	8,13,18	7,8,13,18	564	12,17,22	8,18,19,20	8,10,11,18	8,12
503	10,13,18,22	16,17,22	7,8,11,12	7,8,10,17	565	17,18,22	10,14,20	10,12,18	8,15
504	8,13,18,22	8,9,22	8,15,17	7,8,13,15	566	16,17,22	8,18,19,22	8,10,13	7,8,10,12
505	13,15,16,22	8,12,17,22	8,12,14	7,8,16,17	567	16,18,22	9,14,20	8,10,11,16	8,9,10,12
506	13,15,18,22	14,17,18,22	7,8,13,16	7,8,10,14	568	8,14,22	8,9,14,20	7,8,15,16	8,12,16
507	14,17,18,22	8,15,16,22	8,14,15,18	7,8,13	569	10,13,17,22	8,10,14,20	8,11,12,16	8,10,11,12
508	8,10,15,22	17,18,22	8,10,14,15	7,8,17,18	570	8,13,22	7,8,13,20	8,15,18	8,9,15,16
509	8,13,15,22	13,16,22	8,14,15,16	8,10,14,15	571	8,17,22	7,13,20,22	7,8,14	7,8,11,15
510	13,16,18,22	10,11,22	7,8,11,15	7,8,14,16	572	13,18,22	10,15,20,22	8,11,16,18	8,9,11,15
511	8,17,18,22	13,18,22	7,8,9,17	7,8,17	573	15,17,22	7,10,13,20	8,11,16	8,10,11,18
512	10,14,18,22	14,16,22	7,8,9,11	7,8,13,14	574	14,16,18,22	7,13,20	7,8,9,12	7,8,11,18
513	7,8,15,22	8,9,10,15	8,11,15	7,8,14	575	8,10,11,22	8,16,19,20	8,9,10,15	7,8,9,12
514	8,14,18,22	14,15,17,22	8,9,11,12	7,8,15	576	7,8,15,16	10,15,20	7,10,15,16	8,11,15,16
515	8,16,17,22	13,15,22	8,10,17,18	7,8,13,17	577	8,13,17,22	8,16,19,22	8,9,16,18	8,9,11,18
516	7,13,18,22	13,16,18,22	8,9,10,13	7,8,14,18	578	13,14,15,22	7,17,20,22	8,12,14,18	11,14,15,16
517	8,9,15,22	8,22	8,9,16,17	7,8,15,17	579	13,16,22	7,8,17,20	8,9,10,12	7,8,11,12
518	8,14,16,22	13,15,16,22	8,14,15	8,18	580	10,15,16,22	7,17,20	7,8,10,15	8,11,16,18
519	16,17,18,22	8,14,17	8,14,16,18	8,10,16,18	581	9,13,17,22	7,13,16,20	8,16,17	8,9,11,12
520	8,13,16,22	8,10,11,22	8,9,13	7,8,18	582	14,17,22	8,18,19	7,12,14,18	8,10,12,16
521	11,12,13,22	16,17,18,22	8,10,11,12	8,10,11,16	583	15,16,22	9,13,15,20	7,8,16,18	8,15,16,18
522	11,13,15,22	11,13,15,22	7,8,9,14	7,8,10,15	584	14,16,22	7,14,17,20	8,10,17	7,12,15,17
523	8,10,18,22	8,18,20,22	8,10,11,15	8,11,12,13	585	8,13,14,17	7,13,17,22	8,9,15	9,11,13,17
524	8,11,13,14	10,22	8,16,17,18	7,8,11,16	586	8,14,15,22	8,10,15,20	8,10,15,16	8,10,15,18
525	8,15,17,22	12,22	8,10,14,18	8,9,11,16	587	13,16,17,22	8,16,19	8,10,11	8,11,15,18
526	11,13,22	8,16,20,22	8,11,15,16	8,9,16,18	588	7,10,15,22	11,12,13,22	7,8,10,12	8,11,12,16
527	10,13,14,22	8,18,20	7,8,10,13	8,16	589	14,18,22	7,10,17,20	8,9,12	7,8,12,16
528	7,13,14,22	8,16,17	8,9,14,16	7,8,15,16	590	12,16,17,22	10,16,17,20	8,9,15,16	10
529	7,13,22	8,14,16,17	11,14,15,16	7,8,14,15	591	7,18,22	10,11,13,20	8,14,16	8,10,13,16
530	9,13,22	9,14,18,22	7,8,16,17	7,8,16,18	592	7,8,14,15	13,14,22	8,15,16,18	8,10,13,18
531	8,16,18,22	15,17,22	8,9,11,16	8,9,14,15	593	8,11,22	7,14,20,22	9,10,12,16	8,10,13,15
532	10,13,22	7,14,18,22	7,8,13	8,9	594	13,14,22	7,14,20	7,8,15	8,10,13
533	7,17,22	8,16,20	8,17,18	8,9,10	595	10,11,22	8,9,13,19	8,10,14	8,10,13,14
534	9,17,22	8,17	8,9,11,18	7,8,10	596	7,12,17,22	9,10,13,19	11,12,18	8,10,13,17
535	7,15,17,22	14,18,22	8,10,13,16	12,14,15,16	597	7,8,22	9,16,17,20	7,8,12	7,8,15,18
536	10,17,22	8,12,22	8,11,15,18	8,11,12	598	15,17,18,22	9,13,19,22	8,10,16,18	8,12,18
537	8,12,17,22	13,15,18,22	9,10,14,15	7,8	599	13,17,18,22	9,13,19,20	7,10,12,16	8,9,12,16
538	8,15,16,22	8,9,13,20	7,8,11,18	8,10,12,13	600	8,9,22	7,8,14,20	8,13	10,12,15,17
539	12,13,22	9,10,13,20	8,11,12,15	7,8,12,13	601	8,12,17,18	7,9,17,20	8,15,16	8,11,12,15
540	9,14,22	9,13,20,22	8,9,10,17	8,9,12,13	602	7,8,11,22	7,13,18,20	12,15,16,18	8,9,15,18
541	12,13,14,22	9,13,20	8,9,10,11	8,12,13,16	603	14,15,22	9,13,19	8,9,18	8,12,14,18
542	7,14,18,22	8,14,17,18	7,9,14,15	8,12,13,18	604	8,12,22	8,14,15,17	7,11,13,17	7,9,11,12
543	8,14,17,22	7,15,17,22	7,8,14,16	8,12,14,17	605	13,17,22	7,11,22	9,16	9,12,15,17
544	10,14,22	9,17,20,22	7,8,11,16	8,12,13	606	7,11,22	8,9,17,19	7,12,15,17	10,12,14,16
545	7,14,22	8,9,17,20	7,9,10,12	8,12,13,15	607	9,18,22	9,17,19,20	9,12,14,18	11,13,16,17
546	9,14,18,22	9,13,16,20	8,11,18	8,12,17	608	7,8,18,22	9,17,19,22	10,12,15,17	10,12,14,15
547	10,15,22	9,17,20	8,9,11	8,12,13,14	609	12,13,17,22	9,13,16,19	7,8,18	7,11,13,17
548	9,15,17,22	9,14,17,20	8,9,17	8,10,12,17	610	8,9,11,22	8,16,18,20	8,11	9,10,11,12

Continued on next page

Table A.1 – continued from previous page

Rank	w_{C1} Tx's	w_{G1} Tx's	w_{C2} Tx's	w_{G2} Tx's	Rank	w_{C1} Tx's	w_{G1} Tx's	w_{C2} Tx's	w_{G2} Tx's
611	9,12,17,22	9,17,19	8,10,15	8,12,14,16	673	12,13,16,20	9,16,17,19	10,11,13,22	8,10,17,22
612	10,14,15,22	9,14,17,19	8,10,12	7,9,15,16	674	8,18,20,22	7,14,19	12,13,17,22	8,10,14,22
613	9,10,15,22	11,13,19,22	12,16,18	8,14,16	675	7,13,20,22	7,8,14,19	7,14,17,22	10,16,17,22
614	11,22	11,13,19,20	8,12,16	8,14,18	676	7,17,20,22	7,9,17,19	9,13,15,22	8,10,15,22
615	11,16	10,18,20,22	7,16	8,14,16,18	677	9,10,14,20	7,13,18,19	12,13,14,22	10,17,18,22
616	8,10,12,22	11,13,19	7,12,18	8,14,15	678	8,15,20,22	8,20,22	9,14,17,22	7,9,13,22
617	7,22	15,22	8,16,18	8,14,15,16	679	8,16,20,22	8,16,17,18	12,14,17,22	10,14,16,22
618	9,11,22	10,17,19,20	9,10,15,16	8,14	680	10,17,20,22	8,15,17	7,13,15,22	7,9,17,22
619	9,22	10,17,19,22	8,17	8,12,15	681	9,13,20,22	8,16,18,19	12,13,15,22	8,10,18,22
620	13,15,17,22	10,18,20	8,10,12,16	8,12,15,17	682	10,13,20,22	8,19,20	7,8,12,18	7,9,14,22
621	7,10,11,22	8,10,17,19	8,10,18	8,10,12,18	683	7,11,13,20	7,8,15,20	7,15,17,22	10,15,17,22
622	10,16,18,22	7,13,15,20	8,10,15,18	8,11,13,22	684	11,13,16,20	17,22	9,13,18,22	10,14,18,22
623	12,14,22	7,9,13,19	9	10,11,13,22	685	9,11,13,20	10,18,19,20	12,13,18,22	10,17,22
624	10,12,22	8,11,13,19	7,8,12,16	7,11,13,22	686	12,13,18,20	9,17,18,20	9,15,17,22	11,16,22
625	12,22	10,17,19	7,8,15,18	9,11,13,22	687	10,14,20,22	10,18,19,22	9,12,13,22	8,9,18,22
626	15,18,22	9,10,17,19	8,14	11,13,16,22	688	8,13,18,20	7,13,15,19	7,9,13,22	10,14,22
627	8,15,18,22	10,14,17,19	8,9,15,18	11,13,18,22	689	7,8,15,20	10,18,19	9,17,18,22	10,15,16,22
628	13,22	7,11,13,20	8,15	11,13,22	690	7,17,18,20	7,11,13,19	9,14,18,22	10,15,22
629	17,22	9,13,18,19	8,9,12,16	11,14,17,22	691	9,17,20,22	12,13,14,22	7,17,18,22	10,18,22
630	10,22	9,14,19,20	8,9,10	11,13,15,22	692	8,13,16,20	12,13,20,22	7,13,16,22	10,14,15,22
631	15,22	9,14,19,22	8,12	8,10,11,22	693	18,22	12,13,20	9,14,15,22	10,16,18,22
632	8,22	10,14,19,20	8,12,18	10,11,22	694	9,17,18,20	7,16,17,19	9,13,16,22	9,15,16,22
633	14,22	7,16,17,20	7,8,10	7,8,11,22	695	9,14,20,22	9,20,22	10,17,18,22	7,10,13,22
634	8,10,13,20	10,14,19,22	10,11,13,17	8,11,22	696	7,13,20	8,12,13,20	7,14,15,22	7,14,17,22
635	7,9,13,20	9,18,22	8,18	7,11,22	697	8,14,20,22	8,15,20,22	10,14,15,22	7,8,13,22
636	7,13,16,20	9,10,14,20	9,12,18	8,9,11,22	698	8,18,20	9,10,14,19	7,12,13,22	7,13,16,22
637	9,10,13,20	9,11,13,20	7,9,15,18	7,10,11,22	699	10,15,20,22	9,11,13,19	10,14,18,22	7,10,17,22
638	8,10,17,20	8,9,14,19	8,9	9,11,22	700	12,14,17,20	7,15,19,20	7,14,18,22	7,13,18,22
639	8,10,22	10,14,19	7	9,10,11,22	701	8,17,20,22	8,9,15,20	9,10,13,22	7,8,17,22
640	7,14,17,20	8,10,14,19	7,8	7,9,11,22	702	11,13,20,22	10,12,13,20	7,16,17,22	7,13,15,22
641	7,10,12	7,8,13,19	8,12,15,17	8,16,18,22	703	8,13,15,20	7,15,19,22	7,9,11,22	7,8,14,22
642	9,13,18,20	7,15,20,22	8,16	8,18,22	704	7,14,20,22	8,15,20	12,13,16,22	7,16,17,22
643	7,10,13,20	7,13,19,20	9,12,15,17	11,13,14,22	705	10,17,20	7,20,22	7,10,13,22	7,10,14,22
644	9,13,16,20	10,15,19,20	8,12,14,16	8,16,22	706	9,13,20	7,15,19	9,12,17,22	7,17,18,22
645	9,14,17,20	7,13,19,22	8,10	8,14,15,18	707	8,15,20	7,12,13,20	9,10,11,22	7,8,15,22
646	8,9,13,20	9,14,19	10,12,14,15	9,10,13,22	708	10,13,20	7,17,18,20	9,14,16,22	7,14,16,22
647	8,10,14,20	10,15,19,22	11,17	9,10,17,22	709	8,16,20	7,10,14,19	7,9,14,22	7,13,14,22
648	7,8,13,20	7,10,13,19	7,9,11,12	8,9,13,22	710	8,16,17,20	9,12,13,20	9,16,17,22	11,22
649	7,8,17,20	13,22	8,12,15	9,14,17,22	711	7,17,20	11,13,16,19	10,16,17,22	7,13,22
650	8,9,17,20	7,15,20	10,12,14,16	9,13,16,22	712	7,14,16,20	9,15,19,20	8,11,15,17	7,17,22
651	10,16,17,20	7,13,19	9,10,11,12	9,10,14,22	713	10,14,20	8,19,20,22	10,12,13,22	9,14,15,22
652	7,10,17,20	7,17,19,20	10,11,15,17	9,13,18,22	714	8,10,18,20	10,15,16,22	7,9,17,22	7,14,18,22
653	9,10,11,22	7,17,19,22	8,11,17,18	8,9,17,22	715	12,13,15,20	9,15,19,22	9,10,17,22	7,15,17,22
654	9,10,17,20	10,15,19	16	9,13,15,22	716	7,8,16,18	12,13,16,20	7,10,11,22	7,13,17,22
655	9,13,15,20	7,8,17,19	8,10,12,18	8,9,14,22	717	8,9,15,20	8,10,18,20	7,12,17,22	7,14,22
656	7,13,15,20	7,13,16,19	10,11,14,15	9,16,17,22	718	9,17,20	10,14,16,19	12,17,18,22	10,16,22
657	8,9,14,20	7,17,19	8,11,13,17	9,17,18,22	719	7,9,14,20	13,14,16,22	7,14,16,22	7,15,22
658	7,16,17,20	7,10,14,20	8,11,14	8,9,15,22	720	9,14,16,20	9,15,19	8,12,16,18	8,10,22
659	7,8,14,20	11,13,16,20	9,11,14,15	9,13,14,22	721	9,14,20	10,17,18,19	10,14,16,22	7,10,15,22
660	8,11,13,20	9,13,15,19	7,11,14,15	9,14,16,22	722	8,14,16,20	9,14,16,20	7,13,17,22	7,8,18,22
661	8,10,15,20	7,14,17,19	10	9,13,22	723	11,13,20	7,9,14,20	9,10,14,22	7,18,22
662	9,12,13,20	9,15,20,22	11,16,17	9,13,17,22	724	10,15,20	8,20	12,16,17,22	9,16,18,22
663	7,9,17,20	10,12,17,22	7,8,9	9,14,18,22	725	10,18,20,22	7,14,16,20	7,10,17,22	10,11,16,22
664	9,16,17,20	9,15,20	11,14,17,22	9,15,17,22	726	8,17,18,20	11,20,22	8,11,13,22	9,10,22
665	7,12,13,20	10,14,16,20	11,13,15,22	9,17,22	727	7,14,20	7,20	7,10,14,22	7,8,22
666	10,14,16,20	8,10,15,19	11,13,14,22	9,14,22	728	12,13,20,22	9,19,20,22	10,15,16,22	7,15,16,22
667	10,12,13,20	10,17,18,20	11,13,18,22	9,10,15,22	729	7,15,20,22	7,8,15,19	10,12,17,22	11,12,13,22
668	10,11,13,20	7,10,17,19	11,12,13,22	9,15,22	730	8,10,13,19	9,17,18,19	9,15,16,22	7,14,15,22
669	10,16,22	10,16,17,19	11,13,16,22	8,9,22	731	8,12,14,22	12,13,19,20	15,17,18,22	7,11,16,22
670	8,12,13,20	10,11,13,19	9,11,13,22	9,18,22	732	9,10,12	12,13,19,22	8,11,12,18	9,11,16,22
671	10,17,18,20	7,14,19,20	9,13,14,22	8,11,16,22	733	10,13,16,20	7,19,20,22	9,10,15,22	7,16,18,22
672	7,10,14,20	7,14,19,22	7,11,13,22	10,14,17,22	734	8,10,17,19	12,13,19	7,15,16,22	7,10,22

Continued on next page

Table A.1 – continued from previous page

Rank	w_{C1} Tx's	w_{G1} Tx's	w_{C2} Tx's	w_{G2} Tx's	Rank	w_{C1} Tx's	w_{G1} Tx's	w_{C2} Tx's	w_{G2} Tx's
735	10,14,17,20	9,19,20	9,16,18,22	8,9,10,22	797	10,12,13,19	9,13,14,19	8,13,15,22	9,11,15,22
736	9,10,13,19	15,19,20,22	7,10,15,22	15,16,22	798	10,11,13,19	12,13,15,19	8,10,18,22	8,17
737	7,13,16,19	8,12,13,19	10,16,18,22	11,12,22	799	10,17,18,19	11,13,18,19	8,9,18,22	12,16,22
738	7,9,13,19	8,15,19,20	14,15,17,22	15,18,22	800	13,15,18,20	16,18,19	8,10,15,22	8,12,16,22
739	8,9,13,19	7,19,20	9,11,16,22	8,11,12,22	801	7,14,19,22	15,16,19,22	7,8,18,22	7,9,12,22
740	7,15,16,22	8,19,22	7,16,18,22	11,15,22	802	8,15,17,20	11,14,17,20	8,14,15,22	14,16,17,22
741	7,14,17,19	8,15,19,22	7,11,16,22	7,8,10,22	803	7,10,14,19	10,20	8,17,18,22	14,17,18,22
742	9,13,14,20	7,10,15,22	13,15,17,22	10,12,13,22	804	8,13,20	14,17,20,22	7,11,12,22	14,15,17,22
743	8,10,14,19	12,13,18,20	7,13,14,22	7,12,13,22	805	11,13,19,22	15,16,19,20	14,16,18,22	16,17,18,22
744	9,15,20,22	8,9,15,19	10,11,16,22	8,12,13,22	806	14,15,17,20	10,20,22	10,15,17,22	7,11,12,22
745	7,10,13,19	10,12,13,19	10,11,12,22	9,12,13,22	807	14,17,18,20	8,9,20	9,11,15,22	15,16,17,22
746	7,8,17,19	7,12,13,19	13,15,18,22	12,13,16,22	808	8,18,19	10,15,17,20	7,9,12,22	8,22
747	12,13,20	8,15,19	13,14,15,22	12,13,18,22	809	7,13,19	7,18,20	13,14,16,22	15,17,18,22
748	7,8,13,19	7,17,18,19	8,12,14,15	12,14,17,22	810	12,13,16,19	7,18,20,22	8,9,12,22	14,17,22
749	8,16,18,20	9,12,13,19	10,13,14,22	12,13,15,22	811	14,16,17,20	7,19	10,11,18,22	15,17,22
750	9,13,18,19	9,20	8,9,13,22	12,13,22	812	8,17,20	10,19,20	8,10,12,22	17,18,22
751	9,13,16,19	9,19,22	7,9,15,16	8,12,17,22	813	10,17,19	14,17,20	7,8,12,22	7,9,22
752	8,9,17,19	7,19,22	8,9,11,22	12,17,22	814	16,17,20,22	14,16,17,20	7,13,18,22	16,17,22
753	10,18,20	8,10,18,19	15,16,17,22	10,12,17,22	815	8,12,17,20	11,19	8,14,16,22	7,11,18,22
754	9,14,17,19	12,13,16,19	8,12,13,22	12,13,14,22	816	8,15,19	16,17,20,22	8,16,17,22	11,15,16,22
755	7,15,20	16,18,20,22	8,9,17,22	12,16,17,22	817	8,16,19	7,8,19,20	8,11,15,22	9,11,18,22
756	10,16,17,19	11,20	8,10,13,22	7,12,17,22	818	9,10,14,19	8,9,20,22	11,13,22	14,16,18,22
757	8,18,19,22	12,14,17,20	7,8,13,22	8,10,12,22	819	10,13,19	18,20,22	8,16,18,22	14,18,22
758	8,13,20,22	14,22	7,8,11,22	8,15,16,22	820	9,13,19	15,16,19	9,11,12,22	14,15,22
759	9,10,17,19	11,19,20,22	13,15,16,22	9,12,17,22	821	8,13,18,19	7,13,14,19	8,13,14,22	14,15,16,22
760	8,9,14,19	13,17,22	8,9,14,22	8,12,22	822	7,8,15,19	15,19,22	8,13,17,22	14,16,22
761	7,8,14,19	8,11,20	10,14,17,22	12,13,17,22	823	17,18,20,22	7,8,19	8,11,18,22	13,16,18,22
762	9,13,15,19	15,20,22	8,10,17,22	8,11,15,22	824	7,11,13,19	8,12,17,20	11,15,16,22	13,15,16,22
763	7,13,15,19	8,11,20,22	9,13,17,22	12,14,22	825	7,17,19	16,20,22	8,13,16,22	13,15,18,22
764	8,15,19,22	7,9,14,19	8,14,18,22	10,12,22	826	10,14,19	12,17,19,20	14,15,18,22	13,14,16,22
765	7,10,17,19	9,14,16,19	7,10,12,22	8,12,14,22	827	11,14,17,20	12,17,19	8,9,10,22	13,14,18,22
766	7,13,19,22	7,14,16,19	13,17,18,22	7,8,12,22	828	11,13,16,19	12,17,19,22	9,11,18,22	13,16,17,22
767	8,16,19,22	11,19,20	10,11,15,22	10,11,15,22	829	9,11,13,19	7,8,19,22	7,8,10,22	13,14,15,22
768	9,15,20	9,13,14,20	10,13,15,22	7,12,22	830	10,18,19,22	16,17,20	7,11,18,22	13,17,18,22
769	7,16,17,19	16,18,20	8,10,11,22	8,15,22	831	12,13,18,19	7,8,18,22	7,12,14,15	13,14,22
770	8,10,15,19	11,19,22	10,13,17,22	8,15,18,22	832	14,15,16,22	12,16,17,22	7,13,22	13,15,22
771	8,11,13,19	12,13,15,20	14,17,18,22	9,12,22	833	9,17,19	14,17,18,20	9,13,22	13,17,22
772	10,17,19,22	11,13,18,20	7,8,14,22	8,9,12,22	834	12,13,19,22	8,13,16	9,11,22	13,18,22
773	11,13,18,20	15,16,20,22	14,15,16,22	12,17,18,22	835	7,13,18,20	10,14,18,19	7,11,22	13,16,22
774	8,15,16,20	15,16,17,22	8,9,15,22	7,22	836	7,17,18,19	8,15,16,20	9,17,22	13,15,17,22
775	9,13,19,22	12,13,18,19	13,14,18,22	8,11,18,22	837	9,14,19	17,18,20,22	7,17,22	9,11,12,22
776	13,15,16,20	15,16,20	8,10,14,22	11,18,22	838	7,15,19,22	10,19,20,22	9,14,22	15,16,18,22
777	8,14,18,20	16,19,20,22	8,11,14,15	10,22	839	10,15,19	8,13,18	10,13,22	13,14,17,22
778	7,17,19,22	7,8,20	9,10,12,22	16,18,22	840	8,18,19,20	8,13	10,11,22	8,11,13,20
779	13,16,18,20	7,13,14,20	7,8,17,22	9,22	841	14,17,20,22	8,9,19,20	8,14,17,22	10,11,13,20
780	10,14,18,20	12,14,17,19	8,11,12,22	10,11,12,22	842	11,13,19	11,14,17,19	11,12,22	7,11,13,20
781	10,13,19,22	16,18,19,22	14,16,17,22	7,10,12,22	843	9,17,18,19	7,18,19,20	12,13,22	9,11,13,20
782	10,14,19,22	8,11,19,20	10,13,18,22	9,10,12,22	844	16,17,18,20	14,17,19,22	10,17,22	11,13,16,20
783	10,13,18,20	13,14,18,22	16,17,18,22	12,22	845	13,15,20,22	8,9,11,22	8,12,16,22	11,13,20,22
784	9,17,19,22	14,15,22	8,15,18,22	7,11,15,22	846	7,14,19	10,15,17,19	7,14,22	11,13,18,20
785	9,12,13,19	18,22	8,15,17,22	10,11,18,22	847	8,13,15,19	17,18,20	10,14,22	11,14,17,20
786	9,16,17,19	16,18,19,20	7,8,15,22	7,8,9	848	12,17,20,22	7,18,19,22	9,15,22	8,11,20,22
787	7,9,17,19	12,17,20	13,16,18,22	8,14,16,17	849	16,22	8,13,15	11,16,18,22	11,13,20
788	16,18,20,22	12,17,20,22	13,16,17,22	8,14,17,18	850	8,15,19,20	7,18,19	12,17,22	8,10,11,20
789	10,13,15,20	8,11,19	13,14,17,22	8,14,15,17	851	8,16,19,20	14,17,19,20	9,18,22	10,11,20,22
790	8,14,20	7,8,20,22	10,13,16,22	8,14,17	852	12,14,17,19	8,9,19	7,15,22	11,13,15,20
791	10,14,16,19	8,11,19,22	8,12,14,22	8,16,17,18	853	8,10,18,19	10,11,20	15,16,18,22	7,11,20,22
792	8,12,13,19	14,16,18,22	8,15,16,22	8,17,18	854	8,13,19,22	14,17,19	11,16,22	10,11,20
793	7,12,13,19	18,19,20,22	8,13,18,22	8,16,17	855	7,13,19,20	14,16,17,19	12,14,22	8,11,20
794	10,15,19,22	7,8,11,22	8,11,16,22	8,15,17	856	8,16,17,19	13,16,20,22	10,15,22	7,11,20
795	9,14,19,22	9,11,22	8,12,17,22	8,15,16,17	857	8,17,19,22	10,19,22	10,15,18,22	7,8,11,20
796	10,15,17,20	10,14,18,20	7,11,15,22	8,15,17,18	858	15,16,20,22	10,11,20,22	10,18,22	8,9,11,20

Continued on next page

Table A.1 – continued from previous page

Rank	$\mathbf{w_{C1}}$ Tx's	$\mathbf{w_{G1}}$ Tx's	$\mathbf{w_{C2}}$ Tx's	$\mathbf{w_{G2}}$ Tx's	Rank	$\mathbf{w_{C1}}$ Tx's	$\mathbf{w_{G1}}$ Tx's	$\mathbf{w_{C2}}$ Tx's	$\mathbf{w_{G2}}$ Tx's
859	8,13,16,19	8,9,19,22	7,18,22	9,11,20,22	921	11,13,15,20	14,16,19	11,14,17,20	7,11,19,22
860	10,17,19,20	16,17,19,22	15,18,22	9,11,20	922	11,12,13,20	13,16,18,19	11,13,16,20	7,8,11,19
861	7,14,16,19	8,13,16,18	10,11,17,18	7,10,11,20	923	9,14,18,20	16,22	11,13,18,20	10,11,19
862	8,9,15,19	14,16,20,22	15,17,22	11,16,18,22	924	8,15,16,19	13,15,18,20	11,13,15,20	9,11,19,20
863	9,13,19,20	8,10,22	11,15,22	9,10,11,20	925	15,16,20	13,15,19	10,11,13,20	8,9,11,19
864	8,14,19,22	9,19	11,14,16,18	7,9,11,20	926	7,18,20	10,19	9,11,13,20	7,11,19
865	9,15,19,22	16,17,19,20	10,16,22	11,20,22	927	8,17,19	14,20,22	9,13,14,20	8,11,19
866	10,13,19,20	12,20,22	10,12,16,22	8,16,18,20	928	9,15,19,20	13,19,20,22	14,22	9,11,19,22
867	7,9,14,19	13,18,20,22	15,16,22	8,18,20,22	929	14,16,20	14,18,20	8,11,13,20	9,18,20
868	10,14,19,20	8,12,17,19	9,12,22	8,16,20,22	930	8,14,18,19	8,19	7,11,13,20	11,19,20,22
869	8,14,16,19	13,16,20	8,11,22	8,18,20	931	13,15,16,19	16,19,22	11,12,13,20	7,10,11,19
870	15,17,20,22	16,17,19	7,12,22	8,16,20	932	11,13,18,19	8,15,16,17	9,13,18,20	8,11,16,20
871	8,14,17,20	14,15,17,20	9,10,22	11,13,14,20	933	8,9,20,22	7,15,17,20	10,14,18,20	9,11,19
872	7,17,19,20	13,18,20	10,12,22	10,15,18,22	934	10,14,18,19	12,14,22	10,14,16,20	11,20
873	12,13,15,19	13,15,20,22	8,15,22	9,10,13,20	935	17,18,20	13,15,16,19	10,16,17,20	11,16,20,22
874	8,20,22	14,17,18,19	8,18,22	9,10,17,20	936	10,13,18,19	15,19,20	10,15,17,20	10,14,17,20
875	9,14,16,19	14,16,20	17,18,22	8,9,13,20	937	7,12,22	8,10,11,19	10,17,18,20	8,10,17,20
876	8,17,18,19	8,13,15,16	7,10,22	9,10,14,20	938	17,18,19,22	7,12,17,22	7,13,16,20	8,10,14,20
877	13,18,20,22	12,20	13,15,22	8,9,17,20	939	10,13,15,19	15,18,22	9,10,11,20	10,16,17,20
878	8,11,20,22	13,16,18,20	11,12,16,22	9,14,17,20	940	8,14,19,20	11,13,15,19	7,14,17,20	8,10,15,20
879	12,17,20	13,15,20	14,15,22	9,13,16,20	941	14,17,20	9,15,17,20	11,13,14,20	9,10,11,19
880	12,13,19	8,15,16,19	16,18,22	9,13,18,20	942	8,15,17,19	9,13,17,20	9,13,15,20	7,9,13,20
881	9,17,19,20	17,18,19,22	11,18,22	8,9,14,20	943	12,17,19,22	16,17,18,19	7,16,17,20	10,17,18,20
882	10,18,19	13,16,17,22	8,16,22	9,13,15,20	944	10,15,17,19	8,13,14	9,14,16,20	10,17,20,22
883	13,16,20,22	17,19,20,22	16,17,22	9,16,17,20	945	18,20,22	12,19	7,13,15,20	10,14,16,20
884	9,14,19,20	17,18,19,20	9,12,16,22	8,20,22	946	8,10,11,20	8,12,19,20	7,9,13,20	10,14,20,22
885	7,15,19	17,20,22	8,9,22	9,13,20,22	947	15,19,20,22	15,17,19,22	8,10,17,20	7,9,17,20
886	10,15,19,20	17,18,19	13,18,22	9,17,18,20	948	13,15,19,22	17,19,22	9,10,13,20	10,15,20,22
887	14,16,20,22	13,15,16,20	8,14,22	8,9,15,20	949	8,9,20	7,14,18,19	9,14,17,20	8,10,18,20
888	14,18,20,22	8,10,11,20	7,8,22	9,17,20,22	950	15,17,20	9,14,18,19	8,10,13,20	10,18,20,22
889	13,15,20	13,14,15,22	14,18,22	9,14,16,20	951	8,13,19,20	15,17,19,20	10,14,15,20	7,9,14,20
890	7,14,19,20	10,11,19,20	8,13,22	9,13,14,20	952	13,15,18,19	8,12,19	8,9,11,20	10,14,18,20
891	11,13,19,20	10,11,19	7,12,16,22	9,14,20,22	953	8,19,20,22	8,12,19,22	9,14,18,20	10,15,17,20
892	16,18,20	11,13,15,20	8,10,22	9,15,20,22	954	15,16,19,22	14,18,19,22	7,10,11,20	8,9,18,20
893	9,20,22	13,16,19,22	8,17,22	9,13,20	955	8,12,17,19	11,12,13,20	9,17,18,20	10,17,20
894	8,13,14,20	10,11,19,22	13,17,22	9,13,17,20	956	8,20	15,17,19	9,13,16,20	11,16,20
895	10,13,16,19	12,19,20,22	13,14,22	8,9,20,22	957	7,20	7,13,17,20	7,8,11,20	10,14,20
896	7,20,22	16,17,18,20	8,12,22	8,11,13,19	958	9,15,17,20	14,18,19,20	8,10,14,20	10,15,20
897	7,8,20,22	12,19,20	13,16,22	9,14,18,20	959	14,16,17,19	9,18,20	7,15,17,20	7,9,11,19
898	10,14,17,19	13,16,19,20	14,16,22	10,11,13,19	960	13,16,18,19	13,15,18,19	7,17,18,20	10,18,20
899	8,11,20	14,16,19,22	14,17,22	9,15,17,20	961	8,17,19,20	13,14,20,22	7,9,11,20	10,15,16,20
900	8,16,18,19	18,19,22	9,11,15,17	7,11,13,19	962	14,15,17,19	7,11,20	7,10,13,20	10,11,13,17
901	9,15,19	8,13,15,18	12,16,22	9,11,13,19	963	14,17,18,19	14,18,19	9,10,17,20	8,10,20,22
902	7,18,20,22	13,18,19,22	11,15,18,22	9,17,20	964	7,13,18,19	13,14,20	8,10,11,20	8,16,18,19
903	16,17,20	13,16,19	7,9,22	11,13,16,19	965	8,19,22	13,19,22	10,15,16,20	9,20,22
904	9,13,14,19	15,17,20,22	7,15,18,22	11,13,19,22	966	7,8,12,22	7,15,17,19	9,16,17,20	10,14,15,20
905	16,18,19,22	14,16,19,20	7,11,15,17	11,13,19,20	967	16,20,22	7,11,20,22	8,9,14,20	8,18,19,20
906	15,20,22	13,18,19,20	11,22	9,14,20	968	10,12,17,20	9,18,20,22	9,15,17,20	9,15,16,20
907	7,14,18,20	7,14,18,20	12,14,18,22	11,13,18,19	969	8,19,20	9,15,17,19	7,9,14,20	10,16,18,20
908	10,18,19,20	9,14,18,20	11,12,15,22	11,14,17,19	970	8,11,19,22	9,13,17,19	7,8,17,20	8,16,19,20
909	11,20,22	8,12,20	8,9,12,18	8,11,19,20	971	16,19,20,22	8,10,12,22	7,10,17,20	8,18,19,22
910	7,8,20	12,19,22	9,15,18,22	9,18,20,22	972	9,19,22	8,10,13,22	7,14,18,20	10,16,20,22
911	13,16,20	10,12,22	7,22	9,15,20	973	13,16,19,22	10,13,22	8,9,17,20	8,10,20
912	12,13,19,20	14,15,17,19	12,18,22	8,11,19,22	974	13,18,19,22	9,10,15,22	7,14,16,20	8,16,19,22
913	7,15,19,20	13,18,19	12,22	11,13,19	975	7,19,22	10,13,16,22	8,10,18,20	7,10,13,20
914	8,14,19	8,12,20,22	9,22	10,11,19,20	976	15,17,19,22	14,19,22	8,9,15,20	7,8,13,20
915	7,13,14,20	14,18,20,22	10,22	11,13,15,19	977	10,11,20,22	9,18,19,20	8,9,13,20	7,10,17,20
916	10,13,14,20	14,19,20,22	8,12,18,22	8,10,11,19	978	11,14,17,19	10,12,17,20	9,10,14,20	7,14,17,20
917	13,18,20	13,15,19,22	8,22	8,9,20	979	9,19,20,22	11,12,13,19	7,8,13,20	7,8,17,20
918	8,13,19	13,20,22	13,22	9,10,15,20	980	12,13,14,20	7,13,17,19	10,16,18,20	7,13,16,20
919	7,15,17,20	15,17,20	17,22	10,11,19,22	981	18,19,20,22	10,13,18,22	7,10,14,20	7,13,18,20
920	16,17,19,22	13,15,19,20	15,22	7,11,19,20	982	9,20	10,16,22	7,14,15,20	7,13,15,20

Continued on next page

Table A.1 – continued from previous page

Rank	$\mathbf{w_{C1}}$ Tx's	$\mathbf{w_{G1}}$ Tx's	$\mathbf{w_{C2}}$ Tx's	$\mathbf{w_{G2}}$ Tx's	Rank	$\mathbf{w_{C1}}$ Tx's	$\mathbf{w_{G1}}$ Tx's	$\mathbf{w_{C2}}$ Tx's	$\mathbf{w_{G2}}$ Tx's
983	14,18,20	13,14,19,22	7,8,14,20	7,8,14,20	1045	8,9,19	13,20	8,14,16,20	7,11,16,20
984	12,17,19	9,18,19	8,10,15,20	7,10,14,20	1046	13,14,18,20	8,9,11,20	9,18,20,22	9,14,19,22
985	11,20	7,11,19,20	9,14,15,20	7,13,20,22	1047	7,10,15,20	8,15,18,22	8,16,18,20	9,15,19,20
986	7,19,20,22	13,14,19,20	7,9,17,20	7,16,17,20	1048	15,16,19,20	7,8,18,19	8,14,15,20	9,15,19,22
987	7,8,19,22	7,11,19	9,10,15,20	11,19,20	1049	7,15,17,19	8,10,19,20	7,14,20,22	9,13,17,19
988	16,17,18,19	13,14,19	9,15,16,20	7,17,20,22	1050	15,17,19	8,10,20,22	9,17,20,22	8,9,19,20
989	8,12,20,22	10,13,15,22	7,8,15,20	7,8,15,20	1051	9,14,18,19	8,10,19	8,17,18,20	9,14,18,19
990	17,20,22	7,11,19,22	7,8,18,20	7,17,18,20	1052	13,18,19,20	12,16,17,19	8,9,10,20	9,15,17,19
991	14,16,19,22	7,10,12	7,15,16,20	7,14,20,22	1053	14,17,19	9,10,12	10,18,20,22	7,10,20,22
992	7,9,11,22	9,18,19,22	8,9,18,20	7,14,16,20	1054	9,18,20,22	8,13,16,17	8,13,16,20	9,13,19
993	11,19,22	12,13,14,20	12,13,17,20	7,15,20,22	1055	11,13,15,19	8,9,11,19	10,15,20,22	8,9,19,22
994	10,11,20	10,15,16,20	7,10,15,20	7,13,20	1056	11,12,13,19	13,16,17,20	8,15,17,20	9,11,16,20
995	16,18,19	13,17,18,22	9,12,13,20	10,16,20	1057	7,18,19,20	13,14,15,20	9,11,20	7,10,20
996	10,20,22	18,19,20	8,15,16,20	7,13,14,20	1058	18,19,22	8,10,19,22	7,10,12,20	9,17,19
997	9,12,22	8,13,14,16	9,16,18,20	11,19,22	1059	14,16,19,20	10,12,20	8,14,18,20	7,16,18,20
998	8,11,19	10,14,15,22	8,15,18,20	7,17,20	1060	9,18,20	10,12,20,22	7,15,20,22	9,18,19,20
999	7,18,19,22	10,12,17,19	12,13,18,20	9,14,15,20	1061	10,11,19,22	8,13,14,15	10,11,12,20	9,14,19
1000	8,14,17,19	15,17,18,22	12,13,15,20	7,14,20	1062	17,18,19,20	7,8,15,16	10,11,20	9,10,15,19
1001	13,15,19	13,19,20	7,16,18,20	9,10,20	1063	10,19,22	7,12,17,20	10,16,20,22	9,18,19,22
1002	14,20,22	13,14,16,20	7,12,13,20	7,8,20,22	1064	7,11,20,22	13,19	7,11,20	8,19,20
1003	11,19,20,22	17,19,20	12,14,17,20	7,14,18,20	1065	8,10,11,19	12,14,20	8,16,17,20	9,19,20,22
1004	13,14,20,22	7,10,15,20	12,13,14,20	7,15,17,20	1066	8,9,19,20	9,10,11,22	7,13,20	9,15,19
1005	15,16,17,20	11,16	8,11,16,20	7,18,20,22	1067	8,12,19,22	13,16,17,19	9,10,12,20	8,9,19
1006	8,13,17,20	12,13,14,19	9,12,17,20	7,13,17,20	1068	14,15,20,22	12,14,20,22	8,14,20,22	15,22
1007	8,12,20	16,19,20	12,13,16,20	7,15,20	1069	7,19	15,18,20	8,18,20	8,11,16,19
1008	14,17,19,22	10,15,16,19	10,12,13,20	10,20,22	1070	17,19,22	15,18,20,22	8,11,20	10,14,17,19
1009	13,14,16,20	7,10,11,22	7,12,17,20	8,19,20,22	1071	10,19,20,22	13,14,15,19	7,18,20,22	11,16,19,20
1010	16,17,19	8,13,17	8,12,13,20	7,10,15,20	1072	15,17,19,20	10,12,19,20	8,17,20,22	8,10,17,19
1011	7,19,20	14,19,20	8,11,12,20	9,10,20,22	1073	14,17,19,20	10,12,19	10,17,20	11,16,19,22
1012	16,18,19,20	13,14,16,19	11,13,20,22	10,12,16,22	1074	11,19	8,15,17,18	8,9,20,22	8,10,14,19
1013	9,19,20	13,17,20,22	12,14,16,22	11,13,14,19	1075	14,18,19	10,12,19,22	9,13,20	10,16,17,19
1014	7,8,19	10,16,18,22	10,12,17,20	7,8,20	1076	16,19,22	17,20	8,16,20	9,18,19
1015	10,13,17,20	13,17,20	10,11,16,20	7,18,20	1077	7,11,20	7,12,17,19	9,14,20	8,10,15,19
1016	13,16,19	7,10,15,19	12,16,17,20	7,8,18,20	1078	9,15,17,19	10,13,17,22	8,15,20	7,9,13,19
1017	15,19,22	9,12,17,22	8,12,14,20	9,16,18,20	1079	10,19,20	12,14,19,20	8,10,20,22	10,17,18,19
1018	12,17,19,20	15,16,17,20	8,10,12,20	8,18,19	1080	10,12,17,19	12,14,19	10,14,20	10,14,16,19
1019	8,13,14,19	12,13,17,22	7,11,16,20	10,11,16,20	1081	10,11,19	15,18,19,20	7,17,20	10,17,19,20
1020	10,15,16,20	14,15,20,22	9,11,16,20	8,16,19	1082	13,19,20,22	13,15,17,22	10,13,20	7,9,17,19
1021	13,15,19,20	7,8,11,20	12,17,18,20	7,20,22	1083	13,14,19,22	12,14,19,22	11,16,20,22	10,17,19,22
1022	14,18,19,22	13,17,19,22	8,18,20,22	7,15,16,20	1084	12,20	10,16,20	7,8,20,22	10,14,19,20
1023	13,18,19	13,14,18,20	8,9,12,20	11,12,13,20	1085	14,19,22	9,10,15,20	9,15,20	10,14,19,22
1024	8,9,19,22	9,11,20	7,17,20,22	9,10,13,19	1086	15,16,17,19	8,10,12,20	9,17,20	10,15,19,20
1025	8,14,15,20	13,17,19,20	10,11,20,22	9,10,17,19	1087	8,12,19	15,18,19,22	10,13,17,20	8,10,18,19
1026	15,16,19	14,16,18,20	9,11,20,22	8,9,13,19	1088	12,17,18,22	15,18,19	7,14,20	10,15,19,22
1027	8,11,19,20	13,17,19	8,16,20,22	9,10,14,19	1089	12,13,14,19	15,20	11,12,20,22	7,9,14,19
1028	7,18,19	14,15,20	8,12,17,20	9,14,17,19	1090	13,17,20,22	8,10,13,20	10,15,20	10,18,19,20
1029	13,14,20	8,13,14,18	7,11,20,22	8,9,17,19	1091	14,18,19,20	10,13,20,22	9,18,20	10,15,17,19
1030	7,13,14,19	9,11,20,22	8,11,20,22	9,13,16,19	1092	7,13,17,20	10,13,20	15,16,17,20	10,14,18,19
1031	16,17,19,20	10,13,14,22	8,13,18,20	9,13,18,19	1093	14,15,20	10,13,16,20	10,18,20	10,18,19,22
1032	13,20,22	15,16,17,19	7,13,20,22	9,13,15,19	1094	12,16,17,20	10,16,19,20	7,15,20	8,9,18,19
1033	11,19,20	7,8,18,20	10,17,20,22	8,9,14,19	1095	12,19,22	10,16,20,22	11,13,16,19	10,17,19
1034	17,19,20,22	8,10,20	8,15,20,22	7,14,15,20	1096	13,19,22	10,13,18,20	11,14,17,19	10,14,19
1035	10,13,14,19	14,15,19,22	11,13,20	9,16,17,19	1097	9,13,17,20	10,16,19	11,13,18,19	10,15,16,19
1036	10,20	7,8,11,19	7,8,12,20	9,17,18,19	1098	9,19	7,12,22	7,9,12,16	11,16,19
1037	17,18,19	13,14,18,19	9,13,20,22	9,13,19,22	1099	10,11,19,20	10,13,15,20	12,13,20,22	10,15,19
1038	7,14,18,19	9,11,19,20	10,14,20,22	9,13,19,20	1100	7,8,18,20	9,10,15,19	8,11,15,20	14,15,18,22
1039	7,8,19,20	14,15,19,20	9,14,20,22	8,9,15,19	1101	8,13,17,19	8,10,12,19	10,11,15,20	8,10,19,20
1040	14,16,19	12,16,17,20	10,13,20,22	9,13,14,19	1102	8,12,19,20	14,20	11,13,15,19	10,19,20,22
1041	12,20,22	14,16,18,19	8,13,15,20	9,14,16,19	1103	12,19,20,22	13,17,18,20	8,11,13,19	10,18,19
1042	14,16,18,20	9,11,19	18,22	9,17,19,20	1104	13,14,16,19	8,10,13,19	10,11,13,19	15,16,20,22
1043	13,16,19,20	14,15,19	7,8,10,20	9,17,19,22	1105	13,16,17,20	10,13,19,20	7,18,20	10,14,15,19
1044	14,19,20,22	9,11,19,22	9,15,20,22	9,14,19,20	1106	8,9,12,22	10,13,19,22	9,10,20,22	8,19,22

Continued on next page

Table A.1 – continued from previous page

Rank	$\mathbf{w_{C1}}$ Tx's	$\mathbf{w_{G1}}$ Tx's	$\mathbf{w_{C2}}$ Tx's	$\mathbf{w_{G2}}$ Tx's	Rank	$\mathbf{w_{C1}}$ Tx's	$\mathbf{w_{G1}}$ Tx's	$\mathbf{w_{C2}}$ Tx's	$\mathbf{w_{G2}}$ Tx's
1107	7,8,11,20	10,13,19	10,16,20	8,10,19,22	1169	8,9,11,19	7,8,12,20	10,15,16,19	7,15,16,19
1108	13,17,20	10,14,15,20	7,11,13,19	9,15,16,19	1170	13,20	12,17,18,22	7,9,11,19	15,16,20
1109	10,15,16,19	10,13,16,19	9,13,14,19	10,16,18,19	1171	9,11,19	7,8,12,19	7,15,17,19	10,19,22
1110	9,18,19,22	10,16,19,22	9,11,13,19	10,16,19,20	1172	8,10,19	7,9,11,20	8,9,15,19	7,19,20
1111	8,14,15,19	15,17,18,20	8,9,20	13,22	1173	12,13,17,20	14,15,16,20	9,10,17,19	7,8,10,20
1112	13,14,19	8,12,14,22	15,16,20,22	8,9,10,20	1174	8,10,19,22	8,12,17,18	7,10,13,19	9,20
1113	15,19,20	10,13,18,19	7,10,20,22	10,16,19,22	1175	15,18,20	7,9,11,19	7,14,16,19	11,12,13,19
1114	7,11,19,22	10,13,15,19	8,10,20	7,10,13,19	1176	9,11,19,20	8,11,13,14	10,12,20,22	7,14,15,19
1115	12,19,20	7,10,11,20	10,13,16,20	7,8,13,19	1177	10,12,19,22	14,15,16,19	9,16,17,19	7,19,22
1116	13,14,15,20	8,13,17,18	11,16,20	7,14,17,19	1178	10,16,20,22	8,14,22	16,18,20,22	7,11,16,19
1117	13,14,19,20	13,17,18,19	14,15,16,20	7,10,17,19	1179	8,10,12,19	8,14,16,22	7,9,14,19	8,20
1118	9,18,19	7,15,16,22	10,14,18,19	7,13,16,19	1180	10,16,20	8,9,18,20	7,8,13,19	11,15,20,22
1119	14,15,19,22	9,12,17,20	10,14,16,19	7,13,18,19	1181	10,16,18,20	7,14,15,22	7,14,18,19	7,10,19,20
1120	10,19	10,14,15,19	10,16,17,19	7,8,17,19	1182	8,10,19,20	8,9,12,20	9,15,17,19	8,11,12,20
1121	7,10,15,19	17,19	13,15,18,20	10,20	1183	12,14,19,22	8,9,18,19	10,16,18,19	7,10,19,22
1122	14,16,18,19	15,17,18,19	10,14,17,20	7,13,15,19	1184	10,12,19	8,14,18,22	7,8,14,19	9,11,16,19
1123	8,19	10,16,18,20	9,13,18,19	7,8,14,19	1185	7,10,11,20	8,9,12,19	8,10,15,19	11,15,20
1124	7,12,17,20	9,12,22	11,12,20	7,10,14,19	1186	13,17,18,19	16,19	9,10,14,19	15,18,20
1125	13,14,18,19	7,10,11,19	12,17,20,22	7,16,17,19	1187	15,18,19,22	12,17,18,20	7,10,14,19	7,16,18,19
1126	10,13,17,19	9,12,17,19	10,15,17,19	7,13,19,20	1188	8,15,18,20	12,17,18,19	11,13,19,22	11,19
1127	7,11,19	12,13,17,20	15,18,20,22	7,13,19,22	1189	17,20	7,10,22	8,12,20,22	7,10,19
1128	8,9,11,20	10,16,18,19	11,12,13,19	9,10,19,20	1190	12,14,19	8,14,20,22	7,8,15,19	17,22
1129	9,18,19,20	10,13,14,20	8,10,17,19	7,20	1191	15,17,18,19	8,14,20	13,16,18,20	10,12,13,20
1130	12,19	12,13,17,19	7,13,14,20	7,17,19,20	1192	10,12,19,20	8,14,15,22	7,12,20,22	7,12,13,20
1131	13,17,19,22	18,20	14,15,17,20	7,17,18,19	1193	9,10,15,19	8,14,16,20	11,20,22	8,12,13,20
1132	9,11,20,22	10,13,14,19	10,17,18,19	7,17,19,22	1194	13,19	7,14,15,20	7,9,12,20	9,12,13,20
1133	14,15,19	14,19	9,10,11,19	7,8,15,19	1195	12,14,19,20	9,15,16,22	7,10,17,19	12,13,16,20
1134	7,11,19,20	8,15,18,20	8,10,13,19	7,14,19,20	1196	10,14,15,19	8,14,19,20	14,16,18,20	12,13,20,22
1135	9,11,20	15,19	7,13,16,19	7,14,16,19	1197	9,12,17,19	8,14,19,22	7,14,15,19	12,13,18,20
1136	17,19,20	7,8,12,22	13,15,16,20	7,14,19,22	1198	10,16,19,22	8,14,19	15,17,20,22	12,14,17,20
1137	8,9,18,22	8,15,18,19	7,8,20	7,13,14,19	1199	10,16,19	7,14,15,19	7,10,20	12,13,15,20
1138	18,19,20	9,10,11,20	12,14,20,22	7,15,19,20	1200	15,18,19	8,14,16,19	7,8,18,19	12,13,20
1139	8,10,20	9,10,11,19	8,10,14,19	7,15,19,22	1201	12,13,17,19	8,14,18,20	9,10,15,19	8,12,17,20
1140	7,13,17,19	10,13,17,20	7,16,17,19	7,13,19	1202	15,20	8,14,17,22	12,17,20	12,17,20,22
1141	8,10,12,20	14,15,16,22	8,9,11,19	9,14,15,19	1203	13,15,17,20	8,17,22	7,9,17,19	12,17,20
1142	13,17,19	7,8,14,15	7,14,17,19	7,8,19,20	1204	15,18,19,20	8,16,17,22	10,13,14,20	8,13,16,18
1143	13,19,20	13,15,17,20	7,8,11,19	7,14,18,19	1205	10,16,19,20	8,14,18,19	9,15,16,19	8,13,15,16
1144	14,15,19,20	7,9,11,22	8,11,18,20	7,15,17,19	1206	10,16,18,19	8,17,18,22	9,14,15,19	8,13,15,18
1145	12,16,17,19	7,12,20	7,13,15,19	7,17,19	1207	14,20	7,16,18,22	7,10,15,19	8,12,20,22
1146	7,8,18,19	10,13,17,19	16,17,18,20	7,13,17,19	1208	7,10,11,19	8,15,17,22	8,9,18,19	10,12,17,20
1147	9,13,17,19	7,12,20,22	7,9,13,19	7,18,19,20	1209	8,15,18,19	7,10,20	10,13,15,20	12,13,14,20
1148	13,17,18,20	13,15,17,19	9,13,15,19	9,19,20	1210	9,10,11,20	9,15,16,20	8,18,19,22	8,13,15
1149	8,10,20,22	16,20	9,14,16,19	7,8,19,22	1211	8,12,14,20	7,10,19,20	8,13,14,20	8,13,18
1150	16,19,20	8,12,14,20	9,10,13,19	7,18,19,22	1212	17,19	7,10,19	8,13,20,22	8,13,16
1151	7,8,11,19	8,13,15,17	15,17,18,20	7,14,19	1213	13,15,17,19	7,10,20,22	8,13,17,20	8,13,14
1152	10,12,20,22	7,15,17,18	10,14,15,19	8,10,19	1214	7,15,16,20	9,15,16,19	7,15,16,19	8,13,14,16
1153	15,17,18,20	7,12,19,20	8,10,11,19	7,10,15,19	1215	9,15,16,22	8,14,15,20	8,15,16,19	8,12,20
1154	13,16,17,19	7,12,19	11,13,14,19	7,19,20,22	1216	18,20	7,10,19,22	13,15,17,20	12,16,17,20
1155	12,14,20,22	7,12,19,22	7,10,11,19	9,10,19,22	1217	7,12,20,22	8,13,16,22	10,13,18,20	8,13,14,18
1156	13,17,19,20	7,15,16,20	8,9,14,19	10,16,19	1218	7,12,20	8,13,22	8,15,18,19	8,13,17
1157	10,12,20	8,12,14,19	9,14,18,19	7,15,19	1219	9,10,11,19	8,14,15,19	11,15,20,22	7,12,17,20
1158	9,10,15,20	9,12,20	9,14,17,19	9,10,19	1220	14,19	8,13,18,22	12,14,20	10,12,20,22
1159	7,15,17,18	9,12,20,22	9,13,16,19	7,8,18,19	1221	8,11,12	8,13,15,22	8,16,19,22	8,13,16,17
1160	12,14,20	7,15,16,19	7,8,17,19	10,19,20	1222	8,12,14,19	11,13,14,22	8,11,19,22	8,13,14,15
1161	13,14,15,19	8,9,12,22	9,17,18,19	11,12,20,22	1223	9,12,20,22	8,17,20,22	7,11,15,20	8,10,12,20
1162	15,18,20,22	9,12,19,20	9,10,20	11,12,20	1224	15,19	8,14,17,20	9,12,20	12,14,20,22
1163	9,11,19,22	9,12,19	12,13,20	9,16,18,19	1225	9,12,20	8,17,20	9,16,18,19	8,15,20,22
1164	14,19,20	9,12,19,22	8,10,18,19	10,11,16,19	1226	7,12,19,22	8,16,17,20	9,11,19,22	8,15,16,20
1165	7,12,17,19	8,9,18,22	8,9,13,19	7,18,19	1227	7,8,12,20	8,17,18,20	10,11,19,22	10,12,20
1166	7,14,15,22	8,14,15,16	8,9,17,19	9,19,22	1228	14,15,16,20	8,17,19,20	8,15,19,22	9,12,17,20
1167	9,12,17,20	18,19	9,12,20,22	15,18,20,22	1229	7,15,16,19	8,17,19,22	9,12,13,19	8,11,15,20
1168	10,14,15,20	7,8,16,18	7,17,18,19	7,8,19	1230	7,12,19	8,14,17,19	12,13,17,19	15,16,19,22

Continued on next page

Table A.1 – continued from previous page

Rank	$\mathbf{w}_{C1}$ Tx's	$\mathbf{w}_{G1}$ Tx's	$\mathbf{w}_{C2}$ Tx's	$\mathbf{w}_{G2}$ Tx's	Rank	$\mathbf{w}_{C1}$ Tx's	$\mathbf{w}_{G1}$ Tx's	$\mathbf{w}_{C2}$ Tx's	$\mathbf{w}_{G2}$ Tx's
1231	16,20	8,17,19	7,13,19,22	12,14,20	1293	11,12,20,22	7,10,12,20	8,13,20	9,10,12,20
1232	7,16,18,22	8,13,14,22	10,12,20	12,13,17,20	1294	8,10,11,16	10,11,12	9,11,19	12,19,20,22
1233	7,12,19,20	8,16,17,19	7,11,19,22	8,13,17,18	1295	13,14,17,19	7,10,12,19	8,9,12,19	12,16,17,19
1234	9,12,19,22	9,14,15,22	14,17,18,20	12,20,22	1296	9,10,12,22	11,16,22	12,16,17,19	7,12,17,19
1235	9,12,19	8,17,18,19	10,17,19,22	8,9,10,19	1297	11,12,19,22	8,11,16,22	10,11,19	10,12,19,20
1236	9,12,19,20	7,16,18,20	8,11,16,19	8,12,14,20	1298	11,12,19	9,10,12,20	14,15,20,22	10,12,19,22
1237	7,8,12,19	8,15,17,20	10,11,18,20	7,12,20,22	1299	11,12,19,20	9,10,12,19	8,11,19	12,14,19,20
1238	7,9,11,20	7,16,18,19	7,16,18,19	8,13,15,17	1300	8,11,16,22	12,16	8,18,19	12,14,19,22
1239	7,10,22	8,15,17,19	7,11,12,20	7,12,20	1301	11,16,22	8,11,12,22	7,8,19,22	8,10,12,19
1240	14,15,16,19	9,10,20	8,20,22	9,12,20,22	1302	8,11,12,22	8,10,11,16	9,11,16,19	9,12,17,19
1241	11,13,14,22	8,13,17,22	9,13,19,22	8,15,20	1303	10,13,14,17	11,16,20	7,13,19	15,19,20,22
1242	8,9,16,18	9,10,22	10,14,19,22	15,16,19,20	1304	12,16	11,16,20,22	7,11,16,19	8,15,16,19
1243	8,9,12,20	9,10,19,20	12,13,18,19	7,8,12,20	1305	7,10,12,20	11,16,19,20	7,20,22	8,15,19,20
1244	8,11,16	9,10,19	8,12,16,20	9,12,20	1306	7,10,12,19	11,16,19	11,18,20,22	8,11,15,19
1245	8,9,18,20	8,13,20,22	7,17,19,22	10,11,15,20	1307	9,10,12,20	11,16,19,22	11,16,19,22	12,13,17,19
1246	18,19	8,13,20	9,14,19,22	8,15,18,20	1308	7,8,11,16	8,11,16,20	8,12,17,19	8,12,19
1247	7,9,11,19	8,13,16,20	7,12,13,19	8,9,12,20	1309	9,10,12,19	8,11,16,19	8,17,20	8,15,19,22
1248	9,14,15,22	11,13,14,20	7,12,20	11,12,19,20	1310	8,9,11,16	8,11,12,20	12,17,18,19	12,14,19
1249	12,17,18,20	8,13,18,20	9,17,19,22	11,12,19,22	1311	11,16,20,22	8,11,12,19	7,11,19	10,12,19
1250	8,9,12,19	8,13,15,20	12,13,15,19	12,17,18,20	1312	11,16,20	7,8,10,20	10,17,19	7,12,19,20
1251	8,9,18,19	8,13,19,20	7,9,10	8,13	1313	8,11,16,20	7,8,10,19	8,13,18,19	12,19,20
1252	12,17,18,19	8,13,19,22	12,14,17,19	11,12,19	1314	11,16,19,22	7,8,11,16	8,16,19	8,12,14,19
1253	7,14,15,20	8,13,16,19	9,15,19,22	15,18,19,22	1315	11,16,19	7,8,10,22	15,18,20	7,12,19,22
1254	16,19	8,13,19	10,13,19,22	16,18,20,22	1316	8,11,12,20	8,9,10,22	7,13,18,20	9,12,19,20
1255	7,8,10,12	11,13,14,19	8,12,20	7,8,10,19	1317	11,16,19,20	8,9,11,16	13,14,15,20	9,12,19,22
1256	7,14,15,19	9,14,15,20	7,13,17,20	15,18,19,20	1318	8,11,16,19	10,13,14,17	7,8,12,19	7,8,12,19
1257	9,16,18,22	8,13,18,19	9,18,19,22	15,16,19	1319	8,11,12,19	8,9,10,20	8,15,19	10,11,15,19
1258	9,15,16,20	8,13,15,19	9,13,17,20	11,18,20,22	1320	7,8,10,20	11,15	7,8,10,19	7,12,19
1259	9,10,22	19,20,22	9,12,17,19	8,11,18,20	1321	7,8,10,19	8,9,10,19	11,12,19,22	12,19,22
1260	7,10,20	9,14,15,19	7,14,19,22	12,20	1322	7,8,10,22	10,11,16,22	9,14,19	9,12,19
1261	7,10,20,22	8,9,16,18	10,15,19,22	7,12,16,22	1323	8,9,10,22	10,11,16,20	10,14,19	8,15,18,19
1262	8,9,14,15	8,13,14,20	12,13,16,19	11,18,20	1324	10,11,16,22	10,11,16,19	9,13,19	8,9,12,19
1263	9,15,16,19	8,11,16	13,17,18,20	9,12,16,22	1325	11,15	7,9,12	10,13,19	12,17,18,19
1264	13,14,17,22	8,13,14,19	12,13,14,19	11,12,16,22	1326	8,9,10,20	8,12,16	7,17,19	8,15,19
1265	7,10,19	9,16,18,22	10,12,13,19	11,15,19,20	1327	8,9,10,19	7,11,16,22	13,14,16,20	7,11,15,20
1266	7,10,19,22	8,13,17,20	13,14,18,20	11,15,19,22	1328	8,12,16	9,11,16,22	8,13,15,19	14,22
1267	7,16,18,20	9,10,20,22	10,18,19,22	8,11,12,19	1329	10,11,16,20	7,11,16,20	13,15,20,22	10,11,12,19
1268	7,10,19,20	8,11,12	9,11,15,20	11,15,19	1330	10,11,16,19	7,11,16,19	10,11,12,19	10,11,15,17
1269	10,11,16	8,13,17,19	11,13,19	15,18,19	1331	7,11,16,22	7,10,11,16	8,16,18,19	16,18,19,22
1270	7,8,10	9,10,19,22	8,12,13,19	8,13,14,17	1332	7,9,12	9,11,16,20	8,14,16,19	10,11,18,20
1271	7,16,18,19	10,11,16	17,18,20,22	16,18,20	1333	9,11,16,22	9,11,16,19	8,9,10,19	11,18,19,20
1272	9,10,20	9,16,18,20	8,11,12,19	10,12,13,19	1334	7,10,11,16	10,11,12,19	9,15,19	11,18,19,22
1273	11,13,14,20	9,16,18,19	8,14,20	7,12,13,19	1335	7,11,16,20	12,16,22	8,14,15,19	8,11,18,19
1274	9,14,15,20	13,14,17,22	14,16,17,20	8,12,13,19	1336	7,11,16,19	12,16,20	8,17,18,19	7,19
1275	9,10,19	7,8,10,12	7,12,17,19	9,12,13,19	1337	9,11,16,20	12,16,20,22	9,17,19	15,20,22
1276	9,10,19,20	11,12,22	10,12,17,19	12,13,16,19	1338	12,16,22	12,16,19,20	7,14,19	16,18,19,20
1277	11,13,14,19	7,8,10	13,16,17,20	12,13,18,19	1339	13,14,16,17	12,16,19	10,15,19	11,18,19
1278	11,12,22	13,14,17,20	10,11,14	12,13,19,20	1340	9,11,16,19	12,16,19,22	12,13,19,22	12,18,22
1279	9,14,15,19	11,12,20	7,15,19,22	12,13,19,22	1341	10,11,12,19	8	15,16,17,19	9,11,15,20
1280	9,10,20,22	13,14,17,19	10,16,19,22	12,14,17,19	1342	8,12,16,22	8,12,16,22	8,15,17,19	10,19
1281	19,20,22	11,12,20,22	10,11,16,19	12,13,15,19	1343	12,16,20	13,14,16,17	11,13,19,20	7,10,12,19
1282	9,10,19,22	11,12,19	9,20,22	8,12,17,19	1344	12,16,20,22	8,12,16,20	9,10,19,22	16,18,19
1283	9,16,18,20	11,12,19,20	11,15,20	12,13,19	1345	12,16,19,22	8,12,16,19	16,22	9,10,12,19
1284	8,9,10,12	11,12,19,22	14,18,20,22	12,17,19,20	1346	12,16,19	12,13,15,17	10,18,19	12,16,20,22
1285	9,16,18,19	7,11,16	8,9,19,22	10,11,12,20	1347	12,16,19,20	10,11,12,22	9,18,19	12,16,20
1286	10,11,12	8,9,14,15	8,10,12,19	12,17,19,22	1348	10,11,12,22	9,10,11,16	7,15,19	12,19
1287	7,11,16	8,13,14,17	7,18,19,22	7,10,12,20	1349	8	10,11,12,20	14,17,20,22	8,12,16,20
1288	7,10,12,22	9,11,16	15,16,20	8,12,19,20	1350	9,10,11,16	14,15,18	7,10,12,19	16,19,20,22
1289	8,9,10	7,10,12,22	10,20,22	10,12,17,19	1351	10,11,15	11,18	8,16,17,19	7,11,15,19
1290	13,14,17,20	8,9,10	16,17,20,22	12,17,19	1352	12,13,15,17	10,11,15	7,10,19,22	18,22
1291	9,11,16	8,9,10,12	8,12,14,19	12,13,14,19	1353	8,12,16,20	7,9,12,22	8,14,18,19	10,11,18,19
1292	11,12,20	9,10,12,22	8,10,19,22	8,12,19,22	1354	8,12,16,19	11,15,22	15,16,19,22	9,19

Continued on next page

Table A.1 – continued from previous page

Rank	$\mathbf{w_{C1}}$ Tx's	$\mathbf{w_{G1}}$ Tx's	$\mathbf{w_{C2}}$ Tx's	$\mathbf{w_{G2}}$ Tx's	Rank	$\mathbf{w_{C1}}$ Tx's	$\mathbf{w_{G1}}$ Tx's	$\mathbf{w_{C2}}$ Tx's	$\mathbf{w_{G2}}$ Tx's
1355	14,15,18	8,11,15	11,18,20	18,19,20,22	1417	10,15,18	9,11,15,19	13,16,20,22	17,18,19,20
1356	11,18	7,9,12,20	8,18,19,20	7,9,12,20	1418	7,9,20	15,16,18,20	8,19,20,22	13,14,16,20
1357	10,11,12,20	7,9,12,19	9,12,14,15	11,15,18,22	1419	7,9,19	15,16,18,19	14,15,18,20	13,14,18,20
1358	8,11,15	11,15,20	11,20	9,11,14,15	1420	7,9,19,20	12,16,17,18	7,15,19,20	16,17,19,20
1359	7,9,12,22	11,15,20,22	12,17,19,22	9,11,15,19	1421	7,9,20,22	7,8,11,12	8,9,19,20	14,17,19
1360	11,15,22	11,15,19,20	16,18,20	7,11,12,20	1422	7,9,19,22	15,16,18,22	7,13,14,19	13,15,20,22
1361	7,8,9,12	11,15,19	7,18,19	14,16,17,20	1423	7,8,11,12	7,11,18	10,11,15,19	13,14,15,20
1362	1,9,12	11,15,19,22	9,10,12,19	14,17,18,20	1424	9,11,15,20	10,12,16	10,16,19,20	13,16,17,20
1363	7,9,12,20	7,9,11,16	8,16,19,20	14,15,17,20	1425	9,11,15,19	19,22	8,10,19,20	13,14,20,22
1364	7,9,12,19	11,12,13,15	10,16,19	16,17,18,20	1426	12,16,17,18	9,11,18	15,17,19,22	13,18,20,22
1365	11,15,20,22	7,8,9,12	10,15,18,20	15,16,17,20	1427	7,8,11,15	7,8,11,15	7,10,19	13,16,20,22
1366	11,15,20	20,22	8,11,19,20	7,9,20	1428	15,16,18,22	11,15,16	10,13,16,19	13,17,18,20
1367	8,11,18	8,11,18	9,11,19,20	14,17,20,22	1429	8,9,11,15	8,9,11,15	7,18,19,20	13,17,20,22
1368	11,15,19,22	8,10,11,15	8,15,19,20	7,9,20,22	1430	15,16,18,20	14,15,16,18	12,20,22	15,17,19
1369	11,15,19	8,11,15,22	8,9,19	17,18,20,22	1431	7,11,18	8,10,11,18	11,15,19,22	13,15,17,20
1370	8,10,11,15	9,15,17,18	15,18,19,22	15,17,20,22	1432	15,16,18,19	10,15,18,20	8,19,22	17,18,19
1371	11,15,19,20	7,11,12	10,11,19,20	16,17,20,22	1433	11,15,16	10,15,18,19	12,17,19	13,14,20
1372	7,9,11,16	8,11,15,20	8,10,19	15,17,18,20	1434	9,11,18	9,11,12,22	14,15,16,19	13,17,20
1373	11,12,13,15	8,11,15,19	11,19,22	12,16,19,20	1435	10,12,16	9,11,12,20	10,14,17,19	13,15,20
1374	8,11,15,22	10,11,15,22	13,14,17,20	12,16,19,22	1436	14,15,16,18	9,11,12,19	7,8,19,20	16,17,19
1375	7,11,12	10,11,15,20	9,11,12,20	10,11,14,15	1437	8,10,11,18	7,8,11,18	8,11,18,19	13,18,20
1376	9,15,17,18	10,11,15,19	12,14,19,22	12,16,19	1438	19,22	7,10,11,15	13,15,18,19	13,16,20
1377	20,22	7,11,15	8,13,16,19	14,17,20	1439	8,14,15,18	9,10,11,15	11,16,19,20	7,11,18,19
1378	8,10,11,12	8,10,11,12	7,11,19,20	15,17,20	1440	9,11,12,22	10,12,16,22	16,17,20	11,15,16,19
1379	10,11,15,22	7,10,16,18	7,13,19,20	8,12,16,19	1441	7,8,11,18	10,12,16,20	12,16,20	9,11,18,19
1380	8,11,15,20	11,18,22	14,16,20,22	17,18,20	1442	1,7,12	10,12,16,19	12,14,19	15,16,18,20
1381	7,11,15	8,11,18,22	8,13,19,22	16,17,20	1443	10,15,18,20	7,11,18,22	9,12,19	9,11,12,20
1382	8,11,15,19	14,15,18,22	11,16,19	18,20,22	1444	10,15,18,19	8,14,15,18	14,15,17,19	14,16,18,19
1383	10,11,15,20	14,15,18,20	8,17,19,22	15,19,22	1445	7,10,11,15	7,11,18,20	13,15,16,19	14,18,19,22
1384	14,15,18,22	7,9,14,18	15,17,20	7,11,18,20	1446	9,11,12,20	11,15,16,22	10,19,22	14,16,19,22
1385	10,11,15,19	14,15,18,19	10,17,19,20	16,20,22	1447	9,11,12,19	7,11,18,19	7,20	7,15,18,22
1386	11,18,22	11,18,20	11,15,16,20	11,15,16,20	1448	9,10,11,15	9,11,18,22	16,17,18,19	14,15,19,22
1387	8,11,18,22	11,18,20,22	11,12,19	9,11,18,20	1449	10,12,16,22	11,15,16,20	10,12,19	14,18,19,20
1388	7,10,16,18	11,18,19,20	7,8,19	14,16,18,20	1450	7,11,18,22	11,15,16,19	11,12,19,20	14,16,19,20
1389	10,11,18	11,18,19	9,13,19,20	14,18,20,22	1451	8,11,15,16	9,11,18,20	9,19,22	14,15,19,20
1390	7,9,14,18	11,18,19,22	9,12,19,22	14,16,20,22	1452	11,15,16,22	9,11,18,19	10,20	14,15,16,19
1391	14,15,18,20	10,11,18	14,15,20	14,15,20,22	1453	9,11,18,22	9,12,16	15,17,18,19	13,14,17,20
1392	14,15,18,19	8,11,18,20	9,14,19,20	7,9,12,19	1454	10,12,16,20	8,11,15,16	9,19,20,22	8,19
1393	11,18,20	8,11,18,19	10,14,19,20	14,15,16,20	1455	10,12,16,19	8,10,12,16	9,10,19,20	17,19,20,22
1394	11,18,20,22	7,9	8,14,19,22	7,11,12,19	1456	7,11,18,20	8,9,11,18	7,12,19	10,15,18,19
1395	11,18,19	9,11,15	10,12,19,22	14,17,18,19	1457	7,11,18,19	11,16,18	10,19,20,22	14,15,19
1396	11,18,19,22	7,11,12,22	8,14,17,20	14,16,17,19	1458	8,10,12,16	8,15,16,18	8,12,19	14,18,19
1397	8,11,18,20	15,16,18	9,11,18,20	14,15,17,19	1459	9,12,16	10,15,18,22	17,18,20	17,20,22
1398	11,18,19,20	7,11,12,20	13,18,20,22	16,17,18,19	1460	11,15,16,20	9,12,16,20	14,16,20	14,16,19
1399	8,11,18,19	7,11,12,19	7,11,18,20	7,9,19,20	1461	9,11,18,20	7,12,16	10,13,14,19	13,15,16,19
1400	9,11,15	7,11,15,22	7,17,19,20	15,16,17,19	1462	11,15,16,19	9,12,16,19	7,19,22	13,16,18,19
1401	7,9	8,9,15,16	10,13,19,20	14,15,20	1463	8,9,11,18	8,9,11,12	13,14,20,22	13,15,18,19
1402	4,9,11	7,11,15,20	9,15,19,20	14,18,20	1464	9,11,18,19	11,16,18,22	13,17,20,22	13,14,16,19
1403	7,11,12,22	7,11,15,19	12,16,20,22	10,15,18,20	1465	1,11,13	11,16,18,20	11,19,20	8,11,14
1404	8,9,15,16	10,11,18,22	11,19,20,22	14,17,19,22	1466	1,8,11	11,16,18,19	12,13,19,20	13,14,18,19
1405	15,16,18	10,11,18,20	13,15,20	15,17,18,19	1467	8,15,16,18	7,9,11,15	15,20,22	13,14,15,19
1406	7,11,15,22	10,11,18,19	8,12,19,22	7,9,19,22	1468	11,16,18	10,14,15,18	13,18,20	13,16,17,19
1407	7,11,12,20	7,9,22	16,18,19,22	7,9,19	1469	4,7,11	10,11,13,14	17,18,19,22	13,15,19,22
1408	7,11,12,19	7,9,20	9,10,19	14,16,20	1470	10,15,18,22	12,18	13,16,20	13,14,19,22
1409	10,11,18,22	9,11,12	7,12,19,22	15,17,19,22	1471	8,9,11,12	7,12,16,22	14,18,20	13,18,19,22
1410	7,11,15,20	7,9,19	10,15,19,20	17,18,19,22	1472	7,12,16	9,12,16,22	9,20	13,17,18,19
1411	7,11,15,19	7,9,19,20	7,14,19,20	16,17,19,22	1473	9,12,16,20	7,12,16,20	7,9,12,19	13,17,19,22
1412	10,11,18,20	7,9,20,22	12,13,19	14,17,19,20	1474	9,12,16,19	7,12,16,19	14,16,18,19	13,16,19,22
1413	10,11,18,19	7,9,19,22	9,17,19,20	13,15,16,20	1475	11,16,18,22	10,11,15,16	16,17,19,22	11,16,18,20
1414	9,11,12	10,15,18	9,18,19,20	13,16,18,20	1476	10,11,13,14	9,10,16,18	7,9,20,22	13,14,19,20
1415	7,9,22	9,11,15,22	8,11,15,19	13,15,18,20	1477	10,14,15,18	7,10,11,18	10,13,17,19	13,15,19,20
1416	9,11,15,22	9,11,15,20	10,18,19,20	15,17,19,20	1478	7,9,11,15	11,12,16	8,14,19	13,18,19,20

Continued on next page

Table A.1 – continued from previous page

Rank	$\mathbf{w}_{C1}$ Tx's	$\mathbf{w}_{G1}$ Tx's	$\mathbf{w}_{C2}$ Tx's	$\mathbf{w}_{G2}$ Tx's	Rank	$\mathbf{w}_{C1}$ Tx's	$\mathbf{w}_{G1}$ Tx's	$\mathbf{w}_{C2}$ Tx's	$\mathbf{w}_{G2}$ Tx's
1479	11,16,18,20	10,15,16,18	8,13,14,19	13,15,17,19	1541	12,14,18,19	11,12,15,19	12,16,19,22	13,19
1480	11,16,18,19	8,11,16,18	7,10,19,20	13,17,19,20	1542	10,11,15,18	7,11,15,18	14,16,19,22	7,15,18,19
1481	7,12,16,22	12,18,22	15,16,18,20	13,16,19,20	1543	7,8,15,18	9,14,15,16	12,19,22	17,20
1482	9,12,16,22	12,18,20	7,19,20,22	13,14,19	1544	9,15,18	8,9,15,18	15,17,19	7,12,14,15
1483	10,11,15,16	12,18,19	10,13,15,19	13,17,19	1545	11,12,15	12,13,14,17	9,12,16,20	7,8,12,18
1484	12,18	12,18,19,20	8,20	13,15,19	1546	9,13,14,17	7,12,16,17	13,14,15,19	15,20
1485	7,12,16,20	12,18,20,22	14,15,19,22	13,18,19	1547	8,12,14,18	7,13,14,17	14,15,19	8,12,16,18
1486	7,12,16,19	12,18,19,22	11,15,19	13,16,19	1548	8,11,12,15	7,10,15,18	13,16,19,22	8,10,13,20
1487	9,10,16,18	7,11,15,16	8,13,17,19	18,19,22	1549	9,15,18,22	11,15,16,18	13,14,16,19	10,13,16,20
1488	11,12,16	9,11,15,16	8,13,19	15,16,18,19	1550	9,15,18,20	9,11,15,18	16,19,20,22	10,13,18,20
1489	1,11,17	11,12,16,22	10,13,18,19	9,11,12,19	1551	7,11,16,18	13,14,17,18	18,19,20,22	10,13,15,20
1490	7,10,11,18	11,12,16,20	11,18,19,22	14,19,20,22	1552	9,15,18,19	12,14,16	16,18,19,20	10,13,20,22
1491	8,11,16,18	11,12,16,19	15,16,19	13,20,22	1553	9,11,16,18	12,14,16,22	12,19,20,22	10,13,14,20
1492	10,15,16,18	10,12,17,18	12,17,19,20	16,22	1554	11,12,15,22	12,14,16,20	13,15,19	10,13,20
1493	12,18,22	9,10,11,18	13,15,17,19	14,20,22	1555	11,12,15,20	12,14,16,19	10,15,18,19	10,13,17,20
1494	7,11,15,16	10,14,15,16	11,16,18,20	13,14,17,19	1556	11,12,15,19	9,10,15,18	17,20,22	9,15,18,20
1495	12,18,20	7,14,15,18	8,12,16,19	13,19,20,22	1557	7,11,15,18	13,14,15,17	11,18,19,20	8,12,18,20
1496	9,11,15,16	7,8,12,16	7,11,15,19	16,19,22	1558	9,14,15,16	7,9,10,12	9,11,12,19	14,20
1497	12,18,20,22	9,14,15,18	8,19,20	15,19,20	1559	8,9,15,18	9,12,16,17	15,17,19,20	8,10,13,19
1498	12,18,19	7,15,16,18	9,12,19,20	11,16,18,19	1560	12,13,14,17	7,10,15,16	13,14,17,19	10,13,16,19
1499	12,18,19,20	10,11,16,18	10,11,18,19	8,11,17,18	1561	7,12,16,17	10,11,12,15	8,14,17,19	10,13,18,19
1500	12,18,19,22	8,10,15,18	12,14,19,20	17,19,22	1562	7,13,14,17	7,11,12,15	11,15,16,19	10,13,15,19
1501	11,12,16,22	7,12,17,18	14,17,18,19	10,12,16,20	1563	7,10,15,18	12,15,17,18	12,16,19	10,13,19,20
1502	10,12,17,18	8,11,12,16	8,17,19	13,19,22	1564	1,11,18	9,11,12,15	7,11,18,19	10,13,19,22
1503	11,12,16,20	11,12,14,17	10,12,19,20	8,10,13,22	1565	1,11,16	11,16,17,18	14,15,19,20	10,13,14,19
1504	11,12,16,19	12,14,16,18	7,11,12,19	10,13,16,22	1566	11,15,16,18	9,16	9,11,18,19	12,14,18,20
1505	1,10,12	11,15,18	13,15,19,22	10,13,18,22	1567	13,14,17,18	7,16	16,17,19	10,13,19
1506	9,10,11,18	7,9,11,18	7,9,20	10,13,15,22	1568	9,11,15,18	7,16,22	14,20,22	10,13,17,19
1507	7,8,12,16	7,15,18	13,16,18,19	10,13,14,22	1569	12,14,16	9,16,22	14,17,19,22	9,15,18,19
1508	10,14,15,16	8,11,15,18	10,12,16,20	10,13,22	1570	12,14,16,22	9,16,20	13,14,19,22	11,12,15,20
1509	7,14,15,18	11,15,18,22	8,12,19,20	10,13,17,22	1571	12,14,16,20	9,16,19	13,15,19,20	8,12,18,19
1510	1,11,14	11,15,18,20	15,18,19	14,15,18,20	1572	12,14,16,19	9,16,19,20	7,9,19,22	12,14,18,19
1511	10,11,16,18	11,15,18,19	13,14,20	14,19,22	1573	9,10,15,18	7,16,20	13,17,19,22	17,19
1512	9,14,15,18	7,15,18,22	7,12,19,20	9,15,18,22	1574	13,14,15,17	7,16,19	17,18,19	12,14,16,22
1513	7,15,16,18	7,15,18,20	7,13,17,19	7,9,10	1575	7,9,10,12	7,16,19,20	13,16,19	11,12,15,19
1514	8,10,15,18	7,15,18,19	9,11,15,19	10,12,16,19	1576	9,12,16,17	7,16,20,22	13,18,19	11,16,17
1515	8,11,12,16	9,12,17,18	9,13,17,19	9,12,16,20	1577	7,10,15,16	9,16,20,22	14,15,18,19	9,16,22
1516	7,12,17,18	12,14,18	7,13,18,19	8,12,18,22	1578	10,11,12,15	7,16,19,22	14,18,19	18,20
1517	11,12,14,17	9,15,16,18	13,17,18,19	12,14,18,22	1579	7,11,12,15	9,16,19,22	15,19,22	14,19
1518	12,14,16,18	7,14,15,16	13,14,18,19	14,15,18,19	1580	9,11,12,15	9,10,12,16	12,19,20	7,16,22
1519	11,15,18	8,12,18	8,14,19,20	18,19,20	1581	12,15,17,18	7,10,12,16	7,12,16,20	15,19
1520	7,9,11,18	8,9,12,16	13,17,20	13,19,20	1582	11,16,17,18	12,15	14,16,19	11,14,16,18
1521	8,11,15,18	8,12,18,22	14,17,20	9,12,16,19	1583	9,16	19,20	7,19	16,20
1522	7,15,18	8,12,18,20	14,16,17,19	17,19,20	1584	7,16	7,10,14,15	11,12,16,20	12,14,16,20
1523	4,10,11	8,12,18,19	9,19,20	7,12,16,20	1585	7,16,22	12,15,22	16,17,19,20	12,14,16,19
1524	11,15,18,22	12,14,18,22	10,19,20	11,12,16,20	1586	9,16,22	12,15,20	12,16,19,20	12,15,22
1525	11,15,18,20	12,14,18,20	15,16,19,20	11,12,15,22	1587	9,16,20	12,15,19	10,19	18,19
1526	11,15,18,19	12,14,18,19	13,16,17,19	16,19,20	1588	9,16,19	12,15,19,20	7,9,19	9,16,20,22
1527	7,15,18,22	9,15,18	18,20,22	14,19,20	1589	9,16,19,20	12,15,20,22	13,20,22	9,16,20
1528	7,15,18,20	10,11,15,18	12,20	7,12,16,19	1590	7,16,20	12,15,19,22	14,16,19,20	8,11,13,17
1529	7,15,18,19	7,8,15,18	15,19,20,22	11,12,16,19	1591	7,16,20,22	11,12,13,14	17,19,20,22	7,16,20,22
1530	9,12,17,18	11,12,15	14,18,19,22	12,18,20,22	1592	9,16,20,22	12,15,16,17	17,18,19,20	7,16,20
1531	12,14,18	9,13,14,17	7,19,20	12,18,20	1593	7,16,19	10,12,18	14,18,19,20	9,11,15,17
1532	9,15,16,18	9,15,18,22	8,13,19,20	7,11,14,15	1594	7,16,19,22	11,12,15,16	13,16,19,20	9,16,19,20
1533	8,12,18	9,15,18,20	11,15,19,20	12,18,19,20	1595	9,16,19,22	10,12,14,18	13,18,19,20	9,16,19,22
1534	7,14,15,16	9,15,18,19	11,19	12,18,19,22	1596	7,16,19,20	7,10,11,12	12,19	9,16,19
1535	8,9,12,16	8,12,14,18	11,18,19	12,18,19	1597	1,11,15	9,10,15,16	13,17,19	7,16,19,20
1536	8,12,18,22	7,11,16,18	16,18,19	11,15,18,20	1598	9,10,12,16	10,12,18,22	15,16,18,19	7,16,19,22
1537	8,12,18,20	8,11,12,15	8,17,19,20	7,9,12,16	1599	7,10,12,16	10,12,18,20	14,19,20,22	7,16,19
1538	8,12,18,19	9,11,16,18	15,18,19,20	13,20	1600	12,15	10,12,18,19	14,17,19	8,11,12,18
1539	12,14,18,22	11,12,15,22	16,20,22	11,15,18,19	1601	19,20	8,12,14,16	9,19	10,12,18,22
1540	12,14,18,20	11,12,15,20	13,18,19,22	7,15,18,20	1602	7,10,14,15	9,11,13,14	11,16,18,19	10,11,17,18

Continued on next page

Table A.1 – continued from previous page

Rank	$\mathbf{w}_{C1}$ Tx's	$\mathbf{w}_{G1}$ Tx's	$\mathbf{w}_{C2}$ Tx's	$\mathbf{w}_{G2}$ Tx's	Rank	$\mathbf{w}_{C1}$ Tx's	$\mathbf{w}_{G1}$ Tx's	$\mathbf{w}_{C2}$ Tx's	$\mathbf{w}_{G2}$ Tx's
1603	12,15,22	8,12,15	18,19,22	8,14,16,22	1665	7,12,18,19	9,12,18,22	12,14,16,19	8,16,17,20
1604	12,15,20	8,12,15,22	8,9,16	8,14,18,22	1666	11,13,14,16	12,14,15,22	16,20	8,17,18,20
1605	12,15,19	8,12,15,20	10,12,16,19	8,14,15,22	1667	4,11,13	12,14,15,20	7,8,9,22	8,15,17,20
1606	12,15,19,20	8,12,15,19	7,9,19,20	8,14,22	1668	12,14,15,16	12,14,15,19	7,9,16,18	8,17,20,22
1607	12,15,20,22	9,10,14,15	13,14,19	8,12,14,15	1669	7,12,14,18	7,8,12,18	9,16,20,22	8,17,20
1608	12,15,19,22	11,12,15,18	13,14,19,20	8,12,15,22	1670	11,14,15	8,12,16,18	7,16,20,22	11,14,15,22
1609	11,12,13,14	10,11,12,16	17,19,22	7,9,16,18	1671	7,11,13,14	7,12,15,17	9,16,20	7,8,9,19
1610	12,15,16,17	12,15,17	14,17,19,20	8,9,16	1672	11,14,15,22	8,11,14,22	7,12,18,22	8,14,17,19
1611	11,12,15,16	8,12,15,17	13,17,19,20	8,9,12,18	1673	11,14,15,20	10,12,14,16	7,16,20	8,16,17,19
1612	10,12,18	12,14,15,18	16,19,22	12,15,20	1674	11,14,15,19	11,15,17	9,16,19,22	8,17,18,19
1613	10,12,14,18	8,10,12,18	13,19,20,22	12,15,20,22	1675	7,9,15,18	11,13,14,15	7,16,19,22	8,15,17,19
1614	1,11	12,15,17,22	9,12,16,19	7,11,15,17	1676	5,11,12	11,15,17,22	11,14,15,22	8,17,19,20
1615	1,11,22	12,15,17,20	14,19,22	16,19	1677	8,11,14	11,15,17,20	9,16,19	8,17,19,22
1616	1,11,20	12,15,17,19	9,16,22	8,11,15,17	1678	8,11,14,20	11,15,17,19	7,16,19	8,17,19
1617	7,10,11,12	11,17,18	13,19,22	11,17,18,22	1679	8,11,14,19	11,14,15,18	18,19	12,16,18,20
1618	1,11,19	11,17,18,22	7,16,22	12,15,19,20	1680	8,11,17,18	9,11,13,17	9,16,19,20	12,16,18,19
1619	10,12,18,22	11,17,18,20	11,15,18,20	12,15,19,22	1681	10,12,15,17	11,12,18	7,16,19,20	10,11,14
1620	9,10,15,16	11,17,18,19	8,19	12,15,19	1682	11,15,17,18	11,13,17	12,15,20,22	7,8,9,10
1621	10,12,18,20	11,14	12,18,20,22	9,12,14,15	1683	11,14,15,16	8,11,12,18	10,12,18,20	7,12,18,20
1622	10,12,18,19	7,9,14,15	7,12,16,19	8,11,14,15	1684	4,8,11	11,13,17,18	12,15,20	8,13,18,20
1623	8,12,14,16	11,14,22	11,12,16,19	12,15,17,22	1685	9,12,14,18	10,12,14,15	12,15,19,22	8,13,16,20
1624	9,11,13,14	11,14,20	10,12,18,22	10,12,18,20	1686	9,12,18	8,11,13,17	12,15,16	8,13,15,20
1625	8,12,15	11,14,19	15,19,20	11,14,22	1687	12,14,15	11,12,18,20	12,15,19	8,13,20,22
1626	8,12,15,22	11,14,19,20	12,18,20	10,12,18,19	1688	9,12,18,22	11,12,18,19	9,11,17,18	8,13,14,20
1627	9,10,14,15	11,14,20,22	7,15,18,20	8,14,16,20	1689	9,12,18,20	11,12,18,22	8,12,15,20	8,13,17,20
1628	8,12,15,20	11,14,19,22	17,19,20	8,14,18,20	1690	12,14,15,22	11,13,14,18	10,12,18,19	8,13,20
1629	8,12,15,19	12,16,18	18,19,20	8,14,20,22	1691	9,12,18,19	11,13,17,22	12,15,19,20	7,12,18,19
1630	11,12,15,18	7,8,9	12,18,19,22	8,14,15,20	1692	12,14,15,20	11,13,17,20	16,19	8,13,15,19
1631	10,11,12,16	11,15,16,17	13,19,20	8,14,20	1693	12,14,15,19	11,13,17,19	12,14,15,22	8,13,18,19
1632	12,15,17	12,16,18,22	16,19,20	8,14,16,19	1694	7,8,12,18	8,12,14,15	9,12,18,22	8,13,16,19
1633	8,12,15,17	12,16,18,20	11,15,18,19	8,14,18,19	1695	8,12,16,18	9,10,11,12	8,12,15,19	8,13,14,19
1634	8,10,12,18	12,16,18,19	12,18,19	8,14,19,20	1696	7,12,15,17	8,9,12,18	7,11,17,18	8,13,19,20
1635	12,14,15,18	7,8,9,19	12,14,18,20	8,14,19,22	1697	8,11,14,22	7,9,11,12	12,15,17,20	8,13,19,22
1636	12,15,17,22	7,8,9,20	8,12,18,20	8,14,15,19	1698	10,12,14,16	11,13,14,17	11,17,18,20	8,13,17,19
1637	12,15,17,20	7,8,9,22	9,15,18,20	8,14,19	1699	11,15,17	8,9,16	12,15,17,19	8,13,19
1638	12,15,17,19	12,15,16,18	12,18,19,20	8,12,15,20	1700	4,7,12	8,9,16,20	11,17,18,19	19,20,22
1639	11,17,18	11,12,13,17	14,19,20	8,12,15,19	1701	11,13,14,15	8,9,16,19	11,14,20,22	11,14,15,20
1640	11,17,18,22	7,12,18	11,12,15,20	8,14,17,22	1702	11,15,17,22	8,9,16,22	11,14,20	11,14,15,19
1641	11,17,18,20	7,12,18,20	12,15,22	8,16,17,22	1703	11,15,17,20	8,11,15,17	8,11,14,22	8,11,14,20
1642	11,17,18,19	7,12,18,19	7,15,18,19	8,17,18,22	1704	11,15,17,19	8,11,14,15	7,8,9,20	9,12,18,22
1643	11,14	7,12,18,22	13,20	8,15,17,22	1705	11,14,15,18	11,13,16,17	11,14,19,22	12,14,15,22
1644	7,9,14,15	11,13,14,16	12,15,17,22	8,17,22	1706	9,11,13,17	9,12,15,17	12,16,18,20	8,11,14,19
1645	11,14,22	12,14,15,16	11,17,18,22	7,8,9,22	1707	11,12,18	7,9,15,16	11,14,19	11,14,18
1646	11,14,20	7,12,14,18	8,12,15,22	11,17,18,20	1708	8,11,12,18	11,13,15,17	11,15,17,22	8,11,14,22
1647	11,14,20,22	11,14,15	17,20	12,16,18,22	1709	11,13,17	10,11,13,17	11,14,19,20	12,15,16
1648	11,14,19	7,11,13,14	8,12,18,19	11,17,18,19	1710	8,11,13,17	7,11,13,17	7,8,9,19	9,12,18,20
1649	11,14,19,20	11,14,15,22	12,14,18,19	12,15,17,20	1711	10,12,14,15	10,11,15,17	12,16,18,19	12,14,15,20
1650	11,14,19,22	11,14,15,20	9,15,18,19	12,15,17,19	1712	11,13,17,18	10,11,14,15	7,12,18,20	12,15,18
1651	12,16,18	11,14,15,19	13,19	11,14,20,22	1713	11,12,18,22	7,8,9,10	11,13,17,22	9,12,18,19
1652	7,8,9	7,9,15,18	11,12,15,19	11,14,20	1714	11,12,18,20	7,9,10	11,12,18,22	12,14,15,19
1653	11,15,16,17	8,11,14	15,20	11,14,19,20	1715	11,12,18,19	7,9,10,19	7,12,18,19	11,15,17,22
1654	12,16,18,22	8,11,14,20	14,20	11,14,19,22	1716	11,13,14,18	7,9,10,20	10,11,16,17	11,13,17,22
1655	12,16,18,20	8,11,14,19	17,19	11,14,19	1717	11,13,17,22	7,9,10,22	11,14,15,20	9,11,17,18
1656	12,16,18,19	8,11,17,18	12,14,16,20	7,12,18,22	1718	11,13,17,20	7,9,12,16	12,15,18	11,12,18,22
1657	7,8,9,20	10,12,15,17	18,20	8,13,18,22	1719	11,13,17,19	9,11,14,15	8,11,14,20	11,15,17,20
1658	7,8,9,19	11,15,17,18	14,19	8,13,15,22	1720	8,12,14,15	7,11,14,15	11,14,15,19	8,11,16,17
1659	7,8,9,22	11,14,15,16	7,8,9,10	8,13,16,22	1721	9,10,11,12	7,12,14,15	19,20,22	11,15,17,19
1660	12,15,16,18	9,12,14,18	12,16,18,22	8,13,14,22	1722	8,9,12,18	11,16,17	8,11,14,19	8,9,16,22
1661	11,12,13,17	9,12,18	8,11,16,17	8,13,17,22	1723	7,9,11,12	8,11,16,17	9,12,18,20	7,11,17,18
1662	7,12,18	12,14,15	15,19	8,13,22	1724	11,13,14,17	10,11,17,18	12,14,15,20	11,13,17,20
1663	7,12,18,22	9,12,18,20	11,14,22	7,8,9,20	1725	8,9,16	11,16,17,22	8,9,16,22	11,13,17,19
1664	7,12,18,20	9,12,18,19	11,14,18	8,14,17,20	1726	8,9,16,20	11,16,17,20	9,12,18,19	11,12,18,20

Continued on next page

Table A.1 – continued from previous page

Rank	w_{C1} Tx's	w_{G1} Tx's	w_{C2} Tx's	w_{G2} Tx's	Rank	w_{C1} Tx's	w_{G1} Tx's	w_{C2} Tx's	w_{G2} Tx's
1727	8,9,16,22	11,16,17,19	7,12,14,16	11,12,18,19	1789	2,11,12	10,12,15,20	7,11,14,20	9,12,14,16
1728	8,9,16,19	11,14,16,18	12,14,15,19	8,9,16,20	1790	10,11,16,17	10,12,15,19	9,11,14,19	7,12,15,16
1729	8,11,15,17	7,9,16,18	11,15,17,20	8,9,16,19	1791	5,10,11	10,12,15,22	7,11,14,19	10,12,15,22
1730	8,11,14,15	9,11,15,17	11,15,17,19	10,11,16,17	1792	8,10,11,14	7,10,18	4,9,11	9,10,12,18
1731	11,13,16,17	7,11,15,17	11,13,17,20	7,12,14,16	1793	9,11,17,18	7,10,18,22	20,22	10,12,15,20
1732	4,9,12	10,11,14	11,12,18,20	7,9,15	1794	11,17,22	7,10,18,19	9,12,14,16	10,12,15,19
1733	9,12,15,17	10,11,14,22	11,14,16	7,9,10,22	1795	11,17,20	7,10,18,20	9,12,15,16	10,12,15,16
1734	7,9,15,16	10,11,14,20	11,13,17,19	7,9,10,20	1796	11,17,19,20	9,12,15,16	7,10,18	9,11,12,18
1735	11,13,15,17	10,11,14,19	11,12,18,19	7,9,10,19	1797	11,17,20,22	9,12,14,16	7,12,15,16	7,11,12,18
1736	10,11,13,17	9,12,14,15	8,9,16,20	11,16,17,22	1798	11,17,19,22	7,12,15,16	10,12,15,22	11,12,14,15
1737	7,11,13,17	11,17	7,9,10,22	11,14,16	1799	7,11,17,18	9,10,12,18	9,10,12,18	11,12,17
1738	10,11,15,17	11,17,19	7,9,15	11,16,17,20	1800	8,11,14,18	10,12,15,16	10,12,15,16	9,11,12,17
1739	10,11,14,15	12,15,16	8,9,16,19	11,16,17,19	1801	11,14,18	8,11,17	9,11,12,18	9,12,15,18
1740	7,8,9,10	12,15,16,22	8,11,14,18	9,11,14	1802	7,12,14,16	8,11,17,22	7,11,12,18	10,12,16,18
1741	7,9,10	12,15,16,20	8,10,11,14	8,10,11,14	1803	11,14,18,22	8,11,17,20	10,12,15,20	10,11,12,18
1742	7,9,10,20	12,15,16,19	9,11,14	10,11,14,22	1804	8,12,15,18	8,11,17,19	10,12,15,19	7,10,18,22
1743	7,9,10,19	10,11,16,17	7,11,14	7,11,14	1805	11,14,18,20	9,11,12,18	9,11,12,17	7,11,12,17
1744	4,11,17	8,10,11,14	8,12,15,18	8,11,14,18	1806	11,14,18,19	7,11,12,18	7,11,12,17	7,9,11,14
1745	7,9,10,22	9,11,17,18	11,16,17,22	10,11,14,20	1807	12,15,18	8,12,15,16	10,11,12,18	7,12,15,18
1746	4,11,14	11,17,22	7,9,10,20	8,12,15,18	1808	12,15,18,22	10,12,16,18	11,12,17	8,11,17
1747	1,7,9	11,17,20	7,9,10,19	10,11,14,19	1809	12,15,18,20	10,11,12,18	8,11,17	7,10,18,20
1748	4,10,12	11,17,19,20	7,8,9,15	7,8,9,15	1810	12,15,18,19	7,8,16	11,12,14,15	7,10,18,19
1749	7,9,12,16	11,17,20,22	10,11,14,22	11,17,19	1811	7,8,9,15	7,8,16,19	10,11,12,17	11,12,14,16
1750	1,12,13	11,17,19,22	11,16,17,20	9,11,12,16	1812	1,12,15	7,8,16,20	11,12,14,16	10,11,12,17
1751	9,11,14,15	7,11,17,18	11,16,17,19	7,11,12,16	1813	4,8,12	9,12,15,18	9,12,15,18	11,12,15,17
1752	7,11,14,15	8,11,14,18	9,11,12,16	7,9,10,15	1814	1,7,10	9,11,12,17	10,12,16,18	9,10,11,14
1753	7,12,14,15	11,14,18	7,11,12,16	12,15,16,22	1815	7,9,15	7,11,12,17	7,9,11,14	8,12,15,16
1754	11,16,17	7,12,14,16	8,11,14,16	12,15,16,20	1816	7,9,15,22	7,12,15,18	7,12,15,18	11,12,14,18
1755	8,11,16,17	11,14,18,22	7,9,10,15	12,15,16,19	1817	7,9,15,20	7,9,11,14	7,10,18,22	10,12,15,18
1756	10,11,17,18	11,14,18,20	12,15,16,22	8,11,14,16	1818	7,9,15,19	10,11,12,17	8,12,15,16	7,10,11,14
1757	11,16,17,22	11,14,18,19	10,11,14,20	11,17,22	1819	4,12,13	11,12,14,16	9,10,11,14	9,12,15
1758	11,16,17,20	8,12,15,18	10,11,14,19	11,14,18,22	1820	1,12,16	9,10,11,14	7,10,11,14	8,11,17,22
1759	11,16,17,19	12,15,18	11,17,19	11,17,20,22	1821	1,12,18	10,12,15,18	11,12,14,18	7,8,16
1760	1,8,12	12,15,18,22	12,15,16,20	11,17,20	1822	8,11,14,16	11,12,14,15	10,12,15,18	8,11,17,20
1761	11,14,16,18	12,15,18,20	11,14,18,22	11,17,19,20	1823	11,14,16	7,10,11,14	7,10,18,20	8,11,17,19
1762	4,11,18	12,15,18,19	12,15,16,19	11,17,19,22	1824	11,14,16,22	8,11,12,17	11,12,15,17	7,9,11,17
1763	4,11,15	7,8,9,15	11,17,22	12,15,18,22	1825	11,14,16,20	11,12,17	7,10,18,19	11,12,16,17
1764	7,9,16,18	7,9,15	12,15,18,22	8	1826	11,14,16,19	11,12,17,22	9,12,15	11,12,17,18
1765	5,7,11	7,9,15,20	8,10,16	11,14,18,20	1827	4,7,9	11,12,17,20	11,12,16,17	8,11,12,17
1766	3,11,12	7,9,15,19	7,9,15,22	11,14,18,19	1828	4,12,17	11,12,17,19	7,8,16	9,10,11,17
1767	9,11,15,17	7,9,15,22	11,17,20,22	8,10,16	1829	8,10,16,22	9,12,15	8,11,12,17	9,11,14,16
1768	7,11,15,17	8,11,14,16	11,17,20	7,9,15,22	1830	8,10,16	9,12,15,20	8,11,17,22	7,10,16
1769	10,11,14	11,14,16	11,17,19,22	12,15,18,20	1831	8,10,16,20	9,12,15,19	7,9,11,17	7,8,16,20
1770	10,11,14,22	11,14,16,22	11,14,18,20	12,15,18,19	1832	8,10,16,19	8,9,11,14	1,11,13	8,9,11,14
1771	4,11,16	11,14,16,20	1,9,12	7,9,15,20	1833	3,9,11	9,12,15,22	11,12,17,18	7,8,16,19
1772	10,11,14,20	11,14,16,19	11,17,19,20	7,9,15,19	1834	9,11,14	7,8,10,16	8,9,11,14	7,10,11,17
1773	10,11,14,19	8,10,16,22	11,14,18,19	11,14,16,22	1835	9,11,14,22	7,8,11,14	8,11,17,20	7,11,14,16
1774	9,12,14,15	8,10,16	12,15,18,20	11,14,16,20	1836	9,11,14,20	11,12,14,18	9,10,11,17	7,8,10,16
1775	11,17	8,10,16,19	8	11,14,16,19	1837	9,11,14,19	11,12,16,17	8,11,17,19	19,22
1776	11,17,19	8,10,16,20	12,15,18,19	10,12,15	1838	7,9,10,15	7,9,11,17	7,8,11,14	9,11,17
1777	1,9,10	9,11,14	7,9,15,20	8,10,16,22	1839	7,11,14	11,12,15,17	9,11,17	7,8,11,14
1778	5,9,11	9,11,14,22	11,14,16,22	9,11,14,22	1840	7,11,14,22	9,10,11,17	9,11,14,16	9,10,18
1779	4,11,19	9,11,14,20	7,9,15,19	7,11,14,22	1841	7,11,14,20	7,10,16	7,10,11,17	7,11,17
1780	12,15,16	9,11,14,19	10,12,15	8,10,16,20	1842	7,11,14,19	7,10,16,22	7,11,14,16	10,11,14,16
1781	12,15,16,22	7,9,10,15	8,10,16,22	8,10,16,19	1843	4,9,10	7,10,16,19	7,11,17	9,11,14,18
1782	12,15,16,20	7,11,14	9,11,14,22	9,11,14,20	1844	4,7,10	7,10,16,20	1,7,12	11,12,17,22
1783	12,15,16,19	7,11,14,22	7,11,14,22	9,11,14,19	1845	5,9,12	7,10,11,17	7,8,10,16	11,12,17,20
1784	1,12,17	7,11,14,20	11,14,16,20	7,11,14,20	1846	9,11,12,16	9,11,14,16	7,10,16	11,12,17,19
1785	4,11	7,11,14,19	11,14,16,19	7,11,14,19	1847	5,7,12	9,10,18	10,11,14,16	7,11,14,18
1786	4,11,20	9,11,12,16	8,10,16,20	20,22	1848	4,12,15	9,10,18,22	9,10,18	9,12,15,22
1787	1,12,14	7,11,12,16	8,10,16,19	7,10,18	1849	7,11,12,16	9,10,18,19	7,8,16,20	10,11,17
1788	4,11,22	10,12,15	9,11,14,20	9,12,15,16	1850	3,7,11	9,10,18,20	10,11,17	9,11,16,17

Continued on next page

Table A.1 – continued from previous page

Rank	$\mathbf{w}_{C1}$ Tx's	$\mathbf{w}_{G1}$ Tx's	$\mathbf{w}_{C2}$ Tx's	$\mathbf{w}_{G2}$ Tx's	Rank	$\mathbf{w}_{C1}$ Tx's	$\mathbf{w}_{G1}$ Tx's	$\mathbf{w}_{C2}$ Tx's	$\mathbf{w}_{G2}$ Tx's
1851	1,12,22	7,11,14,16	9,11,14,18	9,12,15,20	1913	5,12,13	7,9,16,22	1,10,12	8,9,10,16
1852	1,12,20	11,12,17,18	7,8,16,19	9,12,15,19	1914	3,9,12	8,9,10,16	1,11,14	8,9,12,15
1853	4,12,18	8,9,11,17	7,11,14,18	7,11,16,17	1915	7,8,16	8,9,12,15	7,12,14,20	7,12,15
1854	1,12	10,11,14,16	19,22	8,9,11,17	1916	7,8,16,20	7,8,12,15	7,12,14,19	7,8,12,15
1855	1,12,19	9,11,17	8,9,11,17	7,8,11,17	1917	7,8,16,19	7,12,15	10,12,14,22	9,10,16
1856	5,11,17	9,11,17,22	11,12,17,22	10,11,14,18	1918	4,8,9	7,12,15,20	10,12,14,20	8,10,12,15
1857	5,11,13	9,11,17,20	9,11,16,17	7,10,16,22	1919	9,12,15,18	7,12,15,19	9,10,12,15	7,12,15,22
1858	5,8,11	9,11,17,19	7,8,11,17	8,10,11,17	1920	9,11,12,17	7,12,15,22	10,12,14,19	7,12,15,20
1859	6,11,12	7,8,11,17	7,11,16,17	7,10,16,20	1921	7,11,12,17	8,10,12,15	7,10,12,15	7,12,15,19
1860	5,11,14	7,11,17	9,12,15,22	7,10,16,19	1922	4,7,8	9,10,16	7,8,9,16	9,10,16,22
1861	3,10,11	7,11,17,22	10,11,14,18	9,10,18,22	1923	7,12,15,18	9,10,16,20	7,9,16	9,10,16,20
1862	5,10,12	7,11,17,20	11,12,17,20	9,10,18,20	1924	7,9,11,14	9,10,16,19	8,9,12,15	9,10,16,19
1863	2,7,11	7,11,17,19	8,10,11,17	9,10,18,19	1925	4,9,14	9,10,16,22	8,9,10,16	7,9,10,18
1864	4,12,14	8,10,11,17	11,12,17,19	9,11,17,22	1926	3,11,14	20	7,9,16,22	9,11,12,14
1865	5,11,15	10,11,17	9,12,15,20	9,11,17,20	1927	10,11,12,17	7,9,10,18	7,8,12,15	7,11,12,14
1866	4,12,22	10,11,17,22	9,12,15,19	7,11,17,22	1928	11,12,14,16	9,11,12,14	7,9,16,20	7,12,16,18
1867	4,12	10,11,17,20	7,10,16,22	9,11,17,19	1929	9,10,11,14	7,11,12,14	7,12,15	7,8,9,18
1868	4,12,20	10,11,17,19	9,10,18,22	7,11,17,20	1930	10,12,15,18	4,11,13	7,9,16,19	7,9,18
1869	4,12,19	9,11,14,18	4,7,11	7,11,17,19	1931	1,7,8	4,11	4,10,11	7,9,18,22
1870	4,12,16	7,11,14,18	7,10,16,20	10,11,17,22	1932	4,7,13	4,11,17	9,10,16	7,9,18,20
1871	10,12,15	9,11,16,17	7,10,16,19	10,11,17,20	1933	11,12,14,15	4,13,17	8,10,12,15	7,9,18,19
1872	10,12,15,20	7,11,16,17	9,11,17,22	10,11,17,19	1934	7,10,11,14	4,17	7,12,15,22	8,9,10,18
1873	10,12,15,19	10,11,14,18	9,10,18,20	11,12,14	1935	4,9,17	4,14,17	7,12,15,20	7,8,10,18
1874	10,12,15,22	9,12,16,18	9,10,18,19	9,12,16,18	1936	5,7,9	4,13,14	7,12,15,19	19,20
1875	5,11,16	10,11,12,14	7,11,17,22	10,11,12,14	1937	5,9,10	4,14	9,10,16,22	7,9,12,14
1876	5,11,18	8,11,12,14	1,8,11	11,12,16,18	1938	8,11,12,17	4,11,14	9,10,16,20	20
1877	5,11,22	9,10,12,14	10,11,17,22	9,10,12,14	1939	3,10,12	4,12,17	9,10,16,19	4,13
1878	5,11,20	11,12,16,18	9,11,17,20	7,9,12,17	1940	5,12,17	4,12,14	9,11,12,14	4,11,13
1879	5,11	11,12,14	9,11,17,19	7,10,12,14	1941	11,12,17	4,12,13	7,9,10,18	4,11
1880	5,11,19	11,12,14,22	7,11,17,20	7,9,10,16	1942	4,9,15	4,11,12	7,11,12,14	4,13,17
1881	2,10,11	11,12,14,20	7,11,17,19	8,11,12,14	1943	11,12,17,22	4,12	7,12,16,18	4,17
1882	2,9,11	11,12,14,19	10,11,12,14	9,10,12,17	1944	11,12,17,20	4,14,15	1,11,18	4,11,17
1883	1,7,13	7,10,12,14	10,11,17,20	9,12,14	1945	11,12,17,19	4,15,17	1,11,16	4,13,14
1884	7,10,18	7,9,12,17	10,11,17,19	7,10,12,17	1946	9,12,15	4,13,15	7,8,9,18	4,14,17
1885	7,10,18,22	7,9,10,16	11,12,14	7,12,14	1947	8,9,11,14	4,12,15	7,9,18	4,14
1886	7,10,18,20	9,10,12,17	9,12,16,18	7,9,12,18	1948	9,12,15,20	4,15	7,9,18,22	4,11,14
1887	7,10,18,19	7,8,16,22	1,11,17	11,12,14,22	1949	9,12,15,19	4,11,15	7,9,18,20	4,12,13
1888	9,12,15,16	7,10,12,17	11,12,16,18	11,12,14,20	1950	9,12,15,22	4,13	7,9,18,19	4,12,17
1889	9,12,14,16	8,9,12,14	9,10,12,14	11,12,14,19	1951	5,12,18	4,18	8,9,10,18	4,12,14
1890	7,12,15,16	9,12,14	8,11,12,14	8,9,12,14	1952	7,8,10,16	4,15,18	7,8,10,18	4,11,12
1891	9,10,12,18	9,12,14,22	7,9,12,17	7,8,12,14	1953	4,7,17	4,17,18	1,11,15	4,12
1892	1,9,13	9,12,14,20	7,10,12,14	10,12,14	1954	7,8,11,14	4,11,18	19,20	4,13,15
1893	5,8,12	9,12,14,19	9,10,12,17	7,8,16,22	1955	1,9,17	4,12,18	7,9,12,14	4,15,17
1894	4,9,13	7,8,12,14	7,9,10,16	8,10,12,14	1956	11,12,14,18	4,14,18	1,11	4,14,15
1895	10,12,15,16	7,12,14	9,12,14	9,12,14,22	1957	3,11,15	4,13,18	1,11,22	4,15
1896	8,11,17	7,12,14,22	7,10,12,17	9,12,14,20	1958	4,9,18	4,9,18	1,11,20	4,11,15
1897	8,11,17,22	7,12,14,20	7,12,14	9,12,14,19	1959	3,11,18	4,9,13	1,11,19	4,12,15
1898	8,11,17,20	7,12,14,19	8,9,12,14	7,10,12,18	1960	2,9,12	4,9,12	4,11,13	4,17,18
1899	8,11,17,19	7,9,12,18	11,12,14,22	7,9,12,15	1961	11,12,16,17	4,9,14	5,11,12	4,15,18
1900	6,9,11	8,10,12,14	7,9,12,18	7,12,14,22	1962	7,9,11,17	4,9,15	4,8,11	4,14,18
1901	6,7,11	10,12,14	7,8,12,14	7,12,14,20	1963	6,10,11	4,9,17	4,7,12	4,13,18
1902	3,11,13	10,12,14,22	10,12,14	7,12,14,19	1964	11,12,15,17	4,9,11	4,9,12	4,18
1903	9,11,12,18	10,12,14,20	11,12,14,20	10,12,14,22	1965	1,9,14	4,9	4,11,17	4,11,18
1904	3,8,11	10,12,14,19	11,12,14,19	10,12,14,20	1966	4,9,16	4,7,17	4,11,14	4,12,18
1905	7,11,12,18	7,10,12,18	8,10,12,14	10,12,14,19	1967	4,10,13	4,7,12	1,7,9	4,9,13
1906	3,7,12	7,9,12,15	7,8,16,22	9,10,12,15	1968	9,10,11,17	4,7,11	4,10,12	4,9,17
1907	8,12,15,16	7,8,9,16	9,12,14,22	7,10,12,15	1969	7,10,16	4,7,15	1,12,13	4,9,14
1908	10,12,16,18	9,10,12,15	7,10,12,18	7,8,9,16	1970	7,10,16,22	4,7,9	1,8,12	4,9,15
1909	1,8,9	7,10,12,15	7,9,12,15	7,9,16	1971	7,10,16,20	4,7	4,11,18	4,9,18
1910	10,11,12,18	7,9,16	7,12,14,22	7,9,16,22	1972	7,10,16,19	4,7,14	4,11,15	4,9,11
1911	3,11,17	7,9,16,20	9,12,14,20	7,9,16,20	1973	4,7,14	4,7,18	5,7,11	4,9,12
1912	5,12,14	7,9,16,19	9,12,14,19	7,9,16,19	1974	5,12,16	4,7,13	3,11,12	4,9

Continued on next page

Table A.1 – continued from previous page

Rank	w_{C1} Tx's	w_{G1} Tx's	w_{C2} Tx's	w_{G2} Tx's	Rank	w_{C1} Tx's	w_{G1} Tx's	w_{C2} Tx's	w_{G2} Tx's
1975	5,12,15	4,16	4,11,16	4,7,17	2037	4,9,22	4,14,19	3,7,12	4,11,20
1976	7,10,11,17	4,13,16	1,9,10	4,7,15	2038	4,7,15	4,17,19	1,8,9	4,13,20
1977	3,11,16	4,11,16	5,9,11	4,7,14	2039	1,8,10	4,18,19	3,11,17	4,20,22
1978	9,11,14,16	4,9,16	4,11,19	4,7,11	2040	6,11,13	4,15,19	5,12,13	4,9,20
1979	9,10,18	4,7,16	4,11	4,7,18	2041	6,8,11	4,12,19	5,12,14	4,12,20
1980	9,10,18,22	4,12,16	1,12,17	4,7,12	2042	6,11,17	4,7,19	3,9,12	4,7,20
1981	9,10,18,20	4,16,17	4,11,20	4,7,9	2043	6,11,14	4,9,19	4,8,9	4,10,20
1982	9,10,18,19	4,14,16	1,12,14	4,7	2044	6,9,12	4,19	4,7,8	4,20
1983	7,11,14,16	4,15,16	2,11,12	4,7,13	2045	5,9,13	4,16,19	4,9,14	4,8,20
1984	4,8,10	4,16,18	4,11,22	4,13,16	2046	6,7,12	4,19,22	3,11,14	4,17,19
1985	5,7,10	4,10,18	5,10,11	4,16,17	2047	3,7,9	4,10,19	1,7,8	4,14,19
1986	11,12,17,18	4,10,17	1,12,15	4,14,16	2048	2,11,15	4,11,19	4,7,13	4,15,19
1987	8,9,11,17	4,10,11	4,8,12	4,16	2049	6,10,12	4,13,19	4,9,17	4,18,19
1988	1,9,15	4,10,15	1,7,10	4,15,16	2050	5,8,9	4	5,7,9	4,16,19
1989	2,7,12	4,10,12	4,12,13	4,11,16	2051	2,11,18	1,4	5,9,10	4,19,20
1990	10,11,14,16	4,9,10	1,12,16	4,9,16	2052	4,10,15	5,11,13	3,10,12	4,13,19
1991	9,11,17	4,7,10	1,12,18	4,12,16	2053	4,7,22	5,11	5,12,17	4,11,19
1992	9,11,17,22	4,10,14	4,7,9	4,7,16	2054	5,7,8	5,11,17	4,9,15	4,19,22
1993	7,8,11,17	4,10,13	4,12,17	4,16,18	2055	9,12,16,18	5,13,17	5,12,18	4,12,19
1994	9,11,17,20	4,10	3,9,11	4,10,17	2056	2,11,16	5,17	4,7,17	4,9,19
1995	9,11,17,19	4,10,16	4,9,10	4,10,13	2057	10,11,12,14	5,14,17	1,9,17	4,7,19
1996	3,11,22	4,8,17	4,7,10	4,10,14	2058	4,7,20	5,14	3,11,15	4,10,19
1997	3,11,20	4,8,18	5,9,12	4,10,15	2059	1,9,19	5,11,14	4,9,18	4,8,19
1998	3,11,19	4,8,11	4,12,15	4,10,18	2060	3,9,10	5,13,14	3,11,18	4,19
1999	3,11	4,8,12	5,7,12	4,10,11	2061	4,7	5,12,17	2,9,12	5,13
2000	7,11,17	4,8,9	3,7,11	4,10,16	2062	4,7,19	5,11,12	6,10,11	5,11,13
2001	7,11,17,22	4,8,15	1,12,22	4,10,12	2063	1,9,20	5,12,14	1,9,14	5,11
2002	7,11,17,20	4,8,13	1,12,20	4,9,10	2064	6,11,18	5,12,13	4,9,16	5,13,17
2003	7,11,17,19	4,8,16	4,12,18	4,7,10	2065	1,9	5,12	4,10,13	5,17
2004	1,10,13	4,8,14	1,12	4,10	2066	6,11,15	5,15	4,7,14	5,11,17
2005	8,10,11,17	4,8,10	1,12,19	4	2067	1,7,15	5,15,17	5,12,16	5,14,17
2006	10,11,17	4,8	5,11,17	1,4	2068	6,11,16	5,13,15	5,12,15	5,14
2007	10,11,17,22	4,7,8	5,11,13	4,8,13	2069	5,7,13	5,12,15	3,11,16	5,11,14
2008	2,11,13	4,13,22	5,8,11	4,8,17	2070	4,10,18	5,14,15	4,8,10	5,13,14
2009	10,11,17,20	4,18,22	6,11,12	4,8,14	2071	3,12,14	5,11,15	5,7,10	5,12,13
2010	10,11,17,19	4,17,22	5,11,14	4,8,15	2072	2,11,20	5,13	1,9,15	5,12,17
2011	9,11,14,18	4,11,22	3,10,11	4,8,18	2073	2,11,19	5,17,18	2,7,12	5,12,14
2012	4,7,18	4,12,22	5,10,12	4,8,11	2074	2,11	5,11,18	3,11	5,11,12
2013	7,11,14,18	4,14,22	2,7,11	4,8,16	2075	5,7,17	5,13,18	3,11,22	5,12
2014	9,11,16,17	4,15,22	4,12,14	4,8,9	2076	4,10,16	5,15,18	3,11,20	5,15,17
2015	2,8,11	4,9,22	5,11,15	4,8,12	2077	3,12,15	5,14,18	3,11,19	5,13,15
2016	2,11,17	4,10,22	4,12,22	4,7,8	2078	8,11,12,14	5,12,18	1,10,13	5,15
2017	7,11,16,17	4,7,22	4,12	4,8,10	2079	2,11,22	5,18	2,11,13	5,14,15
2018	1,9,18	4,22	4,12,20	4,8	2080	9,10,12,14	5,9,13	4,7,18	5,12,15
2019	5,12,22	4,16,22	4,12,19	4,13,22	2081	5,9,17	5,9,15	2,11,17	5,11,15
2020	5,12,20	4,8,22	4,12,16	4,17,22	2082	11,12,16,18	5,9,18	2,8,11	5,17,18
2021	5,12	4,15,20	5,11,16	4,14,22	2083	4,8,13	5,9,14	1,9,18	5,13,18
2022	5,12,19	4,11,20	5,11,18	4,15,22	2084	11,12,14	5,9,17	5,12,22	5,15,18
2023	2,11,14	4,14,20	5,11,22	4,18,22	2085	11,12,14,22	5,9,12	5,12,20	5,14,18
2024	10,11,14,18	4,20	5,11	4,16,22	2086	11,12,14,20	5,9,11	5,12	5,11,18
2025	4,10,17	4,18,20	5,11,20	4,11,22	2087	11,12,14,19	5,9	2,11,14	5,12,18
2026	1,7,17	4,9,20	5,11,19	4,12,22	2088	5,9,14	5,7,14	5,12,19	5,18
2027	4,9,19	4,16,20	2,10,11	4,9,22	2089	6,11,22	5,7,15	4,10,17	5,9,13
2028	1,9,16	4,20,22	2,9,11	4,7,22	2090	6,11,20	5,7,13	1,7,17	5,9,17
2029	4,9,20	4,7,20	1,7,13	4,10,22	2091	1,9,22	5,7,9	4,9,19	5,9,14
2030	2,10,12	4,17,20	1,9,13	4,22	2092	6,11	5,7,11	1,9,16	5,9,15
2031	1,7,14	4,12,20	5,8,12	4,8,22	2093	6,11,19	5,7,12	4,9,20	5,9,18
2032	4,7,16	4,13,20	4,9,13	4,14,20	2094	3,7,10	5,7	1,7,14	5,9,11
2033	4,9	4,10,20	6,9,11	4,15,20	2095	7,10,12,14	5,7,18	2,10,12	5,9,12
2034	3,12,13	4,8,20	6,7,11	4,17,20	2096	3,12,18	5,7,17	4,7,16	5,9
2035	3,8,12	4,19,20	3,11,13	4,18,20	2097	5,10,13	5,11,16	4,9	5,7,13
2036	4,10,14	4,8,19	3,8,11	4,16,20	2098	7,9,12,17	5,9,16	3,12,13	5,7,14

Continued on next page

Table A.1 – continued from previous page

Rank	w_{C1} Tx's	w_{G1} Tx's	w_{C2} Tx's	w_{G2} Tx's	Rank	w_{C1} Tx's	w_{G1} Tx's	w_{C2} Tx's	w_{G2} Tx's
2099	1,7,18	5,7,16	3,8,12	5,7,15	2161	3,7,8	5,7,19	1,10,14	5,11,20
2100	7,9,10,16	5,13,16	4,10,14	5,7,11	2162	2,9,10	5,19,20	3,12	5,20,22
2101	5,9,15	5,16,18	4,7,15	5,7,18	2163	7,10,12,18	5,10,19	4,10	5,12,20
2102	3,12,17	5,16,17	4,9,22	5,7,17	2164	5,7,22	5,11,19	4,10,19	5,9,20
2103	2,12,13	5,12,16	1,8,10	5,7,9	2165	6,12,15	5,9,19	4,10,20	5,7,20
2104	5,8,10	5,16	6,11,13	5,7,12	2166	6,12,14	5,19,22	3,12,19	5,10,20
2105	9,10,12,17	5,14,16	6,8,11	5,7	2167	1,10,15	5,15,19	4,10,22	5,8,20
2106	3,12,16	5,15,16	6,11,17	5,13,16	2168	5,7,16	5,19	6,12,13	5,20
2107	5,7,14	5,10,14	6,11,14	5,16,17	2169	5,10,18	5,12,19	3,12,20	5,13,19
2108	3,12,22	5,10,17	6,9,12	5,16,18	2170	5,9,22	5,8,19	4,13,17	5,17,19
2109	7,8,16,22	5,10,15	5,9,13	5,14,16	2171	5,10,15	5,16,19	4,13,14	5,14,19
2110	1,7,16	5,10,16	6,7,12	5,15,16	2172	6,9,10	7,12,16,18	5,7,18	5,18,19
2111	7,10,12,17	5,10,18	3,7,9	5,16	2173	5,7,20	4,5	5,9,18	5,15,19
2112	8,9,12,14	5,9,10	2,11,15	5,11,16	2174	5,7	5	5,10,17	5,19,20
2113	1,10,14	5,10,12	6,10,12	5,9,16	2175	5,7,19	1,5	6,8,12	5,11,19
2114	3,12	5,7,10	5,8,9	5,12,16	2176	1,7,22	3,11,13	2,8,12	5,19,22
2115	4,10	5,10,11	2,11,18	5,7,16	2177	7,9,12,15	3,11	5,9,16	5,9,19
2116	4,10,19	5,10,13	4,10,15	5,10,17	2178	6,12,18	3,11,17	4,8,17	5,12,19
2117	4,10,20	5,10	4,7,22	5,10,13	2179	4,13,18	3,13,17	1,10,17	5,7,19
2118	3,12,19	5,8,16	5,7,8	5,10,14	2180	1,10,18	3,17	3,9,13	5,10,19
2119	4,10,22	5,8,11	2,11,16	5,10,15	2181	6,7,10	3,14	5,7,15	5,19
2120	9,12,14	5,8,14	4,7,20	5,10,18	2182	3,7,17	3,14,17	2,12,17	5,8,19
2121	9,12,14,22	5,8,17	1,9,19	5,10,16	2183	5,10,16	3,11,14	6,7,9	5,16,19
2122	9,12,14,20	5,8,9	3,9,10	5,10,11	2184	3,9,14	3,13,14	6,12,17	3,13
2123	9,12,14,19	5,8,12	4,7	5,9,10	2185	6,12,16	3,11,12	5,10,14	3,11,13
2124	7,8,12,14	5,8,18	4,7,19	5,10,12	2186	1,7	3,12,17	5,9	3,11
2125	3,12,20	5,8,13	1,9,20	5,7,10	2187	3,9,17	3,12,13	5,9,19	3,13,17
2126	6,12,13	5,8,10	6,11,18	5,10	2188	3,8,9	3,12	4,8,14	3,17
2127	4,13,17	5,8	1,9	4,5	2189	1,7,20	3,12,14	2,12,14	3,11,17
2128	7,12,14	5,7,8	6,11,15	5,8,13	2190	1,7,19	3,11,15	4,13,15	3,14
2129	7,12,14,22	5,8,15	1,7,15	5,8,17	2191	2,12,15	3,13,15	5,9,20	3,14,17
2130	7,12,14,20	5,13,22	6,11,16	5,8,14	2192	3,10,13	3,12,15	2,7,9	3,13,14
2131	7,12,14,19	5,9,22	5,7,13	5,8,18	2193	2,7,10	3,14,15	3,7,13	3,11,14
2132	5,7,18	5,11,22	4,10,18	5,8,11	2194	3,7,14	3,15	3,7,8	3,12,13
2133	4,13,14	5,10,22	3,12,14	5,8,16	2195	7,8,9,16	3,15,17	2,9,10	3,12,17
2134	5,9,18	5,17,22	2,11,20	5,8,15	2196	4,8,15	3,13	6,12,14	3,12,14
2135	5,10,17	5,14,22	2,11,19	5,8,9	2197	9,10,12,15	3,14,18	6,12,15	3,11,12
2136	6,8,12	5,18,22	2,11	5,8,12	2198	4,13,16	3,11,18	5,7,22	3,12
2137	7,9,12,18	5,7,22	5,7,17	5,7,8	2199	4,14,17	3,12,18	1,10,15	3,13,15
2138	2,8,12	5,12,22	4,10,16	5,8,10	2200	2,12,18	3,17,18	5,7,16	3,14,15
2139	5,9,16	5,15,22	3,12,15	5,8	2201	6,12,22	3,13,18	5,10,18	3,15
2140	4,8,17	5,22	2,11,22	5	2202	1,10,16	3,18	5,9,22	3,15,17
2141	8,10,12,14	5,16,22	5,9,17	1,5	2203	6,12	3,15,18	5,10,15	3,11,15
2142	1,10,17	5,8,22	4,8,13	5,13,22	2204	6,12,20	3,9,11	6,9,10	3,12,15
2143	3,9,13	5,11,20	5,9,14	5,17,22	2205	7,10,12,15	3,9,15	5,7,20	3,14,18
2144	5,7,15	5,14,20	6,11	5,14,22	2206	6,12,19	3,9	5,7	3,17,18
2145	10,12,14	5,18,20	6,11,22	5,15,22	2207	5,10,22	3,9,17	5,7,19	3,13,18
2146	10,12,14,22	5,16,20	6,11,20	5,18,22	2208	3,9,15	3,9,14	1,7,22	3,15,18
2147	10,12,14,20	5,7,20	1,9,22	5,16,22	2209	3,9,18	3,9,12	4,13,18	3,18
2148	10,12,14,19	5,20,22	6,11,19	5,11,22	2210	5,10	3,9,18	6,12,18	3,11,18
2149	2,12,17	5,12,20	3,7,10	5,9,22	2211	3,8,10	3,9,13	1,10,18	3,12,18
2150	6,7,9	5,15,20	3,12,18	5,12,22	2212	5,10,20	3,7,14	6,7,10	3,9,17
2151	6,12,17	5,8,20	5,10,13	5,7,22	2213	5,10,19	3,7,11	3,7,17	3,9,14
2152	5,10,14	5,9,20	1,7,18	5,10,22	2214	4,8,18	3,7,18	5,10,16	3,9,15
2153	5,9,19	5,13,20	5,9,15	5,22	2215	2,12,16	3,7,17	3,9,14	3,9,18
2154	5,9	5,17,20	3,12,17	5,8,22	2216	5,8,13	3,7,9	6,12,16	3,9,11
2155	4,8,14	5,20	2,12,13	5,14,20	2217	4,8,16	3,7,12	3,9,17	3,9,13
2156	2,12,14	5,10,20	5,8,10	5,13,20	2218	3,7,15	3,7,13	1,7	3,9,12
2157	4,13,15	5,18,19	3,12,16	5,15,20	2219	3,9,16	3,7,15	3,8,9	3,9
2158	5,9,20	5,14,19	5,7,14	5,18,20	2220	2,12,22	3,7	1,7,20	3,7,13
2159	2,7,9	5,17,19	3,12,22	5,17,20	2221	3,7,18	3,16,18	1,7,19	3,7,17
2160	3,7,13	5,13,19	1,7,16	5,16,20	2222	4,15,17	3,16,17	2,12,15	3,7,14

Continued on next page

Table A.1 – continued from previous page

Rank	$\mathbf{w_{C1}}$ Tx's	$\mathbf{w_{G1}}$ Tx's	$\mathbf{w_{C2}}$ Tx's	$\mathbf{w_{G2}}$ Tx's	Rank	$\mathbf{w_{C1}}$ Tx's	$\mathbf{w_{G1}}$ Tx's	$\mathbf{w_{C2}}$ Tx's	$\mathbf{w_{G2}}$ Tx's
2223	7,9,16	3,16	3,10,13	3,7,18	2285	7,12,15	3,11,19	6,9,13	3,12,20
2224	7,9,16,20	3,14,16	2,7,10	3,7,15	2286	7,12,15,20	3,19,22	6,7,17	3,7,20
2225	7,9,16,19	3,7,16	3,7,14	3,7,11	2287	7,12,15,19	3,12,19	3,10,15	3,10,20
2226	7,9,16,22	3,13,16	4,8,15	3,7,9	2288	7,12,15,22	3,9,19	6,9,14	3,11,20
2227	4,14,15	3,15,16	4,13,16	3,7,12	2289	2,7,8	3,19	4,15,18	3,8,20
2228	4,17,18	3,11,16	4,14,17	3,7	2290	5,8,18	3,7,19	3,10,18	3,20
2229	1,8,13	3,12,16	2,12,18	3,16,17	2291	6,8,10	3,19,20	4,14,16	3,14,20
2230	3,10,17	3,9,16	6,12,22	3,14,16	2292	6,9,15	3,10,19	5,8,15	3,13,20
2231	2,12,19	3,10,14	1,10,16	3,16,18	2293	1,13,14	3,8,19	4,8,22	3,13,19
2232	2,12	3,10,13	6,12	3,13,16	2294	4,15,16	3,14,19	6,9,17	3,17,19
2233	2,12,20	3,10,16	6,12,20	3,15,16	2295	8,10,12,15	3,16,19	5,8,14	3,15,19
2234	5,13,17	3,10,15	6,12,19	3,16	2296	4,17,22	7,8,9,18	5,13,18	3,18,19
2235	5,13,14	3,9,10	5,10,22	3,11,16	2297	6,7,15	3,4	4,8,20	3,14,19
2236	3,9,19	3,10,17	3,9,15	3,12,16	2298	6,9,18	3,5	4,8	3,11,19
2237	3,9	3,10,18	3,9,18	3,9,16	2299	1,13,17	3	6,7,14	3,19,20
2238	3,9,20	3,10,12	5,10	3,7,16	2300	2,8,9	1,3	4,8,19	3,19,22
2239	3,9,22	3,7,10	3,8,10	3,10,13	2301	9,10,16	6,11,13	5,14,17	3,12,19
2240	4,13,20	3,10	5,10,20	3,10,17	2302	9,10,16,20	6,11	6,10,13	3,9,19
2241	3,10,14	3,10,11	5,10,19	3,10,14	2303	9,10,16,19	6,17	5,13,16	3,7,19
2242	4,14,18	3,8,15	4,8,18	3,10,15	2304	9,10,16,22	6,13,17	2,9,13	3,16,19
2243	4,13,19	3,8,18	2,12,16	3,10,18	2305	5,15,17	6,11,17	3,10,16	3,10,19
2244	4,13	3,8,14	5,8,13	3,10,16	2306	5,17,18	6,13,14	2,7,8	3,19
2245	6,8,9	3,8,11	4,8,16	3,10,11	2307	5,14,15	6,11,14	5,8,18	3,8,19
2246	3,7,22	3,8,17	3,7,15	3,9,10	2308	20	6,14,17	6,8,10	6,13
2247	8,9,10,16	3,8,9	3,9,16	3,10,12	2309	3,10,22	6,14	1,13,14	6,11,13
2248	6,7,13	3,8,13	2,12,22	3,7,10	2310	2,7,13	6,12,13	6,9,15	6,11
2249	8,9,12,15	3,8,12	3,7,18	3,10	2311	4,16,18	6,11,12	4,15,16	6,13,17
2250	3,7,20	3,8,16	4,15,17	3,4	2312	5,8,16	6,12,17	4,17,22	6,17
2251	5,8,17	3,7,8	4,14,15	3,8,13	2313	4,17,20	6,12,14	6,7,15	6,11,17
2252	4,16,17	3,8,10	4,17,18	3,8,17	2314	4,17,19	6,12	6,9,18	6,13,14
2253	1,10,22	3,8	3,10,17	3,8,14	2315	4,17	6,14,15	1,13,17	6,14,17
2254	4,13,22	3,15,22	1,8,13	3,8,15	2316	6,7,18	6,12,15	2,8,9	6,11,14
2255	1,10,19	3,17,22	2,12	3,8,18	2317	2,9,14	6,15,17	5,15,17	6,14
2256	5,13,15	3,13,22	2,12,19	3,8,11	2318	6,7,16	6,13,15	5,17,18	6,12,13
2257	1,10	3,11,22	5,13,17	3,8,16	2319	3,10	6,15	5,14,15	6,12,17
2258	1,10,20	3,12,22	2,12,20	3,8,9	2320	3,10,19	6,11,15	20	6,12,14
2259	3,7	3,7,22	5,13,14	3,8,12	2321	6,9,16	6,13	2,7,13	6,11,12
2260	3,7,16	3,10,22	3,9	3,7,8	2322	3,10,20	6,18	4,16,18	6,12
2261	7,8,12,15	3,8,22	3,9,19	3,8,10	2323	4,14,22	6,12,18	3,10,22	6,14,15
2262	3,7,19	3,14,22	3,9,20	3,8	2324	4,14,20	6,11,18	5,8,16	6,15,17
2263	6,7,8	3,22	3,9,22	3,5	2325	5,13,22	6,15,18	4,17,20	6,13,15
2264	6,9,13	3,9,22	4,13	3	2326	2,7,17	6,13,18	4,17,19	6,15
2265	6,7,17	3,16,22	4,14,18	1,3	2327	3,8,13	6,17,18	4,17	6,11,15
2266	3,10,15	3,18,22	3,10,14	3,13,22	2328	5,14,18	6,14,18	6,7,18	6,12,15
2267	6,9,14	3,16,20	4,13,20	3,17,22	2329	5,16,17	6,9,14	2,9,14	6,18
2268	4,15,18	3,20,22	4,13,19	3,15,22	2330	5,13,20	6,9,13	6,7,16	6,15,18
2269	3,10,18	3,7,20	6,8,9	3,14,22	2331	6,10,14	6,9,11	3,10	6,11,18
2270	5,8,15	3,20	3,7,22	3,11,22	2332	3,13,17	6,9,17	6,9,16	6,13,18
2271	4,14,16	3,9,20	6,7,13	3,12,22	2333	6,9	6,9,18	3,10,19	6,12,18
2272	4,8,22	3,8,20	3,7,20	3,9,22	2334	5,13,19	6,9	3,10,20	6,17,18
2273	5,8,14	3,10,20	5,8,17	3,16,22	2335	5,13	6,9,12	4,14,22	6,14,18
2274	6,9,17	3,18,20	4,16,17	3,7,22	2336	6,10,17	6,9,15	4,14,20	6,9,13
2275	5,13,18	3,15,20	1,10,22	3,10,22	2337	4,14	6,7,15	5,13,22	6,9,17
2276	4,8,20	3,17,20	4,13,22	3,18,22	2338	4,14,19	6,7,11	2,7,17	6,9,14
2277	4,8	3,12,20	1,10,19	3,22	2339	6,9,20	6,7,18	3,8,13	6,9,18
2278	6,7,14	3,11,20	5,13,15	3,8,22	2340	6,9,19	6,7,14	5,14,18	6,9,15
2279	4,8,19	3,14,20	1,10	3,15,20	2341	6,7,22	6,7,12	5,16,17	6,9,11
2280	5,14,17	3,13,20	1,10,20	3,16,20	2342	2,10,13	6,7,9	5,13,20	6,9,12
2281	6,10,13	3,15,19	3,7	3,18,20	2343	6,9,22	6,7,13	3,13,17	6,9
2282	5,13,16	3,18,19	3,7,16	3,17,20	2344	2,7,14	6,7	6,10,14	6,7,14
2283	2,9,13	3,13,19	3,7,19	3,20,22	2345	1,8,17	6,7,17	5,13	6,7,13
2284	3,10,16	3,17,19	6,7,8	3,9,20	2346	5,8,22	6,14,16	6,9	6,7,15

Continued on next page

Table A.1 – continued from previous page

Rank	$\mathbf{w}_{C1}$ Tx's	$\mathbf{w}_{G1}$ Tx's	$\mathbf{w}_{C2}$ Tx's	$\mathbf{w}_{G2}$ Tx's	Rank	$\mathbf{w}_{C1}$ Tx's	$\mathbf{w}_{G1}$ Tx's	$\mathbf{w}_{C2}$ Tx's	$\mathbf{w}_{G2}$ Tx's
2347	2,9,17	6,13,16	4,14	6,7,18	2409	2,10,14	6,14,19	2,10,17	6,16,20
2348	6,7,20	6,16	5,13,19	6,7,11	2410	2,9	6,13,19	5,15,22	6,15,20
2349	5,14,16	6,15,16	6,10,17	6,7,17	2411	3,15,17	6,10,19	3,8,18	6,11,20
2350	6,7	6,9,16	4,14,19	6,7,12	2412	6,13,17	6,18,19	6,8,13	6,12,20
2351	6,7,19	6,16,18	6,9,20	6,7,9	2413	2,9,19	6,19,20	6,10	6,20,22
2352	5,15,18	6,11,16	6,9,19	6,7	2414	5,15,20	6,15,19	6,10,20	6,9,20
2353	4,15,22	6,16,17	6,7,22	6,13,16	2415	2,9,20	6,7,19	6,10,19	6,7,20
2354	3,13,14	6,7,16	2,10,13	6,14,16	2416	3,17,18	6,17,19	4,16	6,10,20
2355	3,8,17	6,12,16	2,7,14	6,15,16	2417	3,8,16	6,19	4,16,19	6,8,20
2356	4,15,20	6,10,13	6,9,22	6,16,17	2418	5,15,19	6,19,22	1,8,14	6,20
2357	5,8,20	6,10,16	1,8,17	6,16,18	2419	5,15	6,12,19	1,8,15	6,13,19
2358	5,8,19	6,10,17	2,9,17	6,16	2420	3,14,15	6,16,19	2,9,22	6,14,19
2359	6,10,15	6,10,11	5,8,22	6,11,16	2421	1,13,16	4,6	2,10,14	6,17,19
2360	5,8	6,10,12	6,7,20	6,9,16	2422	5,18,22	5,6	2,9	6,15,19
2361	6,10,18	6,9,10	5,14,16	6,7,16	2423	6,13,14	3,6	6,13,17	6,18,19
2362	4,15,19	6,10,18	6,7	6,12,16	2424	5,18,20	6	3,15,17	6,11,19
2363	1,13,15	6,10,14	5,15,18	6,10,13	2425	2,7,20	2,6	2,9,19	6,19,20
2364	2,9,15	6,7,10	6,7,19	6,10,17	2426	2,7,19	1,6	5,15,20	6,19,22
2365	4,15	6,10	4,15,22	6,10,14	2427	2,7	7,9,18	3,17,18	6,9,19
2366	2,8,10	6,10,15	3,13,14	6,10,18	2428	2,7,22	7,9,18,22	2,9,20	6,7,19
2367	4,18,22	6,8,15	3,8,17	6,10,15	2429	3,13,22	7,9,18,20	3,8,16	6,10,19
2368	2,7,18	6,8,14	4,15,20	6,10,16	2430	5,18,19	7,9,18,19	5,15,19	6,16,19
2369	5,17,22	6,8,18	5,8,20	6,10,11	2431	5,18	8,9,10,18	5,15	6,19
2370	3,13,15	6,8,9	6,10,15	6,10,12	2432	3,16,17	7,8,10,18	3,14,15	6,8,19
2371	2,9,18	6,7,8	5,8,19	6,9,10	2433	3,13,20	2,3	1,13,16	6,12,19
2372	2,9,16	6,8,10	5,8	6,7,10	2434	3,13,19	2,11	5,18,22	2,3
2373	5,15,16	6,8,16	6,10,18	6,10	2435	3,13	2,11,13	6,13,14	2,13
2374	1,13,18	6,8,12	1,13,15	4,6	2436	6,8,17	2,17	5,18,20	2,11
2375	5,17,20	6,8,11	4,15,19	6,8,14	2437	3,14,18	2,13,17	2,7,20	2,11,13
2376	3,13,18	6,8	2,9,15	6,8,15	2438	6,8,14	2,11,17	2,7,19	2,13,17
2377	2,7,15	6,8,17	4,15	6,8,18	2439	5,16,22	2,14,17	2,7	2,17
2378	5,17,19	6,8,13	2,8,10	6,8,16	2440	2,10,18	2,11,14	2,7,22	2,11,17
2379	5,17	6,18,22	2,7,18	6,8,11	2441	7,9,10,18	2,14	3,13,22	2,14,17
2380	3,8,15	6,9,22	4,18,22	6,8,17	2442	3,8,22	2,13,14	5,18,19	2,14
2381	5,14,22	6,7,22	5,17,22	6,8,9	2443	2,10,15	2,12,13	5,18	2,11,14
2382	3,8,14	6,22	3,13,15	6,8,12	2444	3,14,16	2,12,17	3,13	2,13,14
2383	4,18,20	6,12,22	2,9,18	6,7,8	2445	6,13,15	2,11,12	3,16,17	2,12,13
2384	4,18,19	6,8,22	2,9,16	6,8,10	2446	6,13,18	2,12	3,13,20	2,12,17
2385	5,16,18	6,13,22	5,15,16	6,8	2447	5,16,20	2,12,14	3,13,19	2,11,12
2386	4,18	6,10,22	1,13,18	6,8,13	2448	5,16	2,15,17	6,8,17	2,12,14
2387	3,14,17	6,11,22	3,13,18	5,6	2449	5,16,19	2,14,15	3,14,18	2,12
2388	4,16,22	6,16,22	5,17,20	3,6	2450	3,8,20	2,15	6,8,14	2,15,17
2389	3,13,16	6,17,22	2,7,15	6	2451	3,8	2,11,15	5,16,22	2,14,15
2390	5,14,20	6,14,22	5,17	2,6	2452	3,8,19	2,13,15	2,10,18	2,15
2391	6,10,16	6,15,22	5,17,19	1,6	2453	4,20,22	2,12,15	3,8,22	2,13,15
2392	5,14,19	6,14,20	3,8,15	6,13,22	2454	3,15,18	2,13	2,10,15	2,11,15
2393	6,10,22	6,17,20	5,14,22	6,18,22	2455	9,11,12,14	2,12,18	3,14,16	2,12,15
2394	4,16,20	6,7,20	3,8,14	6,16,22	2456	6,8,15	2,13,18	6,13,15	2,13,18
2395	5,14	6,10,20	4,18,20	6,17,22	2457	4,19,22	2,11,18	6,13,18	2,14,18
2396	2,7,16	6,12,20	4,18,19	6,11,22	2458	1,8,18	2,14,18	5,16,20	2,17,18
2397	2,10,17	6,16,20	5,16,18	6,14,22	2459	4,22	2,17,18	5,16	2,11,18
2398	5,15,22	6,11,20	4,18	6,12,22	2460	6,14,17	2,15,18	5,16,19	2,12,18
2399	3,8,18	6,9,20	3,14,17	6,9,22	2461	7,11,12,14	2,18	3,8,20	2,15,18
2400	6,8,13	6,18,20	4,16,22	6,7,22	2462	3,15,16	2,9,13	3,8	2,18
2401	6,10	6,8,20	3,13,16	6,10,22	2463	2,10,16	2,9,18	3,8,19	2,9,13
2402	6,10,20	6,13,20	5,14,20	6,15,22	2464	3,17,22	2,9,14	4,20,22	2,9,17
2403	6,10,19	6,20,22	6,10,16	6,22	2465	4,19,20	2,9	3,15,18	2,9,14
2404	4,16	6,15,20	5,14,19	6,8,22	2466	4,20	2,9,17	6,8,15	2,9,18
2405	4,16,19	6,20	6,10,22	6,17,20	2467	1,14,17	2,9,11	4,19,22	2,9,11
2406	1,8,14	6,11,19	4,16,20	6,13,20	2468	6,13,16	2,9,12	1,8,18	2,9,15
2407	1,8,15	6,9,19	5,14	6,14,20	2469	6,8,18	2,9,15	4,22	2,9,12
2408	2,9,22	6,8,19	2,7,16	6,18,20	2470	3,17,20	2,7,18	6,14,17	2,9

Continued on next page

Table A.1 – continued from previous page

Rank	w_{C1} Tx's	w_{G1} Tx's	w_{C2} Tx's	w_{G2} Tx's	Rank	w_{C1} Tx's	w_{G1} Tx's	w_{C2} Tx's	w_{G2} Tx's
2471	3,17,19	2,7,13	3,15,16	2,7,13	2533	2,13,14	2,12,20	6,17,20	2,17,20
2472	4,19	2,7,14	2,10,16	2,7,14	2534	6,16,18	2,9,20	3,16,22	2,16,20
2473	3,17	2,7,15	3,17,22	2,7,15	2535	1,17,18	2,11,20	6,17	2,11,20
2474	6,8,16	2,7,9	4,19,20	2,7,17	2536	1,13,19	2,20	3,16,20	2,20,22
2475	3,16,18	2,7,11	4,20	2,7,18	2537	3,16	2,16,20	6,17,19	2,12,20
2476	6,15,17	2,7,12	1,14,17	2,7,11	2538	6,14,20	2,18,20	3,16,19	2,9,20
2477	3,14,22	2,7,17	6,13,16	2,7,9	2539	1,13	2,18,19	6,14,22	2,7,20
2478	6,14,15	2,7	6,8,18	2,7,12	2540	6,14,19	2,15,19	3,4	2,10,20
2479	1,8,16	2,16,17	3,17,20	2,7	2541	6,14	2,19,22	2,13,14	2,8,20
2480	5,20,22	2,14,16	3,17,19	2,16,17	2542	3,4	2,19	1,13,20	2,20
2481	4	2,12,16	4,19	2,14,16	2543	3,5	2,8,19	6,16,18	2,18,20
2482	3,14,20	2,7,16	3,17	2,15,16	2544	1,14,18	2,14,19	1,17,18	2,13,19
2483	3,14,19	2,15,16	4	2,13,16	2545	6,15,22	2,9,19	1,13,19	2,14,19
2484	6,17,18	2,13,16	6,8,16	2,16,18	2546	2,13,15	2,13,19	3,16	2,15,19
2485	5,19,22	2,16	6,15,17	2,16	2547	2,8,14	2,16,19	1,13	2,17,19
2486	3,14	2,9,16	3,16,18	2,11,16	2548	6,15,20	2,12,19	6,14	2,18,19
2487	5,22	2,16,18	3,14,22	2,12,16	2549	6,15,19	2,17,19	6,14,20	2,16,19
2488	6,16,17	2,11,16	6,14,15	2,9,16	2550	6,15	2,11,19	6,14,19	2,11,19
2489	6,13,22	2,10,18	1,8,16	2,7,16	2551	4,6	2,10,19	3,5	2,19,22
2490	6,13,19	2,9,10	5,20,22	2,10,14	2552	6,18,22	2,7,19	1,14,18	2,12,19
2491	6,13	2,10,12	3,14,20	2,10,15	2553	2,8,17	2,19,20	6,15,22	2,9,19
2492	6,13,20	2,10,11	6,17,18	2,10,18	2554	3,20,22	2,4	2,13,15	2,19,20
2493	5,19,20	2,10,16	3,14,19	2,10,17	2555	3,19,22	2,5	4,6	2,7,19
2494	6,14,18	2,10,15	3,14	2,10,11	2556	3,22	2	2,8,14	2,10,19
2495	5,20	2,10,14	5,19,22	2,10,16	2557	6,18,20	1,2	6,15,20	2,19
2496	4,5	2,10	5,22	2,9,10	2558	1,8,22	7,9,12,14	6,15	2,8,19
2497	5,19	2,10,17	6,16,17	2,10,12	2559	6,18	1,11,13	6,15,19	1,13
2498	2,10,22	2,7,10	4,5	2,7,10	2560	6,18,19	1,11	6,18,22	1,11,13
2499	3,15,22	2,10,13	6,13,22	2,10,13	2561	5,6	1,17	2,8,17	1,11
2500	7,12,16,18	2,8,18	6,13	2,10	2562	3,19,20	1,13,17	3,20,22	1,13,17
2501	6,8,22	2,8,16	6,13,19	2,4	2563	6,16,22	1,11,17	5,6	1,17
2502	2,8,13	2,8,13	6,13,20	2,8,13	2564	3,20	1,11,14	3,19,22	1,11,17
2503	3,15,20	2,8,17	6,14,18	2,8,17	2565	1,16,17	1,13,14	3,22	1,13,14
2504	5	2,7,8	5,19,20	2,8,15	2566	3,19	1,14,17	6,18,20	1,14,17
2505	3,15,19	2,8,12	5,20	2,8,18	2567	2,13,18	1,14	1,8,22	1,11,14
2506	3,15	2,8,9	5,19	2,8,16	2568	7,8,9,18	1,12,17	6,18	1,14
2507	3,18,22	2,8,10	5	2,8,14	2569	6,16,20	1,12,13	6,18,19	1,12,13
2508	2,10	2,8,15	2,10,22	2,8,11	2570	1,14,16	1,12,14	3,19,20	1,12,17
2509	6,8,20	2,8	3,15,22	2,8,9	2571	6,16,19	1,11,12	6,16,22	1,12,14
2510	2,10,19	2,8,11	6,8,22	2,8,12	2572	6,16	1,12	1,16,17	1,11,12
2511	2,10,20	2,8,14	2,8,13	2,7,8	2573	3	1,12,15	3,20	1,12
2512	6,8	2,18,22	3,15,20	2,8,10	2574	2,14,17	1,15,17	3,19	1,15,17
2513	6,8,19	2,14,22	3,15,19	2,8	2575	2,8,15	1,13,15	3	1,13,15
2514	1,15,17	2,13,22	3,15	2,5	2576	2,8,18	1,11,15	2,13,18	1,14,15
2515	6,14,16	2,11,22	3,18,22	2,13,22	2577	2,13,16	1,14,15	6,16,20	1,11,15
2516	6,15,18	2,12,22	2,10	2,17,22	2578	1,8,20	1,15	1,14,16	1,12,15
2517	2,13,17	2,7,22	6,8,20	2,14,22	2579	1,8	1,13	6,16	1,15
2518	1,14,15	2,17,22	2,10,19	2,18,22	2580	1,8,19	1,14,18	6,16,19	1,13,18
2519	3,18,20	2,10,22	2,10,20	2,15,22	2581	1,15,18	1,13,18	2,14,17	1,14,18
2520	3,18	2,22	6,8	2,16,22	2582	6,20,22	1,15,18	2,8,15	1,15,18
2521	3,18,19	2,9,22	6,8,19	2,11,22	2583	6,19,22	1,12,18	2,8,18	1,17,18
2522	6,17,22	2,8,22	1,15,17	2,12,22	2584	2,15,17	1,11,18	2,13,16	1,18
2523	1,13,22	2,16,22	6,14,16	2,9,22	2585	6,22	1,18	1,8,20	1,11,18
2524	6,15,16	2,15,22	6,15,18	2,7,22	2586	3,6	1,17,18	1,8	1,12,18
2525	6,17,20	2,20,22	2,13,17	2,10,22	2587	6,19,20	1,9,14	1,8,19	1,9,14
2526	3,16,22	2,15,20	1,14,15	2,22	2588	2,8,16	1,9,11	1,15,18	1,9,13
2527	3,16,20	2,10,20	3,18,20	2,8,22	2589	2,14,15	1,9,15	3,6	1,9,15
2528	6,17	2,8,20	3,18	2	2590	6,20	1,9,18	6,20,22	1,9,17
2529	6,17,19	2,13,20	3,18,19	1,2	2591	6,19	1,9,12	2,15,17	1,9,18
2530	3,16,19	2,14,20	6,17,22	2,13,20	2592	1,15,16	1,9,13	6,19,22	1,9,11
2531	6,14,22	2,17,20	1,13,22	2,14,20	2593	2,17,18	1,9	6,22	1,9,12
2532	1,13,20	2,7,20	6,15,16	2,15,20	2594	2,13,22	1,9,17	6,19,20	1,9

Continued on next page

Table A.1 – continued from previous page

Rank	w_{C1} Tx's	w_{G1} Tx's	w_{C2} Tx's	w_{G2} Tx's	Rank	w_{C1} Tx's	w_{G1} Tx's	w_{C2} Tx's	w_{G2} Tx's
2595	6	1,7,14	2,8,16	1,7,13	2657	2,16	1,12,20	2,16,19	1,20,22
2596	1,5	1,7,13	2,14,15	1,7,17	2658	1,18,19	1,20,22	2,16	1,12,20
2597	2,14,18	1,7,15	6,20	1,7,14	2659	1,18	1,8,20	1,18,19	1,9,20
2598	7,9,18	1,7,18	6,19	1,7,15	2660	1,16,22	1,7,20	1,18	1,7,20
2599	7,9,18,22	1,7,11	6	1,7,18	2661	1,16,20	1,20	1,16,22	1,10,20
2600	7,9,18,20	1,7,12	1,15,16	1,7,11	2662	2,20,22	1,15,20	1,16,20	1,8,20
2601	7,9,18,19	1,7,17	2,17,18	1,7,12	2663	2,19,22	1,10,20	2,20,22	1,20
2602	2,13,20	1,7,9	1,5	1,7,9	2664	2,22	1,17,19	2,19,22	1,13,19
2603	2,13,19	1,7	2,13,22	1,7	2665	1,16,19	1,14,19	2,22	1,17,19
2604	2,13	1,16,18	2,14,18	1,16,17	2666	1,16	1,16,19	1,16,19	1,14,19
2605	1,4	1,14,16	1,4	1,14,16	2667	2,19,20	1,19,20	1,16	1,18,19
2606	2,16,17	1,16,17	2,13	1,16,18	2668	2,20	1,18,19	2,19,20	1,16,19
2607	2,8,22	1,16	2,13,20	1,16	2669	2,19	1,13,19	2,20	1,19,20
2608	2,8,20	1,9,16	2,13,19	1,11,16	2670	2	1,11,19	2,19	1,11,19
2609	2,14,16	1,11,16	2,16,17	1,13,16	2671	1,2	1,19,22	2	1,19,22
2610	1,17,22	1,12,16	2,8,22	1,9,16	2672	1,20,22	1,9,19	1,2	1,12,19
2611	1,16,18	1,7,16	2,8,20	1,12,16	2673	1,19,22	1,12,19	1,20,22	1,9,19
2612	2,15,18	1,13,16	2,14,16	1,7,16	2674	1,22	1,8,19	1,19,22	1,15,19
2613	1,14,22	1,15,16	1,17,22	1,15,16	2675	1,19,20	1,19	1,22	1,10,19
2614	2,8,19	1,10,14	2,5	1,10,13	2676	1,20	1,10,19	1,19,20	1,7,19
2615	2,8	1,10,17	1,16,18	1,10,17	2677	1,19	1,7,19	1,20	1,8,19
2616	2,5	1,10,15	2,15,18	1,10,14	2678	7,9,12,14	1,15,19	1,19	1,19
2617	1,3	1,10,11	1,14,22	1,10,15	2679	19	19	1	1
2618	1,17,20	1,10,18	2,8,19	1,10,18	2680	1	1	19	19
2619	1,17	1,10,16	2,8	1,10,11					
2620	1,17,19	1,9,10	1,3	1,10,16					
2621	8,9,10,18	1,10,12	1,17	1,9,10					
2622	2,17,22	1,7,10	1,17,20	1,10,12					
2623	1,14,20	1,10,13	1,17,19	1,7,10					
2624	2,4	1,10	2,4	1,10					
2625	2,15,16	1,8,14	2,17,22	1,8,17					
2626	1,14,19	1,8,15	1,14,20	1,8,14					
2627	1,14	1,8,17	2,15,16	1,8,15					
2628	2,17,19	1,8,11	1,14,19	1,8,11					
2629	2,17	1,8,16	1,14	1,8,16					
2630	2,17,20	1,8,9	2,17	1,8,18					
2631	2,3	1,8,12	2,17,19	1,8,13					
2632	1,6	1,8,10	2,17,20	1,8,9					
2633	2,16,18	1,7,8	2,3	1,8,12					
2634	2,14,22	1,8	1,6	1,7,8					
2635	2,14,20	1,8,18	2,16,18	1,8,10					
2636	7,8,10,18	1,8,13	2,14,22	1,8					
2637	2,6	1,18,22	2,6	1,13,22					
2638	2,14,19	1,13,22	2,14,20	1,17,22					
2639	2,14	1,11,22	2,14	1,14,22					
2640	1,15,22	1,14,22	2,14,19	1,18,22					
2641	2,15,22	1,16,22	1,15,22	1,16,22					
2642	2,15,20	1,17,22	2,15,22	1,11,22					
2643	1,15,20	1,9,22	2,15,20	1,9,22					
2644	2,15,19	1,7,22	1,15,20	1,15,22					
2645	1,15	1,8,22	2,15,19	1,7,22					
2646	2,15	1,10,22	1,15	1,10,22					
2647	2,18,22	1,22	2,15	1,8,22					
2648	1,15,19	1,15,22	2,18,22	1,22					
2649	2,18,20	1,12,22	1,15,19	1,12,22					
2650	2,18,19	1,18,20	2,18,20	1,13,20					
2651	1,18,22	1,17,20	2,18,19	1,17,20					
2652	2,18	1,14,20	1,18,22	1,14,20					
2653	2,16,22	1,13,20	2,18	1,18,20					
2654	2,16,20	1,16,20	2,16,22	1,16,20					
2655	1,18,20	1,9,20	2,16,20	1,15,20					
2656	2,16,19	1,11,20	1,18,20	1,11,20					

Appendix B: Flow Chart of Image Generation Used in Qualitative Demonstration

The images used in Chapter 5 to demonstrate the selection process were generated using Matlab. A general flow chart of the image generation process is shown in Figure B.1. Phase history generation and backprojection follow the approach detailed in Section 2.2.

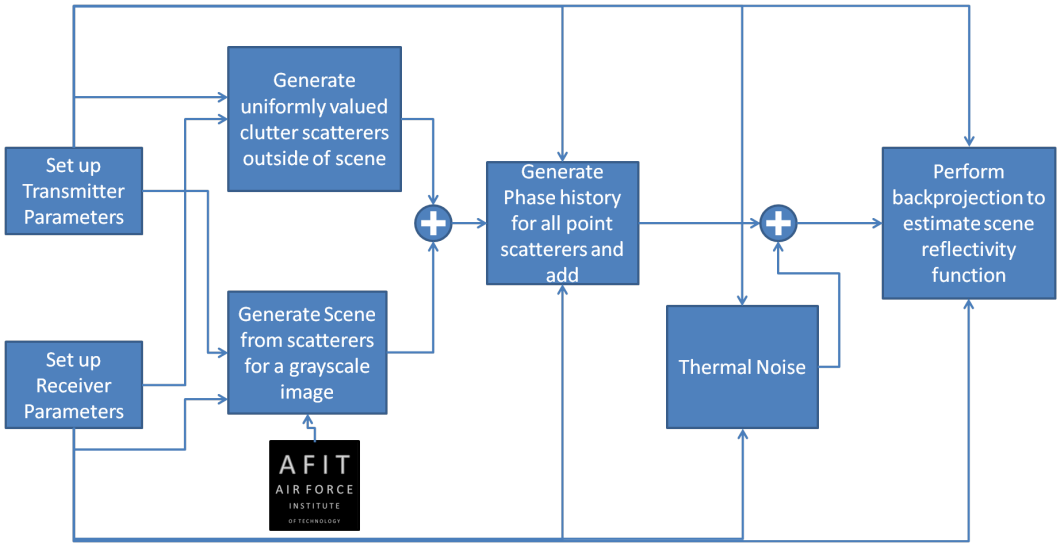

Figure B.1: SAR image generation flowchart

Bibliography

[1] 3rd Generation Partnership Project. "Evolved Universal Terrestrial Radio Access (E-UTRA); Physical Channels and Modulation (Release 8)", Sept. 2008.

[2] Advanced Television Systems Committee. "ATSC Digital Television Standard - Part 2: RF/Transmission System Characteristics", Dec. 2011. URL http://www.atsc.org/cms/standards/a53/a_53-Part-2-2011.pdf.

[3] Akers, G., M. Saville, and T. Hale. "EENG668 2012 Course Notes". School of Electrical and Computer Engineering, Air Force Institute of Technology, Wright-Patterson AFB OH, Winter Quarter 2012.

[4] Bradaric, I., G. T. Capraro, S. H. Brady, M. A. Saville, and M. C. Wicks. "Multistatic measurements in a controlled laboratory environment". *Radar Conference, 2010 IEEE*, 266 –270. May 2010.

[5] Bradaric, I., G. T. Capraro, and M. C. Wicks. "Multistatic ambiguity function - A tool for waveform selection in distributed radar systems". *Waveform Diversity and Design Conference, 2009 International*, 40 –44. Feb. 2009.

[6] Bronshtein, I.N., K.A. Semendyayev, G. Musiol, and H. Muehling. *Handbook of Mathematics*. Springer - Verlag, 4th edition, 2004.

[7] Carrara, W. G., R. S. Goodman, and R. M. Majewski. *Spotlight Synthetic Aperture Radar: Signal Processing Algorithms*. The Artech House Remote Sensing Library. Artech House, 1995.

[8] Chankong, V. and Y. Y. Haimes. *Multiobjective Decision Making: Theory and Methodology*. North Holland series in system science and engineering. New York : North Holland, 1983.

[9] Daout, F., F. Schmitt, G. Ginolhac, and P. Fargette. "Multistatic and Multiple Frequency Imaging Resolution Analysis – Application to GPS-Based Multistatic Radar". *Aerospace and Electronic Systems, IEEE Transactions on*, 48(4):3042 –3057, Oct. 2012.

[10] Desai, M. D. and W. K. Jenkins. "Convolution backprojection image reconstruction for spotlight mode synthetic aperture radar". *Image Processing, IEEE Transactions on*, 1(4):505 –517, Oct. 1992.

[11] FCC Website. "Human Exposure to RF Fields Guidelines For Cellular and PCS Sites", May 2011. URL http: //www.fcc.gov/guides/human-exposure-rf-fields-guidelines-cellular-and-pcs-sites. Accessed Sept. 2012.

[12] FCC Website. "FM Query Broadcast Station Search", Sept. 2012. URL http://www.fcc.gov/encyclopedia/fm-query-broadcast-station-search.

[13] FCC Website. "TV Query Broadcast Station Search", Sept. 2012. URL http://www.fcc.gov/encyclopedia/tv-query-broadcast-station-search.

[14] Goh, A. S., M. Preiss, N. J. S. Stacy, and D. A. Gray. "Bistatic SAR experiment with the Ingara imaging radar". *Radar, Sonar Navigation, IET*, 4(3):426 –437, June 2010.

[15] Gutierrez del Arroyo, Jose. *Passive Synthetic Aperture Radar Imaging Using Commercial OFDM Communication Networks*. Dissertation, Air Force Institute of Technology, Wright Patterson Air Force Base, Sept. 2012.

[16] Howland, P. E. "Target tracking using television-based bistatic radar". *Radar, Sonar and Navigation, IEE Proceedings* -, 146(3):166 –174, June 1999.

[17] Howland, P. E., D. Maksimiuk, and G. Reitsma. "FM radio based bistatic radar". *Radar, Sonar and Navigation, IEE Proceedings* -, 152(3):107 – 115, June 2005.

[18] Jackson, J. "EENG699 2012 Course Notes". School of Electrical and Computer Engineering, Air Force Institute of Technology, Wright-Patterson AFB OH, Summer Quarter 2012.

[19] Jain, A. K. *Fundamentals of Digital Image Processing*. Prentic Hall, Upper Saddle River, NJ, 1989.

[20] Jakowatz, C. J., D. E. Wahl, P. H. Eichel, D. C. Ghihlia, and P. A. Thompson. *Spotlight-Mode Synthetic Aperture Radar: A Signal Processing Approach*. Springer Science + Business Media, Inc., New York, NY, 1996.

[21] Kasischke, E. S. and G. W. Fowler. "A statistical approach for determining radiometric precisions and accuracies in the calibration of synthetic aperture radar imagery". *Geoscience and Remote Sensing, IEEE Transactions on*, 27(4):416 –427, July 1989.

[22] Kay, S. *Intuitive Probability and Random Processes Using Matlab*. Springer, 2006.

[23] Kuperman, G. G. and T. D. Penrod. *Image Quality Analysis of Compressed Synthetic Aperture Radar Imagery*. Technical report, DTIC Document, 1993.

[24] LAN/MAN Standards Committee. "IEEE Standard for Air Interface for Broadband Wireless Access Systems". *IEEE Std 802.16-2012 (Revision of IEEE Std 802.16-2009)*, 1 –2542, 2012.

[25] Levanon, N. and E. Mozeson. *Radar Signals*. John Wiley and Sons, 2004.

[26] Marler, R. T. and J. S. Arora. "Survey of multi-objective optimization methods for engineering". *Structural and Multidisciplinary Optimization*, 26:369–395, 2004.

[27] Munson Jr., D. C., J. D. O'Brien, and W. K. Jenkins. "A Tomographic Formulation of Spotlight-Mode Synthetic Apeture Radar". *Proceedings of the IEEE*, 71(8):917–925, Aug. 1983.

[28] Oppenheim, A. V. and R. W. Schafer. *Discrete-Time Signal Processing*. Prentice-Hall: Englewood Cliffs, NJ, 1989.

[29] Popovic, B. M. and F. Berggren. "Primary Synchronization Signal in E-UTRA". *Spread Spectrum Techniques and Applications, 2008. ISSSTA '08. IEEE 10th International Symposium on*, 426 –430. Aug. 2008.

[30] Proakis, J. G. and M. Salehi. *Communication Systems Engineering*. Prentice Hall, 2nd edition, 2002.

[31] Rapson, M. B. P. *Passive Multistatic Radar Imaging Using an OFDM based Signal of Opportunity*. Thesis, Air Force Institute of Technology, Wright Patterson Air Force Base, Mar. 2012.

[32] Richards, M. A., J. A. Scheer, and W. A. Holm. *Principles of Modern Radar: Basic Principles*. SciTech Publish, Inc., Raleigh, NC, 2010.

[33] Sgrignoli, G., W. Bretl, and R. Citta. "VSB modulation used for terrestrial and cable broadcasts". *Consumer Electronics, IEEE Transactions on*, 41(3):367 –382, Aug. 1995.

[34] Skolnik, M. *Radar Handbook*. McGraw Hill, 3rd edition, 2008.

[35] Strang, G. *Linear Algebra and Its Applications*. Thomson Brooks/Cole, 2006.

[36] Stremler, F. G. *Introduction to Communication Systems*. Addison-Wesley Publish Company, 3rd edition, 1992.

[37] Sullivan, R. J. *Radar Foundations for Imaging and Advanced Concepts*. SciTech Publishing, 2004.

[38] Tsao, T., M. Slamani, P. Varshney, D. Weiner, H. Schwarzlander, and S. Borek. "Ambiguity function for a bistatic radar". *Aerospace and Electronic Systems, IEEE Transactions on*, 33(3):1041 –1051, July 1997.

[39] Voccola, K., B. Yazici, M. Ferrara, and M. Cheney. "On the Relationship between the Generalized Likelihood Ratio Test and Backprojection for Synthetic Aperture Radar Imaging". *Proceedings of SPIE*, 7335(733501-9):1–10, Apr. 2009.

[40] Willis, N. J. and H. D. Griffiths. *Advances in Bistatic Radar*. SciTech Publishing, 2007.

[41] Willis, Nicholas J. *Bistatic Radar*. SciTech Publishing, 2005.

[42] Yu, P. L. and G. Leitmann. "Compromise solutions, domination structures, and Salukvadze's solution". *Journal of Optimization Theory and Applications*, 13:362–378, 1974.

[43] Zeng, T., M. Cherniakov, and T. Long. "Generalized approach to resolution analysis in BSAR". *Aerospace and Electronic Systems, IEEE Transactions on*, 41(2):461 – 474, Apr. 2005.

REPORT DOCUMENTATION PAGE

Form Approved
OMB No. 0704-0188

The public reporting burden for this collection of information is estimated to average 1 hour per response, including the time for reviewing instructions, searching existing data sources, gathering and maintaining the data needed, and completing and reviewing the collection of information. Send comments regarding this burden estimate or any other aspect of this collection of information, including suggestions for reducing the burden, to Department of Defense, Washington Headquarters Services, Directorate for Information Operations and Reports (0704-0188), 1215 Jefferson Davis Highway, Suite 1204, Arlington, VA 22202-4302. Respondents should be aware that notwithstanding any other provision of law, no person shall be subject to any penalty for failing to comply with a collection of information if it does not display a currently valid OMB control number.

PLEASE DO NOT RETURN YOUR FORM TO THE ABOVE ADDRESS.

1. REPORT DATE *(DD-MM-YYYY)*	2. REPORT TYPE	3. DATES COVERED *(From - To)*
22-09-2013	Master's Thesis	Apr. 2010 - Sept. 2013

4. TITLE AND SUBTITLE

Metrics for Emitter Selection for Multistatic Synthetic Aperture Radar

5a. CONTRACT NUMBER

5b. GRANT NUMBER

5c. PROGRAM ELEMENT NUMBER

6. AUTHOR(S)

Stevens, Sean R, Mr.

5d. PROJECT NUMBER

5e. TASK NUMBER

5f. WORK UNIT NUMBER

7. PERFORMING ORGANIZATION NAME(S) AND ADDRESS(ES)

Air Force Institute of Technology
Graduate School of Engineering and Management (AFIT/ENY)
2950 Hobson Way
WPAFB OH 45433-7765

8. PERFORMING ORGANIZATION REPORT NUMBER

AFIT-ENG-13-S-03

9. SPONSORING/MONITORING AGENCY NAME(S) AND ADDRESS(ES)

Dr. Alan Kerrick
Air Force Research Laboratory
2241 Avionics Circle
Area B B620 WPAFB, OH 45433
(937) 938-4350 alan.kerrick@wpafb.af.mil

10. SPONSOR/MONITOR'S ACRONYM(S)

AFRL

11. SPONSOR/MONITOR'S REPORT NUMBER(S)

12. DISTRIBUTION/AVAILABILITY STATEMENT

DISTRIBUTION STATEMENT A. APPROVED FOR PUBLIC RELEASE; DISTRIBUTION UNLIMITED

13. SUPPLEMENTARY NOTES

This material is declared a work of the U.S. Government and is not subject to copyright protection in the United States.

14. ABSTRACT

A bistatic implementation of synthetic aperture radar (SAR) to form images of the ground from an aircraft makes use of separate emitters and receivers. When not using cooperative emitters, ground based communications systems can provide illumination. One way to improve performance of these waveforms, which are not designed for SAR, is a multistatic implementation, formed from multiple bistatic systems. This leads to the problem of selecting a subset from a potentially large set of emitters to use for image formation. A framework for this selection between sets of emitters is proposed using multiple objective optimization. This approach requires use of objective functions to score the inputs to the selection process. The four objective functions selected to score sets of emitters are: signal to noise ratio, waveform ambiguity function's integrated sidelobes , effective multistatic resolution area, and contrast ratio. To speed calculations, an approximation is found for the point spread function. Simulation is used to compare approximation with theory, showing its utility for emitter selection. Finally a qualitative example of emitter selection is presented.

15. SUBJECT TERMS

Multistatic Radar, synthetic aperture radar (SAR), Multistatic, Backprojection, point spread function

16. SECURITY CLASSIFICATION OF:			17. LIMITATION OF ABSTRACT	18. NUMBER OF PAGES	19a. NAME OF RESPONSIBLE PERSON
a. REPORT	b. ABSTRACT	c. THIS PAGE			Dr. Julie A. Jackson, PhD
U	U	U	UU	214	19b. TELEPHONE NUMBER *(Include area code)* (937)255-3636, ext 4678 julie.jackson@afit.edu